https://ntrs.nasa.gov/search.jsp?R=19850024397 2020-03-20T18:21:23+00:00Z

NASA-TM-87570 19850024397

NASA Technical Memorandum 87570

The Global Sulfur Cycle

LIBRARY COPY

JUL [illegible] 1985

LANGLEY RESEARCH CENTER
LIBRARY, NASA
HAMPTON, VIRGINIA

JULY 1985

NASA

NASA Technical Memorandum 87570

The Global Sulfur Cycle

Edited by
Dorion Sagan

Prepared for
Life Sciences Division
NASA Office of Space Science and Applications
Washington, D.C.

NASA
National Aeronautics
and Space Administration

Scientific and Technical
Information Branch

1985

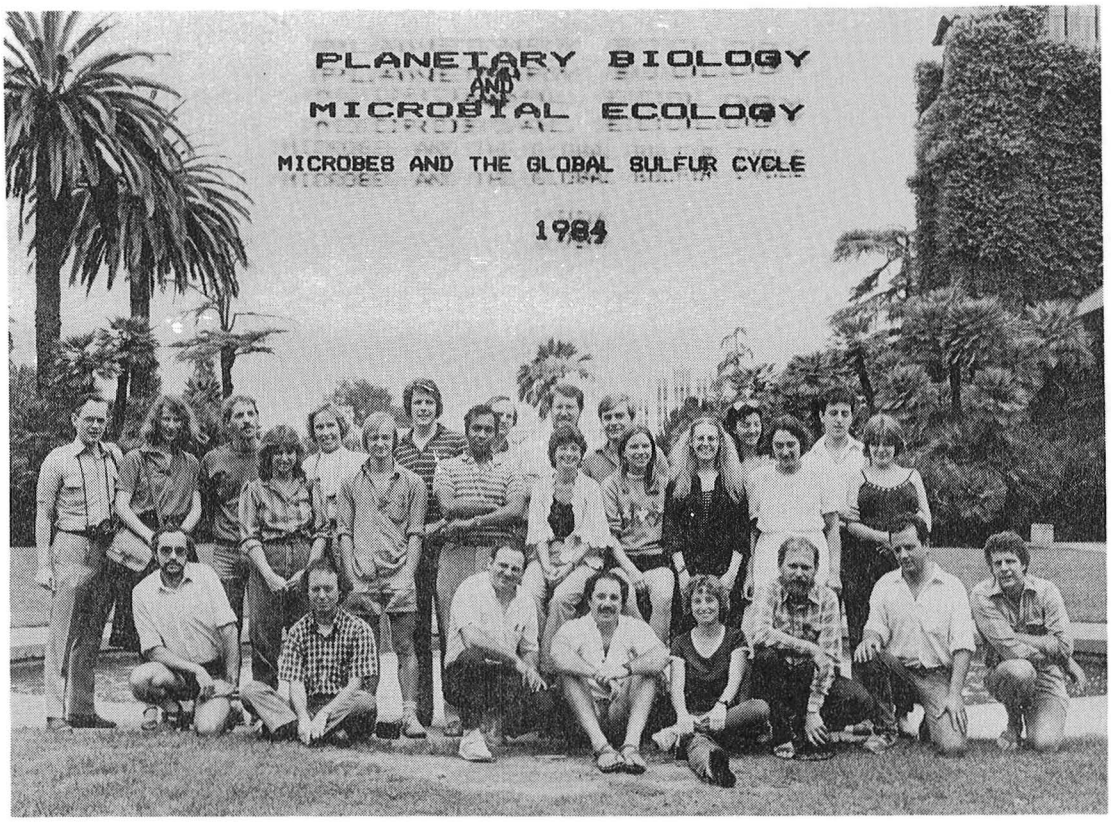

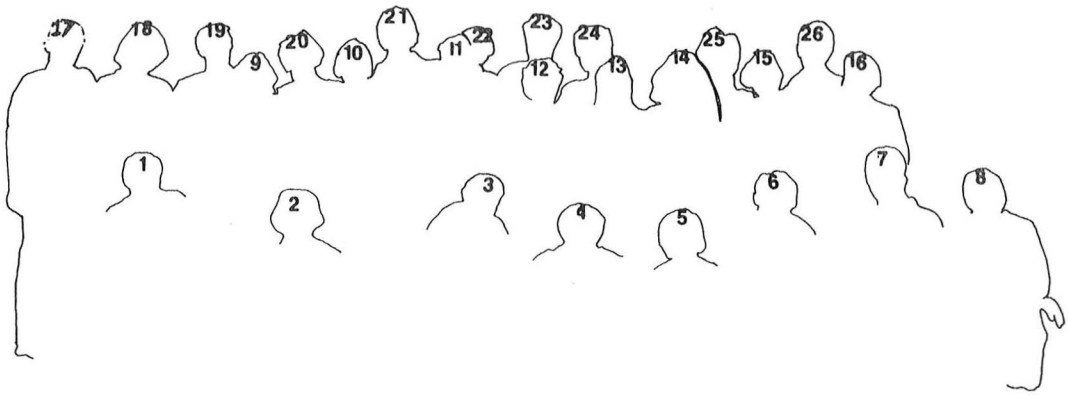

Seated, left to right: (1) U. Fischer, (2) D. Brune, (3) R. Guerrero, (4) R. Haddad, (5) B. Javor, (6) Y. Cohen, (7) D. Bermudes, (8) T. Shaw
Center row: (9) H. Bowers, (10) R. Francois, (11) A. Vairavamurthy, (12) R. Gyure, (13) H. McKhann, (14) P. Boston, (15) L. Margulis, (16) M. Sagan
Rear Row. (17) T. Scheulderman, (18) T. Scheulderman-Suylen, (19) R. Poplawski, (20) E. Weaver, (21) T. Schmidt, (22) John Lawrence, (23) D. Caldwell, (24) M. Klug, (25) L. Prufert, (26) D. Sagan

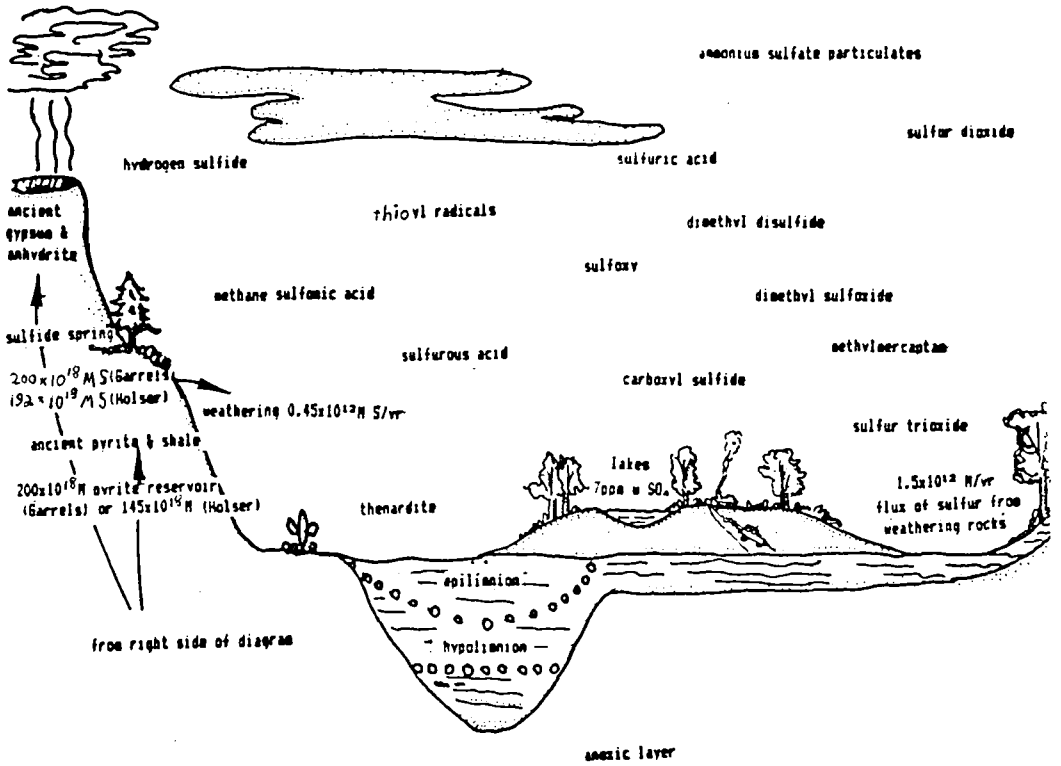

SULFUR MINERALS

troilite
pyrrhotite FeS higher temperatures
pyrite FeS_2
chalcopyrite $CuFeS_2$
galena PbS
sphalerite ZnS
orpiment As_2S_3 - low temperatures, low quantities
covellite CvS weathering, surface of ground water
cinnabar HgS
bornite Cu_3FeS_3

The Global Sulfur Cycle. Drawing by J. Vasko.

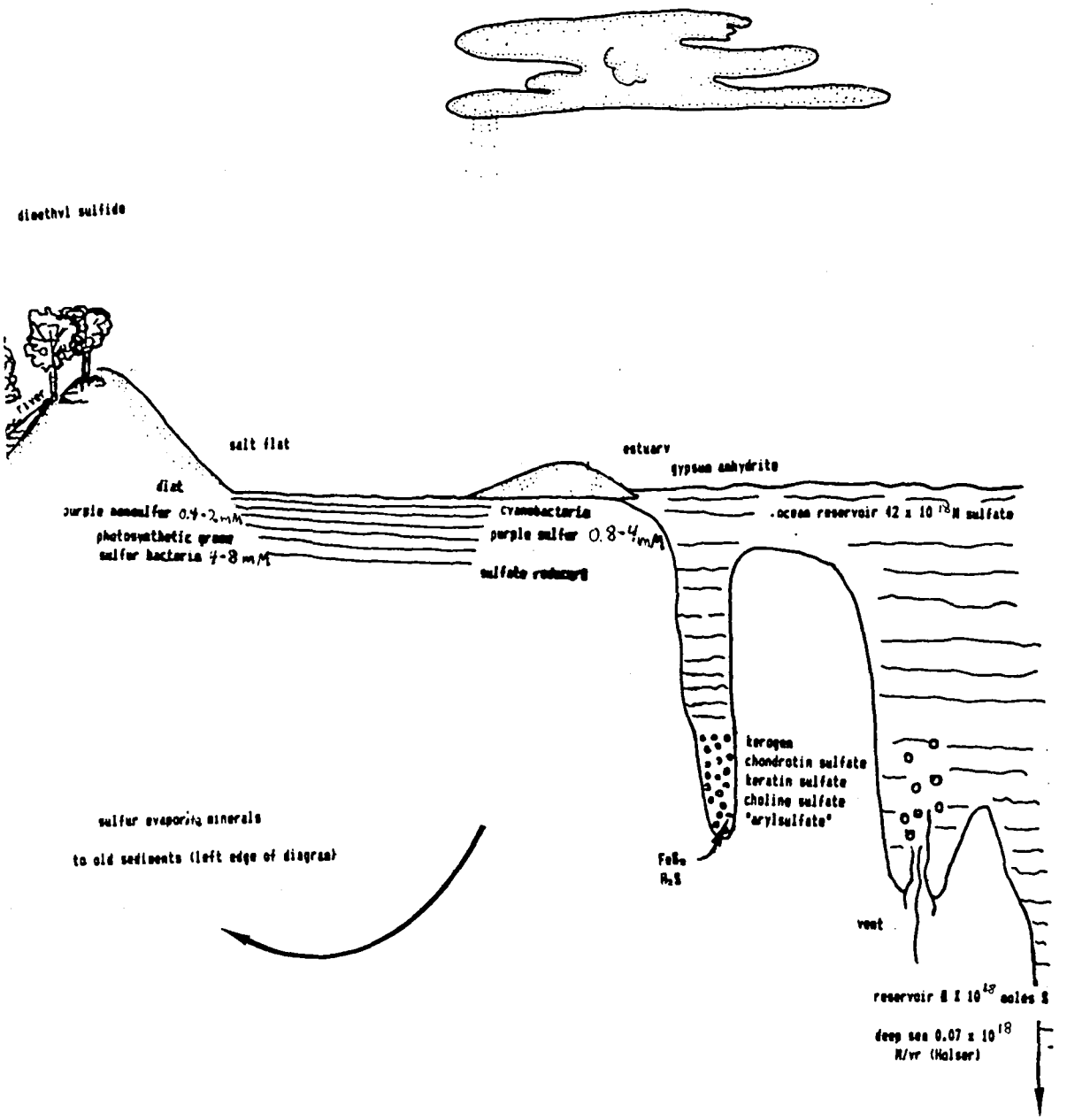
dimethyl sulfide
river
salt flat
flat
purple nonsulfur 0.4-2 mM
photosynthetic green
sulfur bacteria 4-8 mM
cyanobacteria
purple sulfur 0.8-4 mM
sulfate reducers
estuary
gypsum anhydrite
ocean reservoir 42 x 10^18 M sulfate
kerogen
chondrotin sulfate
keratin sulfate
choline sulfate
"arylsulfate"
FeS2
H2S
sulfur evaporite minerals
to old sediments (left edge of diagram)
vent
reservoir 8 X 10^19 moles S
deep sea 0.07 x 10^18
M/yr (Holser)

TABLE OF CONTENTS:
THE GLOBAL SULFUR CYCLE

CHAPTER I.
PBME LECTURE ABSTRACTS AND REFERENCES

CHAPTER II.
SULFUR CYCLING AND METABOLISM OF PHOTOTROPHIC AND FILAMENTOUS SULFUR BACTERIA

CHAPTER III.
SULFUR REDUCTION IN SEDIMENTS OF MARINE AND EVAPORITE ENVIRONMENTS

CHAPTER IV.
RECENT CYANOBACTERIAL MATS: MICROANALYSIS OF COMMUNITY METABOLISM IN PROXIMITY TO THE PHOTIC ZONE IN POTENTIAL STROMATOLITES

CHAPTER V.
FORMATION AND ACTIVITY OF MICROBIAL BIOFILMS ON METAL SULFIDES AND OTHER MINERAL SURFACES

ABBREVIATIONS USED IN THIS BOOK

nM	nanomolar
μM	micromolar
μmol	micromole
mM	millimolar
mmol	millimole
M	molar
mol	mole
nm	nanometer
μm	micrometer (micron)
mm	millimeter
cm	centimeter
m	meter
mV	millivolt
μE	microEinstein
μc	microcurie
wt	weight
ng	nanogram
μg	microgram
mg	milligram
g	gram or gravity
ml	milliliter
l	liter
s	second
h	hour
d	day

dd H_2O distilled deionized water

See Figure I-12 for abbreviations of some common sulfur compounds and their chemical structures.

INTRODUCTION

The manual you hold in your hands is an exciting treatment of the global sulfur cycle - a glimpse, as it were, of the workings of the biosphere we live in and an attempt to both divine and quantify nature's mysterious ways. The manual seems to be made up of disparate and detailed experiments and lectures whose only common thread is that they usually have something to do with sulfur. In fact, however, the work deserves to be seen in the light of a broader perspective. An analogy for the conjoined efforts of the Planetary Biology Microbial Ecology program and NASA is the early anatomical work of the renaissance artist-scientist Leonardo Da Vinci, who ignored religious mores and stole bodies from the grave in order to examine them. Of course, the body being examined by PBME-NASA is not the human body but the Earth, the macro-body which is both a convex container and a virtually animate part of all life.

As Da Vinci imagined the functioning of the human body through an exploration and depiction of its parts, so today's interdisciplinarians theorize about the functioning of the biosphere by exploring its parts, from anaerobic microorganisms living below the surface to satellite-imaged ecosystems. The various layers and parts of the biosphere are analogous to tissues and organs. Science is not yet at the stage where we can say with accuracy how sulfur (or carbon) flows through the many millions of living and chemical species on the Earth's surface. But we are beginning to delve into the anatomy and the physiology of the planet of which we are a part.

In this fledgling anatomy, instead of digging up corpses, Yehuda Cohen and Mike Klug take "cores," withdrawing muds rich with life in cylinders that preserve the order of microbial stratification for later study. Instead of looking at the idealized dead parts cut up from a disinterred man, Douglas Caldwell and Ricardo Guerrero study in situ the behavior of the Earth's living parts, for example, its filamentous and photosynthetic sulfur bacteria and the way they adhere to and make use of the minerals into which, ultimately, or should I say cyclically, they are transformed. The marriage of the microscopically small (the province of microbiologists) to the globally large (the province of geochemists and NASA scientists) is an ambitious scientific undertaking and one which has only recently become possible.

Understanding the sulfur cycle and other chemical pathways of the Earth we live in may eventually lead to a new standard of interspecies or ecological health. I believe this is a logical transition science will make as it extends beyond its traditional attempts to improve only human life. The traditional emphasis has succeeded in the short term by reducing suffering and increasing the human life span, but it is failing in the long term aftermath of overpopulation and industrial self-poisoning. The use of satellite and state-of-the-art NASA technology to discover how species have been able to coexist and even expand their frontiers over a period of longer than three thousand million years - despite natural limitations on the quantities of biologically crucial elements such as sulfur - is an example of an approach that promises a wiser, more peaceful future.

Dorion Sagan
November, 1984

LIST OF FIGURES

LIST OF TABLES

ACKNOWLEDGEMENTS
AND NOTE TO READER

We thank the Department of Biological Sciences and the San Jose State University Foundation for their hospitality and support in all aspects of this program. We are grateful to P.D. Johnson, Refuge Manager, and everyone else at the San Francisco Bay Wildlife Refuge of the U.S. Fish and Wildlife Service who provided us with access to and information about the field sites. Joseph Vasko is to be thanked for his miniaturization of the global sulfur cycle from a wall mural to a neat diagram.

The value of this manuscript lies not in its formation but in its information. Graphs, illustrations, figures, and references should provide the reader with an excellent source material on the global sulfur cycle. Post-course production of this manuscript was accomplished at home with minimal resources by Dorion and Marjorie Sagan. Since we anticipate a wider publication of this NASA technical memorandum and attendant higher quality production we would appreciate receiving corrections, comments, and completion of references now in press. Please send these to Dorion Sagan whose address is listed in the PBME lecturers and participants list. Finally we must acknowledge the many lecturers and participants who ably shared information as well as our four Apples (3 II+ and 1 IIe and our On-Line systems software, the "Screenwriter" word-processing program) without whom and without which this manuscript would not exist.

PBME LECTURERS AND PARTICIPANTS

Visiting Lecturers and Participants

Prof. Meinrat Andreae
Department of Oceanography
Florida State University
Tallahassee FL 32306
D: 904-644-6770
O: 904-644-1221

Prof. Stanley Awramik
Department of Geology
Univerity of California, Santa Barbara
Santa Barbara CA 93106
O: 805-961-3177
ext. 3830

Dr. Sherwood Chang
NASA Ames Research Center 239-11
Moffett Field CA 94035
O: 415-9654-5098

Dr. David Des Marais
NASA Ames Research Center 239-12
Moffett Field CA 94035
O: 415-694-6110

Prof. Robert L. Fahey
Dept. of Chemistry D-006
U.C.S.D.
La Jolla CA 92093
O: 619-452-2163

Prof. George Fox
Dept. of Biochem. and Biophys. Science
University Park
University of Houston
Houston TX 77004
O: 713-749-3980

Prof. Robert M. Garrels
Department of Marine Science
University of South Florida
830 First Street South
St. Petersburg FL 33701
O: 813-893-9538

Dr. Martin Goldhaber
U.S. Geological Survey MS916
Denver Federal Center
Denver CO 80225
O: 303-236-1521
S: 303-236-1644

Prof. William Holser
Department of Geology
University of Oregon
Eugene OR 97403
O: 503-686-4573

Dr. James Kasting
NASA Ames Reseach Center 245-3
Moffett Field CA 94035
O: 415-694-5233

Dr. James Lawless
NASA Ames Research Center
Moffett Field CA 94035
O: 415-694-5098

Prof. Christopher Martens
Department of Marine Science
12-5 Venable Hall 045-A
University of North Carolina
Chapel Hill NC 27514
O: 919-962-1252

Prof. Abdul Matin
Department of Microbiology
Stanford University
Palo Alto CA 94305
O: 415-497-1207

Dr. Ronald Oremland
U.S. Geological Survey Building no. 6
Menlo Park CA 94025
O: 415-323-8111
ext. 2027

Prof. Harold Peck
Department of Biochemistry
University of Georgia
Athens GA 30601
O: 404-542-1334

Dr. David Peterson
NASA Ames Research Center 242-4
Moffett Field CA 94035
O: 415-694-5899

Dr. James Pollack
NASA Ames Research Center 245-3
Moffett Field CA 94035
O: 415-694-5233

Prof. Hans Trueper
Institute of Microbiology
University of Bonn
5300 Bonn
West Germany
West Germany
O: (0228) 732320

Prof. John Yopp
Botany Department
Southern Illinois University
Carbondale IL 62901
O: 618-536-2331

Permanent Faculty

Prof. Douglas Caldwell
Department of Applied
Microbiology & Food Science
University of Saskatchewan
Saskatoon, Saskatchewan
Canada S7N 0W0
Canada
O: 306-966-5027
L: 306-966-5039
H: 306-934-5849

Dr. Yehuda Cohen
Marine Biology Laboratory
Hebrew University
P.O. Box 469
Eilat 88103
Israel
or
NASA Ames Research Center
Moffett Field CA 94035-239-12

Israel
O: 972-59-76181

O: 415-964-6110

Prof. Ricardo Guerrero
Department of Microbiology
Autonomous University of Barcelona
Bellaterra (Barcelona), Spain

Spain
O: 343-692-0200
H: 343-692-7644

Prof. Michael Klug
W.K. Kellogg Biology Station
Hickory Corners, MI 49060-9516

O: 616-671-5117

Co-Directors

Prof. Lynn Margulis
Department of Biology
Boston University
2 Cummington Street
Boston MA 02215

O: 617-353-2443
H: 617-262-0612

Prof. Kenneth Nealson
Scripps Institution of Oceanography
A-002
University of California San Diego
La Jolla CA 92093

O: 619-452-2086
H: 619-459-5186

NASA Coordinator

Dr. John Billingham
NASA Ames Research Center 239-11
Moffett Field CA 94035

O: 415-694-5181

Coordinators

Prof. Ellen Weaver
Department of Biological Sciences
San Jose State University
San Jose CA 95192

O: 408-277-2355
H: 415-851-0517
NASA: 415-694-6182

Dr. Barbara Javor
Scripps Institution of Oceanography
A-002
University of California San Diego
La Jolla CA 92093
O: 619-452-4301
H: 619-571-3846

Editors

Dorion Sagan
351 Utah Avenue
Fort Lauderdale FL 33312
H: 305-797-2815

Heather McKhann
Department of Biology
Middlebury College
Middlebury VT 05753
O: 802-388-3711
ext. 5431

Prof. Lynn Margulis
see Co-Directors.

Prof. Ellen Weaver
see Coordinators

Prof. Kenneth Nealson
see Co-Directors

Production and Layout

Marjorie Sagan
351 Utah Avenue
Fort Lauderdale FL 33312
H: 305-797-2815

Trainees

David Bermudes
Department of Biology
Boston University
2 Cummington Street
Boston MA 02215
O: 617-353-2443
H: 617-787-1409

Dr. Penelope Boston
National Center for Atmospheric Research
PO Box 3000
Boulder CO 80307-3000
O: 303-497-1635
H: 303-665-2283

Dr. Daniel Brune
c/o Professor Hans Trueper
Institute of Microbiology
University of Bonn
5300 Bonn
West Germany
West Germany
O: (0228) 732320

Allen P. Doyle
Institute of Marine Science
University of Alaska
Fairbanks AK 99701
O: 907-474-7533

Dr. Ulrich Fischer
Department of Geomicrobiology
University of Oldenburg
D-2900 Oldenburg
West Germany
West Germany
O: 0441-7983393

Roger François
Department of Oceanography
University of British Columbia
Vancouver, British Columbia
Canada V67 1W5
Belgium
O: 064-228-2936

Ruth Ann Gyure
Department of Biology
Purdue University
West Lafayette IN 47906
O: 317-494-8145

Robert I. Haddad (Planetary Biology Intern)
Department of Marine Sciences
University of North Carolina
Chapel Hill NC 27514
O: 919-962-1253

John Lawrence (Planetary Biology Intern)
Department of Soil Science
University of Saskatchewan
Saskatoon, Canada S7N OWO
Canada
O: 306-343-4201
H: 306-373-8674

Lee E. Prufert
Department of Geology
University of North Carolina
Chapel Hill NC 27514
O: 919-966-4516
H: 919-929-8028

Trudy Scheulderman-Suylen
Laboratory of Microbiology
University of Technology Delft
Julianalaan 67a
Delft, The Netherlands
Netherlands
O: 015-7824.21
H: 070-60.82.11

Thomas Schmidt
Department of Microbiology
Ohio State University
Columbus OH 43210
O: 614-422-8296

Timothy Shaw
Scripps Institute of Oceanography
A-008
University of California San Diego
La Jolla CA 92093
O: 619-452-4257

Alfred R. Sundquist
Department of Chemistry
University of California San Diego
La Jolla CA 92093
O: 619-452-4821

Gordon Tribble
Department of Oceanography
University of Hawaii
Honolulu HI 96822
H: 808-734-7791

Ricardo Poplawski Wainberg
c/o Dr. I. Ohad
Department of Biochemistry
Life Science Institute
Hebrew University
Jerusalem Israel
Uruguay
Israel
O: 972-2-585424

or

Steinitz Marine Biological Laboratory
PO Box 469
Eilat 88103 Israel
Israel
O: 972-59-76181

Appathurai Vairavamurthy
Department of Oceanography
Florida State University
Tallahassee FL 32306
Sri Lanka
Florida
O: 904-694-1730

Technicians

Kamrin MacKnight
San Jose State University

Holly Bowers
San Jose State University

Visitors

Lynne Attiy	Pacific Bell
Nick Bilardello	Harbor High School
Dr. Neal Blair	NASA Ames
Dr. Donald DeVincenzi	NASA Headquarters, Washington, DC
Lauren Fellows	Planetary Biology Intern

Dr. Patricia Grilione	San Jose State University
John Groom	BBC, London
Dr. Fred Iltis	San Jose State University
Linda Jahnke	NASA Ames
Thomas M. Jones	University of California, Berkeley
Dr. Douglas Kent	Stanford University
Tom Kieft	University of California, Berkeley
Dr. Mark Kritz	NASA Ames
Harald Klein	NASA Ames
Emil Kwong	NASA Ames
Mary Lidstrom	University of Washington
William Margulis	Oakland, California
James Marshall	San Jose State University
Dr. John Oro	University of Houston
Dr. T. Satyanarayana	NASA Ames
Dr. Tacheeni Scott	NASA Ames North Arizona University
Joshua Schimel	University of California, Berkeley
Dr. John Stolz	JPL, California Institute of Technology

KEY: D DEPARTMENT O OFFICE H HOME S SECRETARY

PBME PROGRAM

WEEK 1

June 24--Aug 4, 1984

Students and faculty arrived June 23 and June 24

June 24, Sunday

Evening: Reception at International House, San Jose State University

June 25, Monday

0830-1200 hrs

Introduction: K. Nealson and L. Margulis, students and faculty introduced themselves

1330 hrs

Introductory lectures:

K. Nealson, prokaryote physiology and ecology, B. Javor, introduction to microbial ecology. Permanent faculty and students organized lab and office equipment

2000 hrs

Short presentations on potential lab projects by M. Klug, D. Caldwell, R. Guerrero and Y. Cohen. Lab group discussions

June 26, Tuesday

0830 hrs

Lab group planning meetings

1230 hrs

Field trip: Alum Rock Park sulfur springs

1530 hrs

Lecture: Glenn T. Seaborg, Nobel Laureate: *The Transuranium Elements*

June 27, Wednesday

0830 hrs — Lab group meetings

1230 hrs — Field trip: San Francisco Bay estuary

2000 hrs — Reception, home of Dr. John Billingham

June 28, Thursday

NASA life sciences day: NASA Ames Research Center

Schedule

0900 hrs — Introduction to Ames Research Center and the Life Science Directorate: J. Billingham

0930 hrs — Chemical evolution and the origin and early evolution of life: S. Chang

1030 hrs — Evolution of complex life and intelligence: J. Billingham

1115 hrs — Stable carbon isotope biogeochemistry: N. Blair

1135 hrs — Gas chromatographs for solar system exploration: Glen Carle

1200 hrs — Lunch

1300 hrs — Life support systems: J. Billingham

1315 hrs — Controlled ecological life support systems (CELSS): Steven Schwartzkopf

1345 hrs

Biomedical problems of manned space flight: J. Billingham

1430 hrs

Global Biology/ Remote Sensing

J. Lawless: Introduction to NASA Ames new Global Biology Program, the use of remote sensing to solve problems of biogeochemical cycles

James Brass: Earth systems and remote sensing: the view from Landsat 550 miles up

Vincent Ambrosia: Interpretation of remote sensing images

John Arvesen: Visit to U2 and TR1 (Tactical Reconnaissance 1 or Earth Resources aircraft) sampling the stratosphere

1700 hrs

Conclusion

June 29, Friday

0830 hrs

T. Schmidt: Structures of sulfur oxidizing bacteria

0900 hrs

U. Fischer: Cytochromes and sulfur metabolism in purple and green phototrophic bacteria

1100 hrs

Research groups planning discussions

1245-1600 hrs

Lab group meetings

1600 hrs

Plenary session: PBME research and Gaia

June 30, Saturday

0900---1700 hrs

Field trip to West Dumbarton Bridge salt flats

1945 hrs

Saturday Night Lecture: Dr. S. Chang (NASA Ames): Origin of life

WEEK 2

July 2--July 6, 1984

July 2, Monday

0830 hrs

Dr. R. Garrels: Exogenic cycle: ocean, atmosphere and sediments

1030 hrs

Dr. W. Holser: Geology and geochemistry of sulfide and sulfate deposits

July 3, Tuesday

0830 hrs

Dr. C. Martens: Sulfur cycling in marine sediments

1030 hrs

Dr. R. Oremland: studies at Big Soda Lake, Nevada

1900 hrs

Dr. M. Klug: Sulfur cycling in fresh water sediments

July 4, Wednesday

0830 hrs

Dr. C. Martens: Organic carbon mineralization in anaerobic sediments

0945 hrs

Dr. M. Andreae: Algal biosynthesis of organosulfur compounds

July 5, Thursday

0830 hrs

T. Scheulderman: Metabolism of dimethyl sulfoxide and dimethyl sulfide by *Hyphomicrobium* and other bacteria

0900 hrs

Dr. M. Andreae: Role of the oceans in the atmospheric sulfur budget

0945 hrs

Dr. M. Kritz (NASA Ames): gas emissions and measurement with NASA technology

1900 hrs

Dr. M. Kritz: Exchange of sulfur between ocean and atmosphere

July 6, Friday

0830 hrs

Dr. W. Holser: Age curves of sulfur and carbon isotopes

0945 hrs

Dr. R. Garrels: Modeling past variations in sulfur and carbon cycles

July 7, Saturday

1945 hrs

Demonstration: D. Sagan: sleight-of-hand and problems of perception

0830 hrs

Saturday Night Lecture: L. Margulis: From microbial communities to cells (including two short films)

WEEK 3

July 9--July 13, 1984

July 9, Monday

0830 hrs

Dr. M. Goldhaber: Stable isotopes and sulfur compounds in nature

0945 hrs

Dr. J.F. Kasting (NASA Ames): Evolution of the atmosphere I. Before life

0800 hrs

Round table discussion of previous week

July 10, Tuesday

0830 hrs

Dr. S. Awramik: Precambrian evolution and the rock record I

0945 hrs

Dr. J.F. Kasting: Evolution of the atmosphere: II. The Archean and Proterozoic Eons

July 11, Wednesday

0830 hrs

Dr. M. Goldhaber: Sedimentary sulfur and diagenesis

1000 hrs

Dr. S. Awramik: Precambrian evolution II

July 12, Thursday

1000 hrs

Dr. G. Fox: Prokaryotic taxonomy and evolution

2030 hrs

Dr. Y. Cohen: Anoxygenic photosynthesis in cyanobacteria

July 13, Friday

0830 hrs

Dr. R. Fahey: Distribution and abundance of reduced organic sulfur compounds (thiols)

1000 hrs

Dr. G. Fox: Evolution of prokaryotes determined by 5S and 16S ribosomal RNA sequences

July 14, Saturday

0900 hrs

Dr. G. Carle (NASA Ames): Instrumentation for global biology

1945 hrs

Saturday Night Lecture: Dr. James Pollack (NASA Ames): *Global environmental consequences of a nuclear war*

WEEK 4

July 15--July 20, 1984

July 16, Monday

0830 hrs

Dr. B. Javor: The microbiology of solar salt ponds

0930 hrs

Dr. H. Trueper: Phototrophic sulfur bacteria I

2000 hrs

Round table discussion of previous week

July 17, Tuesday

0830 hrs

Dr. H. Trueper: Phototrophic sulfur bacteria II

1030 hrs

Dr. H. Peck: Sulfate reduction I

July 18, Wednesday

0830 hrs

Dr. H. Peck: Sulfate reduction II

1000 hrs

Dr. A. Matin: Chemolithotrophic sulfur oxidizing bacteria

July 19, Thursday

0830 hrs

Dr. A. Matin: Bacterial physiology under nutrient limitation

1000 hrs

Dr. D. Caldwell: Aerobic sulfur oxidizing bacteria

July 20, Friday

0830 hrs

Dr. Y. Cohen: Sulfur cycling in a stratified hypersaline environment

1000 hrs

Dr. R. Guerrero: Sulfur cycling in a lake environment

July 21, Saturday

0900 hrs

Dr. D. Des Marais (NASA Ames): Carbon isotope geochemistry and geobiology

1030 hrs

Dr. D. Peterson (NASA Ames): Remote sensing and the biogeochemistry of forests

July 21--July 22

Field trip to Big Soda Lake, Nevada

WEEK 5

July 23--July 28, 1984

July 23, Monday

2000 hrs

Round table discussion of previous week; faculty skit

July 24, Tuesday

1900 hrs

Gordon Tribble: Christmas Island: Ravings of a displaced naturalist: a slide show

July 25, Wednesday

1930 hrs

Deadline for methods and references for course report

July 27, Friday

0830 hrs

Dr. K.H. Nealson: Manganese redox chemistry and interactions with the sulfur cycle

July 28, Saturday

1945 hrs

Saturday Night Lecture: Dr. J. Lawless (NASA Ames): Chemical evolution revisited

WEEK 6

July 30--August 4, 1984

July 30, Monday

1600 hrs

Wine and cheese reception: President Gail Fullerton, President, San Jose State University

1900 hrs

L. Margulis and J. Stolz: Film: "Miles to Microns" the microbial mat at Laguna Figueroa

July 31, Tuesday

1700 hrs

Deadline for receipt of results and discussion sections and all other material to be included in final course report

August 1, Wednesday

1130-1400 hrs

Relation of 1984 PBME course with NASA Ames (at NASA)

August 2, Thursday

0830 hrs

Dr. J. Yopp: Role of sulfur in osmoregulation: production of DMS and DMSO

1300 hrs

Presentations of results by each research team

August 3, Friday

1300 hrs

Presentations of results by each research team

August 4, Saturday

Final departure

Planetary Biology and Microbial Ecology: The Global Sulfur Cycle, NASA and San Jose State University

Ellen Weaver

We in academe are constantly aware that the function of the university to transmit and to expand knowledge depends as much on students as it does on faculty. The process of intellectual growth requires the energy, curiosity, and naivete of the young people as much as it requires older scholars. Students constantly question, demand, and force us to re-examine our precepts; they make weaknesses in argument or lack of evidence prominent - sometimes even embarrassingly so. The faculty provide perspective, proven principles, and try to focus the efforts of students on problems where new understanding is most urgently needed. Ideally, the faculty also provide an interdisciplinary framework which transcends departmental boundaries, but this element all too easily disappears with specialized courses.

The PBME program combined these elements of students, teachers, and a wide interdisciplinary scope in a setting which also accomodated and integrated the contributions of several highly skilled NASA scientists. The program brought together diverse aspects of the global sulfur cycle in the persons of highly skilled and motivated experts from both academic and governmental laboratories, kept them together long enough for any barriers of reserve to crumble, and incorporated the whole with NASA researchers. The small cadre of dedicated NASA scientists brought indispensible, highly technical skills and instruments. What everyone took away from the program was a truly global view of the sulfur cycle, an understanding of major importance for life on earth. The gaps in our understanding of global sulfur processes were also made evident. Friendships were formed which will make possible a continuing intellectual contribution to matters of NASA's interest. This six week program also advanced knowledge in areas of NASA's specific interests: early evolution of the earth and biosphere, and present processes which affect global habitability.

The PBME program was also valuable to San Jose State University (SJSU). Several students and faculty attended both specialized and public lectures, some attending virtually every lecture. A few science teachers from San Jose secondary schools also attended. If the PBME program takes place again at SJSU, we plan to publicize it more extensively, and provide academic credit for teachers who regularly attend lectures. Thus, the teaching of science will be even more benefitted in the future than it was in 1984. The excellent teaching facilities of SJSU are now better known to both the NASA Ames scientists and the other members of the PBME group. Several of the

SJSU faculty members learned about the bay area field sites from the NASA course visitors and some of us hope to use these sites in teaching our own classes.

The NASA life science program benefits from the PBME summer research by the generation of advanced knowledge in an important field. If knowledge gained per dollar spent were quantified, the PBME would probably prove to be an impressive bargain. The accumulated knowledge will be disseminated in the form of this NASA technical publication, and, we hope, to an even broader public in the form of a published book. Less tangible, however, are the benefits to NASA research which accrue from the infusion of student energy, and from the insights of experts from diverse fields who have no opportunities to interact in any other way. NASA is unique in its ability to view the world synoptically; the value of these world views is increased by an understanding of the processes which it has the potential to observe. The 1984 PBME program went far towards accomplishing this for the biogeochemical processes at the earth's surface which involve sulfur.

UNITED STATES DEPARTMENT OF THE INTERIOR

FISH AND WILDLIFE SERVICE
SAN FRANCISCO BAY REFUGE COMPLEX
REFUGE PERMIT

1. PERMITTEE	2. AUTHORITY-STATUTES: 16USC, 668dd; REGULATIONS (ATTACHED): 50 CFR 25-28
Barbara Javor Dept. of Biological Sciences San Jose State University San Jose, CA 95192	3. NUMBER: SFB-1400-84-12
	4. RENEWABLE: [ ] YES [X] NO; 5. MAY COPY: [X] YES [ ] NO
1 number 01093 key issued	6. EFFECTIVE: 06-29-84; 7. EXPIRES: 08-05-84
8. NAME AND TITLE OR PRINCIPAL OFFICER (IF NO. 1 IS AND ORGANIZATION): Barbara Javor - Program Coordinator	9. TYPE OF PERMIT: Research

10. LOCATIONS WHERE AUTHORIZED ACTIVITY MAY BE CONDUCTED

Saltponds of Coyote Hills Unit - SF Bay NWR

11. CONDITIONS AND AUTHORIZATIONS

A. GENERAL CONDITIONS SET OUT IN SUBPART D OF 50 CFR 25, AND SPECIFIC CONDITIONS CONTAINED IN FEDERAL REGULATIONS CITED IN BLOCK NO. 2 ABOVE, ARE HEREBY MADE A PART OF THIS PERMIT. ALL ACTIVITIES AUTHORIZED HEREIN MUST BE CARRIED OUT IN ACCORD WITH AND FOR THE PURPOSE DESCRIBED IN THE APPLICATION SUBMITTED. CONTINUED VALIDITY, OR RENEWAL, OF THIS PERMIT IS SUBJECT TO COMPLETE AND TIMELY COMPLIANCE WITH ALL APPLICABLE CONDITIONS, INCLUDING THE FILING OF ALL REQUIRED INFORMATION AND REPORTS.

B. THE VALIDITY OF THIS PERMIT IS ALSO CONDITIONED UPON STRICT OBSERVANCE OF ALL APPLICABLE STATE, LOCAL OR OTHER FEDERAL LAWS.

C. VALID FOR USE BY PERMITTEE NAMED ABOVE.

D. Permittee may drive 3 vehicles containing up to 25 people onto the Shoreline Trail for the purpose of collecting water and sediment samples in the saltponds on seperate dates as described in letter of 06-27-84. Permittee is also granted access to saltpond adjacent to 5-mile loop trail.

[X] ADDITIONAL CONDITIONS AND AUTHORIZATIONS ON REVERSE ALSO APPLY

12. REPORTING REQUIREMENTS Permittee agrees to provide at least one (1) copy of any report, paper, publication, etc. produced as a result of this research to the library of the San Francisco Bay NWR.

ISSUED	TITLE	DATE
Roger D. Johnson	Refuge Manager	6/29/84

E. Permitte agrees to acknowledge the US Fish and Wildlife Service and the San Francisco Bay National Wildlife Refuge in any report, publication, or paper produced as a result of this research.

F. Permittee will observe dike road speed limit of 15 mph.

G. Caution should be used when driving dike roads after foggy and/or windy days due to wet and muddy roads.

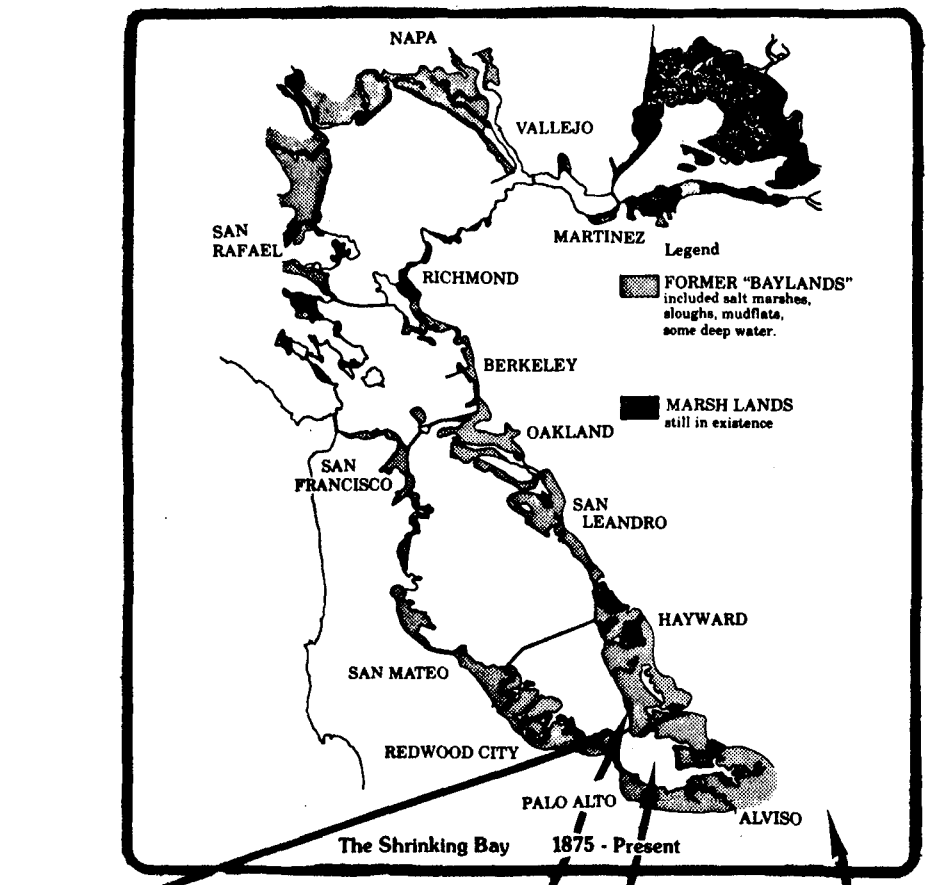

EMBARCADERO ROAD
DUMBARTON BRIDGE
SALT MARSH

ALUM ROCK PARK
SULFUR SPRINGS
SAN JOSE

SAN FRANCISCO
NATIONAL WILDLIFE REFUGE
SALT PONDS

NASA AMES RESEARCH CENTER
MOFFETT FIELD

NASA
PLANETARY BIOLOGY AND MICROBIAL ECOLOGY
JUNE-AUGUST 1984

STUDY SITES

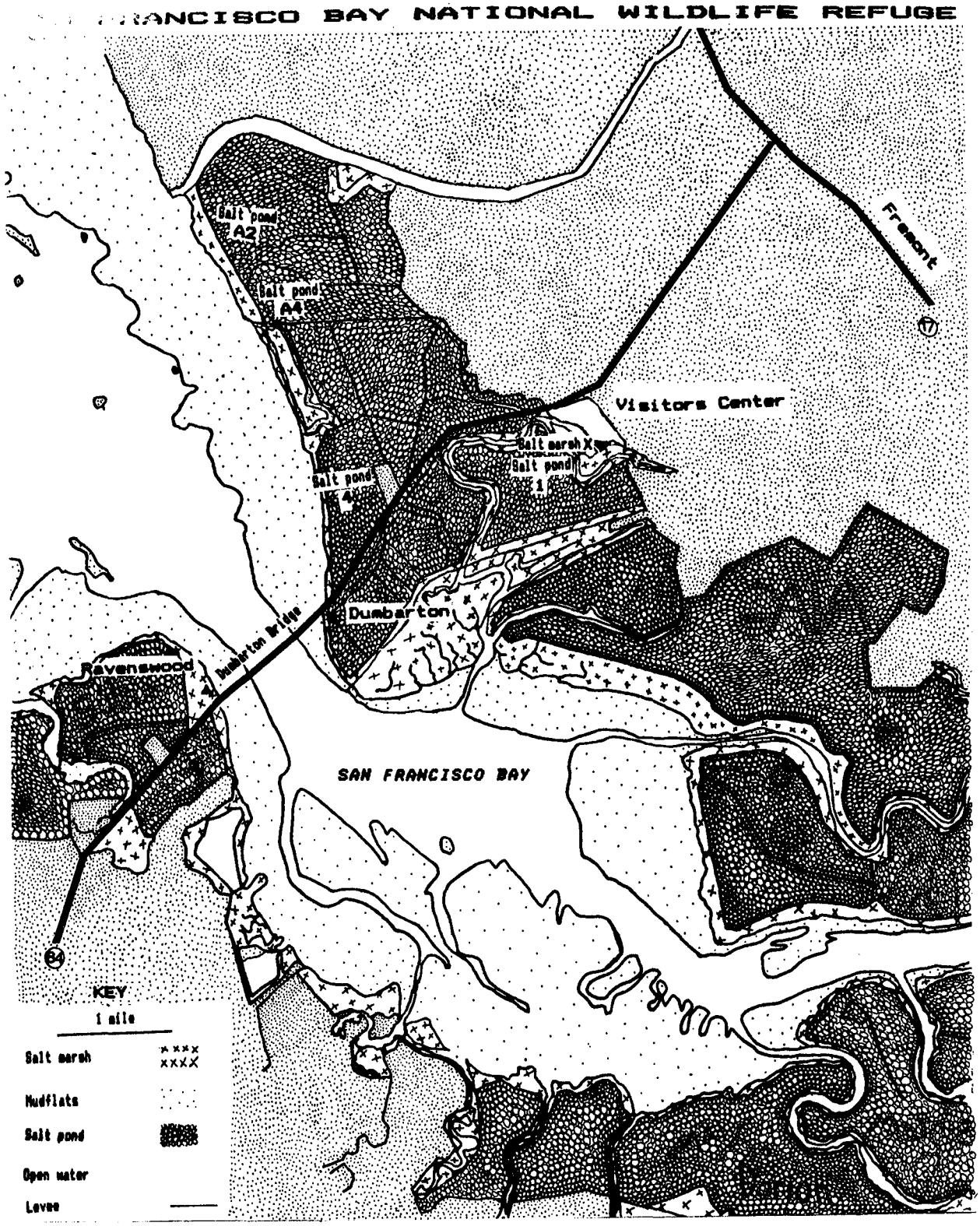
SAN FRANCISCO BAY NATIONAL WILDLIFE REFUGE
Salt pond A2
Salt pond A4
Salt pond 4
Salt marsh
Salt pond 1
Visitors Center
Fremont
17
Dumbarton
Dumbarton Bridge
Ravenswood
SAN FRANCISCO BAY
84
KEY
1 mile
Salt marsh
Mudflats
Salt pond
Open water
Levee

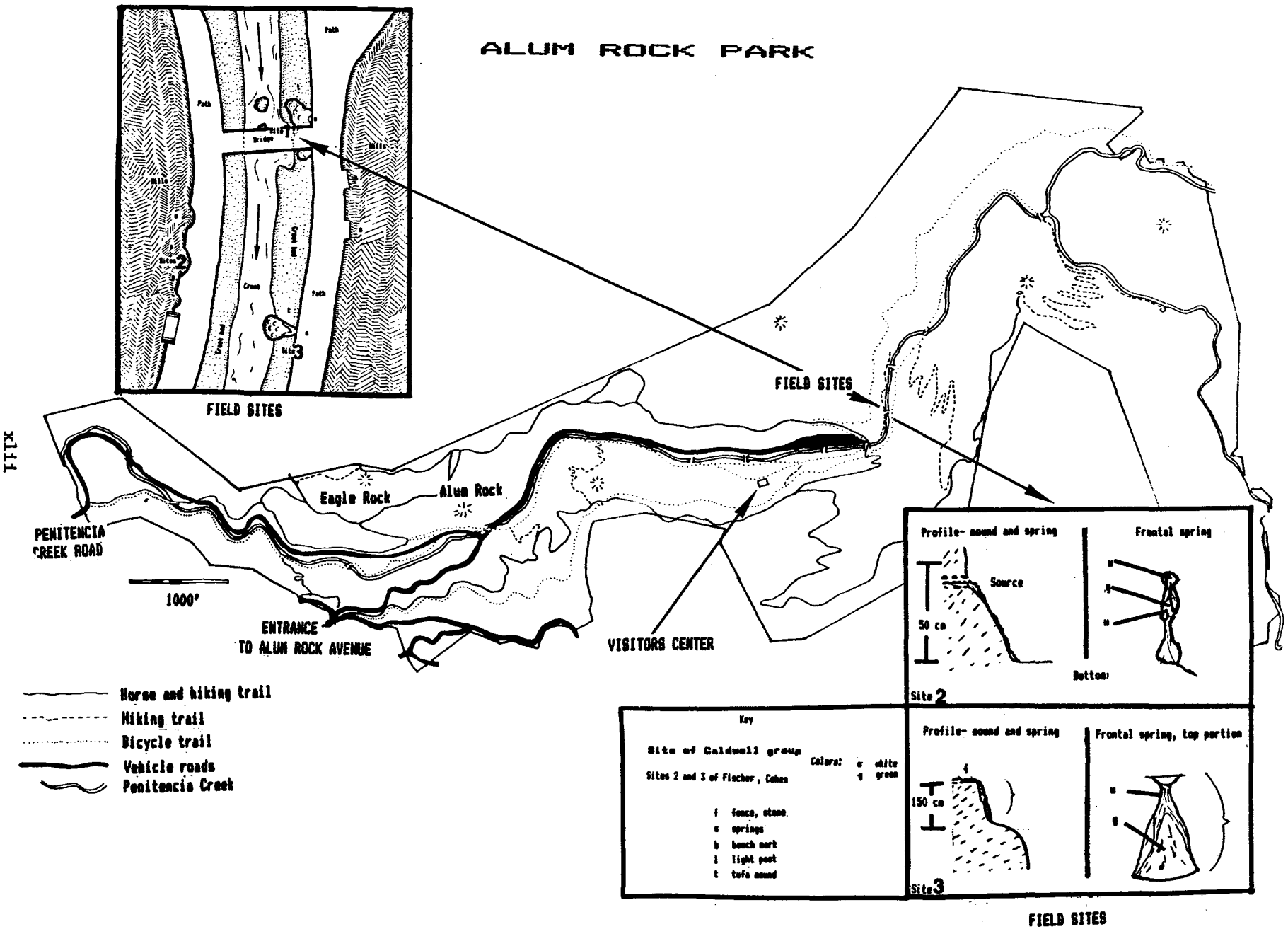
ALUM ROCK PARK
FIELD SITES
FIELD SITES
Eagle Rock
Alum Rock
PENITENCIA CREEK ROAD
1000'
ENTRANCE TO ALUM ROCK AVENUE
VISITORS CENTER
Horse and hiking trail
Hiking trail
Bicycle trail
Vehicle roads
Penitencia Creek
Profile- mound and spring
Source
50 cm
Frontal spring
Bottom
Site 2
Key
Site of Caldwell group
Sites 2 and 3 of Fischer, Cohen
Colors: w white
g green
f fence, stone
s springs
b bench mark
l light post
t tufa mound
Profile- mound and spring
150 cm
Frontal spring, top portion
Site 3
FIELD SITES

CHAPTER I: PBME LECTURE ABSTRACTS AND REFERENCES

M.O. Andreae: BIOGENIC CONTRIBUTIONS TO THE ATMOSPHERIC SULFUR CYCLE

Biological processes emit sulfur gases at rates comparable to the SO_2 flux from fossil fuel burning (order: 100 x 10^{12} g/yr). H_2S from bacterial sulfate reduction in anoxic environments is responsible for only a minor part of this flux. The ultimate source of most of the biogenic sulfur gases released to the atmosphere is the reduction of sulfate and subsequent biosynthesis of organosulfur compounds by plants and algae in oxic environments. Volatile sulfur compounds can then be released either directly from photosynthetic organisms (e.g., dimethyl sulfide from phytoplankton) or through microbial decomposition processes (e.g., in leaf litter, soils, etc.).

Andreae, M.O. and Barnard, W.R., 1984. The marine chemistry of dimethylsulfide, Mar. Chem., 14:267-279.

Andreae, M.O. and Raemdonck, H., 1983. Dimethylsulfide in the surface ocean and the marine atmosphere: a global view, Science, 221:744-747.

Berresheim, H. and Jaeschke, W., 1983. The contribution of volcanoes to the global atmospheric sulfur budget, J. Geophys. Res., 88:3732-3740.

Bolin, B. and Cook, R.B. (eds.), 1983. *The Major Biogeochemical Cycles and Their Interactions*. SCOPE 24. John Wiley and Sons, Inc., New York.

Bremner, J.M. and Steele, C.G., 1978. Role of microorganisms in the atmospheric sulfur cycle. In *Advances in Microbial Ecology*, (M. Alexander, ed.), Vol. 2, Plenum Press, New York, pp. 155-201.

Ferek, R.J. and Andreae, M.O., 1984. Photochemical production of carbonyl sulfide in marine surface waters, Nature, 307:148-150.

Kadota, H. and Ishida, Y., 1972. Production of volatile sulfur compounds by microorganisms, Ann. Rev. Microbiol., 26:127-138.

Liss, P.S. and Slinn, W.G.N. (eds.), 1983. *Air-Sea Exchange of Gases and Particles*. Reidel, Boston.

Vairavamurthy, A., Andreae, M.O., and Iverson, R.L., 1984. Biosynthesis of dimethylsulfide and dimethylpropiothetin by *Hymenomonas carterae* in relation to sulfur source and salinity variations, Limnol. Oceanog., (in press).

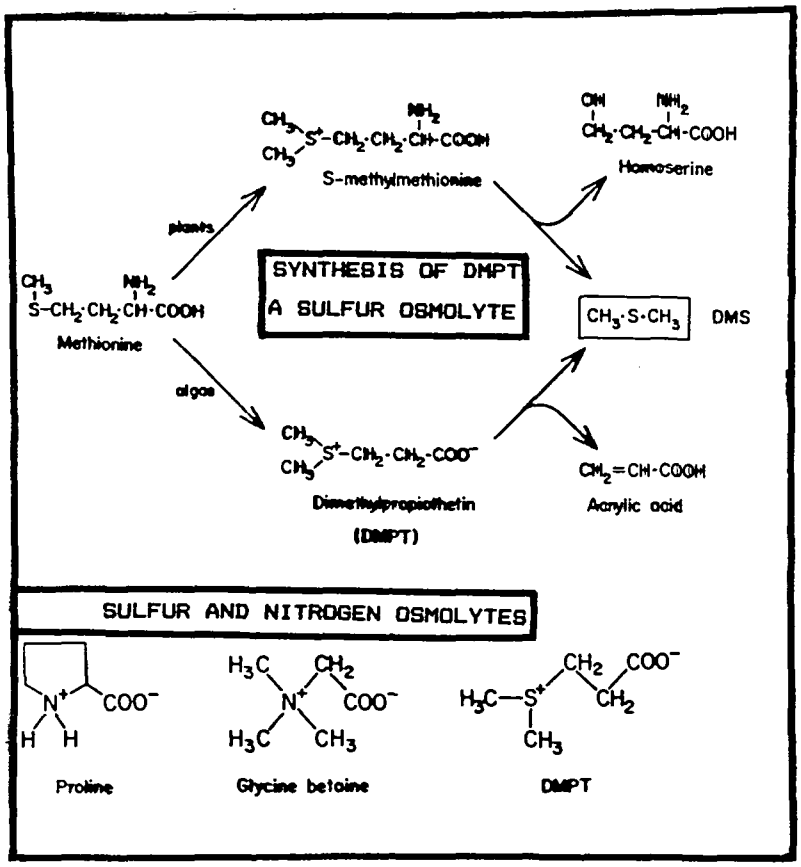

Meinrat O. Andreae

Figure I-1. (Top) Synthesis of DMSP by a marine protist. Sulfur-containing metabolic products that regulate intracellular salt concentration (osmolytes) are sources of atmospheric sulfur gases. This is an example of gas production by a marine haptomonad (synonyms: haptophyte, prymnesiophyte), a coccolithophorid which develops blooms in the ocean. DMPT is known to be **beta-dimethyl sulfoniopropionate (DMSP)**, a less trivial name.

(Bottom) Osmolytes. Nitrogen osmolytes are thought to be more prevalent in terrestrial organisms and sulfur more prevalent in marine organisms where each of these elements is less limiting.

Figure I-2. (Top) The relation between dimethyl sulfide production and the population density of *Phaeocystis poucheti*, (a haptomonad protist). The coefficient of correlation, r, is based on 84 separate measurements and is highly significant.

(Bottom) The linear relation between photosynthetic production and dimethyl sulfide released by laboratory cultures of *Phaeocystis poucheti*.

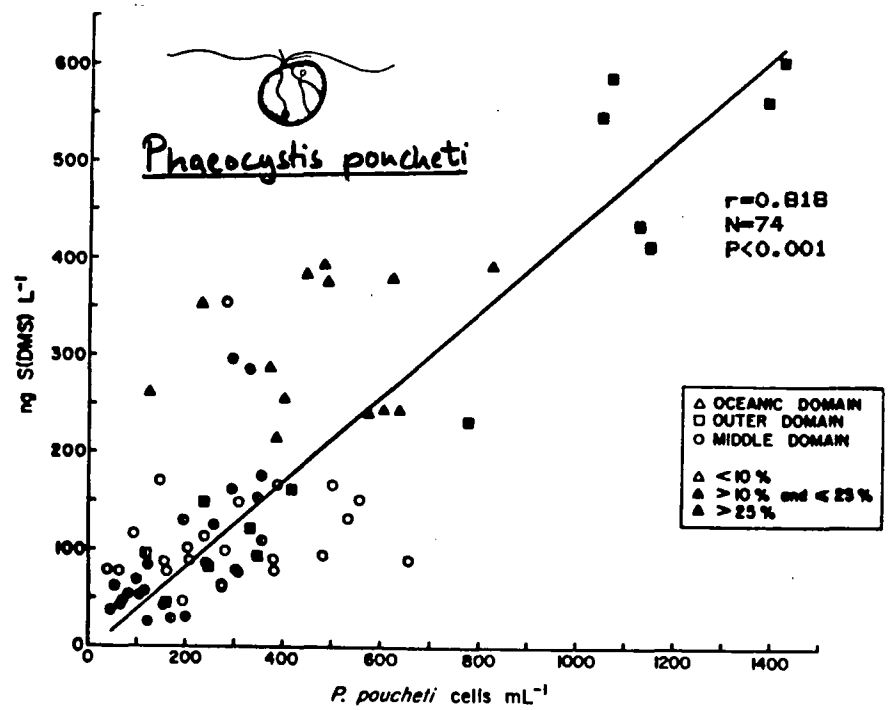

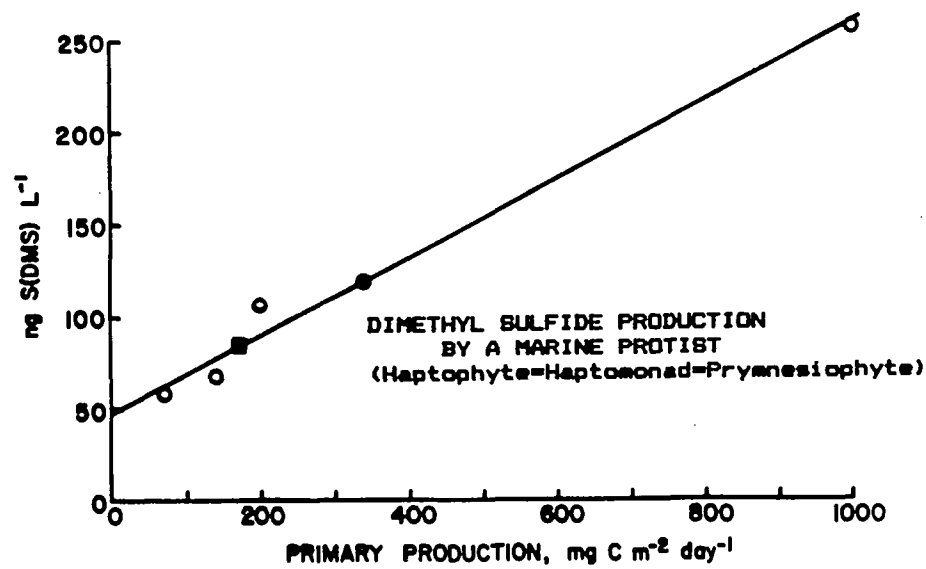

PROCESSES THAT FORM SMALL VOLATILE ATMOSPHERIC SULFUR COMPOUNDS

1) EXCRETION BY LIVE PHYTOPLANKTON: DMS $H_3C-S-CH_3$

Haptomonads such as *Phaeocystis* and *Hymenomonas*

2) EXCRETION BY OTHER MARINE BIOTA OF OTHER SULFUR COMPOUNDS

little known

3) DECOMPOSITION (FERMENTATION AND GROWTH OF BACTERIA)

e.g., cystine:

$$4C_3H_7O_2NS + 6H_2O \longrightarrow 4H_2S + 4NH_3 + 7CO_2 + 5CH_4$$

depending on pathway, many other sulfur compounds may be produced:

CH_3SH, CS_2, polythiols, etc.

4) PULP-MILL TYPE REACTIONS:

terrigenic lignins + sulfide
from dissimilatory sulfate reduction:

CS_2, CH_3SH, COS, DMS, etc.

5) PHOTOCHEMICAL BREAKDOWN OF DMS

O_2 + organic sulfur $\xrightarrow{(light)}$ COS + organic compounds

Meinrat Andreae

Table I-1. Processes that form small volatile atmospheric sulfur compounds include these. There is a paucity of information concerning sulfur trace gas production over the land.

S. Awramik: PRECAMBRIAN EVOLUTION AND THE ROCK RECORD

Precambrian time refers to geological time prior to the first appearance of animals with mineralized hard parts (see Fig I-2.5 for geological time scale). Best estimates for this event are around 570 million years ago. Because the rock record begins some 3,800 million years ago the Precambrian encompasses about 84 percent of geologic time. The fossil record for this immense span of time is dominated by prokaryotes and the sedimentary structures produced by them. The first fossil remains that can confidently be considered eukaryotic are found in 1,000 million year old rocks. The first animals may be as old as 700 million years.

Like life, the Earth has changed through time. An understanding of the interrelationship between the physical evolution of the Earth and its life is one goal of paleontology. During the Archean Eon (3,800 to 2,500 million years ago) solar luminosity was lower than at present yet surface temperatures of the Earth were not unlike those of today. Free atmospheric oxygen was absent, the crust of the Earth was thin, and there were higher geothermal gradients. There existed a preponderance of tectonically short-lived but active marine basins. Around 2,500 million years ago, at the beginning of the Proterozoic Eon, some major changes occurred on the Earth. The crust became thicker and continents emerged above wave base on a larger scale. Intercratonic troughs became common, as did extensive, shallow marine environments with mature, multicycled sediments. Around 2,000 million years ago, significant quantities of free oxygen appeared in the atmosphere and, about 1,500 million years ago, the tectonic style began to change over to a regime that resembled modern plate tectonics with large scale horizontal plate motion. The quantity of oxygen as O_2 increased in the atmosphere though the quantitative details are not known. Extrapolating from the metabolic needs for oxygen by all animals it is inferred that by 700 million years ago, the time the first animals appeared, at least 10 percent of the Earth's present atmospheric level of O_2 was already achieved. No physical or chemical signals have been identified that corelate with the explosion of metazoan evolution at the Precambrian-Cambrian transition.

The oldest fossils are those from the 3,500 million year old Warrawoona Group in Western Australia and the Swaziland Supergroup in South Africa. Organic-walled, micron-sized filaments have been preserved three dimensionally in chert, a cryptocrystalline form of quartz. The chert is laminated and this lamination may have been produced by microbial activity. Stromatolites are organosedimentary structures usually found in the form of laminated rocks. Produced by sediment trapping, binding and/or the precipitation activities of microbial communities, stromatolites are known from both the Warrawoona and the Swaziland rocks. The presence of stromatolites indicates complex microbial activity; presumably photoautotrophic bacteria were involved. The fossilized communities of microbes are of such simple morphology that little can be said about them. The fossil record for the remainder of the Archean Eon is spotty, with only a few

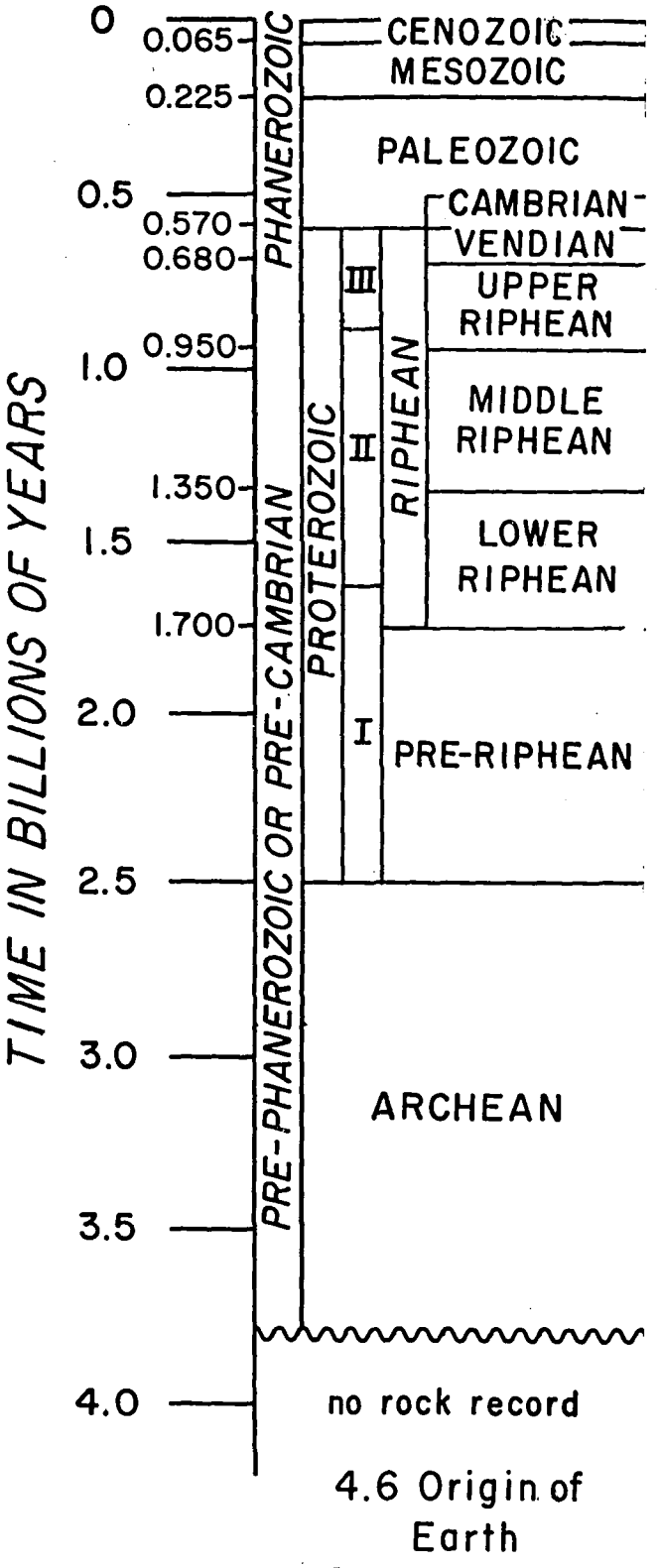

Figure I-2.5. Geological time scale.

good examples of microfossilization. Eventually stromatolites become more noticable in shallow water in tectonically inactive geological environments. By the early Proterozoic, stromatolites become abundant and exhibit diverse and complex morphologies.

A major benchmark in the history of life is recorded by the fossils of the 2,000 million year old Gunflint Iron Formation of Lake Superior, Canada. Well-preserved, abundant and diverse microfossils are found in both stromatolitic and non-stromatolitic cherts. Fossils resembling modern coccoid and filamentous cyanobacteria as well as iron-oxidizing bacteria are common. Bizarre forms of uncertain taxonomic affinity are well represented in the Gunflint. The first plankters are also found in the Gunflint Iron Formation. So, by 2,000 million years ago, stromatolite-building microbes were diverse and plankton had appeared. Generally speaking, early Proterozoic microbes of the Gunflint and other formations were small (less than 10 μm in diameter) and dominated by cyanobacteria-like forms.

Stromatolitic fossil microbes throughout the remainder of the Proterozoic Eon show a tendency towards increased size and morphological complexity. Unlike many modern stromatolites, multitrichomous filaments are very rare. Yet, by the middle and late Proterozoic Eon stromatolitic microbiotas had become surprisingly "modern" in appearance. The diversity of carbonate stromatolites increased markedly during this interval. Stromatolites reached the height of their morphological complexity by about 800 million years ago. Then, from 680 to 570 million years ago, stromatolite diversity sharply decreased. The number of Proterozoic stromatolitic microfossil localities is few, somewhere in excess of 200, but there are thousands of stromatolite localities that do not contain any preserved microfossils.

The first abundant remains of plankton are found around 1,000 million years ago in clastic rocks. These microfossils, which have acid-resistant organic walls, measure from a few to several tens of microns in diameter. Most researchers agree that these microfossils are remains of eukaryotic plankton. Microfossils show an increase in diversity throughout the remainder of the Proterozoic, undergoing some extinctions during the latest Proterozoic (700 to 600 million years ago). Eukaryotic microbes apparently diversified rapidly again in the earliest Cambrian time.

The fossil record of Precambrian life is not representative of all habitats and groups of organisms; there is an obvious bias towards organisms with the greatest preservation potential. Benthic cyanobacteria and cyanobacteria-like microbes within microbial mat habitats had the greatest potential to be preserved. Other prokaryotes are exceptionally rare. Only the form of the microorganism is preserved, and in most cases, this form has been altered by fossilization. Assigning affinities, primarily based on morphological comparisons with modern analogs, involves guesswork. Yet the original reports on the microfossils of the Gunflint delivered 30 years ago by Barghoorn and Tyler were greeted by much skepticism.

Seminal papers did not appear until 1965. The fossil record of the first 84 percent of Earth history is just beginning to become understood and has not come close to reaching its full potential.

Awramik, S.M., 1982. The origins and early evolution of life. In *The Cambridge Encyclopedia of Earth Sciences*. (D.G. Smith, ed.), Cambridge University Press, Cambridge, pp. 349-362.

Awramik, S.M., 1984. Ancient stromatolites and microbial mats. In *Microbial Mats: Stromatolites*. (Y. Cohen, R.W. Castenholz and H.O. Halvorson, eds.), Alan R. Liss, New York, pp. 1-22.

Awramik, S.M., Schopf, J.W., and Walter, M.R., 1983. Filamentous fossil bacteria from the Archean of Western Australia, Precambrian Research, 20:357-374.

Barghoorn, E.S. and Tyler, S.A., 1965. Microorganisms from the Gunflint chert, Science, 147:563-577.

Cloud, P., 1976. Major features of crustal evolution, Geol. Soc. S. Africa, Annexure to 79:1-32.

Glaessner, M.F., 1984. *The Dawn of Animal Life*. Cambridge University Press, Cambridge, 244 p.

Goodwin, A.M., 1981. Precambrian perspectives, Science, 213:55-61.

Knoll, A.H. and Awramik, S.M., 1983. Ancient microbial ecosystems. In *Microbial Geochemistry*. (W. Krumbein, ed.), Blackwell and Sons, Oxford, pp. 287-315.

Schopf, J.W., 1975. Precambrian paleobiology: problems and perspectives, Ann. Rev. Earth Planet. Sci., 3:213-249.

Schopf, J.W.,(ed.), 1983. *Earth's Earliest Biosphere*. Princeton University Press, Princeton, 543 pp.

Walter, M.R., (ed.), 1976. *Stromatolites*. Elsevier, Amsterdam, 790 pp.

Windley, B.F., 1977. *The Evolving Continents*. John Wiley and Sons, New York, 385 pp.

D. Caldwell: AEROBIC SULFUR-OXIDIZING BACTERIA: ENVIRONMENTAL SELECTION AND DIVERSIFICATION

Sulfur-oxidizing bacteria oxidize reduced inorganic compounds to sulfuric acid. In the case of lithotrophic sulfur oxidizers, the energy obtained from oxidation is used for microbial growth. Heterotrophic sulfur oxidizers obtain energy from the oxidation of organic compounds. In sulfur-oxidizing mixotrophs energy may be derived either from the oxidation of inorganic or organic compounds. Sulfur-oxidizing bacteria are usually located within the sulfide/oxygen interfaces of springs, sediments, soil microenvironments, and the hypolimnion. Colonization of the interface is necessary since sulfide auto-oxidizes and because both oxygen and sulfide are needed for growth. The environmental stresses associated with the colonization of these interfaces have resulted in the evolution of morphologically diverse and unique aerobic sulfur oxidizers.

Most sulfur-oxidizing bacteria are sulfur-oxidizing heterotrophs and chemolithoheterotrophs. Variations amongst members of these groups is poorly described partly because of the preoccupation of microbiologists with the morphological and physiological diversity of sulfur autotrophs. However, further studies of heterotrophic sulfur oxidation will be necessary to understand the global sulfur cycle. In the sulfur spring environment there are two groups of sulfur oxidizers: acidophilic and non-acidophilic. Acidophilic communities frequently result when growth rate exceeds dilution. Metabolic wastes, primarily sulfuric acid, accumulate. When the dilution rate exceeds the growth rate, attachment is required to avoid the loss of populations, and sulfuric acid does not accumulate. In sulfur springs the sulfur oxidizing bacteria position themselves within the sulfide/oxygen interface by attaching preferentially to pyrite which is located upstream on the reducing side of the spring. They form streamers, bundles of trichomes (filaments) which extend downstream and into the interface when the organisms are oxygen-limited. Extremely thermophilic sulfur oxidizers from geothermal environments grow at greater rates to higher cell yields than analogous mesophiles. This suggests that the optimum temperature for aerobic sulfur oxidizers exceeds 70°C. The sulfide/oxygen interfaces of hypolimnia are frequently dominated by photosynthetic sulfur bacteria which exclude aerobic sulfur oxidizers. Sulfur-oxidizing bacteria found in sediment environments often migrate diurnally in response to shifting gradients of oxygen and sulfide. This results in the migration of oxidizing equivalents, in the form of elemental sulfur, within the sediment.

Brierley, C.L. and Brierley, J.A., 1982. Anaerobic reduction of molybdenum by *Sulfolobus* species, Zbl. Bakt. Hyg., I. Abt. Orig. C., 3:289-294.

Caldwell, D.E., Kieft, T.L., and Brannan, D.K., 1984. Colonization of sulfide-oxygen interfaces on hot spring tufa by *Thermothrix thiopara*, Geomicrobiol. J., 3:181-200.

Kuenen, J.G. and Veldkamp, H., 1972. *Thiomicrospira pelophila*, gen.n., sp.n., a new obligately chemolithotrophic colourless sulfur bacterium, Antonie van Leeuwenhoek J. Microbiol., 38:241-256.

Nelson, D.C., and Castenholz, R.W., 1982. Light responses of *Beggiatoa*, Arch. Microbiol., 131:146-155.

Starkey, R.L., 1966. Oxidation and reduction of sulfur compounds in soils, Soil Sci., 101:297-306.

S. Chang: ORIGIN OF LIFE

The pathways of organic chemical synthesis, that is of chemical evolution on the early Earth leading to life must have been constrained by the development of the planet by accretion and core formation. No doubt the accretion and differentiation into the core-mantle-crust-atmosphere system strongly influenced the temperature and composition of the atmosphere, surface, and interior; but large gaps persist in our understanding of these processes. We do not know the time-span over which Earth aquired its volatiles, the composition of these volatiles, and the conditions under which outgassing of volatiles occurred to form the atmosphere. Uncertainties in existing models for Earth accretion and early planetary development allow a wide range of possible prebiotic atmospheric compositions at the time and temperature when liquid water appeared and thermally-labile organic compounds could survive. These compositions range from strongly reducing atmospheres (dominated by high abundances of H_2, CO, and CH_4) to mildly reducing ones (containing mostly N_2 with minor to trace amounts of CO_2 and H_2).

Synthesis of organic matter occurs readily in strongly reducing atmospheres as laboratory experiments indicate. Organic chemical syntheses in mildly or non-reducing atmospheres merit much more study. The conversion of N_2 to nitrogen-containing organic compounds in any prebiotic atmosphere by atmospheric photochemical processes must have been limited; production of nitrate by electrical discharges may have been more effective. Prebiotic organic syntheses need not have occurred only in the atmosphere; they could have occurred on land, in the seas, and at a variety of atmosphere, sea, and land interfaces. The involvement of inorganic matter in the origin of life was probably a natural consequence of the geological context within which atmospheric and chemical evolution occurred. Metal ions and minerals, particularly clays, may have served as reactants, catalysts, and even templates for prebiotic organic synthesis.

Considerable success has been achieved in producing the monomeric and oligomeric building blocks of proteins and nucleic acids under putative prebiotic conditions. But the connections between the model environmental conditions and the geologic and meteorologic realities of the prebiotic Earth remain to be established. Until constraints can be imposed on the range of possible prebiotic atmospheric compositions and surface environments, and in the absence of direct evidence of organic chemical evolution on the Archean earth, it is important to explore and assess pathways for organic synthesis in all model environments that are consistent with evidence unveiled in the cosmochemical, geological, and biological records.

Bunch, T.E. and Chang, S., 1980. Carbonaceous chondrites II. Carbonaceous chondrite phyllosilicates and light element geochemistry as indicators of parent body processes and surface conditions, Geochim. Cosmochim. Acta, 44:1543-1577.

Chang, S., 1982. Prebiotic organic matter: possible pathways for synthesis in a geological context, Physics of the Earth and Planetary Interiors, 29:261-280.

Chang, S. and Bunch, T.E., 1985. Clays and organic matter in carbonaceous meteorites: clues to early solar system history and primitive planetary environments. In *Clays and the Origin of Life*. (H. Hartman, A.G. Cairns-Smith and A. Weiss, eds.), Cambridge University Press, Cambridge, (in press).

Chang, S., Des Marais, D., Mack, R., Miller, S.L. and Strathearn, G.E., 1983. Prebiotic organic syntheses and the origin of life. In *Earth's Earliest Biosphere*. (J.W. Schopf, ed.), Princeton University Press, Princeton, 543 pp.

CARBON, HYDROGEN AND NITROGEN ISOTOPE FRACTIONATION VALUES IN ORGANIC MATTER FROM METEORITES AND EARTH SAMPLES

Summary of the range of values [a]

Organic Fraction	^{13}C per mil	D per mil	^{15}N per mil
Soluble compounds in some carbonaceous chondrites	+5 to +40	+100 to +500	+50 to +100
Insoluble compounds in some carbonaceous chondrites	-13 to -21	+600 to +2500	+10 to +150
All natural organic matter on Earth	-90 to -10	-250 to +80	-10 to +25

[a] Delta values are defined in per mil units as follows, as for example in the case of carbon:

$$\delta^{13}C = \left[\frac{\left(^{13}C/^{12}C\right)_{sample}}{\left(^{13}C/^{12}C\right)_{standard}} - 1 \right] \times 1000$$

The standards for C, H and N, respectively, are Peedee Belemnite limestone, mean ocean water and air.

Table I-2. Carbon, hydrogen and nitrogen isotopic fractionation values in organic matter from meteorites and Earth samples. The fractionation values for carbon 13, deuterium (D) and nitrogen 15 are calculated analogously to the example given for carbon below **Table I-3.**

CARBON COMPOUNDS *in the* MURCHISON METEORITE

	relative quantity by weight
Carbonate/CO_2	0.2 to 0.4%
Acid Insoluble "Polymer"	1.2 to 1.6%
Dicarboxylic Acids	200 - 400 ppm
Monocarboxylic Acids	~100 ppm
Hydrocarbons	40 - 70 ppm
Amino Acids	~20 ppm
Ketones & Aldehydes	~5 ppm
Alcohols	~5 ppm
Amines	~5 ppm
All Others	$\leq$ 1 ppm

SUMMARY: 1.44 - 2.07 per cent
BULK CARBON: 2.1 - 2.4 per cent

Table I-3. **Carbon compounds in the Murchison Meteorite.** The Murchison meteorite, a carbonaceous chondrite that landed in Murchison, Australia in 1969, was found to contain an abundance and variety of extraterrestrial organic matter.

Y. Cohen: PROTOCYANOBACTERIA: OXYGENIC AND ANOXYGENIC PHOTOSYNTHESIS IN MAT-FORMING BACTERIA

The oldest record of life, preserved in prePhanerozoic stromatolites dated 3500 million years old, is most likely of filamentous mat-forming cyanobacteria. The sedimentary records of cyanobacterial mats in stromatolites are the most abundant record of life throughout the prePhanerozoic. Stromatolites persisted into the Phanerozoic Eon, yet they become much less pronounced relative to earlier ones. The abundance and persistence of cyanobacterial mats throughout most of geological time point to the evolutionary success of these kinds of microbial communities and their possible role in the evolution of the earth and atmosphere.

Recent cyanobacterial mats are restricted to hypersaline environments, sulfur springs, and alkaline lakes where the grazing organisms are excluded or their populations drastically reduced. Solar Lake cyanobacterial mats serve as good models for the study of the physiology of recent mat-forming cyanobacteria.

Facultative anoxygenic photosynthesis utilizing H_2S as an alternative electron donor for PS I (photosystem I)-dependent photosynthesis was described for *Oscillatoria limnetica* isolated from Solar Lake. Other PS I-dependent characteristics of this cyanobacterium include the use of H_2 as an electron donor alternatively to H_2S, H_2 production from H_2S under CO_2 limitation, sulfide-dependent N_2 fixation, and anaerobic respiration with elemental sulfur as the electron acceptor. These PS I characteristics are found also in other mat-forming cyanobacteria.

While PS II of *Oscillatoria limnetica* is fully inhibited at sulfide concentrations as low as 10 uM, other mat-forming cyanobacteria can operate oxygenically even under 5 mM H_2S. *Microcoleus chthonoplastes*, a cosmopolitan mat-forming cyanobacterium, as well as several isolates from sulfur springs, have a different PS II which is significantly more resistant to H_2S toxicity than planktonic cyanobacteria, algae, and plants. Several isolates carry out exclusively oxygenic photosynthesis under high sulfide concentrations, while others operate oxygenic photosynthesis in concert with anoxygenic photosynthesis. Recently Fe^{++} ions were found to serve as a sole electron donor to PS II in several benthic cyanobacteria under anaerobic reduced conditions. Fe^{++}-dependent CO_2 photoassimilation is DCMU-sensitive. However, about 20 percent of the Fe^{++}-dependent carbon dioxide photoassimilation is carried out in the presence of 5 um DCMU. This indicates that there may be two different sites of Fe^{++}-dependent CO_2 photoassimilation, one at PS II which is sensitive to DCMU and another at PS I.

^{13}C values for organic matter in the Solar Lake mats were found to range between -6 and -8 per mil and thus represent the heaviest values for organic matter recorded. Preliminary observations point to the fact that the ribulose bisphosphate carboxylase system in several mat-forming cyanobacteria is different from other cyanobacteria.

The differences in PS I, PS II, and possibly the ribulose bisphosphate carboxylase in mat cyanobacteria may point to the antiquity of this group among cyanobacteria. Mat-forming "protocyanobacteria" may well represent the prePhanerozoic forms responsible for Archean stromatolites and possibly for the Banded Iron Formations (BIF's). Fe^{++}-dependent carbon dioxide photoassimilation by cyanobacteria may be related to the deposition of BIFs in the absence of free oxygen.

Note: The compound DCMU, 3-(3,4) dichlorophenyl -1,1 dimethyl urea, is a selective inhibitor of photosystem II, i.e., of the oxgen process in photosynthesis.

Cohen, Y., 1984. Oxygenic photosynthesis, anoxygenic photosynthesis and sulfate reduction in cyanobacterial mats. In *Current Perspectives in Microbial Ecology*, (M.J. Klug and C.A. Reddy, eds.), A.S.M., Washington, pp. 435-442.

Cohen, Y., Castenholz, R.W., and Halvorson, H.O. (eds.), 1984. *Microbial Mats: Stromatolites*, Alan R. Liss, New York, 492 pp.

Padan, E. and Cohen, Y., 1982. Anoxygenic photosynthesis. In *The Biology of Cyanobacteria*. (M.C. Carr and B.A. Whitton, eds.), Blackwell Scientific Press, Oxford, pp. 215-235.

Y. Cohen: SULFUR TRANSFORMATIONS AT THE HYDROGEN SULFIDE/OXYGEN INTERFACE IN STRATIFIED WATERS AND IN CYANOBACTERIAL MATS

Stratified water bodies allow the development of several microbial plates along the water column. The microbial plates develop in relation to nutrient availability, light penetration, and the distribution of oxygen and sulfide. Sulfide is initially produced in the sediment by sulfate-reducing bacteria. It diffuses along the water column creating a zone of hydrogen sulfide/oxygen interface. In the chemocline of Solar Lake (Sinai) oxygen and sulfide coexist in a 0-10 cm layer that moves up and down during a diurnal cycle. The microbial plate at the chemocline is exposed to oxygen and hydrogen sulfide, alternating on a diurnal basis. The cyanobacteria occupying the interface switch from anoxygenic photosynthesis in the morning to oxygenic photosynthesis during the rest of the day. This activity results in a temporal build up of elemental sulfur during the day which disappears at night due to both oxidation to thiosulfate and sulfate by thiobacilli, and reduction to hydrogen sulfide by *Desulfuromonas* sp. and anaerobically respiring cyanobacteria.

High dark CO_2 fixation, which can be stimulated by sulfide, elemental sulfur, and thiosulfate in the presence of oxygen or nitrate, is found in the chemocline. Over 90 percent of the primary production in the stratified Solar Lake occurs under sulfide conditions because of the activities of several cyanobacteria, plates of *Chromatium* sp., and *Prosthecochloris* sp.. These sulfur bacteria exist above the major cyanobacterial plate of *Oscillatoria limnetica* which is found at the deepest part of the hypolimnion. The relative contribution of anoxygenic photosynthesis to overall primary productivity is a function of light penetration to the hydrogen sulfide/oxygen interface layer. When only 1 percent of surface light reaches this layer, anoxygenic photosynthesis accounts for about 5 percent of the overall primary productivity whereas if 20 percent of the surface light reaches the chemocline (the case in Solar Lake), anoxygenic photosynthesis accounts for more than 90 percent of the photosynthetic carbon dioxide assimilation.

The study of the hydrogen sulfide/oxygen interface in sediments requires the use of microelectrodes for pO_2, pH, pS^{2-}, pH_2, and pCO_2. These electrodes, now used in several laboratories, were introduced to microbial ecology by N.P. Revsbech of Aarhus University in Denmark. Sharp gradients of all measured parameters are observed in microscale (the top 1-10 mm of the sediment column). These result from intense microbial activities in this thin photic zone.

Diurnal fluctuations at the hydrogen sulfide/oxygen interface in sediment are much more pronounced than those of stratified water bodies, since the established gradients in sediment are very steep and diffusion in these dimensions is very fast. Because of this close

proximity, the diurnal fluctuations expose cyanobacteria to sulfide at night and sulfate-reducing bacteria to high concentrations of oxygen during the day.

The cyanobacteria cope with exposure to sulfide either by carrying out facultative anoxygenic photosynthesis or by performing oxygenic photosynthesis in the presence of sulfide. When pH_2 electrodes were introduced to the Pmax zone, a transient peak of H_2 was observed upon turning on the light, possibly indicating photolysis of water by cyanobacteria under these conditions. *Oscillatoria limnetica* were shown to produce H_2 in a CO_2-limited environment under both aerobic and anaerobic conditions.

Sulfate reduction was found to be enhanced in the light at the surface of the cyanobacterial mats. Microsulfate reduction measurements showed enhanced activity of sulfate reduction even under high oxygen concentrations of 300-800 μM. Apparent aerobic SO_4 reduction activity can be explained by the co-occurence of H_2. The physiology of this apparent sulfate reduction activity is currently being studied.

Cohen, Y., 1984. The Solar Lake cyanobacterial mats: Stategies of photosynthetic life under sulfide. In *Microbial Mats: Stromatolites*. (Y. Cohen, R.W. Castenholz, and H.O. Halvorson eds.), Alan R. Liss, New York, pp. 133-148.

Cohen, Y., 1984. Microtechnique for in situ sulfate reduction measurement in proximity to oxygen, Arch. Microbiol., (in press).

Cohen, Y., 1984. Sulfate reduction under oxygen in cyanobacterial mats and its coupling to primary production, Limnol. Oceanog., (in press).

Cohen, Y., Aizenstat, Z., Stoler, A., and Jørgensen, B.B., 1980. Microbial geochemistry of Solar Lake Sinai. In *Biogeochemistry of Ancient and Modern Environments*. (P.A. Trudinger and M.R. Walter, eds.), Australian Academy of Science, Canberra, pp. 167-177.

Cohen, Y. and Gack, E., 1984. Fe^{++} dependent photosynthesis in cyanobacteria, Nature, (in press).

Cohen, Y., Padan, E., and Shilo, M., 1975a. Facultative anoxygenic photosynthesis in the cyanobacterium *Oscillatoria limnetica*, J. Bacteriol., 12:855-861.

Cohen, Y., Jørgensen, B.B., Padan, E., and Shilo, M., 1975b. Sulphide-dependent anoxygenic photosynthesis in the cyanobacterium *Oscillatoria limnetica*, Nature, 257:489-491.

Cohen, Y., Goldberg, M., Krumbein, W.E., and Shilo, M., 1977a. Solar Lake (Sinai). 1. Physical and chemical limnology, Limnol. Oceanog., 22:597-607.

Cohen, Y., Krumbein, W.E., and Shilo, M., 1977b. Solar Lake (Sinai). 2. Distribution of photosynthetic microorganisms and primary production, Limnol. Oceanog., 22:609-610.

Jørgensen, B.B., Revsbech, N.P., and Cohen, Y., 1983. Photosynthesis and structure of benthic microbial mats: Microelectrode and SEM studies of four cyanobacterial communities, Limnol. Oceanog., 28:1075-1093.

Jørgensen, B.B., Revsbech, N.P., Blackburn, T.H., and Cohen, Y., 1979. Diurnal cycle of oxygen and sulfide microgradients and microbial photosynthesis in a cyanobacterial mat sediment, Appl. Environ. Microbiol., 38:46-58.

Oren, A., Padan, E., and Malkin, S., 1979. Sulfide inhibition of photosystem II in cyanobacteria (blue green algae) and tobacco chloroplasts, Biochem. Biophys. Acta, 546:270-279.

Oren, A. and Shilo, M., 1979. Anaerobic heterotrophic dark metabolism in the cyanobacterium *Oscillatoria limnetica*: sulfur respiration and lactate fermentation, Arch. Microbiol., 122:77-84.

Padan, E. and Cohen, Y., 1982. Anoxygenic photosynthesis. In *The Biology of Cyanobacteria*, (M.C. Carr and B.A. Whitton, eds.), Blackwell Scientific, Oxford, pp. 215-235.

Revsbech, N.P., Jørgensen, B.B., Blackburn, T.H., and Cohen, Y., 1983. Microelectrode studies of the photosynthetic and O_2, H_2S and pH profiles of a microbial mat, Limnol. Oceanog., 28:1062-1074.

Skyring, F.W., 1984. Sulfate reduction in marine sediments associated with cyanobacterial mats, Australia. In *Microbial Mats: Stromatolites*, (Y. Cohen, R.W. Castenholz, and H.O. Halvorson eds.), Alan R. Liss, New York, pp. 265-276.

D. Des Marais: CARBON ISOTOPE GEOCHEMISTRY AND GEOBIOLOGY

The Earth's carbon cycle involves crustal reservoirs that include atmospheric CO_2, oceanic inorganic and organic carbon, carbon in sedimentary organic matter such as that in shales, sedimentary carbonate, and igneous rocks. There also seems to be a relatively low but nontrivial rate of exchange between the carbon reservoir in the Earth's mantle and crustal carbon.

Certain processes moving carbon between these reservoirs are isotopically selective. Photosynthetic carbon fixation produces organic matter which can be between 0.3 and 3 percent depleted in ^{13}C relative to sources of inorganic carbon (Degens, 1969; Deines, 1980). This preference for ^{12}C is principally due to catalysis in the first step of carbon dioxide fixation (e.g., the Calvin cycle enzyme ribulose bisphosphate carboxylase; Estep, 1978). The amount of fractionation is often attenuated by processes which transport inorganic carbon to cellular cytoplasm (e.g., O'Leary, 1981). The respiration of organic carbon is also associated with a discrimination against ^{13}C. The carbon dioxide produced is typically depleted between 0 and 1.2 percent in ^{13}C relative to the organic carbon source (De Niro, 1977; Kaplan and Rittenberg, 1964).

The organic carbon buried in sediments can be isotopically fractionated by sulfate reduction (Fuchs, 1979). Work in our laboratory has shown that even fermentation can produce striking discrimination against the ^{13}C isotope.

More deeply buried organic carbon becomes progressively more reduced by thermal decomposition. If this carbon is heated to several hundred degrees Celsius, it can be converted to graphite. The ^{13}C content of this residual organic matter changes very little until its elemental carbon to hydrogen ratio falls below 0.2 (Schopf, 1983). Below 0.2 the residual carbon becomes more ^{13}C-enriched. Because the ^{13}C value of sedimentary carbon is so well preserved, we are assured that the ^{13}C values in the better preserved sedimentary rocks as old as 3.5 billion years reflect ancient microbial processes.

Carbon issuing from the midocean ridges is about 0.5 percent depleted in ^{13}C relative to marine carbonates, and about 2 percent enriched in ^{13}C relative to sedimentary organic carbon (Des Marais and Moore, 1984). This midocean ridge carbon represents the largest single carbon flux from the mantle, and its isotopic composition is the same as the average of all the crustal reservoirs. The crust/mantle exchange of carbon was more intense during the early Precambrian Eon and, very likely, the crust had a larger carbon inventory then than now (see Des Marais' article in Sundquist and Broeker, 1984).

Carbon isotope fractionation values have been used to understand the history of the biosphere. For example, plankton analyses confirmed that marine extinctions at the end of the Cretaceous period were indeed severe (see Hsu's article in Sundquist and Broeker, 1984). Variations in the isotopic compositions of carbonates and evaporitic sulfates during the Paleozoic might reflect the relative abundances of euxinic (anoxic) marine environments and organic deposits from terrestrial flora (Berner and Raiswell, 1983). The carbon isotopic composition of Precambrian sediments suggest that the enzyme ribulose bisphosphate carboxylase has existed for perhaps 3.5 billion years (Schopf, 1983). Future work in our laboratory seeks to elucidate the relationship between the carbon isotopic composition of stromatolites, atmospheric CO_2, and oxygen inventories.

Abelson, P.H. and Hoering, T.C., 1961. Carbon isotope fractionation in formation of amino acids by photosynthetic organisms, Proc. Nat. Acad. Sci., 47:623-632.

Berner, R.A. and Raiswell, R., 1983. Burial of organic carbon and pyrite sulfur in sediments over Phanerozoic time: a new theory, Geochim. Cosmochim. Acta, 47:855-862.

Degens, E.T., 1969. Biogeochemistry of stable carbon isotopes. In *Organic Geochemistry*. (G. Eglinton and M.T.J. Murphy, eds.), Springer-Verlag, New York, pp. 304-329.

Deines, P., 1980. The isotopic composition of reduced organic carbon. In *Handbook of Environmental Isotope Geochemistry*, (P. Fritz and J.C. Fontes, eds.), Elsevier, New York, pp. 329-406.

De Niro, M.J., 1977. I. Carbon isotope distribution in food chains, Ph.D. thesis, California Institute of Technology.

Des Marais, D.J., Mitchell, J.M., Hayes, J.M., and Meinschein, W.G., 1980. The carbon isotope biogeochemistry of the individual hydrocarbons in bat guano and the ecology of insectivorous bats in the region of Carlsbad, New Mexico, Geochim. Cosmochim. Acta, 44:2075-2086.

Des Marais, D.J. and Moore, J.G., 1984. Carbon and its isotopes in midoceanic basaltic glasses, Earth and Planetary Science Letters, (in press).

Estep, M.F., Tabita, R., Parker, P.L., and Van Baalen, C., 1978. Carbon isotope frationation by ribulose-1, 5-bisphosphate carboxylase from various organisms, Plant Physiol., 61:680-687.

Fuchs, G., Thauer, R., Ziegler, H., and Stichler, W., 1979. Carbon isotope fractionation by *Methanobacterium thermoautotrophicum*, Arch. Microbiol., 120:135-139.

Hoefs J., 1980. *Stable Isotope Geochemistry*, Springer-Verlag, New York, 208 pp.

Kaplan, I.R. and Rittenberg, S.C., 1964. Carbon isotope fractionation during metabolism of lactate by *Desulfovibrio desulfuricans*, J. Gen. Microbiol., 34:213-217.

Melander, L. and Saunders, W.H. Jr., 1980. *Reaction Rates of Isotopic Molecules*, John Wiley and Sons, New York, 331 pp.

O'Leary, M.H., 1981. Carbon isotope fractionation in plants, Phytochem., 20:553-567.

Schopf, J.W., (ed.), 1983. *The Earth's Earliest Biosphere--Its Origins and Evolution*, Princeton University Press, Princeton, 543 pp.

Sundquist, E.T. and Broecker, W.S., 1984. *Proceedings of the Chapman Conference on Natural Variations in Carbon Dioxide and the Carbon Cycle*, American Geophysical Union Monograph, (in press).

Figure I-3. Metabolic carbon isotope values for classes of biological compounds as determined by mass spectrometry.

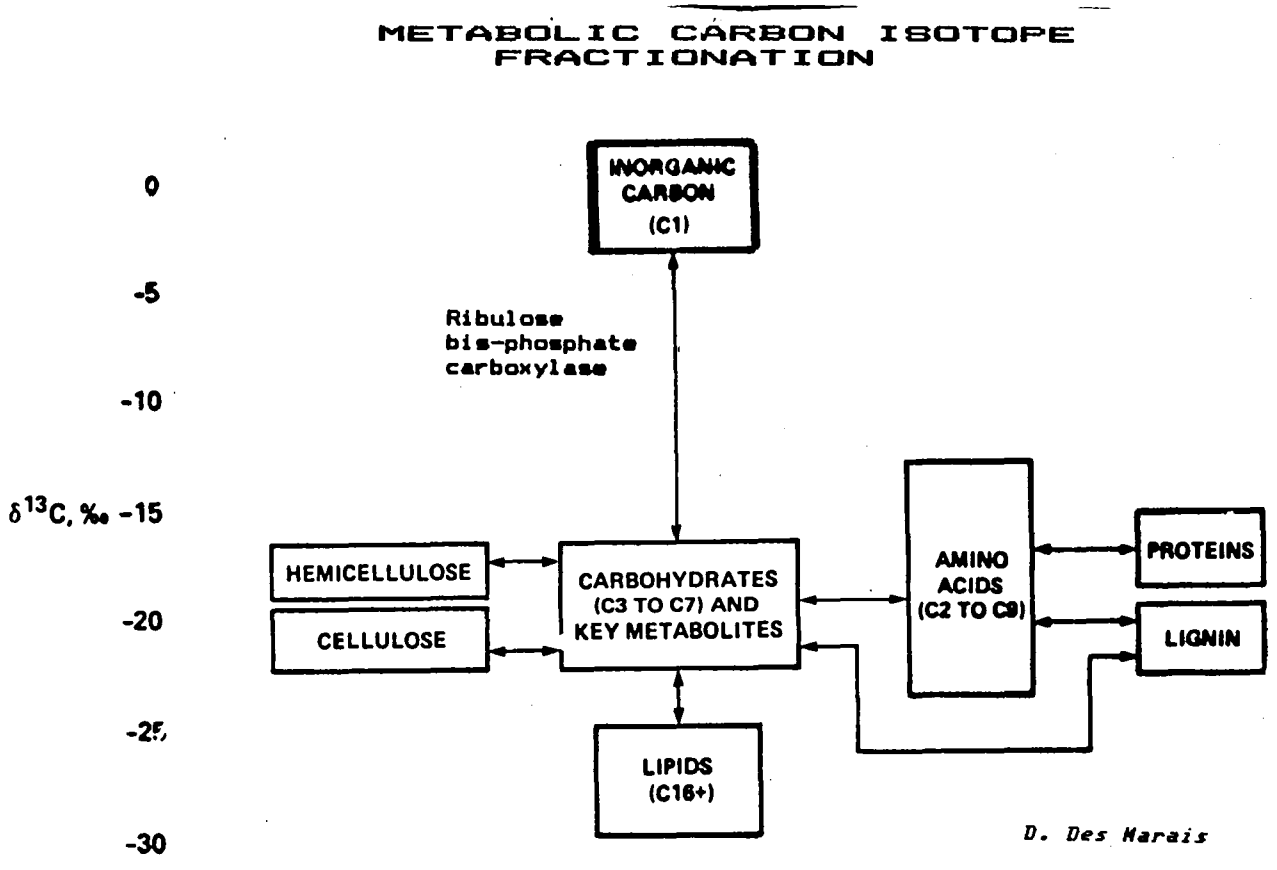

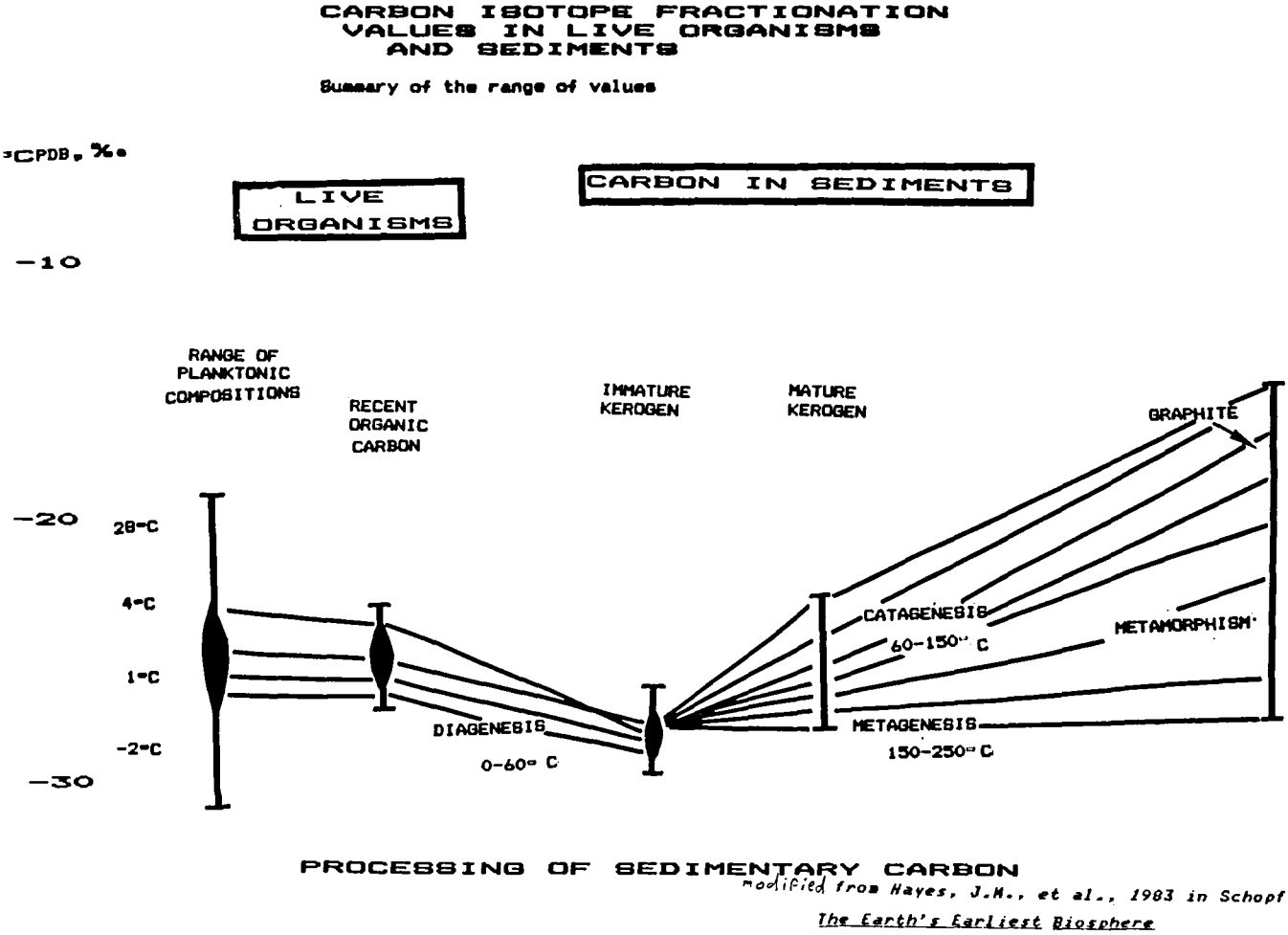

Figure I-4. Carbon isotope fractionation values in live organisms and sediments. The ^{13}C values are a function of temperature in live marine organisms, and these values are altered by temperature alteration in sediments.

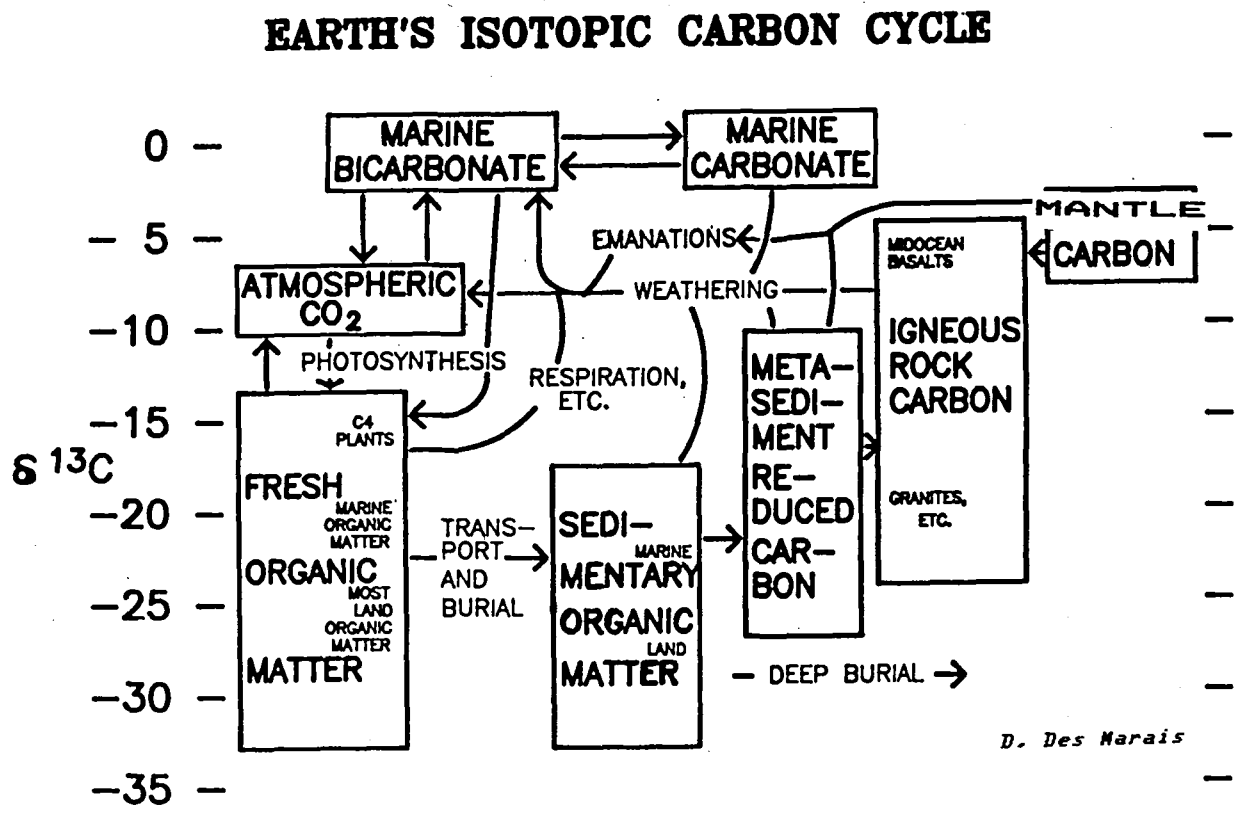

Figure I-5. Carbon isotopic fractionation ranges for extant carbon samples from terrestrial sources. Delta ^{13}C scale at left, boxes represent major reservoirs, arrows represent major processes that transport and convert the carbon between the reservoirs.

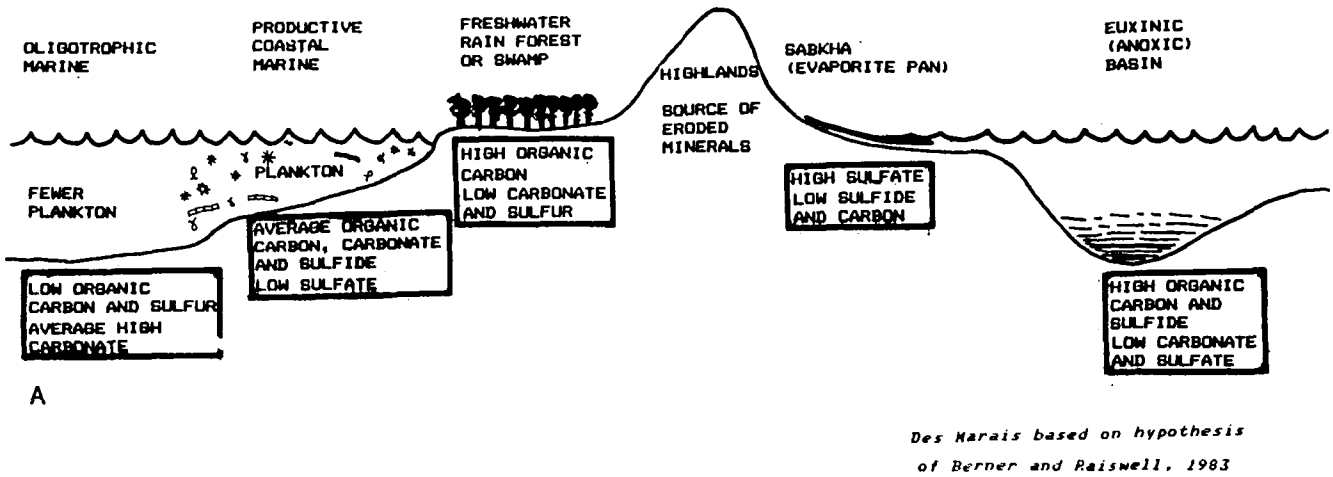

Figure I-6. Reconstruction of the extent of depositional environments based on carbon and sulfur isotope fractionation measurements from ancient sedimentary rocks.

A. Major extant environments where sulfur and carbon compounds are sedimented indicating the relative distribution now.

B. Environmental reconstruction of the Cambrian Period based on interpretations of carbon and sulfur isotope data.

C. Environmental reconstruction of the Permian Period based on interpretations of carbon and sulfur isotope data.

CAMBRIAN TIME 540 MILLION YEARS AGO

Sulfates with high delta S34

Carbonates with low delta C13

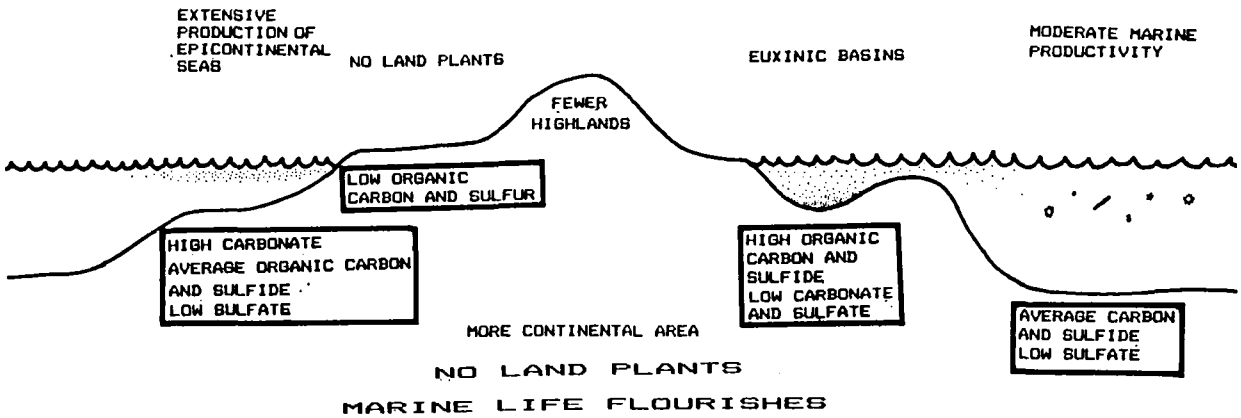

B

PERMIAN TIME 190 MILLION YEARS AGO

Sulfates with low S34

Carbonates with high delta C13

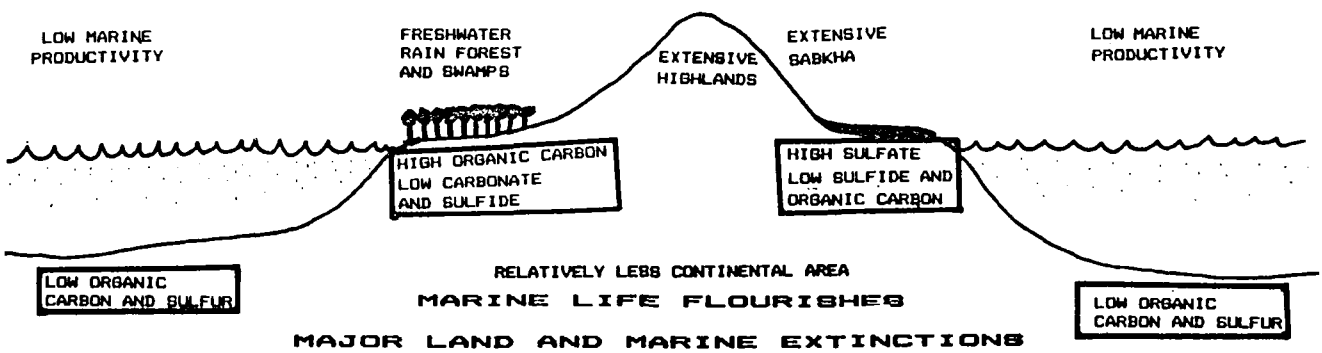

C

Des Marais based on hypothesis of Berner and Raiswell. 1983

R.C. Fahey: DISTRIBUTION AND ABUNDANCE OF ORGANIC THIOLS

The role of glutathione (GSH) in protecting against the toxicity of oxygen and oxygen byproducts is well established for all eukaryotes studied except *Entamoeba histolytica* which lacks mitochondria, chloroplasts, and microtubules. GSH is not universal among prokaryotes. *Entamoeba histolytica* does not produce GSH or key enzymes of GSH metabolism (Fahey, 1984). A general method of thiol analysis based upon fluorescent labeling with monobromobimane and HPLC separation of the resulting thiol derivatives was developed in order to determine the occurrence of GSH and other low molecular weight thiols in bacteria. Glutathione is the major thiol in cyanobacteria and in most bacteria closely related to the purple photosynthetic bacteria, but GSH was not found in archaebacteria, green bacteria, or Gram positive bacteria. This suggests that glutathione metabolism may have been incorporated into eukaryotes at the time that mitochondria and chloroplasts were acquired by endosymbiosis. In Gram positive aerobes, bacteria not thought to be ancestral to eukaryotic organelles, coenzyme A occurs at millimolar levels and CoA disulfide reductases have been identified. CoA, rather than glutathione, may function in the oxygen detoxification processes of these organisms.

Fahey, R.C., Brown, W.C., Adams, W.B., and Worsham, M.B., 1978. Occurrence of glutathione in bacteria. J. Bacteriol., 133:1126-1129.

Fahey, R.C., Dorian, R., Newton, G.L., and Utley, J., 1983. Determination of intracellular thiol levels using bromobimane fluorescent labeling: Applications involving radioprotective drugs. In *Radioprotectors and Anticarcinogens*, (O.F. Nygaard and M.G. Simic, eds.), Academic Press, New York, pp. 103-120.

Fahey, R.C., and Newton, G.L., 1983. Occurrence of low molecular weight thiols in biological systems. In *Functions of Glutathione: Biochemical, Physiological, Toxicological, and Clinical Aspects* (A. Larsson *et al*, eds.), Raven Press, New York, pp. 251-260.

Fahey, R.C., Newton, G.L., Arrick, B., Overdank-Bogart, T., and Aley, S.B., 1984. *Entamoeba histolytica*: A eukaryote without glutathione metabolism, Science, 224:70-72.

Meister, A., and Anderson, M.E., 1983. Glutathione. Ann. Rev. Biochem., 52:711-760.

Newton, G.L., and Javor, B., 1985. Glutamylcysteine and thiosulfate are the major low molecular weight thiols in halobacteria. J. Bacteriol., (in press).

U. Fischer: CYTOCHROMES AND IRON SULFUR PROTEINS IN SULFUR METABOLISM OF PHOTOTROPHIC BACTERIA

Dissimilatory sulfur metabolism in phototrophic sulfur bacteria provides the bacteria with electrons for the photosynthetic electron transport chain and, therefore, with energy. On the contrary, assimilatory sulfate reduction is necessary for the biosynthesis of sulfur-containing cell components, such as amino acids. Sulfide, thiosulfate, and elemental sulfur are the sulfur compounds most commonly used by phototrophic bacteria as electron donors for anoxygenic photosynthesis. Cytochromes or other electron transfer proteins, like high-potential-iron-sulfur protein (HIPIP) function as electron acceptors or donors for most enzymatic steps during the oxidation pathways of sulfide or thiosulfate. Yet heme- or siroheme-containing proteins themselves undergo enzymatic activities in sulfur metabolism. Sirohemes comprise a porphyrin-like prosthetic group of sulfate reductase. Flavocytochromes (cytochrome c reductase, elemental sulfur reductase, or adenylylsulfate (APS) reductase) of phototrophic bacteria react with sulfide. High-spin cytochrome c' exhibits sulfite acceptor oxidoreductase, while sulfite reductases may contain siroheme as a new type of heme prosthetic group.

Reduced sulfur compounds at oxidation levels below that of sulfate serve as electron donors for anoxygenic photosynthesis and carbon dioxide fixation in most phototrophic bacteria. When sulfide is oxidized to sulfate by purple sulfur bacteria (Chromatiaceae) and green sulfur bacteria (Chlorobiaceae), one intermediate product formed is elemental sulfur (S^o). This is stored as sulfur globules inside the cells of Chromatiaceae. The purple sulfur genus *Ectothiorhodospira*, however, stores the S^o outside cells (as is common for the Chlorobiaceae). Purple nonsulfur bacteria (Rhodospirillaceae) capable of utilizing sulfide as the electron donor oxidize it either to sulfate without the formation of elemental sulfur or only to S^o which is then deposited outside the cells and which cannot be further oxidized by them to sulfate. The end product of anoxygenic sulfide oxidation by cyanobacteria is S^o which can be stored inside or outside the cells. As an electron donor for photosynthesis, sulfite (SO_3^{2-}) is used by only a few species of phototrophic bacteria; tetrathionate, as far as known, is used only by the thiosulfate-utilizing green *Chlorobium limicola (forma thiosulfatophilum)*. The ability to consume S^o is typical of Chromatiaceae and Chlorobiaceae, but not of Rhodospirillaceae and cyanobacteria. The use of thiosulfate as an electron donor is more extensive in Chromatiaceae and Rhodospirillaceae than in Chlorobiaceae.

Sulfur compounds can be either oxidized or reduced by metabolism. Electron carrier proteins are necessary for sulfur redox reactions. Electron transfer proteins include cytochromes, sirohemes, and non-heme iron proteins, such as ferredoxin, rubredoxin, and HIPIP.

Figure I-6.5 summarizes the enzymatic steps of sulfur metabolism where electron transfer proteins are involved.

All enzymatic reactions with the exception of ADP sulfurylase and adenylate kinase involve transfer of electrons. Electron donors or acceptors are necessary for each of these reactions. Cytochromes and iron sulfur proteins, probably components of the plasma or photosynthetic membranes, are able to transfer electrons.

Bartsch, R.G., 1978. Cytochromes. In *The Photosynthetic Bacteria*. (R.K. Clayton and W.R. Sistrom, eds.), Plenum Press, New York, pp. 249-279.

Fischer, U., 1984. Cytochromes and iron sulfur proteins in sulfur metabolism of phototrophic sulfur bacteria. In *Sulfur - The Significance for Chemistry, Biology, Geology, Technology and the Cosmosphere*. (A. Mueller and B. Krebs, eds.), Elsevier Scientific Publishing Co., Amsterdam, pp. 383-408.

Steinmetz, M.A. and Fischer, U., 1981. Cytochromes of the non-thiosulfate-utilizing green sulfur bacterium *Chlorobium limicola*, Arch. Microbiol., 130:31-37.

Steinmetz, M.A. and Fischer, U., 1982. Cytochromes of the green sulfur bacterium *Chlorobium limicola* f. *thiosulfatophilum*: Purification, characterization and sulfur metabolism, Arch. Microbiol., 131:19-26.

Steinmetz, M.A. and Fischer, U., 1981. Cytochromes, rubredoxin, and sulfur metabolism of the non-thiosulfate-utilizing green sulfur bacterium *Pelodictyon luteolum*, Arch. Microbiol., 132:204-210.

Steinmetz, M.A., Trueper, H.G., and Fischer, U., 1983. Cytochrome c-555 and iron-sulfur-proteins of the non-thiosulfate-utilizing green sulfur bacterium *Chlorobium vibrioforme*, Arch. Microbiol., 135:186-190.

Trueper, H.G., 1975. The enzymology of sulfur metabolism in phototrophic bacteria - a review, Pl. Soil, 43:29-39.

Trueper, H.G., 1978. Sulfur metabolism. In *The Photosynthetic Bacteria*. (R.K. Clayton and W.R. Sistrom, eds.), Plenum Press, New York, pp. 677-690.

Trueper, H.G., 1981. Photolithotrophic sulfur oxidation. In *Biology of Inorganic Nitrogen and Sulfur*. (H. Bothe and A. Trebst, eds.), Springer Verlag, New York, pp. 199-211.

Trueper, H.G. and Fischer, U., 1982. Anaerobic oxidation of sulfur compounds as electron donors for bacterial photosynthesis, Phil. Trans. R. Soc. Lond. B., 298:529-542.

Wermter, U. and Fischer, U., 1983. Cytochromes and anaerobic sulfide oxidation in the purple sulfur bacterium *Chromatium warmingii*, Z. Naturforsch., 38c:960-967.

Wermter, U. and Fischer, U., 1983. Molecular properties of high potential iron sulfur protein of *Chromatium warmingii*, Z. Naturforsch., 38c:968-971.

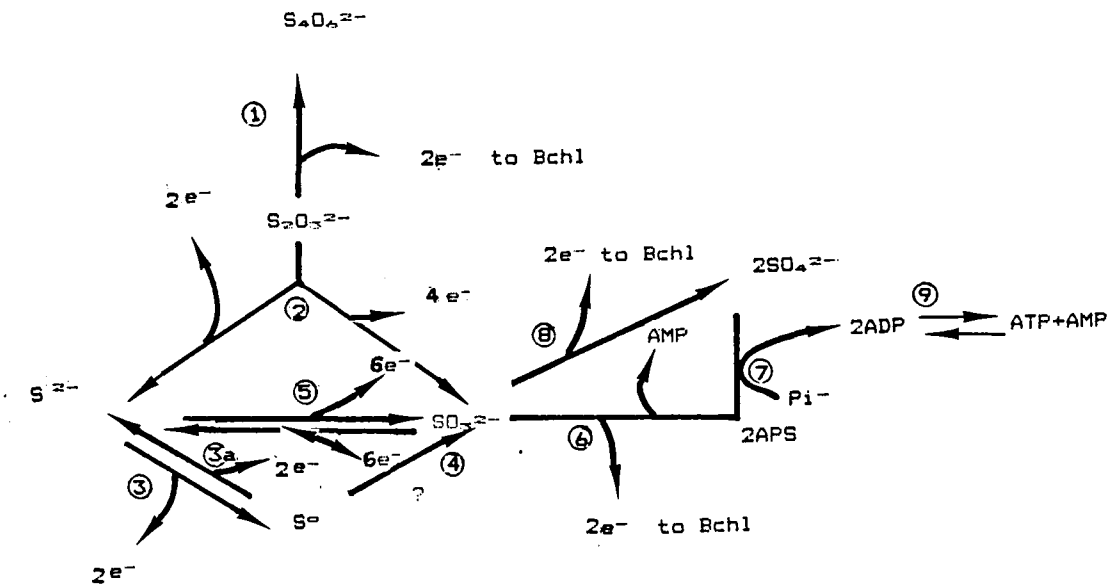

Figure I-6.5. Sulfur oxidation in phototrophic bacteria. 1 = thiosulfate: acceptor oxidoreductase; 2 = thiosulfate reductase; 3 = sulfide oxidizing enzyme; 3a = elemental sulfur reductase; 4 = elemental sulfur-oxidizing enzyme; 5′= sulfite reductase (siroheme); 6 = APS reductase; 7 = ADP sulfurylase; 8 = sulfite: acceptor oxidoreductase; 9 = adenylate kinase. Abbreviations APS = adenosine-5′-phosphosulfate; AMP = adenosine-5′-triphosphate; P*i* = inorganic phosphate; Bchl = Bacteriochlorophyll.

G.E. Fox: INSIGHTS INTO THE PHYLOGENETIC POSITIONS OF PHOTOSYNTHETIC BACTERIA OBTAINED FROM 5S rRNA AND 16S rRNA SEQUENCE DATA

Comparisons of complete 16S ribosomal ribonucleic acid (rRNA) sequences have established that the secondary structure of these molecules is highly conserved. Earlier work with 5S rRNA secondary structure revealed that when structural conservation exists the alignment of sequences is straightforward. Furthermore the constancy of structure implies minimal functional change. Under these conditions a reasonably uniform evolutionary rate can be expected so that conditions are favorable for phylogenetic tree construction.

The sequences of all the 16S ribosomal RNA oligonucleotides produced by complete digestion with ribonuclease T1 allows the construction of rRNA "catalogs" from a large variety of organisms. Binary comparisons of these catalogs are used to generate a matrix of association coefficients (S_{AB} values) from which dendrograms, thought to be partial phylogenies, can be constructed. Complete 5S rRNA sequences exist for many of the same organisms such that separate dendrograms can be made from 5S rRNA data.

The major finding of these studies is that three well-separated evolutionary lines of descent can be detected which are at present represented by eukaryotes, archaebacteria, and eubacteria (Fig. I-7). Presumably, all three lines of descent have diverged from the same ancestral bacterial populations. This branching may have occurred, however, before the evolution of the genetic apparatus was complete. These three lineages differ in morphology of the small ribosomal subunit as well (Fig. I-8).

Within the two prokaryotic lines of descent at least twelve major groups are detected; two archaebacterial and ten eubacterial. Five of the eubacterial groups contain photosynthetic organisms so that it is apparent that the various types of photosynthesis are polyphyletic (Fig. I-9). Only seven species of cyanobacteria are represented but even so it is clear that this cyanobacterial lineage includes both *Prochloron* and the rhodoplast of *Porphyridium*. The plant and *Euglena* chloroplasts share a common ancestry with those seven cyanobacteria as they are currently represented on these trees. Together then the cyanobacteria and chloroplasts define a single major group of photosynthetic eubacteria. The photosynthetic flexibacterium *Chloroflexus aurantiacus* and the Chlorobiaceae apparently represent unrelated groups. The recently discovered *Heliothrix* belongs to the Gram positive bacteria and for the first time brings photosynthesis to that order. The nonsulfur

purple photosynthetic bacteria cluster exclusively into the fifth group with many non-photosynthetic respiring bacteria (Fig. I-10).

The three best-characterized branches of the purple bacteria are referred to as the alpha, beta, and gamma subgroups. The majority of the Rhodospirillaceae contain lamellar or vesicular intercytoplasmic membranes and are in the alpha subgroup where they can be further subdivided according to criteria such as helical form, asymmetric cell division, and the presence of a split 23S rRNA. Each of the subgroups contains non-photosynthetic genera, suggesting that photosynthesis has been gained and/or lost several times during bacterial evolution. The Rhodospirillaceae with tubular intracytoplasmic membranes are similarly interspersed among non-photosynthetic organisms in the "beta" subgroup (Fig. I-10). The Chromatiaceae, including members of the genera *Chromatium*, *Thiocapsa*, and *Ectothiorhodospira* are localized in the "gamma" subgroup.

The purple group is of special interest because several of its members have been suggested as being involved in endosymbiotic relationships which ultimately gave rise to eukaryotic mitochondria. 5S rRNA sequence has already given strong support for the origin of plant mitochondria from the alpha subgroup. Mitochondria are, however, probably of polyphyletic origin, as they can be readily divided between those with tubular cristae and those with flattened (lamellar or vesicular) cristae. Since the alpha and beta subgroups of the purple bacteria can be distinguished by the same criteria, it seems likely that each subgroup may have separately given rise to some eukaryotic mitochondria. In the future it may be possible to localize mitochondrial origins in these two subgroups with even greater precision.

Bonen, L., Doolittle, W.F. and Fox, G.E., 1979. Cyanobacterial evolution: Results of 16S ribosomal ribonucleic acid sequence analysis, Can. J. Biochem., 57:879-888.

Fox, G.E., Luehrsen, K.R. and Woese, C.R., 1982. Archaebacterial 5S ribosomal RNA, Zbl. Bakt. Hyg. I Abt. Orig C, 117:330-345.

Fox, G.E., Pechman, K.R. and Woese, C.R., 1977. Comparative cataloging of 16S ribosomal RNA - A molecular approach to prokaryotic systematics, Int. J. Syst. Bacteriol., 27:44-57.

Fox, G.E., Stackebrandt, E., Hespell, R.B., Gibson, J., Maniloff, J., Dyer, T.A., Wolfe, R.S., Balch, W.E., Tanner, R.S., Magrum, L.J., Zablen, L.B., Blakemore, R., Gupta, R., Bonen, L., Lewis, B.J., Stahl, D.A., Luehrsen, K.R., Chen, K.N. and Woese, C.R., 1980. The phylogeny of prokaryotes, Science, 209:457-463.

Seewaldt, E. and Stackebrandt, E., 1982. Partial sequence of 16S ribosomal RNA and the phylogeny of *Prochloron*, Nature, 295:618-620.

Sobieski, J., Chen, K.N., Filieatreau, J., Pickett, M.H. and Fox, G.E., 1984. 16S rRNA oligonucleotide catalog data base, Nucleic Acid Res., 12:141-148.

Stackebrandt, E. and Woese, C.R., 1981. The evolution of prokaryotes. In *Molecular and Cellular Aspects of Microbial Evolution*. (M.J. Carlile, J.F. Collins and B.E.B. Moseley, eds.), 32nd Soc. Gen. Microbiol. Symposium, 31:1-32.

Stackebrandt, E., Ludwig, W., and Fox, G.E., 1985. 16S ribosomal RNA oligonucleotide cataloging, Methods in Microbiol., 19, (in press).

Stewart, K.D. and Mattox, K.R., 1984. The case for a polyphyletic origin of mitochondria: morphological and molecular comparisons, J. Mol. Evol., 21:54-57.

Villanueva, E., Luehrsen, K.R., Gibson, J., Delihas, N., and Fox, G.E., 1985. Localization and the phylogenetic origin of the plant mitochondrion based on a comparative analysis of 5S ribosomal RNA sequences, J. Mol. Evol, (in press).

Woese, C.R., Gibson, J., and Fox, G. E., 1980. Do genealogical patterns in purple photosynthetic bacteria reflect interspecific gene transfer? Nature, 283:212-214.

Woese, C.R., Stackebrandt, E., Weisburg, W.G., Pasteur, B.J., Madigan, M.T., Fowler, V.J., Hahn, C.M., Blanz, P., Gupta, R., Nealson, K.H. and Fox, G.E., 1984. The phylogeny of purple bacteria: The alpha subdivision, Syst. Appl. Microbiol., 5:315-326.

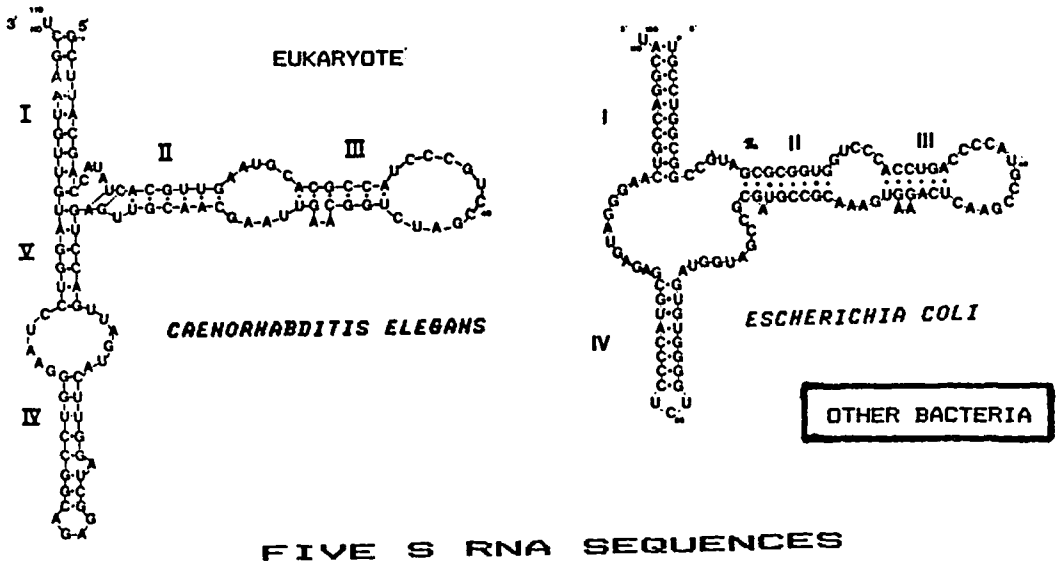

FIVE S RNA SEQUENCES

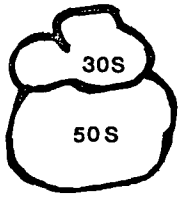

COMPOSITION OF BACTERIAL RIBOSOMES

Subunits	Type of molecules	Number of molecules	Size of subunits
50S	23S rRNA	1	2900 nucleotides
	5S rRNA	1	120 nucleotides
	proteins	34	different proteins (L1-L22)
30S	16S rRNA	1	1540 nucleotides
	proteins	22	different proteins (S1-S22)

Figure I-7. Comparison of ribosomal macromolecules. Five S ribosomal RNA sequences showing structures of (left) a nematode (*C. elegans*) and *E. coli*, a eubacterium. A summary of the structure and macromolecular composition of bacterial ribosomes is shown at the bottom. (Right) Five S RNA from five "archaebacteria." Note the 108 nucleotide insertion in *Halococcus*, nearly the size of the rest of the 5S RNA molecule.

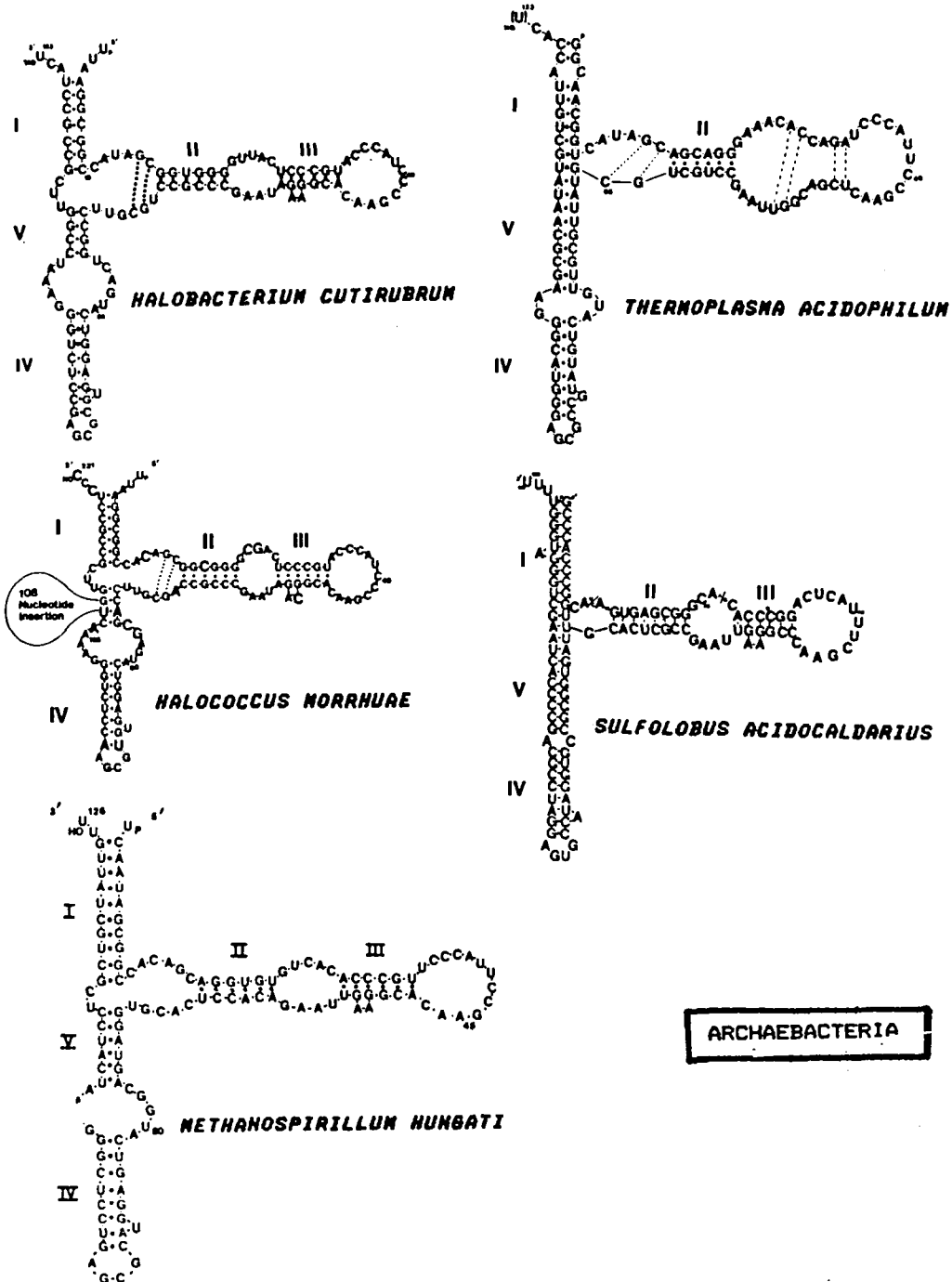

FIVE 8 RNA SEQUENCES

Table I-4.

ARCHAEBACTERIA

Defining Criteria of Archaebacterial Prokaryotes

1. Major lipids are ether linked with phytanol side chains (C_{20}). In other bacteria and eukaryotes major lipids are ester linked.

2. Based on 16S ribosomal RNA oligonucleotide catalogues these organisms are more closely related to each other than they are to eukaryotic or other bacterial 16S RNAs. (16S rRNA from small ribosomal subunits is about 1540 nucleotides long).

3. Based on the sequence of nucleotides in 5S ribosomal RNA these organisms are more closely related to each other than they are to eukaryotic or other bacterial 5S RNAs. (5S rRNA from large ribosomal subunit is about 120 nucleotides long, Fig. I-7).

4. Archaebacteria lack peptidoglycan in their cell walls.

5. A single DNA dependent-RNA polymerase with complex subunit structure (more than 6 subunits) is present in archaebacteria.

6. Archaebacteria ribosomes have a distinctive shape. (Fig. I-8), (Lake, 1983.)

7. Archaebacteria include:

   All methanogenic bacteria
   Halophilic and thermoacidophilic bacteria:

Sulfolobus	*Halococcus*
Thermoproteus	*Halobacterium*
Desulfurococcus	*Thermoplasma acidophilum*

Table I-4.
continued

Ranges of S_{ab} values: 16S ribosomal RNA

The lower limit of the range of Sab values from oligonucleotide catalogues amongst the archaebacteria are 0.18 to 0.24, amongst the eubacteria 0.17 - 0.22. The data for the chloroplasts (0.28 - 0.32 with cyanobacteria) and rhodoplasts (0.40 - 0.43 with cyanobacteria) are included. The Sab values between the archaebacteria and eubacteria are between 0.06 to 0.10, between the eukaryotes and archaebacteria 0.07-0.10, and between the eukaryotes and eubacteria 0.06 - 0.10. Catalogues are available for about 400 genera.

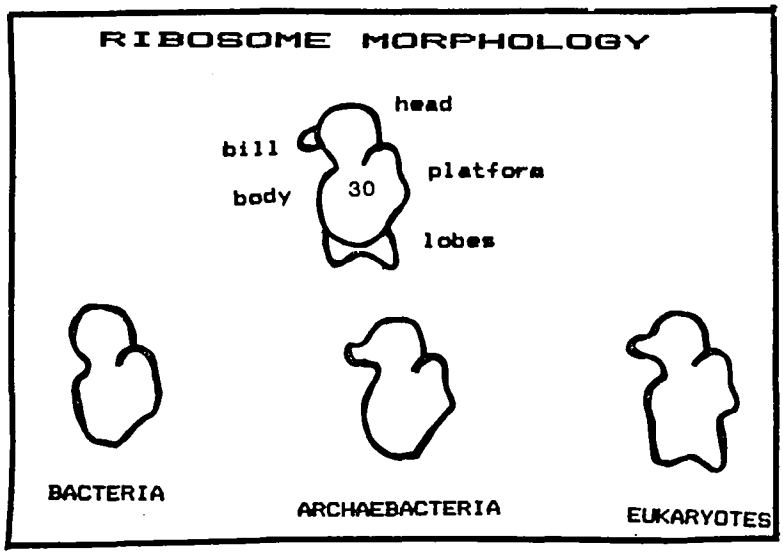

Figure I-8.

Comparative morphology of the 30S ribosomal subunit.

Fox, G.E., 1981. Archaebacteria, ribosomes and origin of eucaryotic cells. In *Evolution Today. Proc. 2nd Intn. Cong. of Syst. and Evol. Biol.*. (Scudder and Reveal, eds.), Univ. Maryland Press, College Park, MD, pp. 235-244.

Lake, J.A., 1983. Ribosome evolution - the structural basis for protein synthesis in archaebacteria, eubacteria and eukaryotes, Cell, 33:318-319.

Woese, C.R. and Fox, G.E., 1977. Phylogenetic structure of the prokaryotic domain: The primary kingdoms, Proc. Natl. Acad. Sciences, USA, 74:5088-5090.

Woese, C.R., Magrum, L.J. and Fox, G.E., 1978. Archaebacteria, J. Molec. Evol., 11:245-252.

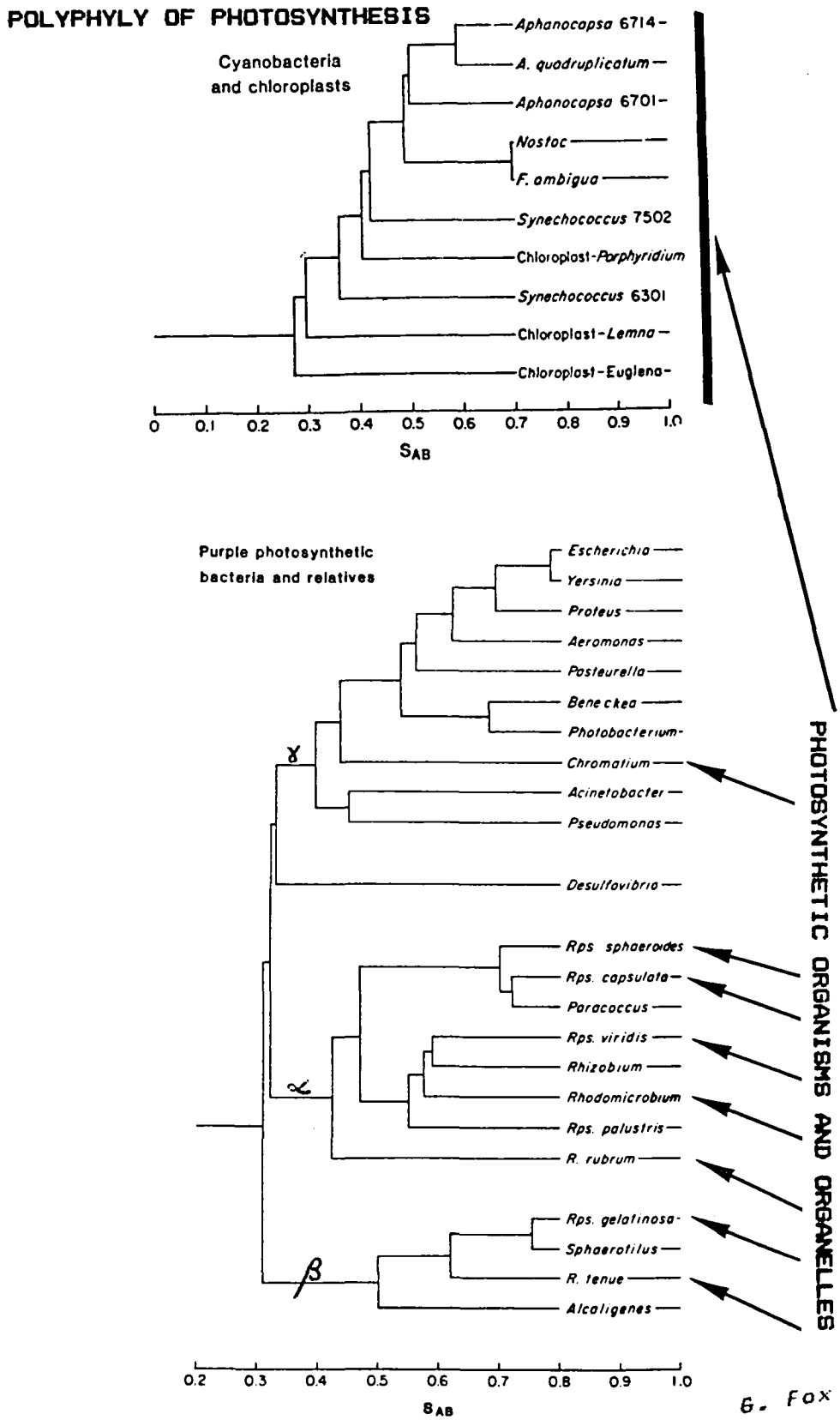

Similarity coefficients based on 16S ribosomal RNA oligonucleotide catalogues

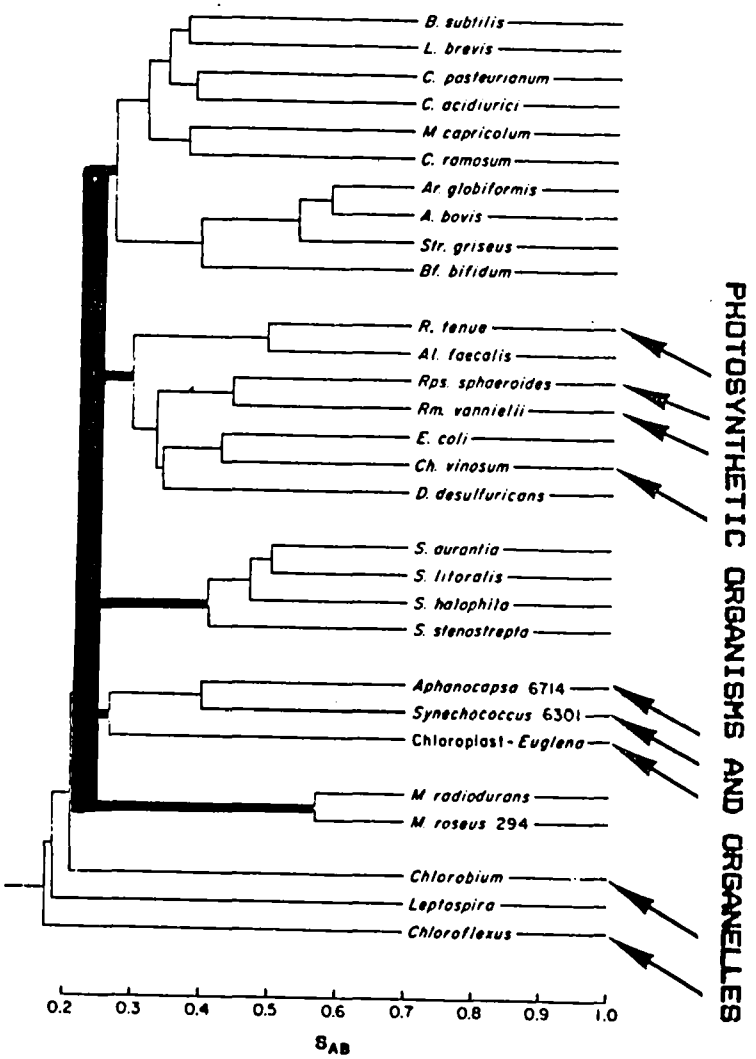

Similarity coefficients based on 16S ribosomal RNA oligonucleotide catalogues

G. Fox

POLYPHYLY OF PHOTOSYNTHESIS

Figure I-9. Partial phylogenies based on 16S RNA comparative data suggest that photosynthesis evolved separately in different bacterial lineages. It probably evolved at least three times (green photosynthetic bacteria, e.g., *Chlorobium* (left), purple photosynthetic bacteria (left and right) and cyanobacteria/plastids (left and right). The relationship between certain respiring and their presumed photosynthetic relatives is shown in more detail at right.

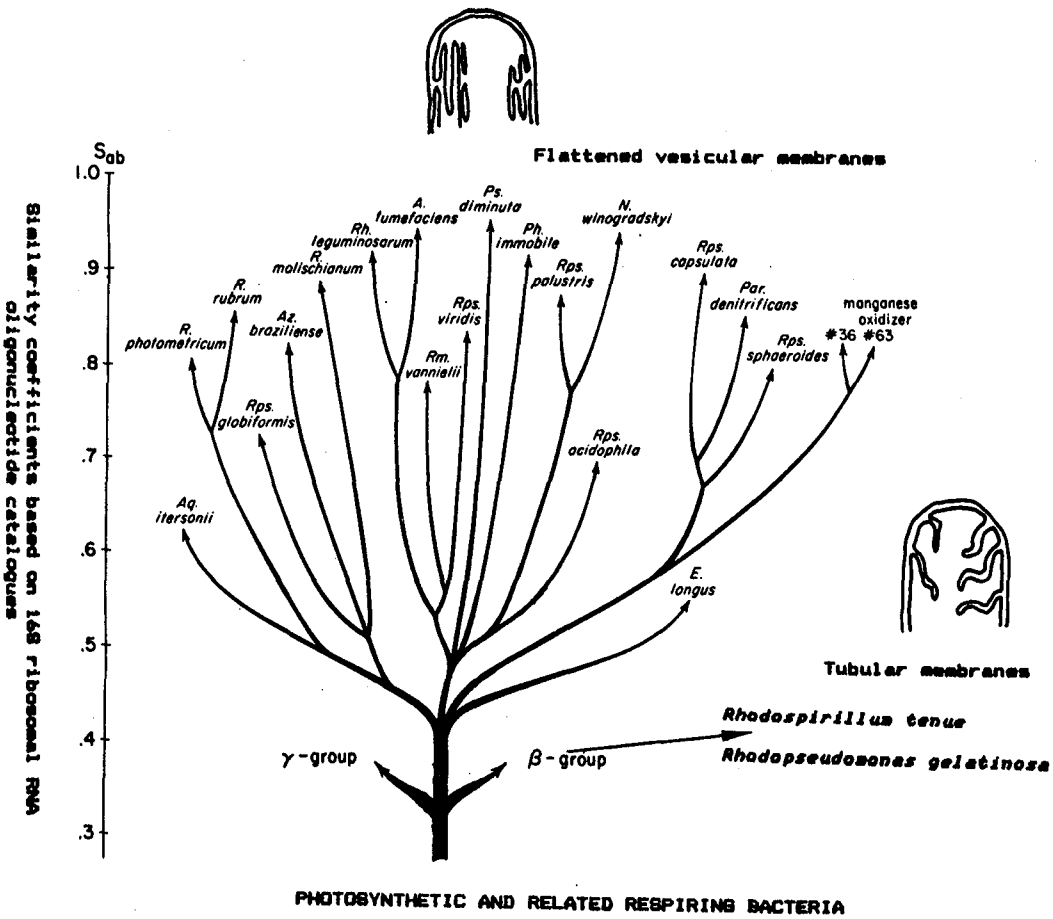

Figure I-10. Based on 16S RNA oligonucleotide catalogues there are at least three groups of photosynthetic/respiring bacteria. One of which (*Rhodomicrobium*, *Paracoccus* and many *Rhodopseudomonas* species, those with flattened membranes) is shown in detail here. Another presumed lineage, the beta group (lower right), has tubular membranes. Mitochondria of eukaryotes are thought to derive from these bacterial lineages. Most likely they too are polyphyletic, those with flattened cristae (e.g., animals and plants) coming from the alpha group and those with tubular cristae (e.g., ciliates, chrysophytes) from the beta group.

R.M. Garrels: CARBON AND SULFUR CYCLING THROUGH GEOLOGIC TIME

Mathematical models of the coupled global systems of sedimentary reservoirs and fluxes can be used to infer variations in reservoir sizes and rates of sedimentation over periods of hundreds of millions of years. Perhaps most interesting is the coupled sulfide/sulfate-carbon/carbonate system that controls global oxygen and carbon dioxide production and consumption.

Berner, R.A., LaSaga, A.M. and Garrels, R.M., 1983. The carbonate-silicate geochemical cycle and its effect on atmosphere carbon dioxide over the past 100 million years, Amer. J. Sci., 283:641-683.

Berner, R.A. and Raiswell, R., 1983. Burial of organic carbon and pyrite sulfur in sediments over Phanerozoic time: a new theory, Geochim. Cosmochim. Acta, 47:855-867.

Garrels, R.M. and Perry, E.A., 1974. Cycling of carbon, oxygen, and sulfur through geologic time. In *The Sea*. (E. Goldberg, ed.), Vol. 5, John Wiley and Sons, pp. 303-336.

Garrels, R.M. and Lerman, A., 1984. Coupling of the sedimentary sulfur and carbon cycles - an improved model, Amer. J. Sci., 284: 989-1007.

Holland, H., 1973. Systematics of the isotopic composition of sulfur in the oceans during the Phanerozoic and its implications for atmospheric oxygen, Geochim. Cosmochim. Acta, 37:2605-2616.

Schidlowski, M. and Junge, C.E., 1981. Coupling among the terrestrial sulfur, carbon, and oxygen cycles: Numerical modeling based on revised Phanerozoic carbon isotope records, Geochim. Cosmochim. Acta, 45:589-594.

Schopf, J.W. (ed.), 1984. *The Earth's Earliest Biosphere: Its Origin and Evolution*. Princeton University Press, Princeton, 543 pp.

ORGANIC CARBON CONTENT OF SHALES AND SLATES AS A FUNCTION OF AGE (AFTER SCHIDLOWSKI, 1982)

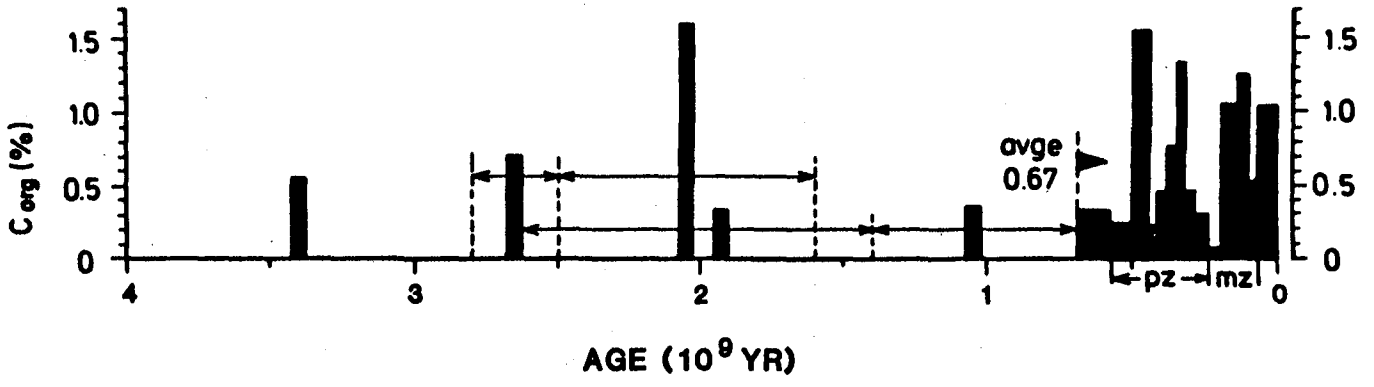

Robert Garrels

Figure I-11 Carbon isotope fractionation ranges (left) and carbon content (right) in organic matter found in shales and slates. pz=Paleozoic Era, mz=Mesozoic Era. The stretch of time left of pz is the prePhanerozoic.

M. Goldhaber: SULFUR DIAGENESIS IN MARINE SEDIMENTS

Bacterial sulfate reduction occurs in all marine sediments that contain organic matter. Aqueous sulfide (HS^-, H_2S), one of the initial products of bacterial sulfide reduction, is extremely reactive with iron-bearing minerals: sulfur is fixed into sediments as iron sulfide (first FeS and then FeS_2). The sequence of biological and chemical alterations that occur in sediment once the sulfur has been deposited is called sulfur diagenesis. Diagenesis involves variable and complex reactions at different rates. The rate of the first step, sulfate reduction, varies in different environments by a factor of as much as 10^3. Such variation is due to the kind and amount of organic matter utilizable by sulfate-reducing bacteria. Sediment accumulation rate dramatically influences the kind of organic matter buried and brought to the zone of sulfate reduction by controlling the exposure of organic matter to degradative oxic conditions near the sediment/water interface.

Aqueous sulfide reacts during sulfur diagenesis with hydrated iron oxide (goethite), which is the major form of reactive iron in most sediments. At the pH of marine pore waters the product of this reaction is mackinawite (tetragonal $FeS_{0.9}$). Subsequently mackinawite transforms to greigite (cubic Fe_3S_4) and finally to pyrite (cubic FeS_2). I believe there occurs in the sediments an addition of elemental sulfur to mackinawite and greigite but the source of this sulfur and its transformations remains obscure.

The quantity of sulfur in pyrite which accumulates in marine sediments is frequently much greater than the sum of the quantities trapped in the pore fluid as sulfate ions plus that entering the sediment as detrital organic sulfur. The excess sulfur is supplied by interchange of pore fluids with overlying sea water caused by the bioturbational activities of the animals and the diffusion of sea water sulfate into sediments. These sources of sulfate are abundant enough to insure that pyrite formation is not limited by sea water sulfate availability. Since the amount of pyrite measured in marine sediments is directly proportional to that of organic carbon, I suggest that the quantity and quality of organic matter controls pyrite formation.

Berner, R.A., 1975. Diagenetic models of dissolved species in the interstitial waters of compacting sediments, Amer. J. Sci., 275:88-96.

Berner, R.A., 1978. Sulfate reduction and the rate of deposition of marine sediments, Earth and Planetary Science Letters, 37:492-498.

Berner, R.A., Baldwin, T., and Holdren, G.R., 1979. Authigenic iron sulfides as paleosalinity indicators, J. Sed. Petrol., 49:1345-1350.

Chambers, L.A. and Trudinger, P.A., 1979. Microbiological fractionation of stable sulfur isotopes: a review and critique, Geomicrobiol. J., 1:249-293.

Goldhaber, M.B. and Kaplan, I.R., 1974. The sulfur cycle. In *The Sea*. (E.D. Goldberg, ed.), Vol. 4, John Wiley and Sons, Inc., New York, pp. 569-655.

Goldhaber, M.B. and Kaplan, I.R., 1975. Controls and consequences of sulfate reduction rates in recent marine sediments, Soil Science, 119:42-55.

Goldhaber, M.B. and Kaplan, I.R., 1980. Mechanisms of sulfur incorporation and isotope fractionation during early diagenesis in sediments of the Gulf of California, Mar. Chem., 9:95-143.

Goldhaber, M.B., Aller, R.C., Cochran, J.K., Rosenfeld, J.K., Martens, C.S., and Berner, R.A., 1977. Sulfate reduction, diffusion, and bioturbation in Long Island Sound sediments: report of the FOAM group, Amer. J. Sci., 277:193-237.

Jørgensen, B.B., 1977. The sulfur cycle of a coastal marine sediment (Limfjorden, Denmark), Limnol. Oceanog., 22:814-832.

Jørgensen, B.B., 1979. A theoretical model of the stable isotope distribution in marine sediments, Geochim. Cosmochim. Acta, 43:363-374.

Kaplan, I.R. and Rittenberg, S.C., 1964. Microbiological fractionation of sulfur isotopes, J. Gen. Microbiol., 34:195-212.

Kaplan, I.R., Emery, K.O., and Rittenberg, S.C., 1962. The distribution and isotopic abundance of sulphur in recent marine sediments of southern California, Geochim. Cosmochim. Acta, 27:297-331.

Pyzik, A.J. and Sommer, S.E., 1981. Sedimentary iron monosulfides: kinetics and mechanism of formation, Geochim. Cosmochim. Acta, 45:687-698.

Rees, C.E., 1973. A steady-state model for sulphur isotope fractionation in bacterial reduction processes, Geochim. Cosmochim. Acta, 37:1114-1162.

Sweeney, R.E. and Kaplan, I.R., 1973. Pyrite framboid formation: Laboratory synthesis and marine sediments, Econ. Geol., 68:618-634.

Westrich, J.T. and Berner, R.A., 1984. The role of sedimentary organic matter in bacterial sulfate reduction: The G model tester, Limnol. Oceanog., 29:236-249.

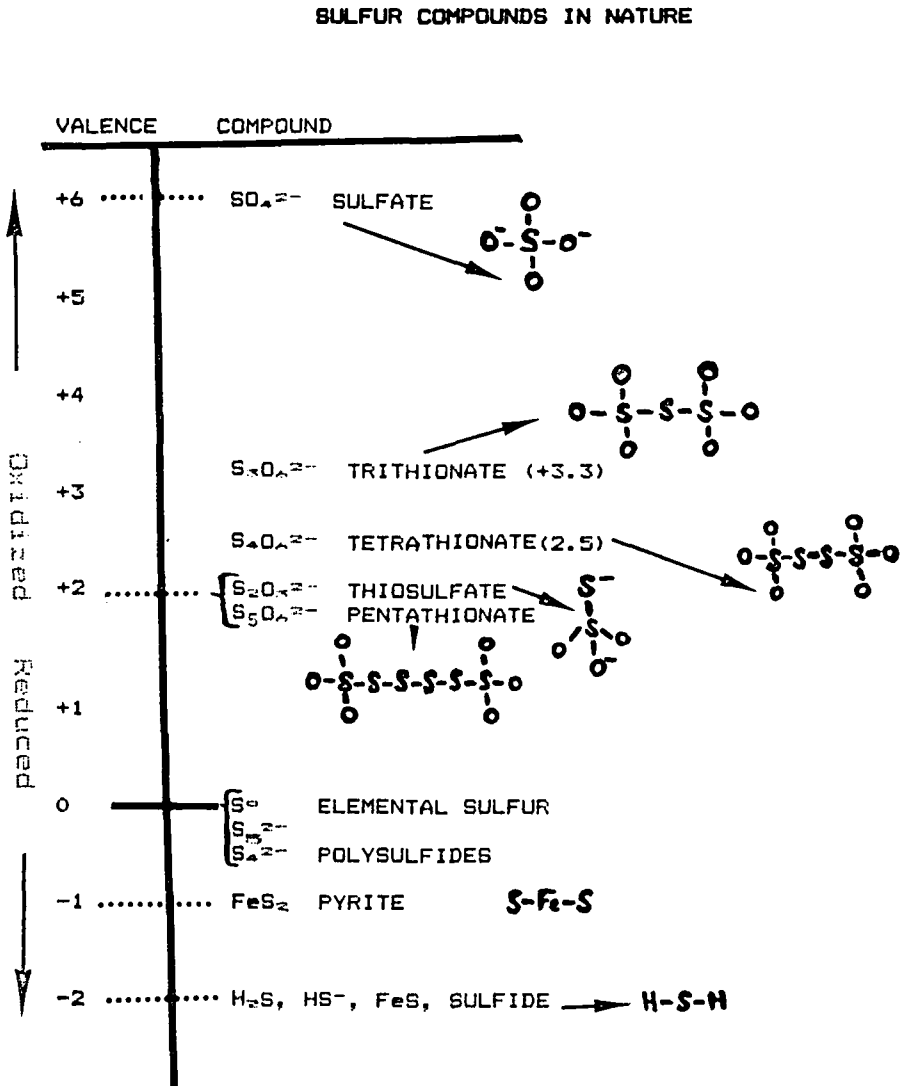

Figure I-12. Sulfur is easily oxidized and reduced: its valence in nature varies from -2 to +6. Sulfates, elemental sulfur and sulfides are the most common forms of the element.

R. Guerrero: ECOPHYSIOLOGY OF PHOTOTROPHIC SULFUR BACTERIA IN LAKES: VERTICAL DISTRIBUTION OF PLANKTONIC POPULATIONS

Purple and green sulfur bacteria typically stratify in sulfide-containing anaerobic waters, often accumulating massively and placing themselves at the depth where physico-chemical conditions most favor their growth. The three main prerequisites for photosynthesis of purple sulfur (Chromatiaceae) and green sulfur (Chlorobiaceae) bacteria are light, absence of oxygen, and the availability of a suitable electron donor, usually sulfide (van Gemerden and Beeftink, 1983). In the present ecosphere, this is a combination only achieved in aquatic, shallow, and oligotrophic or mesotrophic environments such as ponds, lakes, and estuaries. Under such conditions, planktonic purple and green sulfur bacteria may periodically form thick, spectacularly colored layers, the most frequent being brown, green, pink, and variations of pink (Biebl and Pfennig, 1979).

During stratification in summer Chromatiaceae frequently dominate in these bacterial layers, constituting up to 90 percent of the total biomass (Guerrero et al., 1980). Although the physiology of purple sulfur bacteria has been extensively studied in the laboratory (Pfennig, 1978; van Gemerden, 1983), little attention has been devoted to their metabolism in nature. In natural habitats, very sharp physico-chemical gradients are often established. As a consequence, heterogeneous conditions within the bacterial layer result in differences of the physiological state of the cells along the gradients (Fig I-13).

The study of purple and green sulfur bacterial populations in nature is of interest for the following reasons: (a) high quantities of biomass, with low species diversity can be collected (b) study of planktonic life permits us to understand the mechanisms, structural as well as physiological, used to maintain their vertical position without sinking, and (c) because they are capable of sulfur oxidations and reductions that act as important intermediates in the global sulfur cycle. Purple and green photosynthetic bacteria, moreover, may be responsible for certain geological deposits.

The purpose of our research was the analysis of planktonic phototrophic sulfur bacteria in relation to their vertical distribution in the water column, to assess the factors, including competition for light, that determine their sedimentation rates and the numerical changes in species and populations.

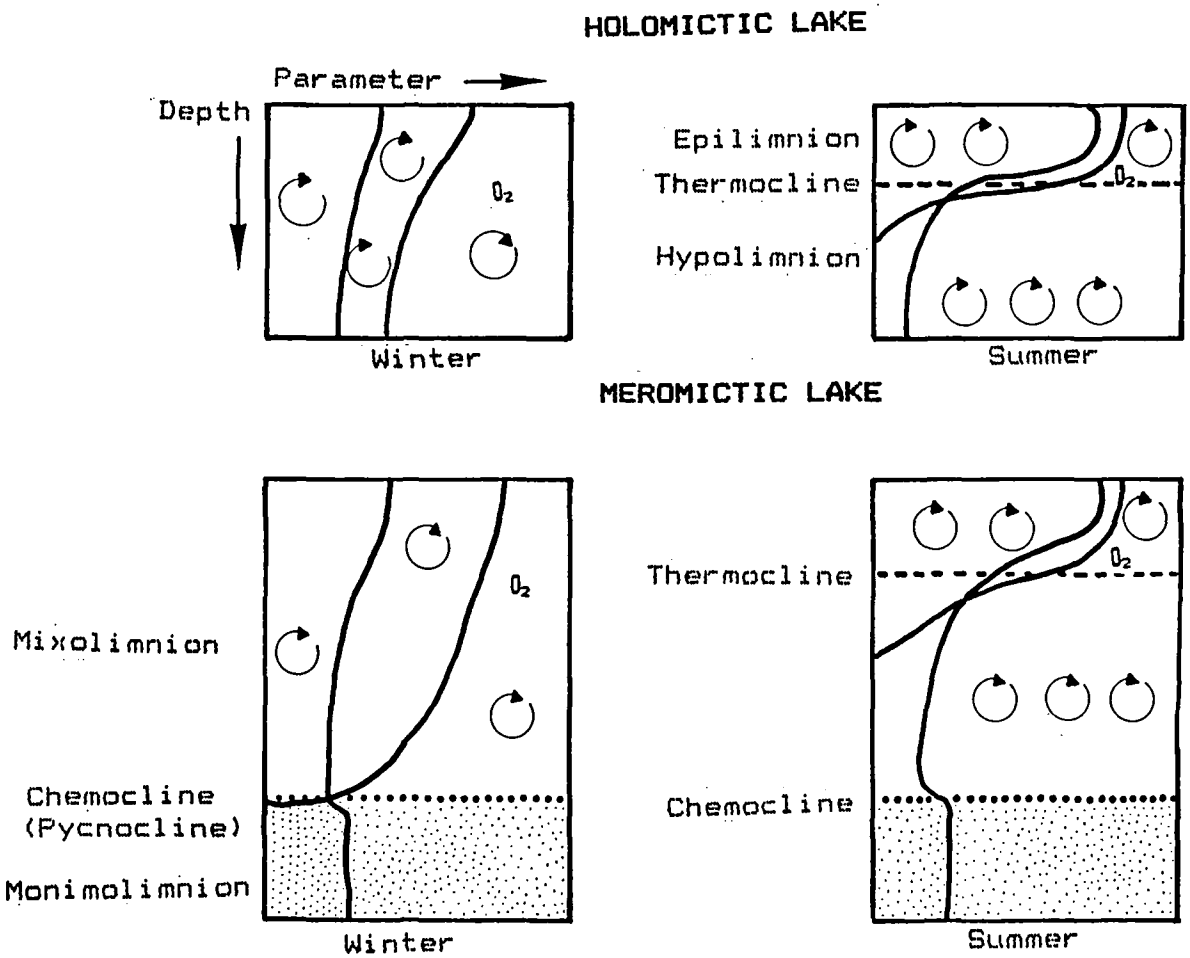

Figure I-13. Vertical structure of the water column in lakes of temperate regions. When sulfide and light are present massive populations of phototrophic sulfur bacteria can develop at the hypolimnion during the summer and in the monimolimnion of meromictic lakes during the remainder of the year.

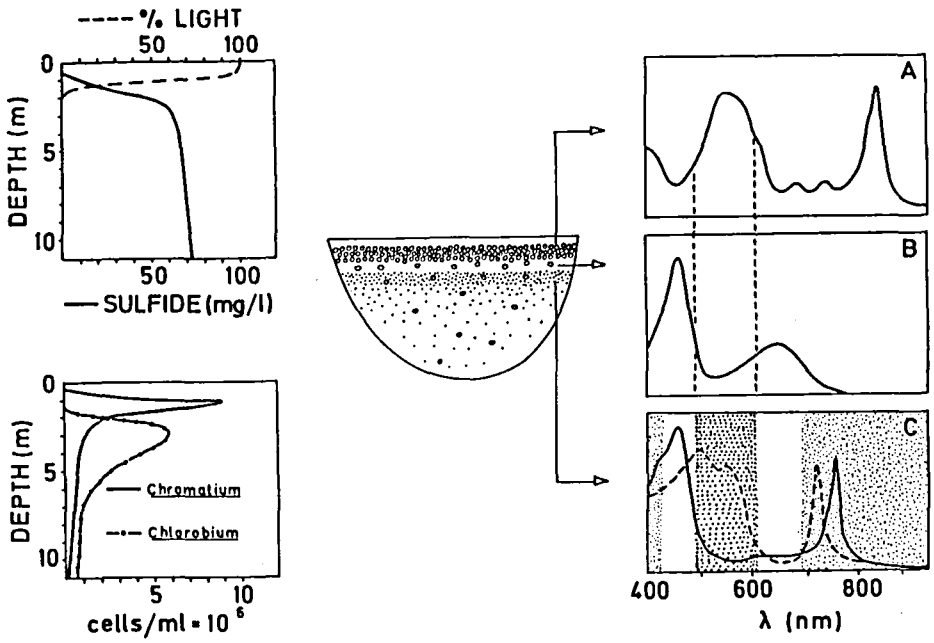

Figure I-14. Shading and light filtering effect of *Chromatium* and *Chlorobium* and resulting competition in Lake Ciso, Spain. (**Left**) Vertical distribution of light, sulfide, *Chromatium* and *Chlorobium* during stratification. (**Right**) **(A)** *Chromatium* layer, in vivo absorption spectrum. **(B)** Spectral distribution of the light below the *Chromatium* layer, which was at 0.5 meters. **(C)** Absorption spectra of *Chlorobium phaeobacteroides* (- - - - - - -) and *Chlorobium limicola* (———) cultures isolated from the layers of *Chlorobium*. Stippled areas represent the bands of light absorbed by water and by the *Chromatium* layer.

In correlated field and laboratory experiments the buoyant densities of populations of selected Chromatiaceae and Chlorobiaeae were measured and investigated for the association between cell density and cytoplasmic inclusions (Guerrero, 1984). The influence of buoyant density on sedimentation was also studied.

Annual changes in *Chromatium* and *Chlorobium* populations were documented (Pedros-Alio, 1983) as was competition, both intra- and interspecific, for light. The competition observed was between two species of *Chlorobium*, *C. limicola* and *C. phaeobacteroides* (Montesinos, 1983) and between *Chromatium* sp. and different chlorobia. The species of *Chlorobium* that develops depends on the presence of *Chromatium* sp. When conditions of light and sulfide are adequate *Chromatium* easily forms as the overlying layer; because it is motile, it resists low concentrations of oxygen, and it tolerates a high light intensity. *Chlorobium limicola* develops under this *Chromatium* layer because it can use the light either filtered by water or by the overlying purple photosynthetic bacteria whereas *Chlorobium phaeobacteroides*, which requires greater light intensity, does not develop underneath (Fig. I-14).

These bacteria, found vertically stratified in lakes, are not equally capable of reproduction: only the *Chromatium* cells receiving sufficient light at the surface of the bacterial layer grow and divide. Cells incapable of maintaining themselves at the top of the layer progressively accumulate at a lower level in the water column, one which is more densely populated but in which the cells are less active. Cells of this layer are replete (from their previous photosynthetic metabolism) with sulfur globules and glycogen and have a correspondingly higher buoyant density (Guerrero, 1984).

As the *Chromatium* cells slowly sink further and further away from the light, they may remain viable for variable periods of time (van Gemerden, submitted for publication). This is apparently done by the conversion of glycogen into poly-beta-hydroxybutyrate, the accumulation of which also leads to high buoyant densities of the cells (Guerrero, submitted for publication). Thus, as the populations develop throughout the year, the bottom of the bacterial layer increases in width and in cell concentration. The sinking cells eventually reach the anaerobic sediment at the bottom where rich populations of sulfate-reducing bacteria are present (Fenchel and Reidl, 1970; Nedwell, 1982). The remains of the photosynthetic bacteria contribute a significant portion of the organic matter necessary to complete the anaerobic carbon and sulfur cycles of lakes. This anaerobic, photosynthetically-driven cycling of carbon and sulfur probably provides an example of the kinds of processes typical of the early ecosystems on Earth.

Biebl, H. and Pfennig, N., 1979. Anaerobic CO_2 uptake by phototrophic bacteria. A review, Archives fur Hydrobiologie, 12:48-58

Fenchel, T. M. and Reidl, R. J., 1970. The sulfide system: a new biotic community underneath the oxidized layer of marine sand bottoms, Marine Biology, 7:255-268.

Guerrero, R., Montesinos, E., Esteve, I., and Abella, C., 1980. Physiological adaptation and growth of purple and green sulfur bacteria in a meromictic lake as compared to a holomictic lake. In *Shallow Lakes*, (M. Dokulil, H. Metz and D. Jewson, eds.) W. Junk, Publishers, The Hague, pp. 161-171.

Guerrero, R., Mas, J., and Pedros-Alió, C., 1984. Buoyant density changes due to intracellular content of sulfur in *Chromatium warmingii* and *Chromatium vinosum*, Arch. Microbiol., 137:350-356.

Montesinos, E., Guerrero, R., Abella, C., and Esteve, I., 1983. Ecology and physiology of the competition from light between *Chlorobium limicola* and *Chlorobium phaeobacteroides* in natural habitats, Appl. Environ. Microbiol., 46:1007-1016.

Nedwell, D. B., 1982. The cycling of sulfur in marine and freshwater sediments. In *Sediment Microbiology*, (D.B. Nedwell and C.M. Brown, eds.), Academic Press, London and New York, pp. 73-106.

Pedros-Alió, C., Montesinos, E., and Guerrero, R., 1983. Factors determining annual changes in bacterial photosynthetic pigments in holomictic Lake Ciso, Spain. Appl. Environ. Microbiol., 46:999-1006.

Pfennig, N., 1978. General physiology and ecology of photosynthetic bacteria. In *The Photosynthetic Bacteria*, (R.K. Clayton and W.R. Sistrom, eds.), Plenum Press, New York, pp. 3-14.

van Gemerden, H., 1983. Physiological ecology of purple and green bacteria, Ann. Microbiol., (Institute Pasteur) 134B: 73-92.

van Gemerden, H., and Beeftink, H.H., 1983. Ecology of phototrophic bacteria. In *The Phototrophic Bacteria: Anaerobic Life in the Light*, (J. G. Ormerod, ed.), Blackwell Scientific, Oxford, pp. 146-185.

W.T. Holser: GEOLOGY AND GEOCHEMISTRY OF SULFIDE AND SULFATE DEPOSITION

Sulfide deposition is dominated by the bacterial reduction of marine sulfate to HS^-, which is then sequestered as $Fe_{1-x}S$, and eventually reacts with another sulfur source to be permanently deposited as pyrite, FeS_2. That shallow and shelf marine sites are more important than the deep sea is shown by the fact that the flux rate from the shallow marine zones is 5.5×10^{11} moles per year whereas that from the deep ocean sediments is about 0.7×10^{11} moles per year (Holser, 1985). Sulfate deposition is dominated by the geological accidents leading to evaporite formation that deposit gypsum/anhydrite, halite, and potash facies minerals (potassium minerals, primarily carnallite and sylvite), in that order. The special conditions of high net evaporation and semi-isolation (but not complete isolation) from sea water input and reflux occur only sporadically in geological time, but when they do occur they fill up any pre-formed basins with these evaporite minerals at a catastrophically high depositional rate.

The isotope ratio of sulfur in sea water, as recorded in the "age curve" of sulfate in evaporite rocks, provides a running account of the relative importance of sulfide (heavier sulfate isotopes) and sulfate (lighter isotopes) in the world reservoirs. Comparison of sulfur and carbon (in carbonate) isotope age curves reflects the balance of oxidation and reduction in these two global cycles.

Berner, R.A., 1982. Burial of organic carbon and pyrite sulfur in the modern ocean: its geochemical and environmental significance, Amer. J. Sci., 282:451-473.

Claypool, G.E., Holser, W.T., Kaplan, I.R., Sakai, H., and Zak, I., 1980. The age curves of sulfur and oxygen isotopes in marine sulfate and their mutual interpretation, Chemical Geology, 28:199-260.

Goldhaber, M.B. and Kaplan, I.R., 1974. The sulfur cycle. In *The Sea* (E.D. Golberg, ed.), Vol. 7, John Wiley and Sons, Inc., New York, pp. 569-655.

Handford, C.R., Loucks, R.G., and Davies, G.R. (eds.), 1982. Depositional and diagnetic spectra of evaporites---A core workshop. *SEPM Core Workshop No. 3*, Society of Economic Paleontologists and Mineralogists, Tulsa, 395 p.

Hardie, L.A., 1984. Evaporites: marine or non-marine?, Amer. J. Sci., 284:193-240.

Holser, W.T., 1982. Mineralogy of evaporites, Reviews in Mineralogy, 6:211-294.

Holser, W.T., 1984. Gradual and abrupt shifts in ocean chemistry during Phanerozoic time. In *Patterns of Change in Earth Evolution.* (H.D. Holland and A.F. Trendall, eds.) Dahlem Konferenzen/Springer-Verlag, Berlin (in press).

Holser, W.T., Maynard, J.B. and Cruikshank, K.M., 1985. Modelling the natural cycle of sulfur through geological time. In *Evolution of the Global Sulfur Cycle.* (W.E. Krumbein and A. Yu Lein, eds.), SCOPE, (submitted).

Holser, W.T., Maynard, J.B., Mackenzie, F.T. and Schidlowski, M., 1985. The cycles of carbon, sulfur, and oxygen. In *Chemical Cycles in the Evolution of the Earth.* (C. Gregor *et al.*, eds.), John Wiley and Sons, Inc., New York (in press).

Kendall, A.C., 1979. Facies models 14. Subaqueous evaporites, Geoscience Canada Reprint Series, 1:159-174.

Kirkland, D.W. and Evans, R. (eds.), 1973 *Marine Evaporites: Origin, Diagenesis, and Geochemistry.* Dowden, Hutchinson and Ross, Inc., Stroudsburg, 246 pp.

Leventhal, J.S., 1983. An interpretation of carbon and sulfur relationships in Black Sea sediments as indicators of environments of deposition, Geochim. Cosmochim. Acta, 47:133-137.

Orr, W.N., 1974. Sulfur. 16L. Biogeochemistry. In *Handbook of Geochemistry*, (K.H. Wedepohl, ed.), 16-L:1-19.

Ruckmick, J.C., Wimberly, G.J., and Edwards, A.F., 1979. Classification and genesis of biogenic sulfur deposits, Economic Geology, 74:469-474.

Volkov, I.I. and Rozanov, A.G., 1983. The sulfur cycle in oceans. Part 1. Reservoirs and fluxes. In *The Global Biogeochemical Sulphur Cycle* (M.V. Ivanov and J.R. Freney, eds.), SCOPE 19. John Wiley and Sons, Inc., New York, pp. 357-423.

Veizer, J., Holser, W.T., and Wilgus, C.K., 1980. Correlation of $^{13}C/^{12}C$ and $^{34}S/^{32}S$ secular variations, Geochim. Cosmochim. Acta, 44:579-587.

Zharkov, M.A., 1981. *History of Paleozoic Salt Accumulation.* Springer-Verlag, Berlin, 308 p.

EVAPORATION SEQUENCE

NAME	SALT	CONCENTRATION OF SEA WATER WHEN SALT PRECIPITATES
Anhydrite	Calcium sulfate $CaSO_4$	3-4 times
Gypsum	Calcium sulfate.2 waters $CaSO_4.2H_2O$	3-4 times
Salt	NaCl	10 times
Potash facies	Potassium chloride KCl	60-70 times
	Magnesium sulfate $MgSO_4$	
	Potassium magnesium chloride $KMgCl_3.6H_2O$	
	Tachyhydrite Magnesium calcium chloride $MgCaCl_4.H_2O$	

(In nature, tachyhydrite is found in the evaporation sequence whereas in the lab bischoffite ($MgCl.6H_2O$) is produced at a concentration of about 70 times

MAJOR MINERALS OF THE POTASH FACIES ("BITTERNS")

Sylvite KCl
Carnellite $KMgCl_3$
Kieserite
Kainite
Schoenite

Figure I-15. As sea water evaporates salts come out of solution in this determined sequence.

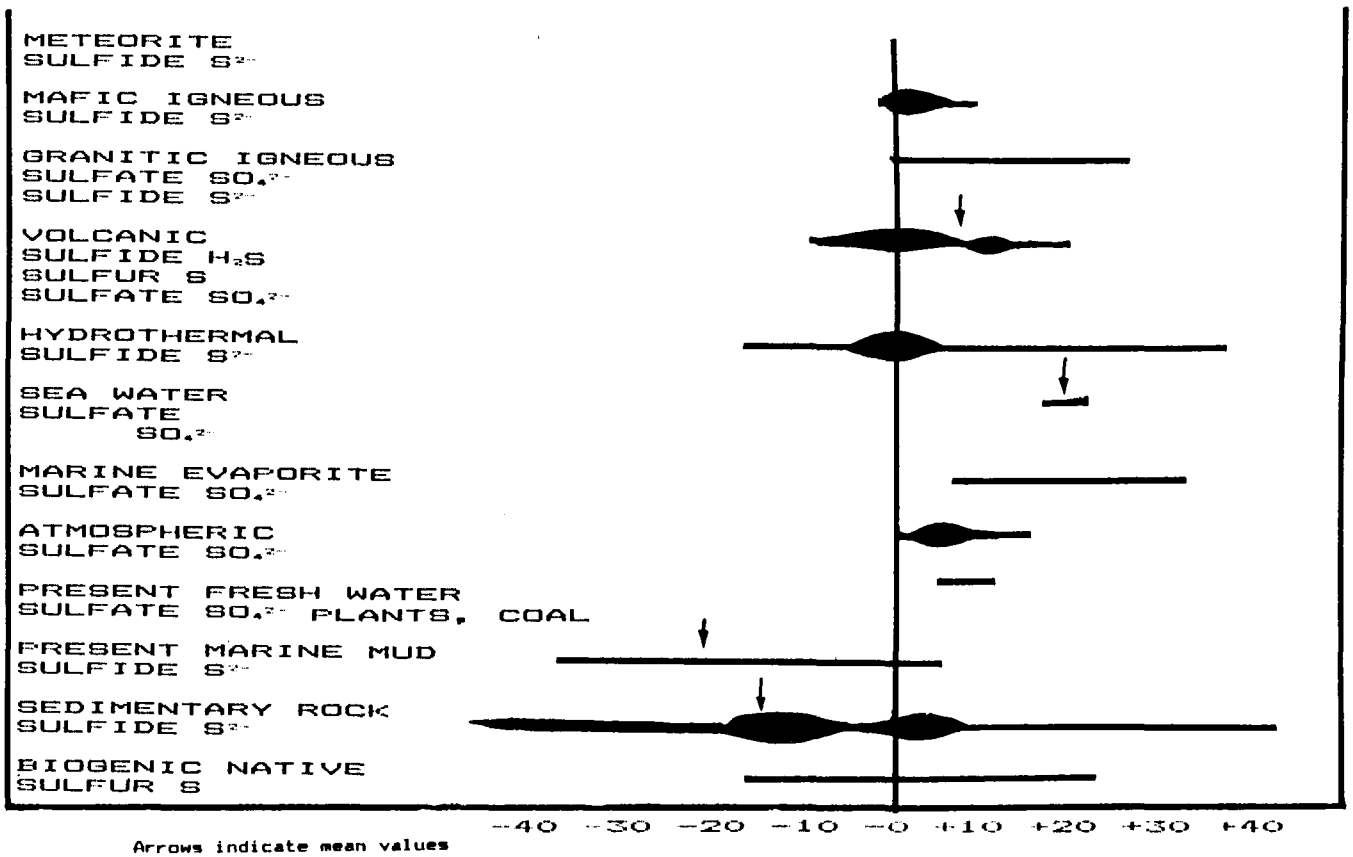

SUMMARY OF SULFUR ISOTOPE FRACTIONATION DATA

δS^{34}

Figure I-16. Summary of literature values. Delta 34S in natural samples varies from over -40 to over +40 depending on several factors, including its source. The width of the black bars approximate the distribution of the values.

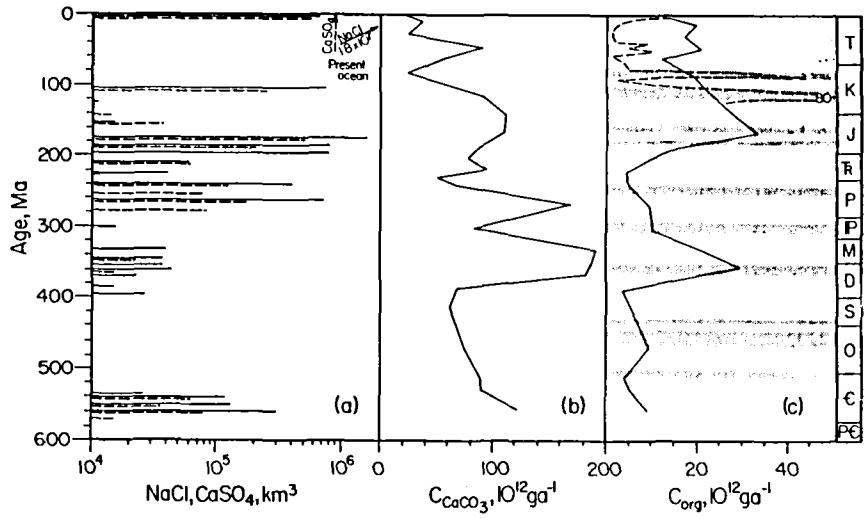

Figure I-17. Phanerozoic marine evaporites and carbon deposition, (a) Nacl and $CaSO_4$ in marine evaporites, scaled logarithmically; content in the present ocean is also shown. Data from Zharkov for Cambrian through Pennsylvanian time, and from Holser et al. for the Permian through the Cenozoic. **(b)** Rate of deposition of C_{carb} **(c)** Rate of deposition of C_{org}. Solid lines in (b) and (c) are carbon in sediments present today on the continents, aggregated to epochs; dashed line in (c) is based mainly on deep-sea cores and aggregated by stages or substages (2). Shaded areas in (c) are times of recognized anoxic events. Note that the scale in (c) is expanded relative to (b).

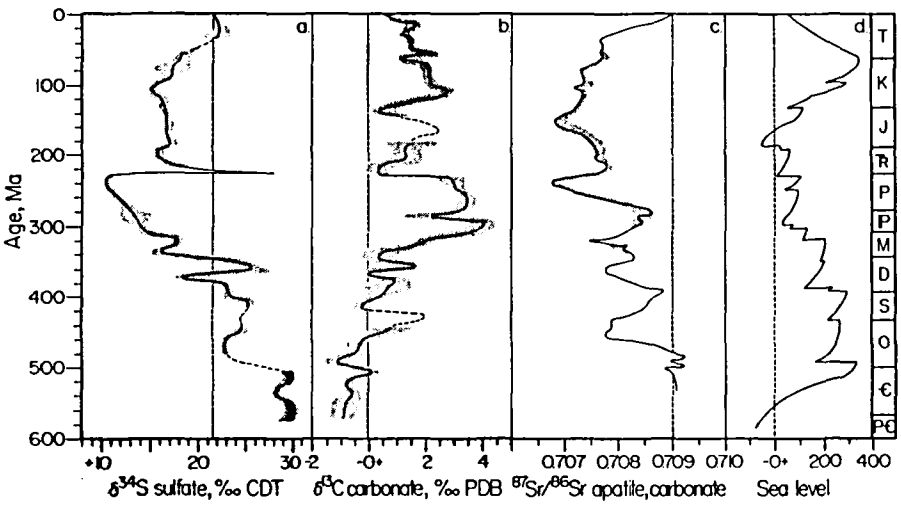

Figure I-18. Age curves of (a) sulfur isotopes in evaporite sulfate; (b) carbon isotopes in carbonate; (c) strontium isotopes in carbonate and in fossil apatite; and (d) sea level. Shading gives range of uncertainty; dashed lines, lack of data.

William Holser

B. Javor: MICROBIOLOGY OF SOLAR SALT PONDS

Solar salt ponds are shallow ponds of brines that range in salinity from that of normal seawater (3.4 percent) through NaCl saturation. Some salterns evaporate brines to the potash stage of concentration (bitterns). All the brines (except the bitterns, which are devoid of life) harbor high concentrations of microorganisms. Oligotrophic brines, ranging from ca. 2X to 4X seawater, have thick bottom mat communities whereas very eutrophic systems harbor dense planktonic populations or benthic and planktonic microbial communities. Gypsum precipitates as grains or solid rock in brines that are concentrated ca. 4X to 7X from seawater. Planktonic populations dominate these brines perhaps because mat-forming communities cannot develop due to rapid burial by $CaSO_4$. The diversity of eukaryotes decreases with increasing salinity, and only one metazoan thrives in 20 percent NaCl brines (the brine shrimp *Artemia salina*). In NaCl-saturated brines, which harbor plankton only, the microbiota consists of the green alga, *Dunaliella*, halobacteria, and some moderately halophilic bacteria. Population densities increase with increasing brine concentration in NaCl-saturated brines, but this increase may be due to passive concentration as a result of evaporation. The bitterns may be devoid of life because concentrations of essential ions are too high or too low, or because the low water activity of such brines (less than 68 per cent) precludes life.

Borowitzka, L.J., 1981. The microflora: adaptations to life in extremely saline lakes, Hydrobiologia, 81:33-46.

Carpelan, L.H., 1957. Hydrobiology of the Alviso salt ponds, Ecology, 38:375-390.

Cohen, Y., Krumbein, W.E., and Shilo, M., 1977. Solar Lake (Sinai). 2. Distribution of photosynthetic microorganisms and primary productivity, Limnol. Oceanog., 22:609-620.

Davis, J.S., 1978. Biological communities of a nutrient salina, Aquat. Bot., 4:23-42.

Hermann, A.G., Knake, D., Schneider, J., and Peters, H., 1973. Geochemistry of modern seawater and brines from salt pans: main components and bromine distribution, Contrib. Mineral. Petrol., 40:1-24.

Javor, B.J., 1983. Planktonic standing crop and nutrients in a saltern ecosystem, Limnol. Oceanog., 28:153-159.

Javor, B.J., 1984. Nutrients and ecology of the western salt and Exportadora de Sal saltern brines. In *Sixth Symposium on Salt*, (in press).

Kushner, D.J., 1978. Life in high salt and solute concentrations: halophilic bacteria. In *Microbial Life in Extreme Environments.* (D.J. Kushner, ed.), Academic Press, New York, pp. 317-368.

Nissenbaum, A., 1975. The microbiology and biogeochemistry of the Dead Sea, Microb. Ecol., 2:139-161.

Post, F.J., 1977. The microbial ecology of the Great Salt Lake, Microb. Ecol., 3:143-165.

J.F. Kasting: EVOLUTION OF THE ATMOSPHERE

The Earth's atmosphere must be of secondary origin; that is, it was outgassed from the interior rather than captured from the solar nebula. The evidence for this is the strong fractionation of rare gases (Ne, A, Kr, Xe) relative to solar abundances. These gases could not have been lost over time by escape to space or by chemical interactions with the crust; hence, their concentrations would be much higher today if the atmosphere were originally derived from nebular materials. If the Earth's crust has always been close to its present oxidation state, as seems likely, the "excess volatiles" that were outgassed would have consisted primarily of H_2O, CO_2 and N_2, with smaller amounts of CO, H_2, SO_2, CH_4, and H_2S. The composition of such an atmosphere might be described as weakly reducing.

The climate of the Archean Earth would have been influenced by the fact that solar luminosity was approximately 25-30 percent lower than it is today. Since liquid water existed on the Earth's surface, the early atmosphere must have contained some infrared absorbing "greenhouse" gases in addition to those present today to compensate for the low solar flux. The most likely scenario involves greatly enhanced levels, perhaps 100-1000 the PAL (Present Atmospheric Level) of CO_2. There are additional reasons to believe CO_2 levels were higher in the past, involving differences in the carbonate-silicate geochemical cycle. Because of increased volcanic and tectonic activity the weathering of calcium silicate ($CO_2+CaSiO_3 \rightarrow CaCO_3+SiO_2$) would have been slower, while the reverse reaction, which occurs during metamorphism, would have been faster.

The O_2 content of the prebiotic atmosphere can be estimated by balancing sources and sinks of H_2. The governing equation may be written as:

$$\Phi esc(H) + 4 \times R(H_2CO) = \Phi out(H) + 2 \times R(H_2O_2)$$

where esc(H) is the rate at which hydrogen escapes to space, $\Phi out(H)$ is the volcanic flux of reduced gases, and $R(H_2CO)$ and $R(H_2O_2)$ are the rainout rates of formaldehyde and hydrogen peroxide, respectively. The rainout terms become important at CO_2 levels much higher than those of today. Model calculations yield H_2 mixing ratios on the order of 10^{-4} to 10^{-3} and extremely low surface O_2 mixing ratios ($\lesssim 10^{-12}$.)

The effect of life on the atmosphere was probably small until the evolution and subsequent widespread distribution of bacterial photosynthesis. With bacterial photosynthesis H_2 levels would have been lowered and atmospheric CH_4 levels would have risen as a result of the activities of methanogens. Distribution of methanogens on a global scale may be recorded by the wide spread in delta ^{13}C values in the organic material in sediments around

2.8 billion years ago.

Evidence in the geological record for oxygenic photosynthesis dates from at least 2.5 billion years ago, the time at which the Hamersley iron formations of Western Australia were deposited. However, the oxygen-producing photosynthetic process of bacteria may have originated much earlier. The effect of oxygenic photosynthesis on the atmosphere depends upon the relative rates of supply of reduced and oxidized materials to the atmosphere, surface ocean, and deep ocean. The surface ocean and atmosphere may have switched from reducing to oxidizing about 2.4 billion years ago, based on evidence from detrital uraninites, fluvial deposits (redbeds), and paleosols. The deep ocean apparenty remained anaerobic until approximately 1.7 billion years ago, at which time the banded iron formations disappeared. The interpretation of the geologic record is clouded by the possible importance of atmospheric oxidants other than O_2, specifically H_2O_2.

Atmospheric O_2 levels must have reached some relatively high, stable value (10^{-3}–10^{-2} PAL) by about 1.4 billion years ago, the time at which eukaryotes first appeared. The origin of metazoa, some 600 million years to 1.0 billion years ago, presumably required still higher O_2 levels (10^{-2}–10^{-1} PAL? – see Schopf, chapter 13). The emergence of land life during the late Silurian (480 million years ago) indicates that O_2 levels probably exceeded 10^{-1} PAL, the amount required to generate an effective ozone screen against solar ultraviolet radiation. These are all lower limits on atmospheric O_2. Oxygen concentrations may have been much higher than this, perhaps reaching the present level as early as 1.7 billion years ago. In this case the appearance of shelled organisms at the beginning of the Cambrian and the emergence of land life during the Silurian would be completely unrelated to changes in atmospheric oxygen, contrary to suggestions by Cloud (1972) and Berkner and Marshall (1964). Further analysis of the geologic record is needed to more accurately estimate the history of atmospheric oxygen.

Berkner, L.V. and Marshall, L.L., 1964. On the origin and rise of oxygen concentration in the Earth's atmosphere, J. Atmos. Sci., 22:225-261.

Chapman, D.J. and Schopf, J.W., 1983. Biological and biochemical effects of the development of an aerobic environment. Chapter 13. In *The Earth's Earliest Biosphere: Its Origin and Evolution.* (J.W. Schopf, ed.), Princeton University Press, Princeton, 543 p.

Cloud, P.E., 1972. A working model of the primitive Earth, Am. J. Sci., 272:537-548.

Cogley, J.J. and Henderson-Sellers, A., 1984. The origin and earliest of the Earth's hydrosphere, Rev. Geophys. Sp. Phys., 22:131-175.

Holland, H.D., 1984. *The Chemical Evolution of the Atmosphere and Oceans*. Princeton University Press, Princeton, 582 pp.

Kasting, J.F. and Donahue, T.M., 1980. The evolution of atmospheric ozone, J. Geophys. Res., 85:3255-3263.

Kasting, J.F., Pollack, J.B., and Crisp, D., 1984. Effects of high CO_2 levels on surface temperature and atmospheric oxidation state of the early earth, J. Atmos. Chem., 1:402-428.

Lewis, J.S. and Prinn, R.G., 1984. *Planets and Their Atmospheres: Origin and Evolution*. Academic Press, New York, NY, 470 pp.

Schneider, S.H. and Londer, R., 1984. *The Coevolution of Climate and Life*. Sierra Club Books, San Francisco, 563 pp.

Schopf, J.W. (ed.), 1983. *The Earth's Earliest Biosphere: Its Origin and Evolution*. Princeton University Press, Princeton, 543 pp.

Walker, J.C.G., 1977. *Evolution of the Atmosphere*. MacMillan, New York, 318 pp.

Michael J. Klug: SULFUR CYCLING IN FRESHWATER SEDIMENTS

Organic sulfur-containing compounds represent greater than 80 percent of the total sulfur in sediments of eutrophic freshwater lakes. Although sedimentary sulfur is predominantly in the form of organic compounds, more sulfur is transformed by sulfate reduction than by any other process. Rates of sulfate reduction in these sediments average 7 mmol/m^2/day. This rate is 19 times greater than the net rate of production of inorganic sulfur from organic compounds on an annual basis.

Ingvorsen, K., Zeikus, J.G., and Brock, T.D., 1982. Dynamics of bacterial sulfate reduction in a eutrophic lake, Appl. Environ. Microbiol., 42:1029-1036

Ivanov, M.V., 1983. The sulfur cycle in lakes and continental reservoirs. In *The Global Biogeochemical Sulphur Cycle*. (M.V. Ivanov and J.R. Freney, eds.), John Wiley and Sons, New York.

King, G.M. and Klug, M.J., 1982. Comparative aspects of sulfur mineralization in sediments of a eutrophic lake basin, Appl. Environ. Microbiol., 43:1406-1412.

Laanbroek, H.J. and Pfennig, N., 1981. Oxidation of short-chain fatty acids by sulfate-reducing bacteria in freshwater and marine sediments, Arch. Microbiol., 128:330-335.

Lovley, D.R. and Klug, M.J., 1982. Intermediary metabolism of organic matter in the sediments of a eutrophic lake, Appl. Environ. Microbiol., 43:552-560.

Lovley, D.R. and Klug, M.J., 1983. Sulfate reducers can outcompete methanogens at freshwater sulfate concentrations, Appl. Environ. Microbiol., 45:187-192.

Lovley, D.R., Dwyer, D.F., and Klug, M.J., 1982. Kinetic analysis of competition between sulfate reducers and methanogens in sediments, Appl. Environ. Microbiol., 43:1373-1379.

Nriagar, J.O., 1968. Sulfur metabolism and sedimentary environment: Lake Mendota, Wisconsin, Limnol. Oceanog., 13:430-439.

Smith, R.L. and Klug, M.J., 1981. Reduction of sulfur compounds in the sediments of a eutrophic lake basin, Appl. Environ. Microbiol., 41:1230-1237.

Smith, R.L. and Klug, M.J., 1981. Electron donors utilized by sulfate-reducing bacteria in eutrophic lake sediments, Appl. Environ. Microbiol., 42:116-121.

Winfrey, M.R. and Zeikus, J.G., 1977. Effect of sulfate on carbon and electron flow during microbial methanogenesis in freshwater sediments, Appl. Environ. Microbiol., 33:275-281.

J.E. Lovelock: SOME THOUGHTS ON GAIA AND THE SULFUR CYCLE

Hypotheses are tested by the accuracy of their predictions. The gaia hypothesis states that the composition, oxidation-reduction state, and temperature of the troposphere are actively regulated by the biota for the biota (Lovelock, 1979). One of the early predictions of the gaia hypothesis was that there should be a sulfur compound made by the biota in the oceans. It would need to be stable enough against oxidation in water to allow its transfer to the air. Either the sulfur compound itself or its atmospheric oxidation product would have to return sulfur from the sea to the land surfaces. The most likely candidate for this role was dimethyl sulfide.

This gaian prediction has been handsomely confirmed by observations of M. Andreae. DMS was found to be abundantly produced by algal blooms, particularly those over the continental shelf regions. The production is so large that DMS can be considered to be the principal sulfur carrier of the natural environment.

Many biologists who might otherwise favor the gaia hypothesis find it difficult to comprehend the channel of communication that instructs marine microorganisms to produce DMS for the "benefit" of the land biota. The scenario that follows is one possible explanation of the development of this link.

The synthesis of propiothetin (that is, beta dimethyl sulfonioproprionate or DMSP), DMS, and DMSO probably began as a device for the protection of marine microorganisms against salt stress (see Fig. I-2). It may not be so well known that DMSO is the most effective neutral solute for protection against the adverse effects of dehydration or freezing. I proposed its use for this purpose in 1957 and it has been used since then, perhaps unwisely, to freeze human embryos in a viable state. Propiothetin and betaines are able to protect against salt stress (they are osmolytes) (see Fig. I-1). The protective action of betaines and their relation to DMS has been noted (Andreae and Raemdonck, 1983). DMS is a byproduct and an end product of the metabolism of DMSO and of DMSP.

Imagine some early, possibly Archean ecosystem existing on the tidal reaches of the shore of a land mass. When the tide receded the organisms left behind would be subject to severe desiccation and salt stress. The production of the DMSO family of compounds would be one answer to these immediate problems. An unintended consequence would be the escape of DMS to the air as a byproduct. On-shore breezes would deliver sulfur from the DMS to the land biota that previously had been depleted in sulfur. They would then flourish and in time this would lead to an increase in the runoff of nutrients such as nitrates and phosphates from the land. This would encourage the further growth of algae and so on. This process could easily be modeled: there would be a spread of land biota inwards as the DMS penetrated further inland and a spread of the DMS producers as the nutrients spread into the ocean waters. These arguments apply to

the production of volatile compounds of other essential elements (e.g., selenium and iodine).

Do the phaeophyte algae, *Laminaria*, that produce methyl iodide in surprisingly large quantities, contain an iodonium betaine?

$$CH_3.I^+.CH_2.CH_2.COO^-$$

Laminarians might be the major source of tropospheric methyl iodide.

Another sulfur compound of interest from a gaian viewpoint is CS_2 (carbon disulfide). If CS_2 is a biological product arising from anaerobic biosynthesis in the sediments, then its production could provide an economic form of climate regulation. CS_2 oxidizes to COS (carbonyl sulfide) in the atmosphere. The compound COS has a residence time of months, long enough to ensure its transfer to the stratosphere. Once in the stratosphere it oxidizes further to form the sulfuric acid aerosol and the presence of this aerosol alters the Earth's radiation balance causing a cooling of the surface.

Bob Garrels wonders if CS_2 played a major role in early Archean biogeochemistry as a surrogate for CO_2 in the metabolism of the photosynthetic sulfur bacteria. Can CS_2 be used as a carbon source instead of CO_2 in anaerobic photosynthetic sulfur bacteria or cyanobacteria? The biochemistry of CS_2 production might be rewarding to study.

Andreae, M.O. and Raemdonck, H., 1983. Dimethyl sulfide in the surface ocean and the marine atmosphere: a global view, Science 221: 744-747.

Lovelock, J.E., 1979. *Gaia: A New Look at Life on Earth*, Oxford University Press, Oxford, U.K.

NOTE: Unfortunately Dr. Lovelock was unable to attend the PBME course. That his enthusiasm for it was unbounded is attested to by this voluntary contribution which he submitted on July 15, 1984. For further references, please see the lecture abstract of M. Andreae at the beginning of this volume.

L. Margulis: FROM MICROBIAL COMMUNITIES TO CELLS

The eukaryotic cell, the unit of structure of protoctists, plants, fungi, and animals, is not at all homologous to prokaryotic cells. Instead the eukaryotic cell is homologous to communities of microorganisms such as those of the sulfuretum. Waste of some members became food of others just as *Desulfuromonas* and *Chlorobium* or *Prosthecochloris* form symbiotrophies. We are testing the hypothesis that at least four different interacting community members entered the original associations that, when stabilized, led to the emergence of eukaryotic cells. These are: host nucleocytoplasm (*Thermoplasma*-like archaebacteria), mitochondria (*Paracoccus* or *Bdellovibrio*-like respiring bacteria; the alpha group of bacteria on p. 33), plastids (cyanobacteria) and undulipodia (spirochetes). We have recently found tubulin-like protein in the free-living spirochete *Spirochaeta bajacaliforniensis* and in several other spirochetes. Robert Obar, who has purified the tubulin-like protein, is determining amino acid sequence to see if the spirochete protein is homologous to the tubulin of undulipodial and mitotic spindle microtubules. The symbiotic theory is considered to have been demonstrated for plastids and mitochondria (Gray, 1983). Even if the spirochete aspect of the symbiotic theory fails to be proved the recognition of the microbial community status of eukaryotic cells still leads to the concept that plant and animal development and cell differentiation are aspects of the evolution of co-evolved microbial communities.

Fracek, S.J. and Stolz, J.F., 1985. *Spirochaeta bajacaliforniensis* sp. n. from a microbial mat at Laguna Figueroa, Baja California, Mexico, Arch. Microbiol., (in press).

Gray, M.W., 1983. Bacterial ancestry of plastids and mitochondria, Bioscience, 33:693-699.

Gray, M.W. and Doolittle, W.F., 1982. Has the endosymbiont hypothesis been proven? Microbiol. Rev., 46:1-42.

Margulis, L., 1982. *Early Life*, Science Books International, Boston, MA.

Margulis, L., 1981. *Symbiosis in Cell Evolution*, W.H. Freeman Co., San Francisco.

Margulis, L., Chapman, D., and Corliss, J.O., (eds.), 1985. *The Protoctista: The Structure, Cultivation, Habitats and Life Cycles of the Eukaryotic Microorganisms and Their Descendants*. Jones and Bartlett Publishing Co., Boston, (in preparation).

Margulis, L. and Sagan, D., 1985. *Origins of Sex*. Yale University Press, New Haven, CT, (in press).

Margulis, L. and Schwartz, K. V.. 1982. *Five Kingdoms: An Illustrated Guide to the Phyla of Life on Earth.* W. H. Freeman Co., San Francisco.

Margulis, L. and Stolz, J.. 1983. Microbial systematics and a Gaian view of the sediments. In *Biomineralization.* (P. Westbroek and E. deJong, eds.). Reidel Publishing Co., Dordrecht, The Netherlands, pp.27-54..

Obar, R., 1985. The purification of a tubulin-like protein from *Spirochaeta bajacaliforniensis*, PhD Thesis, Boston University Graduate School.

Sagan, D. and Margulis, L.. 1985. *The Expanding Microcosm. Four Billion Years of Evolution.* Summit Books, New York, (in press).

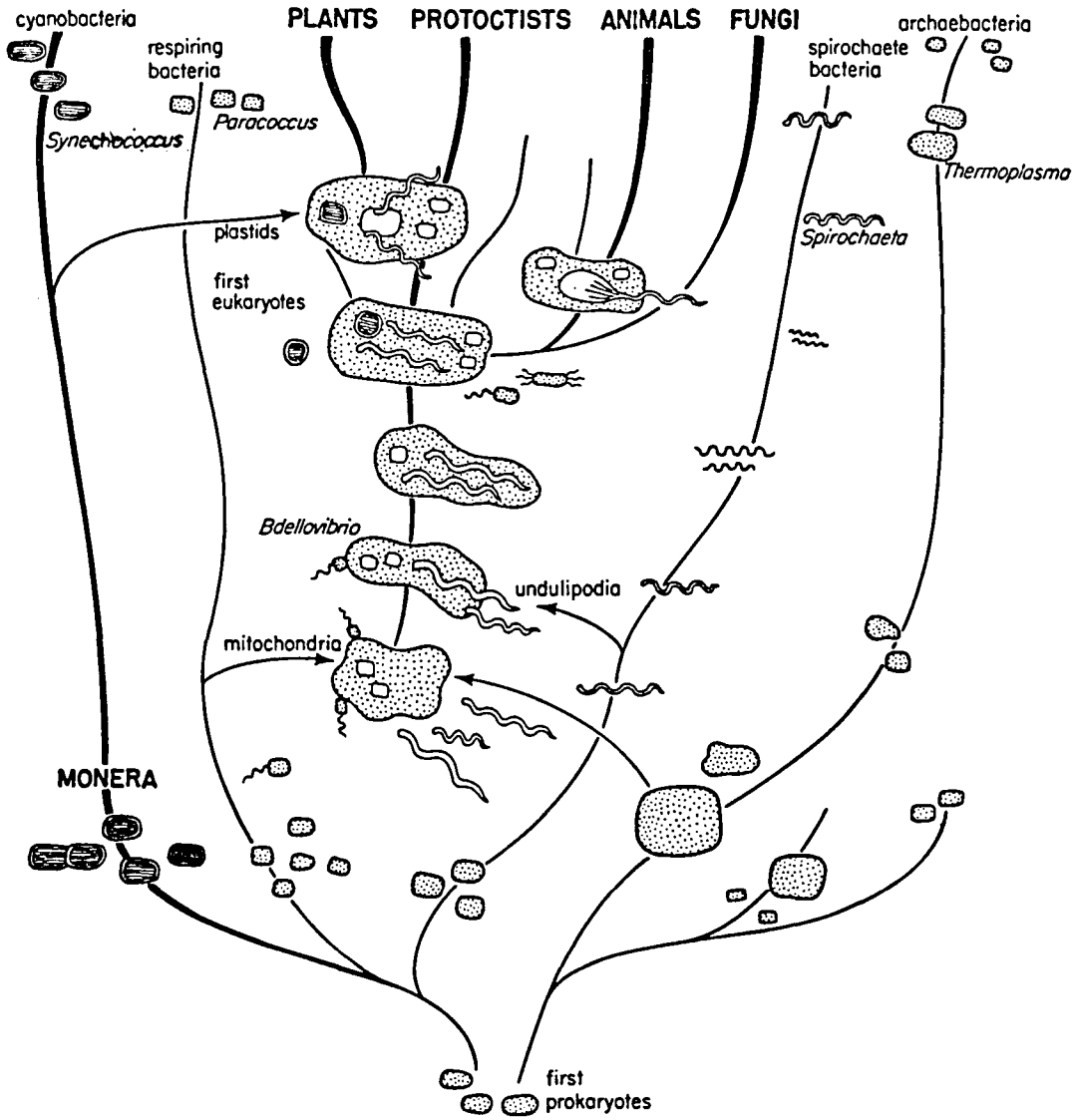

Figure I-19. The emergence of eukaryotic cells from bacterial communities. (from Margulis and Sagan, Origins of Sex, Yale University Press, 1985, in press).

C.S. Martens: SULFUR AND CARBON CYCLING IN ORGANIC-RICH MARINE SEDIMENTS

Nearshore, continental shelf, and slope sediments are important sites of microbially-mediated carbon and sulfur cycling. Marine geochemists have investigated the rates and mechanisms of cycling processes in these environments by chemical distribution studies, *in situ* rate measurements, and steady-state kinetic modeling. Pore water chemical distributions, sulfate reduction rates, and sediment-water chemical fluxes were used to describe cycling on a ten year time scale in a small, rapidly depositing coastal basin, Cape Lookout Bight, and at general sites on the upper continental slope off North Carolina, U.S.A. In combination with ^{210}Pb sediment accumulation rates, these data were used to establish quantitative carbon and sulfur budgets as well as the relative importance of sulfate reduction and methanogenesis as the last steps in the degradation of organic matter.

Berner, R.A., 1980. *Early Diagenesis, A Theoretical Approach.* Princeton University Press, Princeton, 241 pp.

Berner, R.A., 1984. Sedimentary pyrite formation: An update, Geochim. Cosmochim. Acta, 48:605-615.

Crill, P.M. and Martens, C.S., 1983. Spatial and temporal fluctuations of methane production in anoxic coastal marine sediments, Limnol. Oceanog., 28:1117-1130.

Goldhaber, M.B. and Kaplan, I.R., 1974. The sulfur cycle. In *The Sea*, (E.D. Goldberg, ed.), Vol. 4, John Wiley and Sons, Inc., New York, pp. 569-655.

Goldhaber, M.B. and Kaplan, I.R., 1980. Mechanisms of sulfur incorporation and isotope fractionation during early diagenesis in sediments of the Gulf of California, Mar. Chem., 9:95-143.

Jorgensen, B.B., 1977. The sulfur cycle of a coastal marine sediment (Limfjorden, Denmark), Limnol. Oceanog., 22:814-832.

Jorgensen, B.B., 1982. Ecology of the bacteria of the sulfur cycle with special reference to anoxic-oxic interface environments, Phil. Trans. R. Soc. Lond. B, 298:543-561.

King, G.M. and Klug, M.J., 1982. Comparative aspects of sulfur mineralization in sediments of a eutrophic lake basin, Appl. Environ. Microbiol., 43:1406-1412.

Laanbroek, H.J. and Pfennig, N., 1981. Oxidation of short chain fatty acids by sulfate-reducing bacteria in freshwater and in marine sediments, Arch. Microbiol., 128:330-335.

Martens, C.S. and Goldhaber, M.B., 1978. Early diagenesis in transitional sedimentary environments of the White Oak River Estuary, Limnol. Oceanog., 23:429-443.

Martens, C.S. and Klump, J.V., 1984. Biogeochemical cycling in an organic-rich coastal marine basin. 4. An organic carbon budget for sediments dominated by sulfate reduction and methanogenesis, Geochim. Cosmochim. Acta, 48:1987-2004.

Reeburgh, W.S., 1983. Rates of biogeochemical processes in anoxic sediments, Ann. Rev. Earth Planet. Sci., 11:269-298.

Sansone, F.J. and Martens, C.S., 1982. Volatile fatty acid cycling in organic-rich marine sediments, Geochim. Cosmochim. Acta, 46:1575-1589.

Troelsen, H. and Jorgensen, B.B., 1982. Seasonal dynamics of elemental sulfur in two coastal sediments, Estuarine, Coastal and Shelf Science, 15:255-266.

A. Matin: CHEMOLITHOTROPHY AND PHYSIOLOGY OF BACTERIAL NUTRIENT LIMITATION

An overview of the physiology of chemolithotrophic bacteria, particularly the thiobacilli, was presented. In these bacteria unique physiological traits are expressed during nutrient-limited growth. Different physiological types of chemolithotrophs, pathways of sulfur oxidation, and electron transport in the thiobacilli, problems encountered by chemolithotrophs in the generation of reducing power, and some explanations of the phenomenon of obligate chemolithotrophy were considered. Mixotrophy in the thiobacilli has been studied extensively both under nutrient excess and limitation. In nature, bacteria usually grow under nutrient limitation. Yet the bulk of our knowledge of microbial metabolic function is derived from bacteria grown in laboratory batch cultures containing a great abundance of nutrients. Microbial behavior in these two types of environments can be very different, indicating the need for basing an understanding of microbial ecology on studies that rely on cultivation of microorganisms under nutrient limitation. Nutrient-limited bacteria differ in several ways from those growing in large quantities of nutrients. They have different surface structures and make a much fuller use of their metabolic potential, especially by the synthesis of unique pathways of catabolic enzymes.

Harder, W. and Dijkhuizen, L., 1983. Physiological responses to nutrient limitation, Ann. Rev. Microbiol., 37:1-23.

Kelly, D.P., 1978. Bioenergetics of chemolithotrophic bacteria. In *Companion to Microbiology*, (A.T. Bull and P.M. Meadow, eds.), Longman, London, 363 p.

Lu, W.P. and Kelly, D.P., 1984. Oxidation of inorganic sulfur compounds by thiobacilli. In *Microbial Growth on C$_1$ Compounds*, (R.L. Crawford and R.S. Hanson, eds.), American Society for Microbiology, Washington, D.C., p. 34.

Matin, A., 1978. Organic nutrition of chemolithotrophic bacteria, Ann. Rev. Microbiol., 32:433-468.

Matin, A., 1979. Microbial regulatory mechanisms at low nutrient concentrations as studied in chemostat. In *Life Sciences Research Report*, (M. Shilo, ed.), Vol. 13, Verlag Chemie, Weinheim, FL.

Matin, A., 1984. Mixotrophy in facultative thiobacilli. In *Microbial Chemoautotrophy*, (W.R. Strohl and O.H. Tuovinen, eds.), Ohio State University Press, Columbus, Ohio, pp. 57-78.

Matin, A., 1984. Mixotrophy and chemiosmotic apects of acidophilism in facultative thiobacilli. In *Microbial Growth on C-1 Compounds*, (R.L. Crawford and R.S. Hanson, eds.), American Society of Microbiology, Washington, D.C., p. 62.

K.H. Nealson: POSSIBLE ROLES OF MANGANESE REDOX CHEMISTRY IN THE SULFUR CYCLE

Manganese commonly exists in two valence states, which are easily interchangable by chemical redox reactions. These are the soluble Mn(II) ion, and the Mn(IV) ion, which is usually found as one of several possible insoluble oxides or manganates (designated as MnO_2). Oxidation is favored in alkaline (high pH) and oxidizing (high Eh) environments, whereas reduction is favored by acidic and reducing conditions. Bacteria can catalyze both oxidation and reduction.

Sulfate-reducing bacteria (SRB) are very potent MnO_2 reducers by virtue of their sulfide production: H_2S reacts rapidly with MnO_2 to yield Mn(II), elemental sulfur, and water. In manganese-rich zones, Mn cycles rapidly if sulfate is present to drive the reduction and the MnO_2 precipitates and sinks into anaerobic zones. The production of sulfide (by organisms requiring organic carbon compounds) to reduce manganese oxides might act to couple the carbon and sulfur cycles in water bodies in which the two cycles are physically separated. Iron has been proposed for this provision of reducing power by (Jorgensen, 1983), but since MnS is soluble and FeS is very insoluble in water, it is equally likely that manganese rather than iron provides the electrons to the more oxidized surface layers.

Burdige, D.J., 1983. Biogeochemistry of Mn redox reactions, Ph.D. thesis, Scripps Institution of Oceanography, Univ. California, San Diego, La Jolla, CA.

Jørgensen, B.B., 1983. Ecology of the bacteria of the sulfur cycle, Phil. Trans. R. Soc. London B, 298:543-561.

Stone, A.T., 1983. Reduction and dissolution of Mn(III) and Mn(IV) oxides by organics, Ph.D. thesis, Division of Earth and Planetary Science, California Institute of Technology, Pasadena, CA.

H.D. Peck: SULFATE-REDUCING BACTERIA: MICROBIOLOGY AND PHYSIOLOGY

Recent discoveries have changed our concept of the sulfate-reducing bacteria: formerly considered a small group of anaerobes with limited metabolic capabilities we now recognize that they are a large group of bacteria with diverse metabolic capabilities. The sulfate bacteria are essential members of the microbial food chain in anaerobic high sulfate marine water but they also flourish in low sulfate fresh water as hydrogen-producing bacteria (they produce hydrogen for interspecies hydrogen transfer). The sulfate-reducing bacteria vary greatly in their modes of growth: dissimilatory sulfate reducers can grow heterotrophically using a large number of organic substrates including acetate and long-chain fatty acids up to C_{18}, aromatic compounds, alcohols, and hydroxy acids; they can grow autotrophically with hydrogen or formate plus sulfate; they can ferment the simple organic compounds pyruvate, fumarate, lactate, choline; they can utilize inorganic pyrophosphate as a source of energy for growth; they can reduce nitrate rather than sulfate as a terminal electron acceptor, growing in association with photosynthetic bacteria; and they can grow using hydrogen derived from other bacteria. All sulfate-reducing bacteria are strict anaerobes. Thydrogenases are important in the bioenergetics and biochemistry of dissimilatory sulfate reduction. The sulfate reducing bacteria contain two types of periplasmic hydrogenase, a nickel-non-heme iron hydrogenase with four redox centers and a (non-nickel) non-heme iron hydrogenase with three redox centers. Both hydrogenases utilize periplasmic cytochrome c_3 (MW = 13,000) as their cofactor for the reduction of low molecular weight electron transfer proteins.

The sulfate reducing bacteria, the first non-photosynthetic anaerobic bacteria demonstrated to contain c-type cytochromes, perform electron transfer coupled to phosphorylation. A new bioenergetic scheme for the formation of a proton gradient for growth of *Desulfovibrio* on organic substrates and sulfate involving vectors/electron transfer and consistent with the cellular localization of enzymes and electron transfer components has been proposed. Hydrogen is produced in the cytoplasm from organic substrates and, as a permease molecule diffuses rapidly across the cytoplasmic membrane, it is oxidized to protons and electrons by the periplasmic hydrogenase. The electrons only are transferred across the cytoplasmic membrane to the cytoplasm where they are used to reduce sulfate to sulfide. The protons are used for transport or to drive a reversible ATPase. The net effect is the transfer of protons across the cytoplasmic membrane with the intervention of a proton pump. This type of H_2 cycling is relevant to the bioenergetics of other types of anaerobic microorganisms.

Akagi, J.M., 1981. Dissimilatory sulfate reduction: mechanistic aspects. In *Biology of Inorganic Nitrogen and Sulfur*. (E. Bothe and A. Trebst, eds.), Springer Verlag, pp. 169-177.

Biebl, H. and Pfennig, N., 1977. Growth of sulfate reducing bacteria with sulfur as electron acceptor, Arch. Microbiol., 112:115-117.

Bramlett, R.N. and Peck, H.D. Jr., 1975. Some physical and kinetic properties of adenylyl sulfate reductase, J. Biol. Chem., 250:2979-2786.

Lui, C.L., Hart, N., and Peck, H.D. Jr., 1982. Utilization of inorganic pyrophosphate as an energy source for the growth of the sulfate reducing bacteria, Science, 217:363-364.

Lui, C.L., DerVartanian, D.V., and Peck, H.D. Jr., 1979. On the redox properties of three bisulfite reductases from the sulfate reducing bacteria, Biochem. Biophys. Res. Commun., 91:962-970.

LeGall, J., DerVartanian, D.V. and Peck, H.D. Jr., 1979. Flavoproteins, iron proteins and hemoproteins as electron transfer components of the sulfate reducing bacteria, Current Topics in Bioenergetics, 9:237-265.

Murphy, M.J. and Siegel, L.M., 1973. Siroheme and sirohydrochlorin. The basis for a new type of porphyrin-related prosthetic group common to both assimilatory and dissimilatory sulfite reductases, J. Biol. Chem., 248:6911-6919.

Pfennig, N., Widdel, F., and Trueper, H. G., 1981. The dissimilatory sulfate reducing bacteria. In *The Prokaryotes*. (M. P. Starr et al., eds.), Vol. I, Springer Verlag, New York.

Peck, H.D. Jr., 1984. Physiological diversity of the sulfate reducing bacteria. In *Microbial Chemoautotrophy*. (W.R. Strohl and O.H. Tuovinen, eds.), Ohio State University Press, Columbus.

Postgate, J.R., 1979. *The Sulphate Reducing Bacteria*, Cambridge University Press, Cambridge, U.K.

Steenkamp, D.J. and Peck, H.D. Jr., 1981. Protein translocation associa Tuovinen, eds.), Ohio State University Press, Columbus.

Postgate, J.R., 1979. *The Sulphate Reducing Bacteria*, Cambridge University Press, Cambridge, U.K.

Steenkamp, D.J. and Peck, H.D. Jr., 1981. Protein translocation associated with nitrile repiration in *Desulfovibrio desulfuricans*, J. Biol. Chem., 256:5450-5458.

Wolin, M.J. and Miller, T.L., 1982. Interactions of microbial populations in cellulose fermentations, Fed. Proc., 42:109-113.

D.L. Peterson: BIOGEOCHEMICAL CYCLING AND REMOTE SENSING

Research is underway at the NASA Ames Research Center that is concerned with aspects of the nitrogen cycle in terrestrial ecosystems. An interdisciplinary research group is attempting to corelate nitrogen transformations, processes, and productivity with variables that can be remotely sensed. Recent NASA and other publications concerning biogeochemical cycling at global scales identify attributes of vegetation that could be related or explain the spatial variation in biologically functional variables. These functional variables include net primary productivity, annual nitrogen mineralization, and possibly the emission rate of nitrous oxide from soils.

Leaf area index of temperate coniferous forests has been estimated using remote sensing. Leaf area index (LAI), the one-sided projected area of canopies to a unit of ground area, has been consistently identified as a key structural variable. Canopy radiation models show that increased leaf layers in a canopy produce increased reflectance in the infrared region and that this property is asymptotic at LAI=7-8 (Fig. I-20). The reflectance in the infrared region is measured by band 4 (0.90 microns) on the Thematic Mapper (TM) satellite or by simulated TM data obtained by the Daedalus scanner on the NASA U-2 aircraft. Photosynthetically active radiation, especially in the red region, is strongly absorbed by leaves. In fully developed forests, the reflectance in the red region is very low and asymptotic at only LAI=2-3. The red region measurements are complicated by radiance added due to atmospheric scattering and the variation due to transmittance as a function of path length through air masses. We are evaluating these effects with helicopter measurements directly above the canopies of our chosen research sites using a portable field radiometer. In addition, the lack of reliable atmospheric correction algorithms for land scenes force us to compensate by using only relative values or ratios. We use band 3 to normalize the band 4 measurements which compensate for small differences between sites. However, this ratio does not remove the influence on sensitivity that preliminary calculations show reduce the sensitivity to LAI by a factor of about four.

To obtain a range of LAI, we selected sites that follow a temperature-moisture gradient across west-central Oregon. Leaf development in Oregon coniferous forests respond to this gradient from mild and moist temperatures on the coast to hot temperatures and dry sites in the desert (Fig. I-21). Net primary productivity was related to LAI by Henry Gholz (Fig. I-22). Most of the forest stands (sites) are dense, mature forests with nearly closed canopies (a major source of variation in remotely sensed data). Dimensional measurements were made at each site and applied to allometric relations to derive stand level leaf biomass and area. The relationship of these LAI estimates to the ratio of bands 4/3 (infrared/red reflectance) is shown in

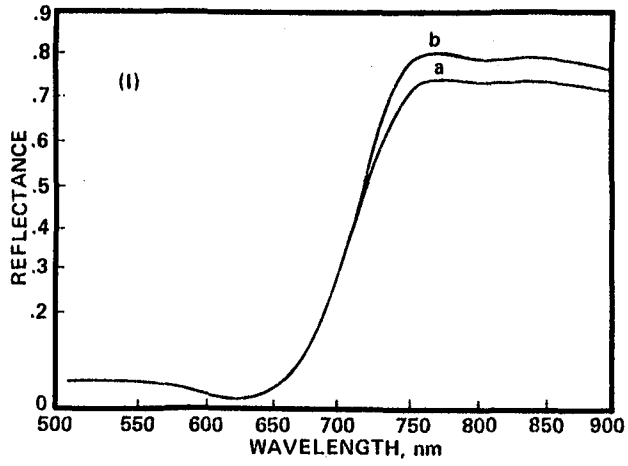

Figure I-20. Theoretical models of reflected radiation using deterministic methods for plant canopies. Courtesy of NASA Ames Research Center.

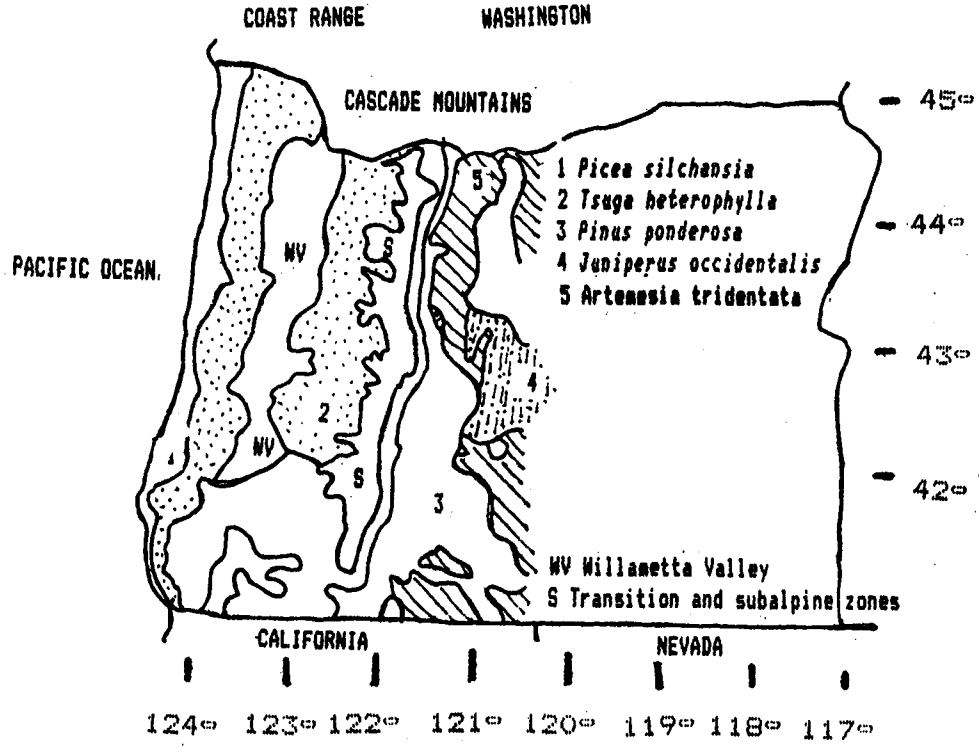

Figure I-21. Location of transect and vegetation zones in Oregon.

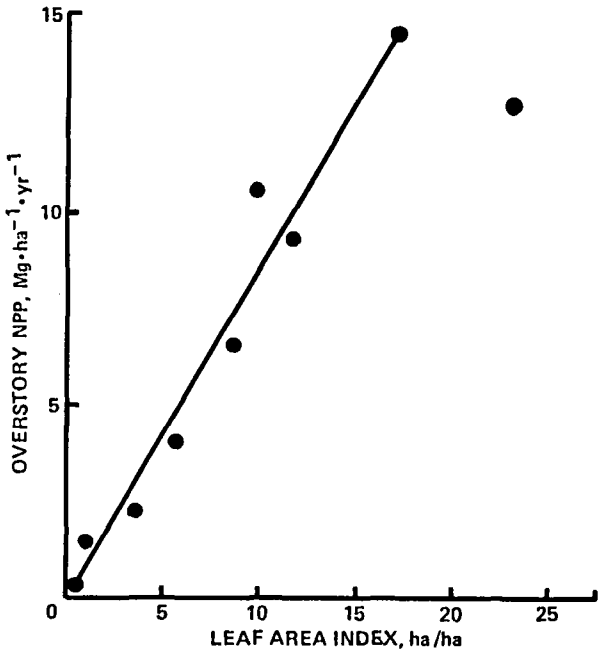

Figure I-22. Relationship between overstory net primary productivity (NPP in Mg/hectare/year) and leaf area (in hectare/hectare) for Oregon transect. Courtesy of Gholz, H.L., 1982.

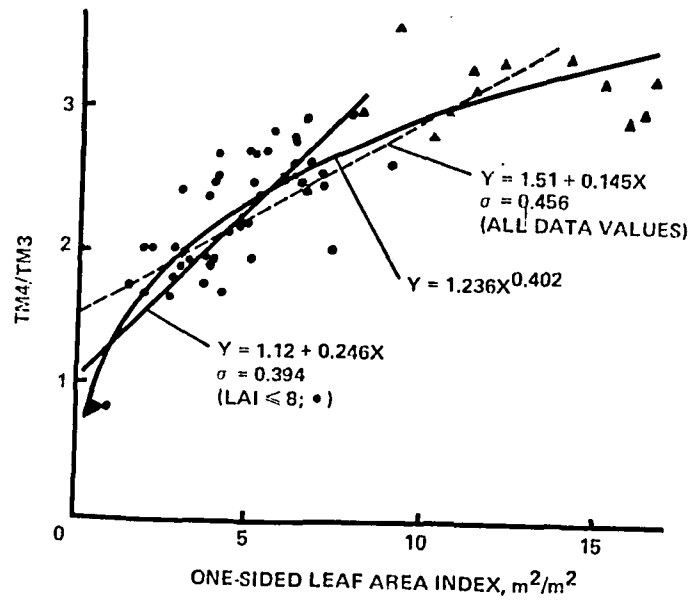

Figure I-23. Relationship of leaf area index (LAI) of secondary sample units to the ratio of thematic mapper (TMS) band 4/band 3.

Figure I-23. A good predictive relationship exists between both the linear and logarithmic curves. The log relationship appears to match the asymptotic behavior best, and this is more consistent with model expectations.

We are beginning to use high spectral resolution remote sensing data for deriving canopy biochemistry. Data are being synthesized from several well-established research sites in Alaska and Wisconsin and other areas for forests of different fertilities and contrasting environments. The synthesis will be used to develop and test a semi-mechanistic process-level model that combines plant-water relations, carbon assimilation-allocation, and nitrogen-phosphorus cycling. Estimates of total canopy nitrogen, phosphorus, and lignin content together with microclimate will be used to drive the model. This model is designed to use remotely sensed inputs, particularly leaf chemistry.

Total canopy nitrogen, phosphorus, and lignin content are the required inputs for remote sensing. Nitrogen, for example, is bound up primarily in chlorophylls and the proteins of leaves. Each organic constituent of leaves has unique absorption properties due to specific stretching frequencies of the chemical bonds. This fine spectral information cannot be observed with broad-band satellites such as the TM. However, new scanners are now available to make high spectral resolution (10 nm) between 1400 and 2400 nm (later from 400 to 2400 nm) measurements using the Airborne Imaging Spectrometer from JPL. The spectral curves for the four major leaf constituents - proteins, water, oils, and carbohydrates - are shown in Figure I-24. Through a combination of wet chemical and spectrophotometric analyses, we plan to develop multi-linear regressions and related corelation techniques which can be used to infer these biochemical variables from the scanner.

Chance, J.E. and LeMaster, E.W., 1977. Suits reflectance models for wheat and cotton: theoretical and experimental tests, Applied Optics, 16: 407-412.

Spanner, M.A., Peterson, D.C., Hall, M., Wrigley, R., and Running, S.W., 1984. Atmospheric effects on remote sensing of forest leaf area index. Proc. 18th International Symp. Remote Sensing of Environment, Paris.

Gholz, H.L., 1982. Environmental limits on above ground net primary production, leaf area, and biomass in vegetation zones of the Pacific Northwest, Ecology, 61:469-481.

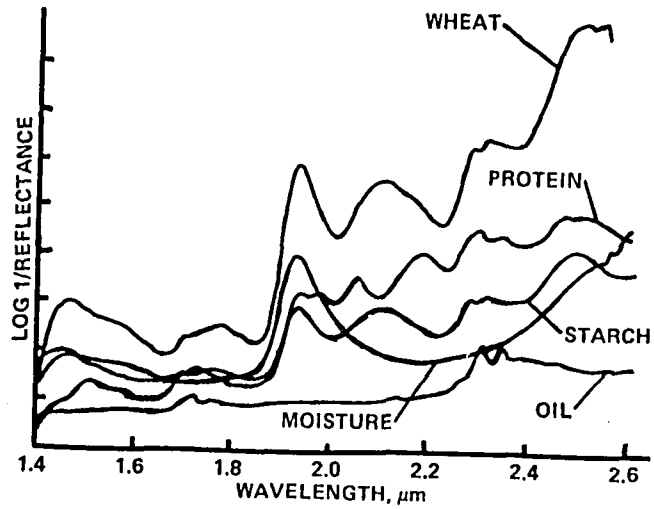

Figure I-24. Organic constituent spectra and typical composite spectra for grain (wheat berries).

Spanner, M. A., Teuber, K., Acevedo, W., Peterson, D. L., Running, S. W., and Card, D. H., 1984. Remote sensing of the leaf area index of temperate coniferous forests. Proc. 10th International Symp. Machine Processing of Remotely Sensed Data, pp. 362-370.

Hruschka, W. R. and Norris, K. H., 1982. Least squares curve fitting of near-infrared spectra predicts protein and moisture contents of ground wheat, Applied Spectroscopy, 36:261-265.

Goetz, A. F. H., Rock, B. N., and Rowan, L. C., 1983. Remote sensing for exploration: An overview, Economic Geology, 78:573-590.

T.M. Schmidt: STRUCTURE AND PHYSIOLOGY OF *BEGGIATOA* AND *THIOTHRIX*

Beggiatoa and *Thiothrix* are genera of filamentous, colorless, sulfide-oxidizing bacteria. These organisms are microaerophilic, oxidizing sulfide to sulfur in the presence of oxygen. The sulfur accumulates in intracellular sulfur globules - the outstanding morphological feature of these bacteria. Some strains are able to further oxidize the sulfur to sulfate aerobically or reduce the sulfur to sulfide anaerobically. This metabolic versatility makes these bacteria important links in aquatic sulfur cycles.

Jørgensen, B.B., 1982. Ecology of the bacteria of the sulphur cycle with special reference to anoxic-oxic interface environments Phil. Trans. R. Soc. Lond., B298:543-61.

Jørgensen, B.B., an and *Thioploca* Ann. Rev. Microbiol., 37:341-67.

Nelson, D.C., and Castenholz, R.W., 1981. Use of reduced sulfur compounds by *Beggiatoa* sp., J. Bacteriol., 147:140-154.

Nelson, D.C. and Jannasch, H.W., 1983. Chemoautotrophic growth of a marine *Beggiatoa* in sulfide-gradient cultures, Arch. Microbiol., 136:262-69.

Strohl, W.R. and Larkin, J.M., 1978. Enumeration, isolation, and characterization of *Beggiatoa* from freshwater sediments Appl. Environ. Microbiol., 36:755-70.

Strohl, W.R. and Schmidt, T.M., 1984. Mixotrophy of the colorless, sulfide-oxidizing gliding bacteria *Beggiatoa* and *Thiothrix*, In *Microbial Chemoautotrophy* (W.R.Strohl and O.H. Tuovinen, eds.), Ohio State University Press, Columbus.

+ positive
- negative
+/- some strains positive
? unknown

CHARACTERISTIC	*BEGGIATOA*	*THIOTHRIX* *	*THIOPLACA*
Trichome formation	+	+	+
Sheath	-	+	+ (common)
Holdfast	-	+	-
Rosette formation	-	+	-
Hormogonium formation	+/-	+	? (horm.)**
Gliding of intact trichomes	+	-	+
Gliding of hormogonia	+	+	?
Sulfur inclusions from sulfide	+	+	+
Sulfur inclusions from thiosulfide	+/-	+	?
Cytochromes	*b,c,a,o*	*c*, (others?)	?
Quinones	Q_8	Q_8	?
Acetate assimilation	+	+	+
Acetate oxidation to CO_2	+	?	?
CO_2 assimilation	low	moderate	?
Reduced sulfur requirement	-	+	?
Sulfide-dependent oxygen consumption	+	+	?

* Data pertaining to *Thiothrix* used in this study

** *Thioploca* has not been cultured axenically, horm. = hormogonia

Table I-5. Morphological and physiological comparison of *Thiothrix*, *Beggiatoa*, and *Thioploca*.

H.G. Trueper: PHOTOTROPHIC BACTERIA AND THEIR ROLE IN THE BIOGEOCHEMICAL SULFUR CYCLE

An essential step that cannot be bypassed in the biogeochemical cycle of sulfur today is dissimilatory sulfate reduction by anaerobic bacteria. The enormous amounts of sulfides produced by these are oxidized again either anaerobically by phototrophic bacteria or aerobically by thiobacilli and large chemotrophic bacteria (*Beggiatoa*, *Thiovulum*, etc.) Phototrophic bacteria use sulfide, sulfur, thiosulfate, and sulfite as electron donors for photosynthesis. The most obvious intermediate in their oxidative sulfur metabolism is a long chain polysulfide that appears as so-called sulfur globules either inside (Chromatiaceae) or outside (Ectothiorhodospiraceae, Chlorobiaceae, and some of the Rhodospirillaceae) the cells. The enzymes involved in phototrophic bacterial sulfur metabolism are cytochrome c, flavocytochrome c, reverse siroheme sulfite reductase, thiosulfate sulfur transferase, thiosulfate:acceptor oxidoreductase, adenylylsulfate reductase, ADP sulfurylase, ATP sulfurylase, and sulfite:acceptor oxidoreductase. Molecular oxygen is not involved in any of these steps. The amount of carbon assimilated by phototrophic bacteria per mole sulfide oxidized to sulfate is about 10 fold higher than that assimilated by chemolithotrophic sulfur-oxidizing bacteria. Phototrophic sulfur bacteria therefore are the predominant primary producers in the sulfuretum. During dark periods under anoxic conditions phototrophic bacteria perform a slow fermentative maintenance metabolism, during which they reduce elemental sulfur and polysulfides to H_2S. At low partial pressures of oxygen several species of the Chromatiaceae (e.g., *Chromatium vinosum*, *Thiocystis violacea*) are also capable of oxidizing reduced sulfur compounds in the dark. They possess an energy metabolism like that of chemolithotrophic bacteria. The assimilation of sulfur compounds in phototrophic bacteria is in principle identical with that of non-phototrophic bacteria. However the Chlorobiaceae and some of the Chromatiaceae and Rhodospirillaceae, unable to reduce sulfate, rely upon reduced sulfur for biosynthetic purposes.

Kondratieva, E.N., Ivanovsky, R.N., and Krasilnikova, E.N., 1981. Light and dark metabolism in purple sulfur bacteria, Soviet Scientific Reviews, 2:325-364.

Pfennig, N., and Trueper, H. G., 1983. Taxonomy of the photosynthetic green and purple sulfur bacteria, Annales de Microbiologie (Institut Pasteur), 134B:9-20.

Trudinger, P.A. and Loughlin, R.E., 1981. Metabolism of simple sulphur compounds. In *Comprehensive Biochemistry*. (M. Florkin and E.H. Stotz, eds.), Vol. 19A (A. Neuberger and L.L.M. van Deenen, eds.), Elsevier, Amsterdam, pp. 165-256.

Trueper, H. G., 1981. Photolithotrophic sulfur oxidation. In *Biology of Inorganic Nitrogen and Sulfur*. (H. Bothe and A. Trebst, eds.), Springer Verlag, New York, pp. 199-211.

Trueper, H. G. 1984a. Microorganisms and the sulfur cycle. In *Sulfur - The Significance for Chemistry, Biology and Geology*. (A. Mueller and B. Krebs, eds.), Elsevier, Amsterdam.

Trueper, H. G. 1984b. Phototrophic bacteria and their sulfur metabolism. In *Sulfur - The Significance for Chemistry, Biology and Geology*. (A. Mueller and B. Krebs, eds.), Elsevier, Amsterdam.

Trueper H. G. and Fischer, U., 1982. Anaerobic oxidation of sulphur compounds as electron donors for bacterial photosynthesis, Phil. Trans. R. Soc. London B, 298:529-542.

Starr, M.P., Stolp, H., Trueper, H.G., Balows, A., and Schlegel, H.G., (eds.), 1981. *The Prokaryotes*, Springer Verlag, New York.

Metabolic type (all anaerobic)	Mechanisms	Microorganisms
Dissimilatory Sulfate Reduction	Electron acceptors: Sulfate, Thiosulfate, Sulfite Electron donors: Organic compounds or H_2 Product: H_2 Carbon source: organic compounds or CO_2	*Desulfovibrio* *Desulfotomaculum* *Desulfomonas* *Desulfobacter* *Desulfobulbus* *Desulfococcus* *Desulfosarcina* *Desulfonema* *Thermodesulfobacterium*
	Electron acceptors: Sulfur Electron donors: Organic compounds or H_2 Product: H_2S Carbon source: organic compounds or CO_2	*Desulfuromonas* *Desulfovibrio (some)* *Campylobacter (some)* *Wolinella* Chromatiaceae (dark) Chlorobiaceae (dark) *Beggiatoa* *Thermoproteus* *Thermodiscus* *Pyrodictium* *Thermococcus*

For list of references see Trueper, 1984 b.

Table I-6. Inorganic sulfur compounds as electron acceptors in bacteria.

Metabolic type	Mechanism	Microorganisms
Phototrophic Sulfur Oxidation (anaerobic)	Electron donors: Sulfide Sulfur Thiosulfate (Sulfite) Photosynthesis (CO_2 Fixation) Product: Sulfate Carbon source: CO_2 and/or organic compounds	Chlorobiaceae Chromatiaceae *Ectothiorhodospira* Rhodospirillaceae (some) Chloroflexaceae Cyanobacteria (some)
Chemotrophic Sulfur Oxidation (anaerobic)	Electron donors: Sulfide Sulfur Thiosulfate (Sulfite) Electron acceptor: Nitrate Product: Sulfate Carbon source: CO_2	*Thiobacillus denitrificans* *Thiomicrospira denitrificans*
Chemotrophic Sulfur Oxidation (aerobic)	Electron donors: Sulfide Sulfur Thiosulfate (Sulfite) Electron acceptor: O_2 Product: Sulfate Carbon source: CO_2 or organic compounds	*Thiobacillus* *Thiomicrospira* *Sulfolobus* *Thermothrix* *Paracoccus* *Pseudomonas* *Beggiatoa* *Thiothrix* *Thiospira* *Thioploca* *Macromonas* *Achromatium* *Thiobacterium* Chromatiaceae (dark, some species) Many heterotrophs

For list of references see Trueper, 1984b.

Table I-7. Inorganic sulfur compounds as electron donors in bacteria.

J.H. Yopp: THE ROLE OF SULFUR IN OSMOREGULATION AND SALINITY TOLERANCE IN CYANOBACTERIA, ALGAE, AND PLANTS

Organosulfur compounds are involved in osmoregulation and salinity tolerance in some cyanobacteria and photosynthetic eukaryotes.

Glycinebetaine, the osmolyte of the halotolerant cyanobacterium, *Aphanothece halophytica*, requires the sulfonium compound, S-adenosyl-methionine (SAM) for its synthesis. Glutamate is the nitrogen source, SAM is the methyl-carbon and serine the carbon "backbone" source of this unique osmolyte. Inhibitor studies suggest that photorespiration interacts with sulfur metabolism to control betaine synthesis in cyanobacteria. The limiting factor for SAM synthesis is formate from photorespiration. SAM is, in turn, the methyl donor for betaine synthesis from serine. The nitrogen component of serine is from glutamate (Fig. I-26). Betaine synthesis is hypothesized to be regulated via potassium.

The biosynthesis of dimethyl-B-propiothetin (DMPT, which is the same as beta-dimethyl sulfoniopropionate - see Fig I-1), and diacylsulfoquinovosylglycerol have been elucidated as have their roles in osmoregulation and salinity tolerance. The relation between these sulfolipids and the sulfur cycle was discussed.

Challenger, F., Bywood, R., Thomas, P., and Haywood, B.J., 1957. Studies on biological methylation. XVII. The natural occurence and chemical reactions of some thetins, Arch. Biochem. Biophys., 69:514-523.

Craigie, J.S. and McCandless, E., 1979. Sulfated polysaccharides in red and brown algae, Ann. Rev. Pl. Physiol., 30:41-53.

Greene, R.C., 1962. Biosynthesis of dimethyl-I-propiothetin, J. Biol. Chem., 237(7):2251-2254.

Ishida, Y. and Kadota, H., 1968. Participation of dimethyl-3-propiothetin in transmethylation reaction in *Gyrodinium cohnii*, Nippon Suisan Gakkaishi, 34:699-705.

Kylin, A., Kuiper, P.J.C., and Hansson, G., 1972. Lipids from sugar beet in relation to the preparation and properties of sodium and potassium-activated ATPases, Physiol. Plant., 26:271-278.

Larker, F., Hammelin, J., and Stewart, G.R., 1977. 3-Dimethylsulfonium propanoic acid from *Spartine anglica*, Phytochem., 16:2019-2020.

Miller, D.M., Jones, J.H. and Yopp, J.H., 1976. Ion metabolism in a halophilic blue-green alga, *Aphanothece halophytica*, Arch. Microbiol., 11:145-149.

Reed, R.H., 1983. Measurement and osmotic significance of B-dimethylsulfonio-propionate in marine organisms, Mar. Biol. Lett., 4(3):173-182.

Stuiver, C.E.E., Kuiper, P.J.C., and Marshner, H., 1978. Lipids from bean barley and sugar beet in relation to salt resistance, Physiol. Plantar., 42:124-128.

Tindall, D.R., Yopp, J.H., Schmid, W.E., and Miller, D.M., 1977. Protein and amino acid composition of the obligate halophile, *Aphanothece halophytica*, J. Phycol., 13:127-133.

Pavlicek, K.V. and Yopp, J.H., 1982. Betaine as a compatible solute in the complete relief of salt inhibition of glucose-6-phosphate dehydrogenase from a halophilic blue-green alga, Plant Physiol., 69:585.

Venable, W.C., Miller, D.M., and Yopp, J. H., 1979. Pulsed NMR study of an obligately halophilic blue-green alga, Physiol. Chem. Phys., 10(5):405-414.

Yopp, J.H., Miller, D.M., and Tindall, D.R., 1978. Isolation, purification and evidence of the obligately halophilic nature of the blue-green alga, *Aphanothece halophytica*, Phycologia, 17:172-178.

Yopp, J.H., Tindall, D.R., Miller, D.M., and Schmid, W.E., 1978. Regulation of intracellular water potential in the halophilic blue-green alga, *Aphanothece halophytica*. In *Energetics and Structure of Halophilic Microorganisms*, (S.R. Kaplan and M. Ginzburg, eds.), Elsevier Press, pp. 619-624.

Yopp, J.H., Miller, D.M., and Albright, G., 1979. Effects of antibiotics and UV radiation on growth and mutation of the halophilic blue-green alga, *Aphanothece halophytica*, Bot. Mar., 22:267-272.

Yopp, J.H., Pavledes, R., Solarz, J., and Shasteen, P., 1984. Origins of the osmolyte glycinebetaine in the halophilic cyanobacterium, *Aphanothece*, Plant Physiol., 75:65-S.

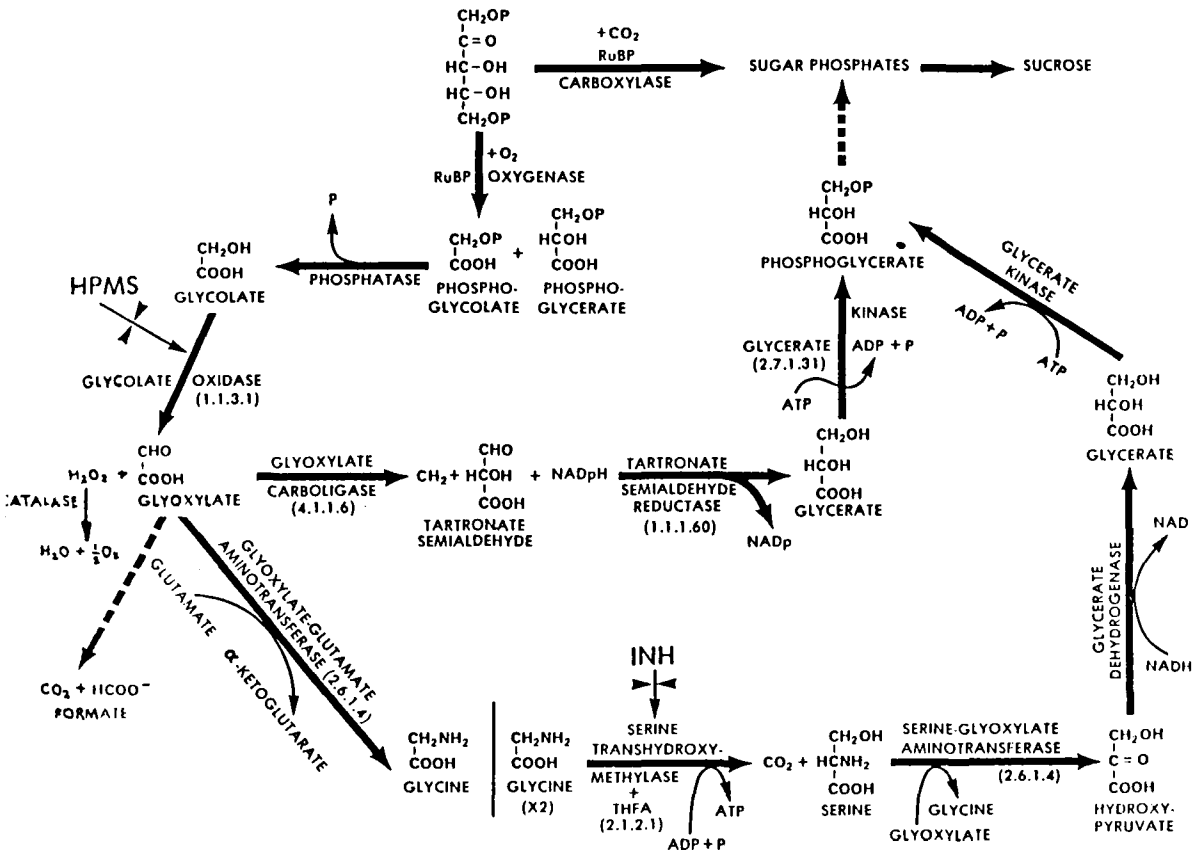

Figure I-25. Photorespiratory pathways in cyanobacteria.

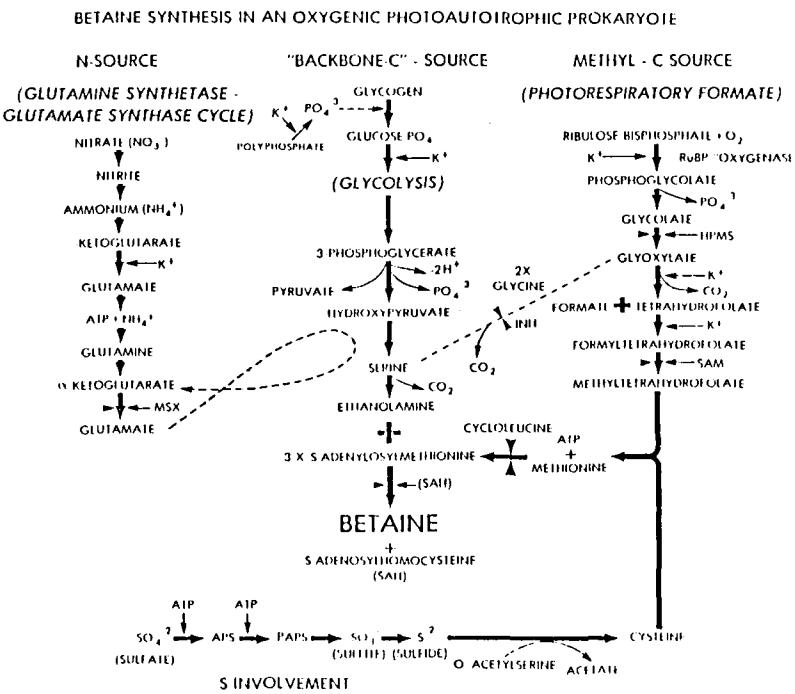

Figure I-26. Role of photorespiration, nitrogen metabolism, and sulfur metabolism in betaine synthesis by the cyanobacterium *Aphanothece halophytica*.

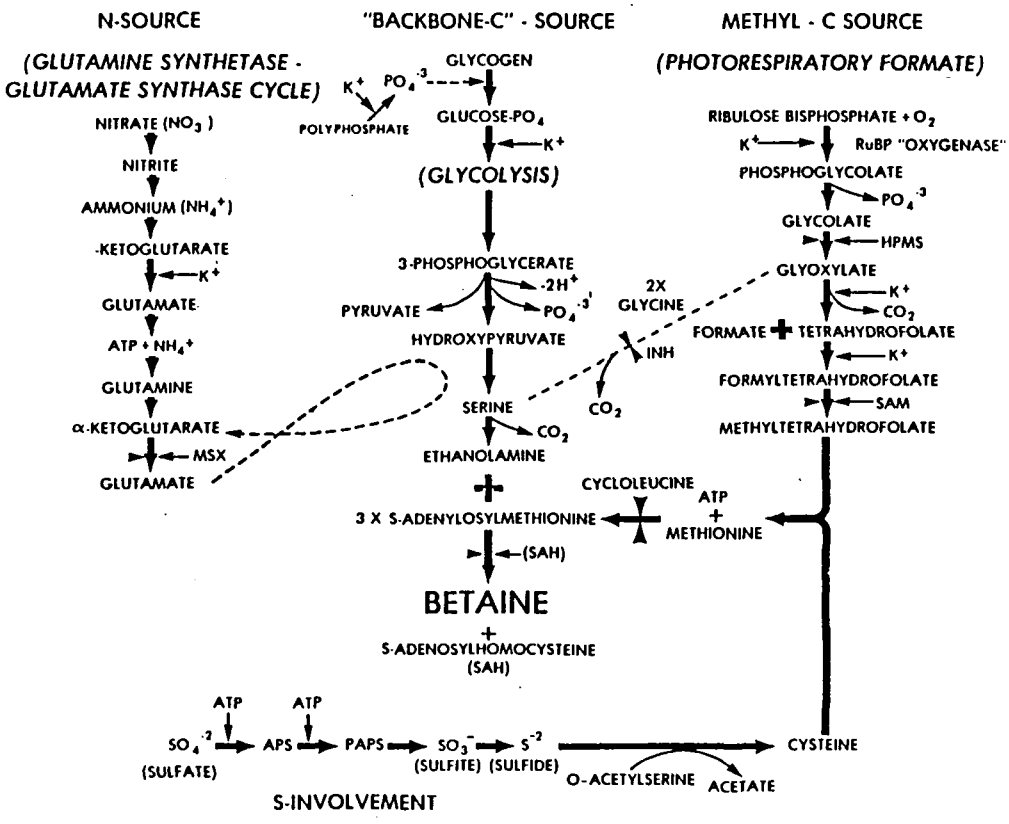

Figure I-27. Betaine synthesis in an oxygenic photoautotrophic prokaryote.

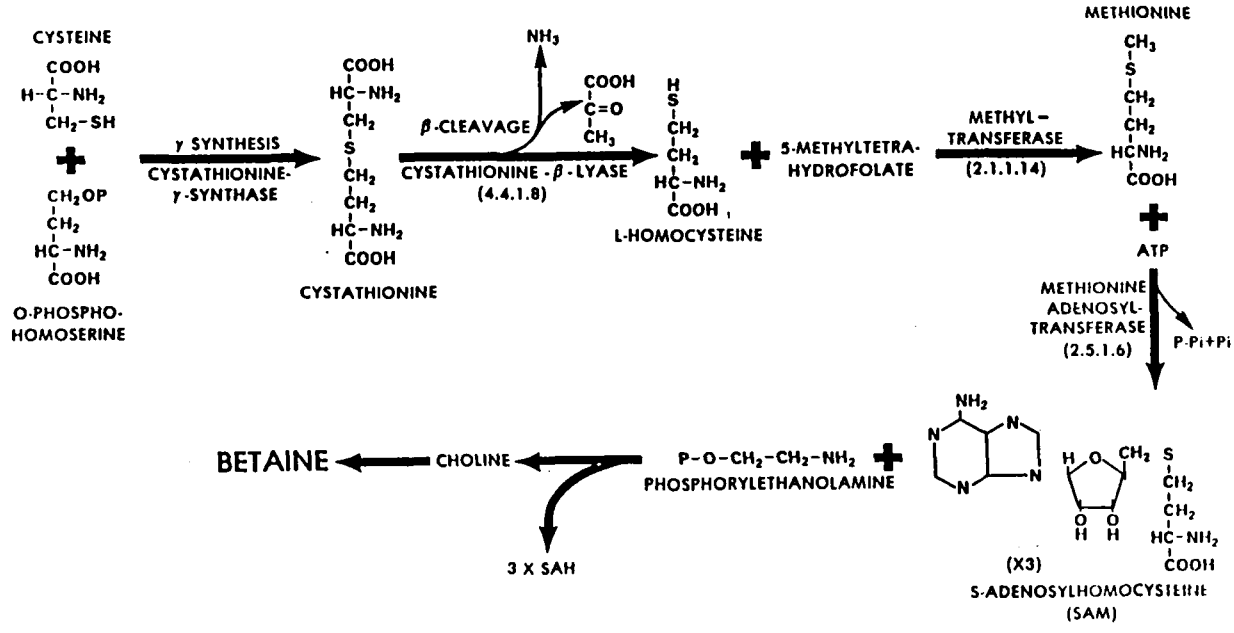

Figure I-28. Formation of the methyl donor of betaine - SAM.

CHAPTER II

SULFUR CYCLING AND METABOLISM OF PHOTOTROPHIC AND FILAMENTOUS SULFUR BACTERIA

Prof. R. Guerrero
D. Brune
R. Poplawski
T.M. Schmidt

Introduction

Sulfur, an abundant element in the biosphere, is rarely a limiting nutrient for organisms. Its proportion in living material has been estimated to be 1 atom of S for 15 atoms of N and 100 atoms of C. The element sulfur exists in oxidation states from -2 to +6 in organic and inorganic molecules. Microorganisms catalyse the oxidation and reduction of different forms of sulfur, establishing a cycle that involves sulfur incorporation into organic matter (anabolic, structural, slow cycling) or the use of different sulfur compounds as acceptors or donors of electrons (catabolic, energetic, rapid cycle). Nonassimilatory sulfur metabolism coupled with the carbon cycle may represent the oldest energy cycle in the biosphere, one used by the earliest autotrophic prokaryotes to obtain energy (Clark, 1981).

Hydrogen sulfide is a highly reactive, extremely toxic compound subject to both biological and nonbiological oxidation. Sulfide can be oxidized to sulfur and sulfate by bacteria under aerobic as well as anaerobic conditions. Some bacteria oxidize sulfide aerobically to generate energy. *Beggiatoa* and *Thiothrix*, for instance, are filamentous, microaerophilic bacteria capable of oxidizing sulfide, and depositing sulfur globules within the cells:

$$2\ H_2S + O_2 \longrightarrow 2S + 2\ H_2O$$

In the absence of sulfide, the sulfur globules are oxidized further to sulfate. These are typical "gradient organisms," positioning themselves in the interfaces of anaerobic environments (sulfate-reducing sediment or sulfide-rich layers of water) with overlying, partially oxygenated waters.

Hydrogen sulfide is also subject to biological photooxidation in anaerobic environments. Phototrophic sulfur bacteria (Chromatiaceae and Chlorobiaceae) are able to photoreduce carbon dioxide while oxidizing sulfide, first to elemental sulfur and later to sulfate (CH_2O symbolizes photosynthate):

$$CO_2 + 2\ H_2S \longrightarrow CH_2O + 2S + H_2O$$
$$3\ CO_2 + 2S + 5\ H_2O \longrightarrow 3\ CH_2O + 2\ H_2SO_4$$

Chromatiaceae are also capable of accumulating internal sulfur globules (the genus *Ectothiorhodospira* is the only exception, and accordingly will be separated into a new family). Some Chromatiaceae can tolerate low concentrations of oxygen and thus are also considered "gradient organisms."

Although oxidation of sulfide to sulfate by different microorganisms is well known, the use of internal sulfur globules as electron acceptors to oxidize or derive energy from storage compounds such as glycogen in the absence of an external source of energy (endogenous metabolism) was hypothesized a long time ago (Dawes and Ribbons, 1964; van Gemerden, 1968) but not definitively demonstrated.

To investigate different aspects of the ecophysiology of purple and green bacteria the following studies were performed:

1. Phototrophic sulfur bacteria taken from different habitats (Alum Rock State Park, Palo Alto salt marsh, and Big Soda Lake) were grown on selective media, characterized by morphological and pigment analysis, and compared with bacteria maintained in pure culture.

2. A study was made of the anaerobic reduction of intracellular sulfur globules by a phototrophic sulfur bacterium (*Chromatium vinosum*) and a filamentous aerobic sulfur bacterium (*Beggiatoa alba*).

3. Buoyant densities of different bacteria were measured in Percoll gradients. This method was also used to separate different chlorobia in mixed cultures and to assess the relative homogeneity of cultures taken directly or enriched from natural samples (including the purple bacterial layer found at a depth of 20 meters at Big Soda Lake.)

4. Interactions between sulfide-oxidizing bacteria were studied. Pairs of sulfide-oxidizing species competed for electrons (sulfide was the only available electron donor in the medium common to a purple sulfur bacterium (*Chromatium vinosum*), a green sulfur bacterium (*Chlorobium phaeobacteroides*) and a cyanobacterium (*Oscillatoria limnetica*)). These bacteria, selected because of their sulfide requirements and the fact that they can co-exist in aquatic enviroments where intense gradients occur, were handled pairwise by placement in a common medium separated by a membrane filter. Competition between two of these species at a time was measured under conditions where metabolites and toxins (but not cells) passed easily through the common culture medium.

References

Clark, B.C., 1981. Sulfur: Fountainhead of life in the universe? In *Life in the Universe* (J. Billingham, ed.), pp. 47-60, MIT Press, Cambridge.

Dawes, E.A. and Ribbons, D.W., 1964. Some aspects of the endogenous metabolism of bacteria, Bacteriol. Rev., 28:126-149.

van Germeden, H., 1968. On the ATP generation of *Chromatium* in darkness, Arch. Mikrobiol., 64:118-124.

ENRICHMENTS FOR PHOTOTROPHIC BACTERIA AND CHARACTERIZATION BY MORPHOLOGY AND PIGMENT ANALYSIS

D. Brune

Introduction

The purpose of this investigation was to examine several sulfide-containing environments for the presence of phototrophic bacteria and to obtain enriched cultures of some of the bacteria present. The field sites were Alum Rock State Park, the Palo Alto salt marsh, the bay area salt ponds (see map 1), and Big Soda Lake (near Fallon, Nevada). Bacteria from these sites were characterized by microscopic examination, measurement of *in vitro* absorption spectra, and analysis of carotenoid pigments.

Field observations at one of the bay area salt ponds, in which the salt concentration was saturating (about 30 percent NaCl) and the sediments along the shore of the pond were covered with a gypsum crust, revealed a layer of purple photosynthetic bacteria under a green layer in the gypsum crust. Samples of this gypsum crust were taken to the laboratory to measure light transmission through the crust and to try to identify the purple photosynthetic bacteria present in this extremely saline environment.

Materials and Methods

Water samples from Alum Rock State Park and from the Palo Alto salt marsh were collected in small screw-cap bottles or tubes. Pieces of the gypsum crust from the salt pond were placed in plastic bags. Water samples taken from different depths in Big Soda Lake using a sampling bottle were transferred to 150 ml glass bottles and to 500 ml and 1 liter plastic bottles that were completely filled and kept on ice during transportation to the laboratory.

In order to stop the movement of motile bacteria and to compress the bacterial cells being examined into one focal plane, agar slides were used for microscopic examination. The agar slides were prepared as follows (Dr. D. Caldwell, personal communication):

1. Difco bacto agar was dissoved in boiling H_2O to form a 0.75 percent solution.

2. The 0.75 percent agar was poured into 250 ml flasks to a depth of about 1 cm and allowed to solidify.

3. Salts were dialysed from the agar by washing with 3 changes of distilled H_2O over a 24 hour period while swirling on an orbital shaker.

4. A layer of clean microscope slides was placed on a clean, wet surface. (Water under the slides and on the edges of touching, adjacent slides inhibits seepage of agar around and under the slides.)

5. The agar was melted by autoclaving and poured over the slides to a depth of about 3 mm.

6. A glass plate was placed a few inches above the slides to protect them from gathering dust and the slides were allowed to dry over night.

7. The slides were then separated and stored in a box at room temperature for future use.

Water samples from the study areas were used to inoculate a culture medium for green and purple sulfur bacteria prepared as described by van Gemerden and Beeftink (1983). Pure bacterial cultures provided by Dr. R. Guerrero were also grown in this medium. NaCl (3 percent) was added to the medium for bacteria from the Palo Alto salt marsh. Samples of gypsum crust containing a distinct purple layer were placed in the same culture medium modified by including autoclaved water from the salt pond (500 ml/l of medium), thus giving a final salt concentration of about 15 percent. To discourage the growth of algae and cyanobacteria in this medium the inoculum was illuminated through a filter made from 2 layers of red and 2 layers of blue cellulose acetate. This filter absorbs visible light required for algal and cyanobacterial growth but transmits infrared light used in bacterial photosynthesis. The transmission spectrum of this filter is shown in Figure II-1.

Absorption and transmission spectra were obtained using a Varian Techtron model 635 UV-Vis spectrophotometer equipped with an X-Y recorder. Two methods were examined for obtaining *in vivo* spectra of photosynthetic sulfur bacteria. In the simplest method, cells in aqueous suspension were placed in the sample cuvette and water in the reference cuvette. The cuvettes were oriented so that the measuring beam of the spectrophotometer passed through the frosted rather than the clear glass faces of the cuvettes. This minimized the effect of light scattering by the bacterial cells by imposing a larger and nearly identical

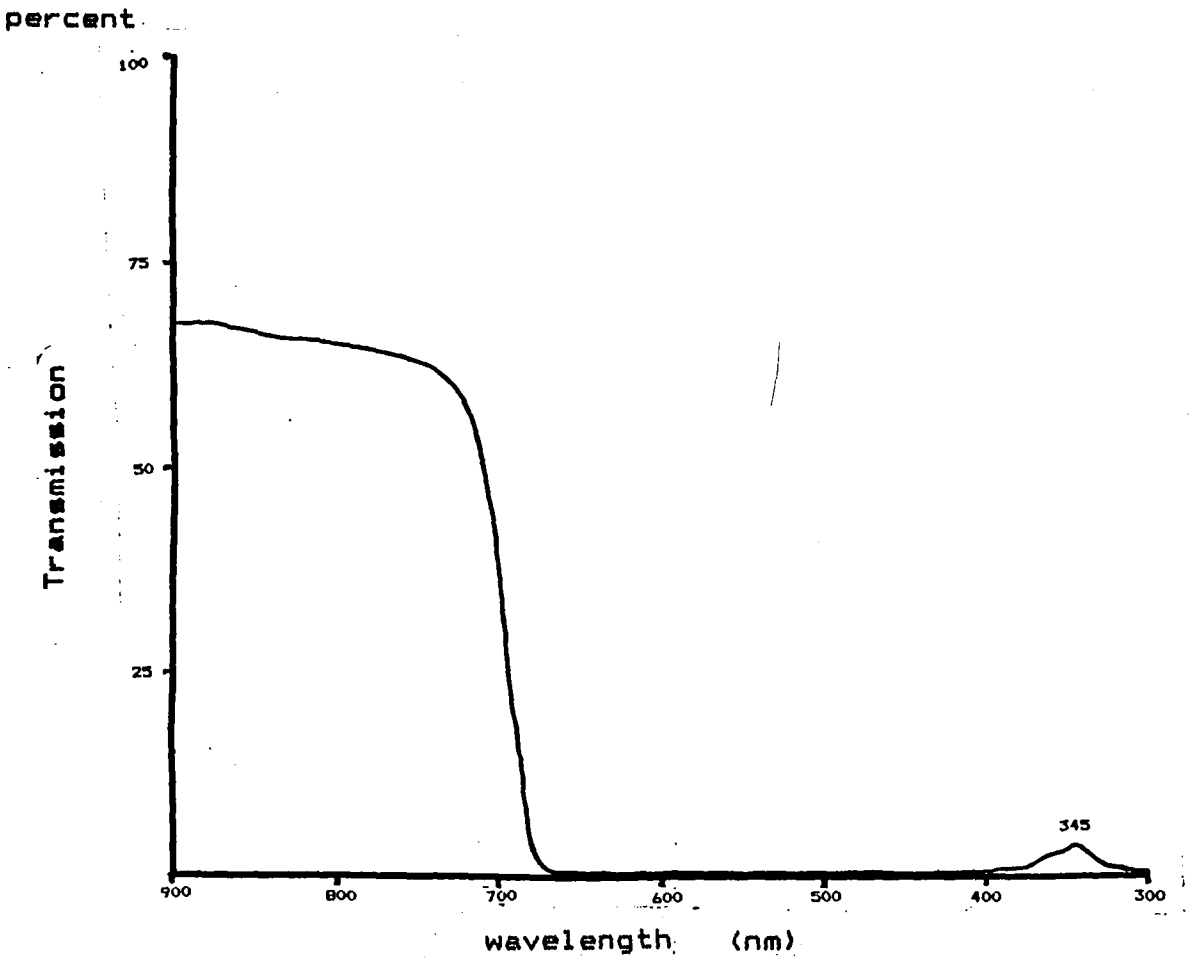

Figure II-1. Transmission spectrum of cellophane filter.

scattering on the light beams passing through the reference and sample cuvettes.

In the other method (Trueper and Yentsch, 1967), the bacterial cell suspension was loaded into a syringe. The bacteria were then collected by forcing the suspension through a Swinney filtration device with a fiberglass or millipore filter. Pieces of aluminum foil with rectangular slits about 15 mm x 4 mm were placed over the windows separating the spectrophotometer sample compartment from the photomultiplier compartment, with the slits aligned so that the reference and measuring light beams passed through them. The filter with the collected bacterial cells was taped over the slit on the sample side while an identical filter moistened with distilled water was taped over the slit on the reference side of the spectrophotometer.

Pieces of the gypsum crust from the salt pond sediment were prepared for light absorption measurement as follows. Loose particulate matter on top of the crust and black mud below the crust were removed by washing with tap water. Sections of crust about 1 cm x 2 to 2.5 cm were cut out using a hack saw blade. Four distinct layers seen in cross section through the gypsum crust could be observed. The uppermost layer was tan and about 2 mm thick. Under this was a green layer of similar thickness. Below the green layer was a thinner, somewhat irregular purple layer, and below this a very irregular, rather crumbly black layer. Using sand paper on the 1 cm x 2-2.5 cm blocks, it was possible to remove layers from the lower surface selectively and thus to obtain slabs consisting of the tan and green layers and the tan layer only. An attempt to obtain the purple layer only by removing the layers above was unsuccessful, although it was possible to obtain discontinuous patches of the purple layer attached to a green layer backing. Spectra of these layers were obtained by placing them in the sample cuvette holder of the spectrophotometer or taping them over a slit on a piece of aluminum foil taped over the window of the spectrophotometer sample compartment. (A piece of white tissue paper was placed over the window to the photomultiplier on the reference side of the sample compartment to partly offset light scattering by the gypsum crust.)

Carotenoids were extracted from bacterial cells and separated by thin layer chromatography as described by Montesinos et al (1983) with minor modifications. Chromatography was performed on both neutral alumina (Merck Type E, 60 F 254) and silica gel (Merck Kieselgel 60) plates without activation by heating prior to use. Colored spots were scraped from the chromatography plates and extracted with about 1 ml of acetone. After centrifugation to sediment the powdered silica gel or alumina, the liquid was decanted and placed in a microcuvette (1 cm pathlength, 0.6 ml volume) for measurement of the absorption spectrum.

Cells from Big Soda Lake used for carotenoid determination were collected by centrifugation from 1 liter of water collected from a depth of 20 m. The extract from the purple layer of the gypsum crust was made using a culture somewhat enriched in purple sulfur bacteria by growth under infrared illumination. This was not a pure culture, however, and also contained some filamentous cyanobacteria.

Carotenoids from these natural samples were chromatographed simultaneously with extracts of known carotenoid composition from cells of *Thiocapsa roseopersicina*, *Rhodopseudomonas capsulata*, *Chromatium vinosum*, and *Thiocystis gelatinosa* for comparison. These extracts were provided by Dr. R. Guerrero.

Results and Discussion

Figures II-2 through II-5 show the *in vivo* absorption spectra of 4 species of purple sulfur bacteria. These spectra were obtained using the first of the methods described, although similar spectra could be obtained using the second method (cells collected on filters). The first method is generally preferable with pure cultures because of its simplicity. The second method is useful, however, for concentrating cells from large dilute samples (e.g., the bacterial plate from Big Soda Lake) or samples in which settling of bacterial cells from an aqueous suspension prevents using the first method.

Figures II-2 through II-5 demonstrate that the absorption spectra of the pure cultures of purple sulfur bacteria differ significantly in wavelength, which ranges between 800 and 900 nm and between 430 and 550 nm. Light absorption between 800 and 900 nm is due to bacteriochlorophyl (Bchl a). Differences in absorption in this part of the spectrum are due to different interacti .. of Bchl a molecules with each other and with proteins (Thornber et al., 1978). Differences in absorption from 430 and 550 nm is due to the presence of different carotenoids. Although the absorption spectrum of a bacterial species depends on culture conditions, particularly light intensity (Thornber et al., 1978), Figure II-5 demonstrates, that absorption spectra may be characteristic enough to distinguish bacterial species.

The absorption of an enriched culture of a green sulfur bacterium obtained from a Palo Alto salt marsh water sample is shown in Figure II-6. The absorption maxima at 756 and 457 nm are characteristic of Bchl c (Pfennig, 1978). The cells failed to grow without NaCl added to the culture medium. Microscopic examination showed spherical cells about 1 um in diameter. This green bacterial species was identified as *Prosthecochloris aestuarii*.

The absorption spectrum of a green sulfur bacterial culture obtained from Alum Rock State Park is shown in Figure II-7. Bchl

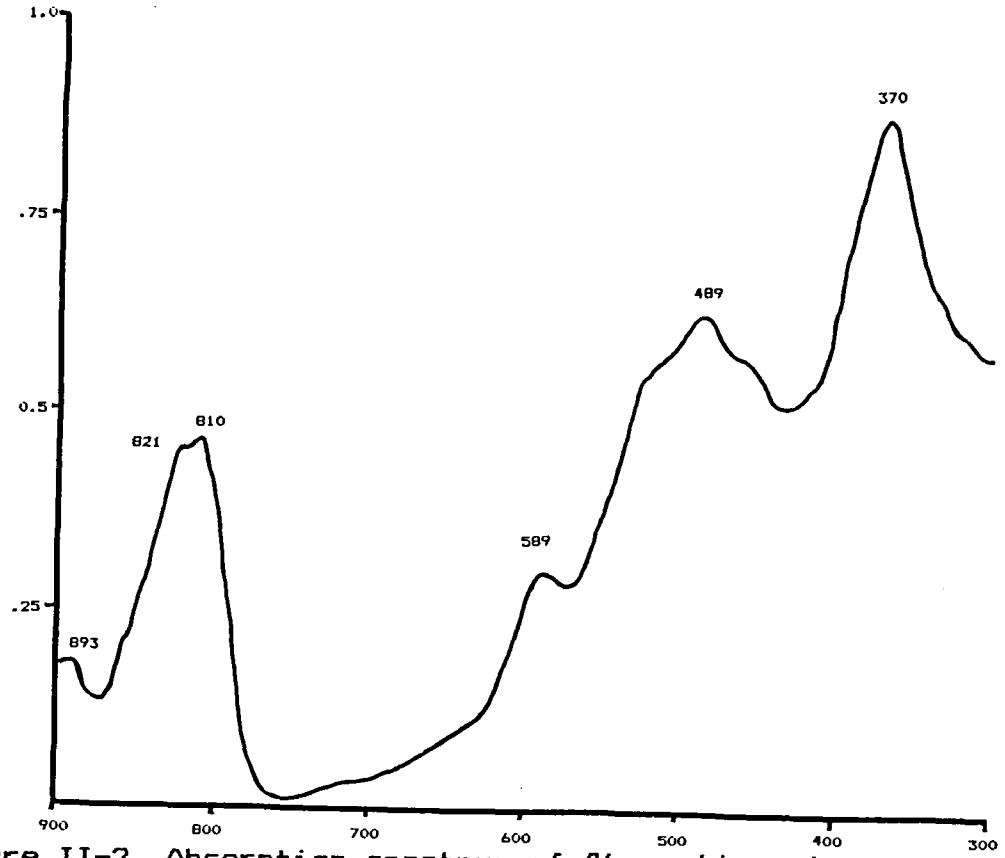

Figure II-2. Absorption spectrum of *Chromatium vinosum*.

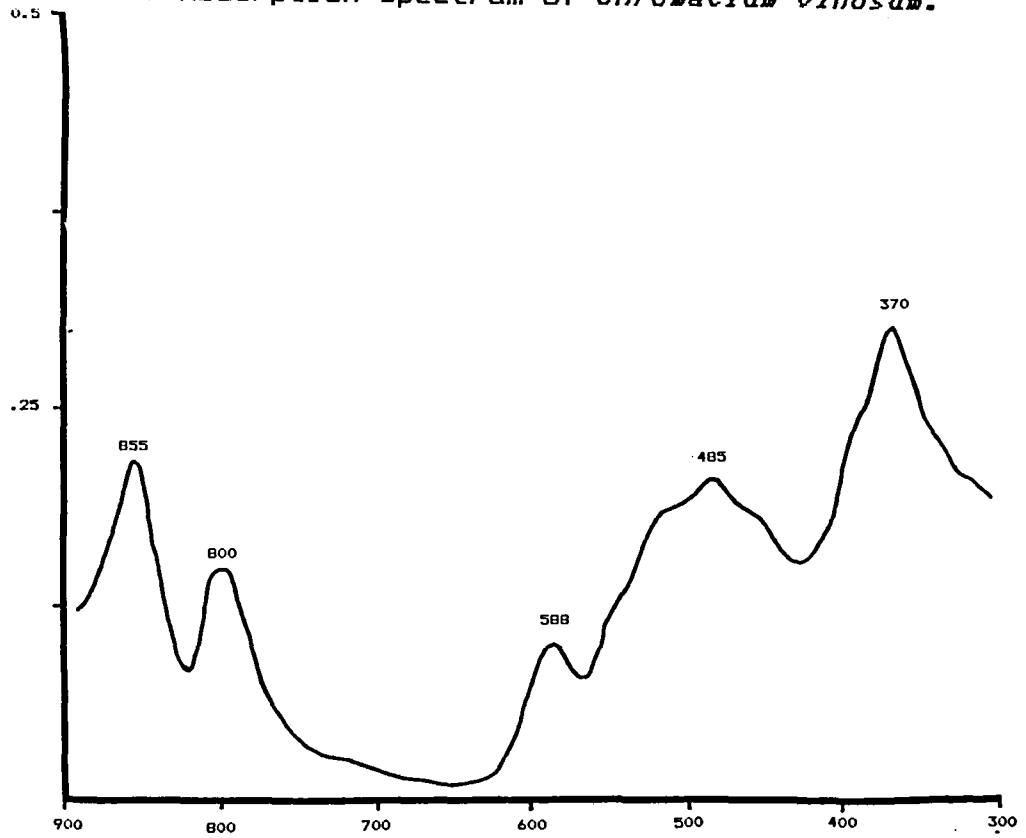

Figure II-3. Absorption spectrum of *Chromatium minutissimum*.

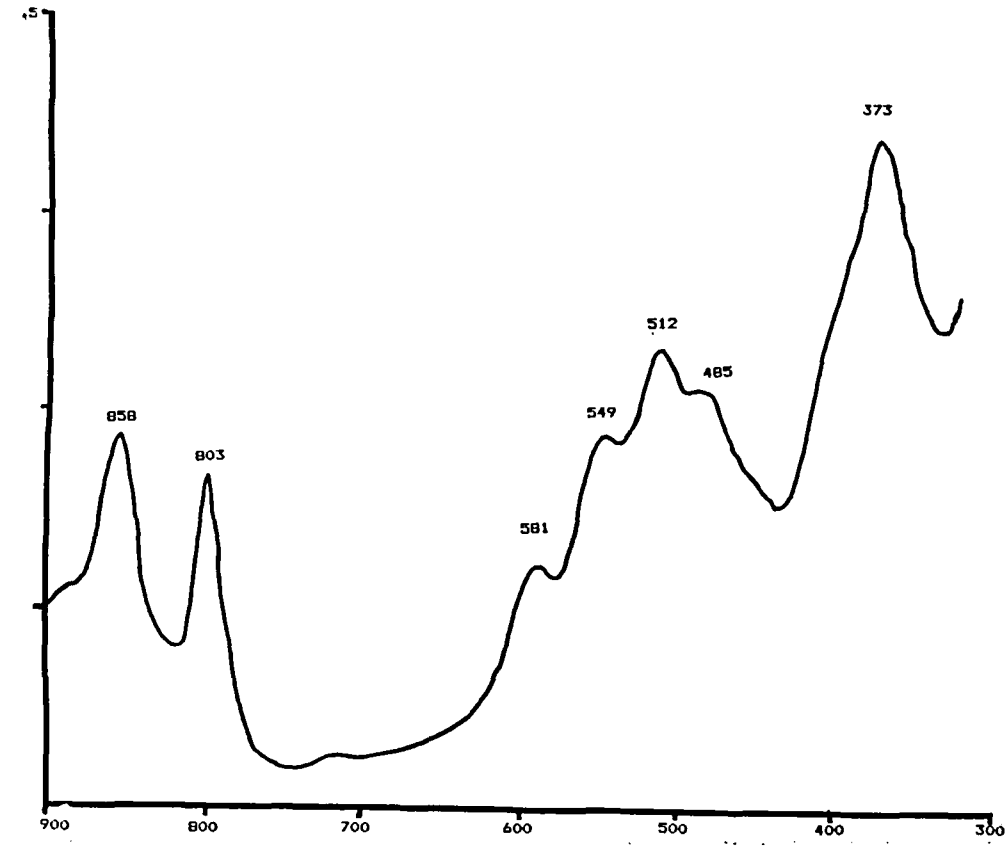

Figure II-4. Absorption spectrum of *Thiocapsa roseopersicina*.

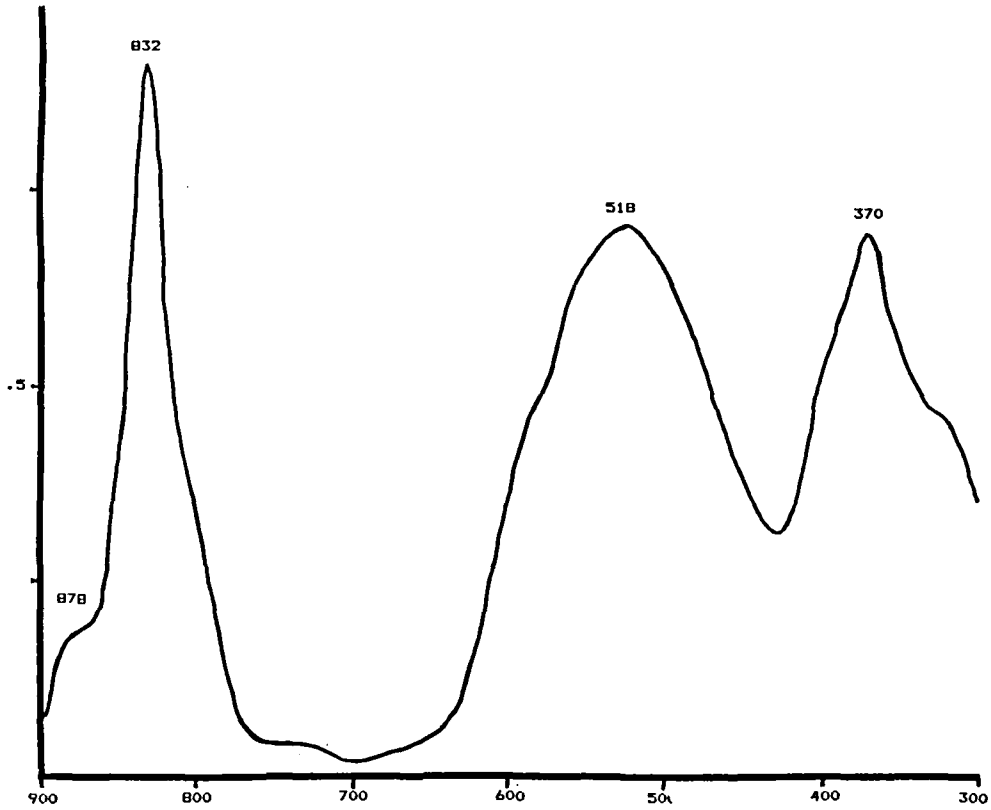

Figure II-5. Absorption spectrum of *Thiocystis gelatinosa*.

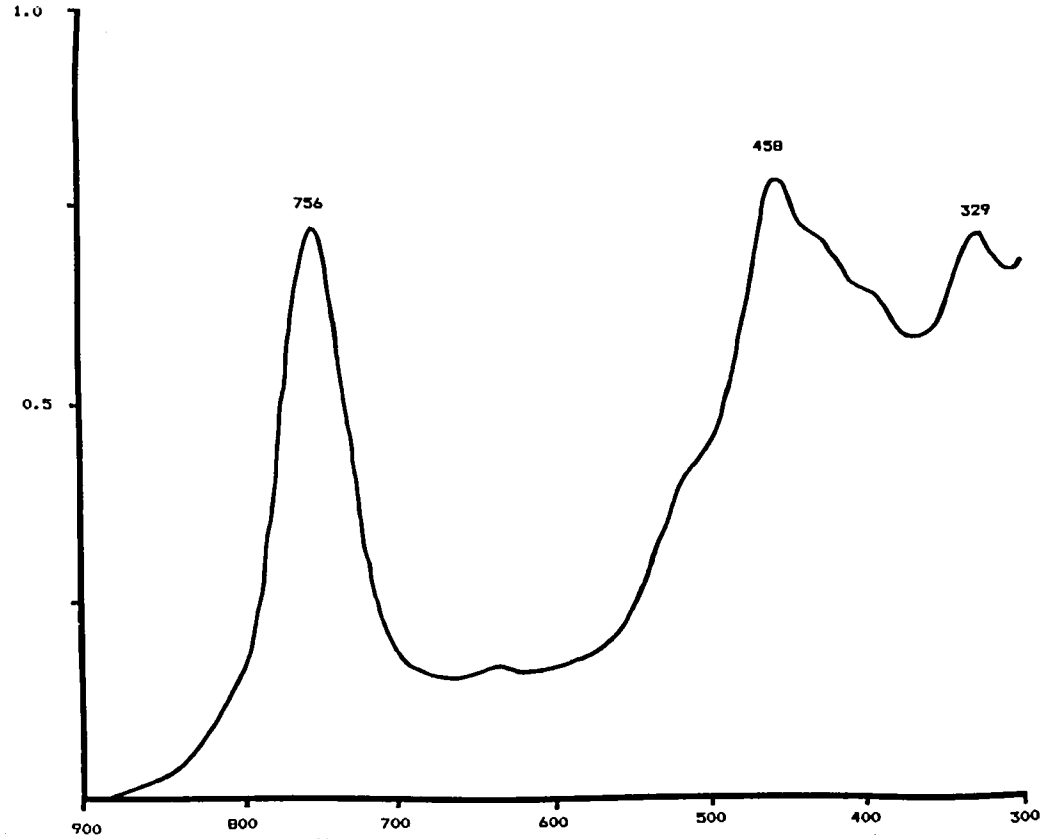

Figure II-6. Absorption spectrum of *Prosthecochloris aestuarii*.

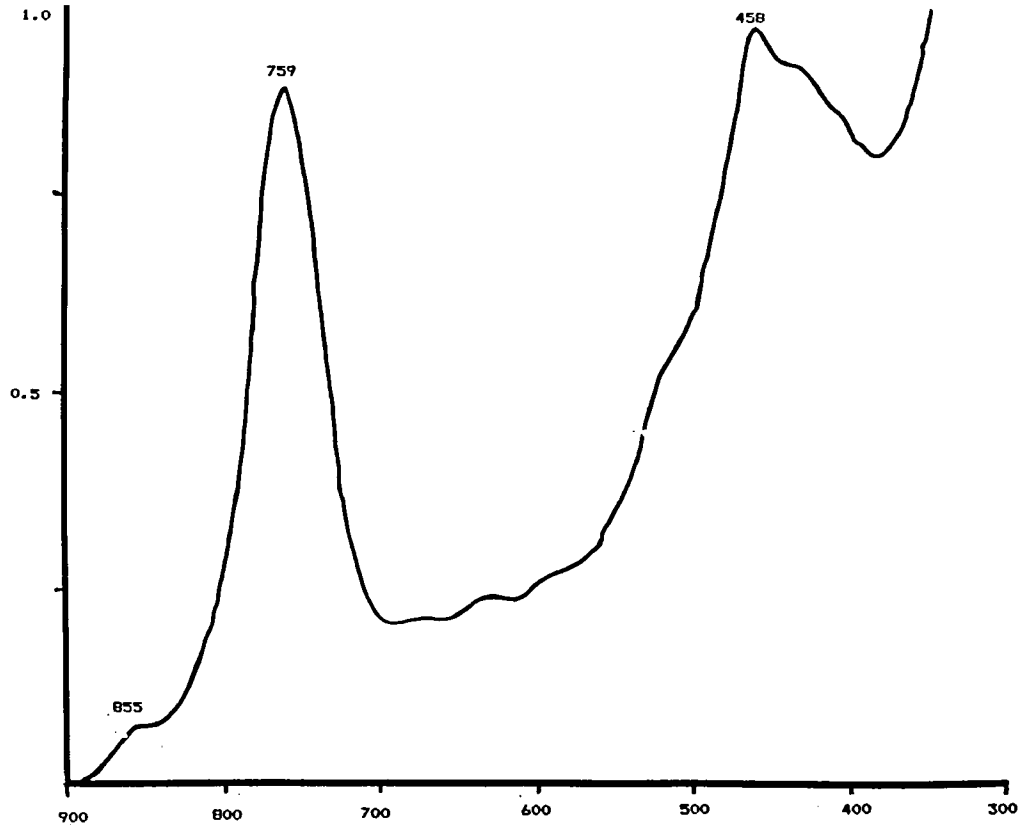

Figure II-7. Absorption spectrum of *Chlorobium limicola*.

c is the principle photosynthetic pigment. (An absorption band at 855 nm is due to the presence of unidentified purple photosynthetic bacteria in the culture.) No added salt was required for growth. The cells were short rods, often joined end to end to form chains. On this basis these bacteria were identified as *Chlorobium limicola*.

The absorption spectra of the tan upper layer of the gypsum crust and of this layer together with the adjacent green layer are shown in Figures II-8 and II-9. The absorption spectrum of the green layer alone was obtained from another piece of the crust; it was practically identical to the spectrum in Figure II-9. The gypsum crust itself absorbs short wavelength light very strongly and becomes increasingly transparent with increasing wavelength (Figure II-8). This crust is sufficiently transparent to red light to permit growth of cyanobacteria, which contribute a prominent absorption peak (about 675 nm) in the red part of the spectrum. Both filamentous and coccoid cyanobacteria were observed during microscopic examination of scrapings from the gypsum crust. The filamentous form grew profusely in bacterial culture medium with about 15 percent NaCl. The tan and green layers together absorb most of the incident light at wavelengths below about 700 nm but are transparent to longer wavelength (infrared) radiation. The ability of Bchl to absorb infrared light clearly is important for the growth of purple sulfur bacteria in the gypsum crust.

The relatively high transmission of infrared light by the gypsum crust makes this natural light filter rather similar to the artificial filter constructed from red and blue cellophane (Fig. II-1). Bacterial cultures grown by illumination through this artificial filter were dominated by purple sulfur bacteria while a control culture grown in unfiltered light was completely overgrown by cyanobacteria. Thus the artificial filter mimics the natural filter in providing a light environment which selectively encourages the growth of purple sulfur bacteria in the presence of cyanobacterial competitors.

Attempts to obtain a continous piece of the purple bacterial layer large enough to obtain an absorption spectrum were unsuccessful. However, the absorption spectrum of a portion of the green layer with discontinuous purple patches adhering to it is shown in Fig. II-10. Infrared absorption bands at about 850 and 795 nm, typical of Bchl a in purple photosynthetic bacteria, are present in this spectrum.

Figure II-11 shows the absorption spectrum of photosythetic bacterial cells taken from a plate located 20 m below the surfae of Big Soda Lake. To obtain this spectrum cells from 1 liter of lake water were concentrated to a volume of about 2.5 ml by centrifuging and resuspending. This spectrum strongly resembles the absorption spectrum of a pure culture of *Thiocystis gelatinosa* (Fig. II-5), except for the presence of a small absorption band at about 675 nm. This absorption peaks at 675

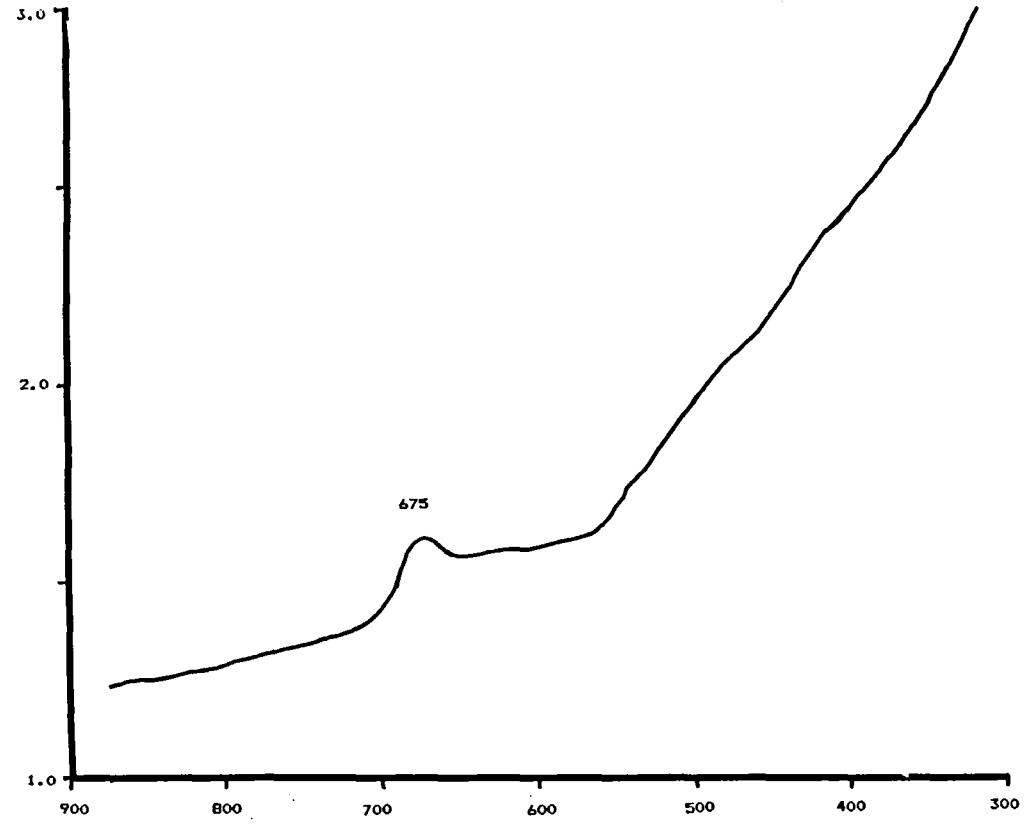

Figure II-8. Absorption spectrum of the tan layer of gypsum crust.

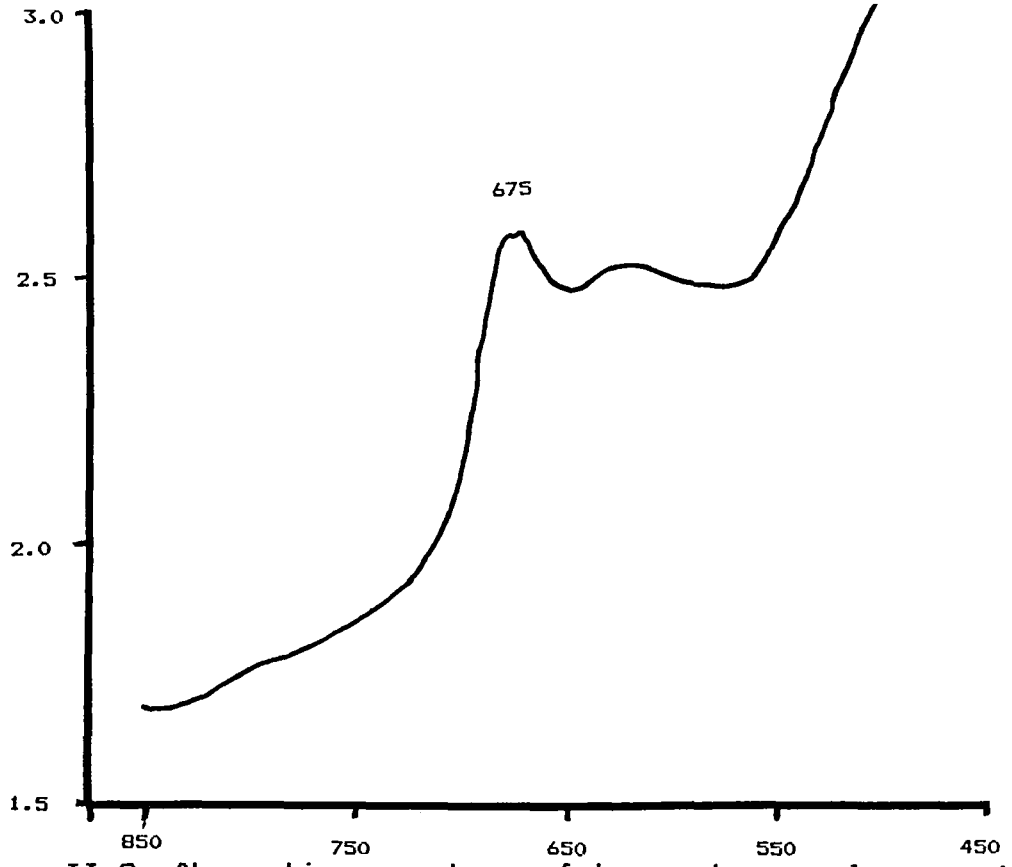

Figure II-9. Absorption spectrum of tan and green layers of gypsum crust.

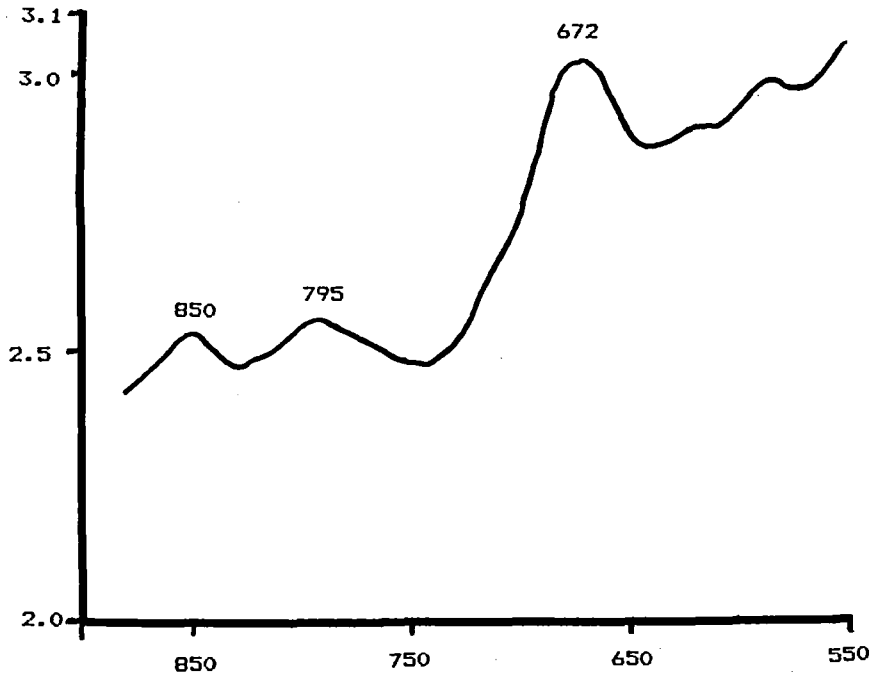

Figure II-10. Absorption spectrum of photosynthetic bacterial layer and part of the overlying layer of gypsum crust.

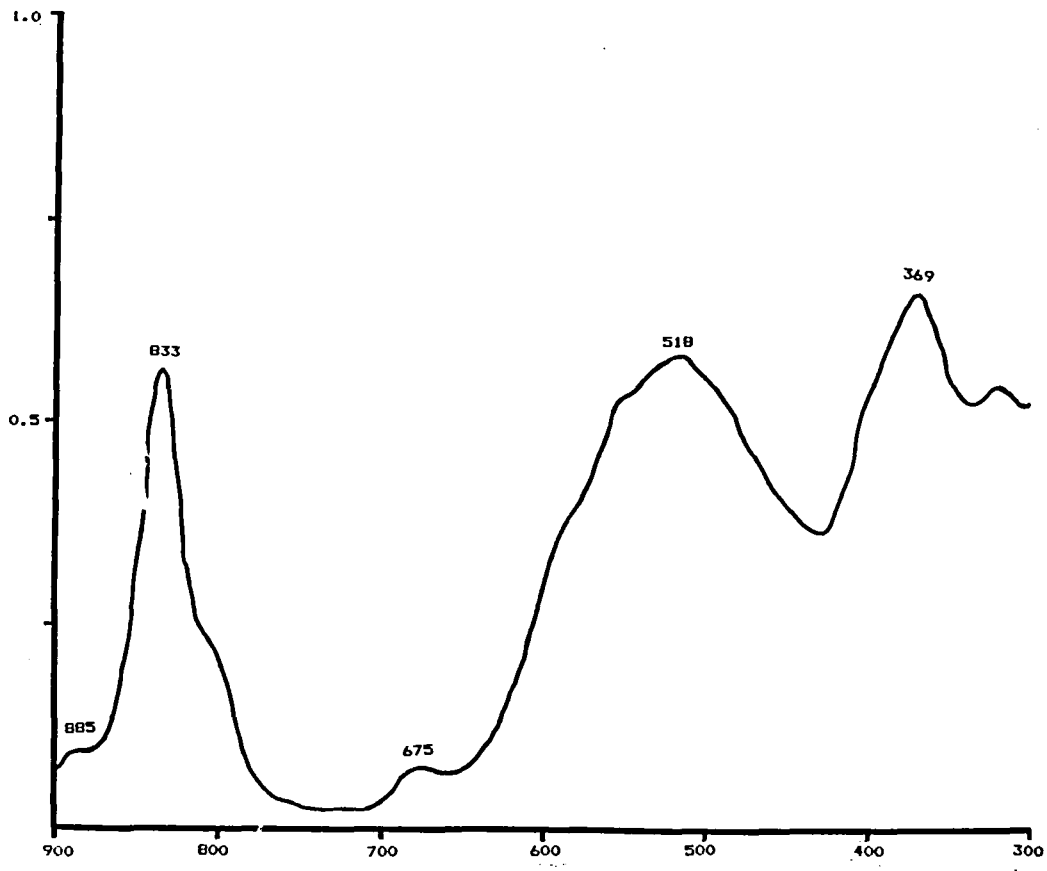

Figure II-11. Absorption spectrum of the bacterial plate sample from Big Soda Lake.

nm, apparently due to the green algae observed on microscopic examination of the bacterial sample from Big Soda Lake. These algae, clusters of cells enclosed in a thick gelatinous sheath, were tentatively identified as *Oocystis* sp. When a portion of the bacterial sample was centrifuged on a percoll density gradient, a heavy band of purple bacterial cells collect at a density of 1.030 g/cm^3, and a lighter unidentified purple band at 1.020 g/cm^3. The green algae separated into a still lighter band having a buoyant density of 1.017 g/cm^3.

Although the similarity of the absorption spectrum of the bacterial cells from Big Soda Lake to that of a pure culture of *Thiocystis gelatinosa* suggests that the dominant organism in the bacterial plate is *T. gelatinosa*, this evidence is not conclusive. A definitive identification of the dominant bacteria species in the plate at the time of sampling is of particular interest, since a previous study (Cloern et al., 1983) reported that *Ectothiorhodospira vacuolata* was the dominant organism in the bacterial plate two years ago. To further characterize this bacterial sample, carotenoids were extracted, separated by thin layer chromatography, and identified on the basis of their Rf values and absorption spectra.

These results and the results of similar experiments of chromatographic separation on silica gel and alumina were performed using purple sulfur bacteria that grew out of the gypsum crust and are shown in Tables I and II. Carotenoids on the plates were identified from their absorption spectra after extraction into acetone or petroleum ether. These spectra were compared with published spectral data (Good, 1973) and with spectra of okenone, rhodopin, and spirilloxanthin in petroleum ether provided by Dr. R. Guerrero.

The sample from Big Soda Lake contained only a single carotenoid identified as okenone. The spectrum of okenone extracted from this sample is shown in Figure II-12. An identical spectrum was obtained for okenone from the *Thiocystis gelatinosa* extract. The Rf values for okenone from the Big Soda Lake sample and from the *Thiocystis gelatinosa* extract were different on alumina. (An excessive amount of okenone was probably applied in the *T. gelatinosa* extract so that the solvent was unable to dissolve and transport all of it simultaneously).

The extract from the bacteria obtained from the gypsum crust contained spirilloxanthin and two other major carotenoids. The absorption spectrum of spirilloxanthin from *Thiocapsa roseopersicina* is shown in Figure II-13. The spectrum of spirilloxanthin from the bacteria under the gypsum crust was identical. One of the other major carotenoids appeared as a yellow spot which ran slightly ahead of spirilloxanthin on the chromatograms. (This carotenoid was not completely separated from spirilloxanthin on alumina.) The other major carotenoid was

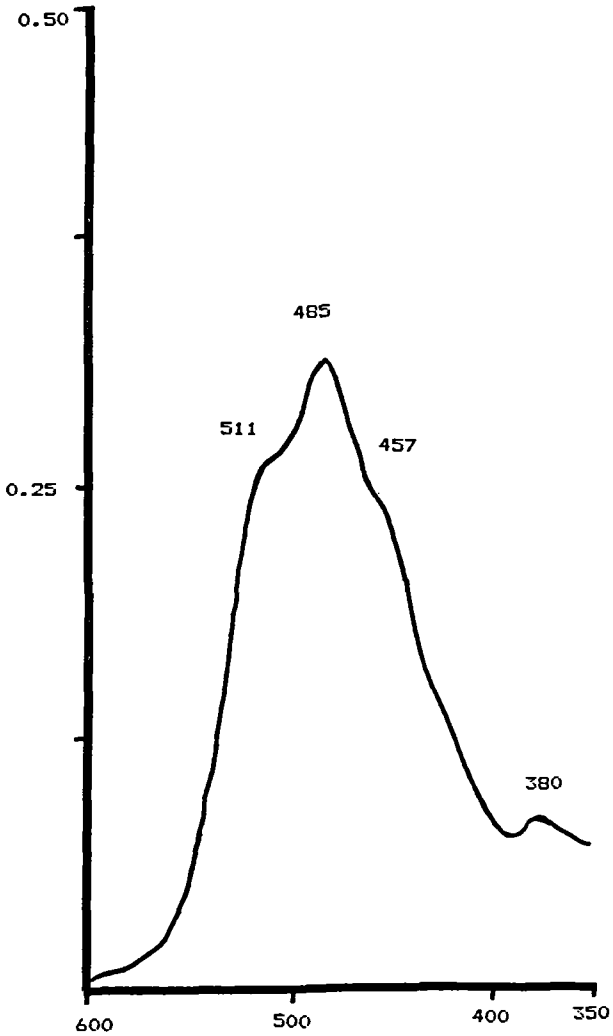

Figure II-12. Okenone (from *Thiocystis gelatinosa*) in acetone.

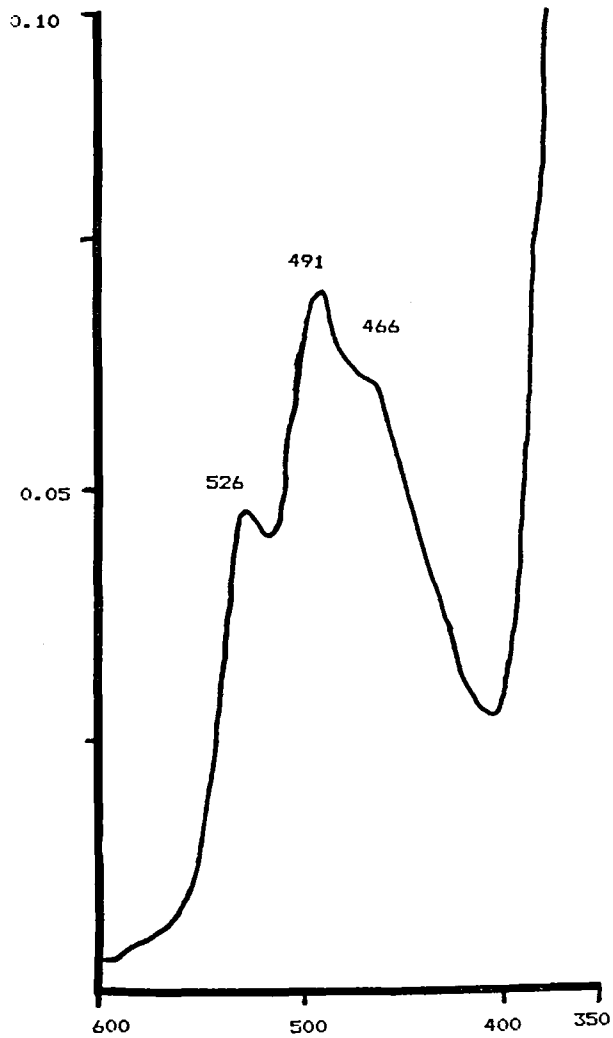

Figure II-13. Absorption spectrum of spirilloxanthin (from *Thiocapsa roseopersicina*) in acetone.

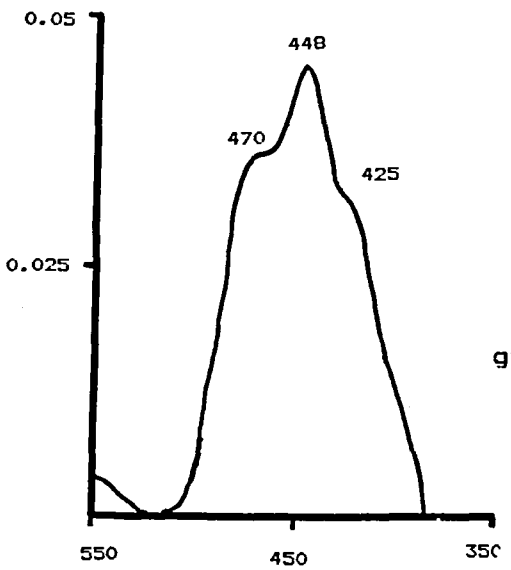

Figure II-14. Absorption spectrum of yellow carotenoid (Rf = 0.73 on silica) from bacteria in gypsum crust in petroleum ether.

a very tightly adsorbed (Rf=0) orange pigment. The absorption spectrum of this orange carotenoid is shown in Figure II-15. Neither the yellow nor the orange carotenoid was identified. It is possible that one or both of these are cyanobacterial pigments, since the culture from which the extract was made still contained cyanobacteria and the initial extract in 90 percent acetone contained about 40 percent as much Chl a as Bchl a, judging from the absorption spectrum of the extract.

Although an extract from *Chromatium vinosum* was used as the standard for rhodopin, the spot for spirilloxanthin in the chromatograms of the *C. vinosum* extract was slightly larger than the spot for rhodopin. An absorption spectrum obtained from the spot identified as rhodopin is shown in Figure II-16.

To complete the identification of the bacterial cells obtained from Big Soda Lake, they were examined microscopically and are described as follows: Individual cells that contain intracellular sulfur globules were spherical and about 2-3 *um* in diameter. Slime capsules surrounded the cells that occur as diplococci, tetrads, and larger clumps. Gas vacuoles were absent; motility was not observed. Pigments were Bchl a and okenone. Except for the lack of motility, these characteristics describe *Thiocystis gelatinosa*, which may be immobile in natural samples (Pfennig and Trueper, 1974). These bacteria were therefore identified as *Thiocystis gelatinosa*.

The bacteria grown from the gypsum crust were also examined microsocpically and may be described as follows: Cells, containing intracellular sulfur globules, were thick rods (3-4 *um* wide and 6-9 *um* long; dividing cells sometimes more than 10 *um* long). Individual cells were colorless; clumps were pink-violet. Cells formed large aggregates, but individual cells were motile, especially when the aggregates were disrupted. Slime capsules and gas vacuoles were absent. The cells occur in highly saline environments and were grown in medium with 15 percent NaCl. Bchl a, spirilloxanthin, and 2 unidentified carotenoids were found in an extract from an enriched culture. On the basis of these characteristics, these bacteria were probably *Chromatium buderi*, although the carotenoid present in described strains of *Chromatium buderi* is rhodopinal rather than spirilloxanthin (Pfennig and Trueper, 1974; Trueper and Pfennig, 1978). Rhodopin has a single absorption maximum at 498 nm (Good, 1973) and therefore cannot be one of the unidentified carotenoids.

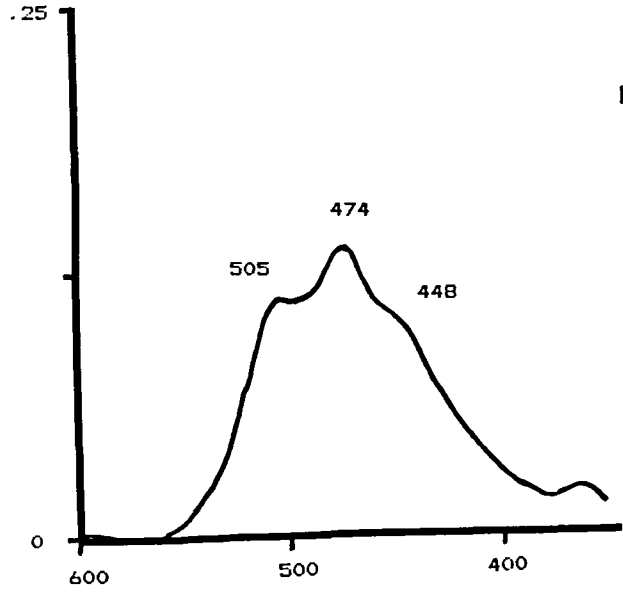

Figure II-15. Absorption spectrum of orange carotenoid (Rf = 0) from bacteria in gypsum crust (in 90% acetone).

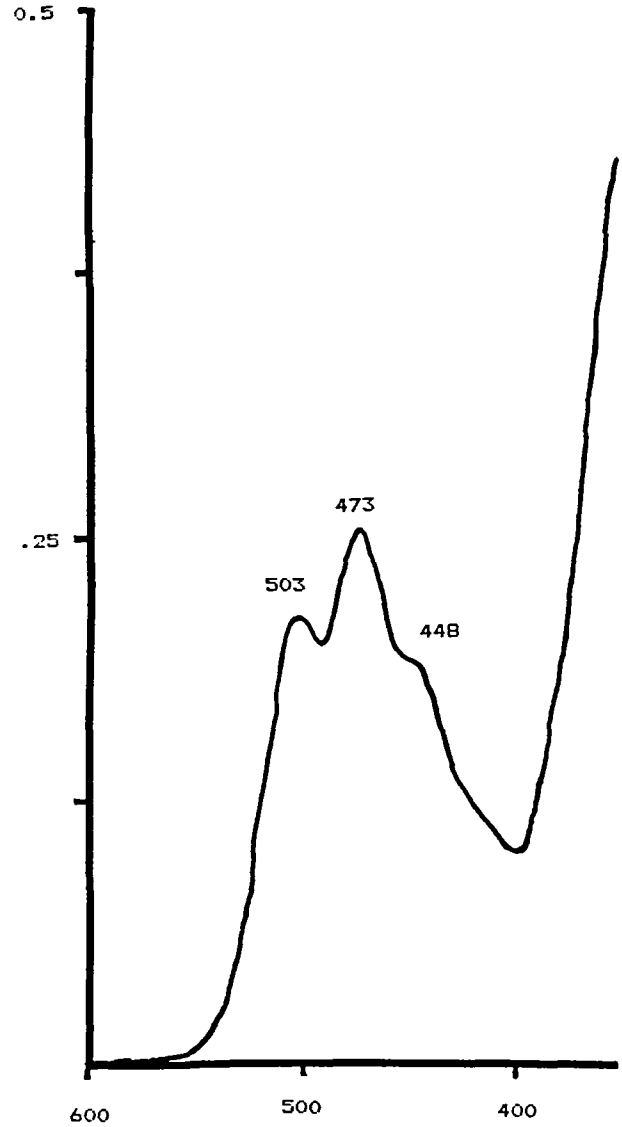

Figure II-16. Absorption spectrum of rhodopin (from *Chromatium vinosum*) in acetone.

Thiocapsa roseopersicina (Spirilloxanthin standard)		
Rf	Color	Identity
0	Blue	Bchl a?
0.62	Pink	Spirilloxanthin
0.73	Pale yellow	n.d.

Rhodopsuedomonas capsulata (Spirilloxanthin should be present)		
Rf	Color	Identity
0.48	Pale yellow	n.d.
0.66	Pink	Spirilloxanthin?

Chromatium vinosum (Rhodopin standard)		
Rf	Color	Identity
0	Blue	Bchl a?
0.44	Peach	Rhodopin
0.60	Pink	Spirilloxanthin

Thiocystis gelatinosa (Okenone standard)		
Rf	Color	Identity
0.48	Pink	Okenone

Big Soda Lake Sample		
Rf	Color	Identity
0.56	Pink	Okenone

Gypsum Crust Purple Bacteria		
Rf	Color	Identity
0	Orange	n.d.
0.62	Pink	Spirilloxanthin
0.73	Yellow	n.d.
(Several other faint bands were also observed.)		

n.d. Not determined

? The spot was not examined spectroscopically, but a likely identity is suggested.

Table II-1. Separation of bacterial carotenoids on silica gel with Rf values, colors of observed spots and the identities of the spots listed under each bacterial species.

Thiocapsa roseopersicina			*Rhodopsuedomonas capsulata*			*Chromatium vinosum*		
Rf	Color	Identity	Rf	Color	Identity	Rf	Color	Identity
0	Blue	Bchl a?	0.62	Peach	n.d.	0	Blue	Bchl a?
0.77	Pink	Spirilloxanthin	0.75	Pink	Spirilloxanthin?	0.65	Peach	Rhodopin
						0.75	Pink	Spirilloxanthin

Thiocystis gelatinosa			Big Soda Lake Sample			Gypsum Crust Purple Bacteria		
Rf	Color	Identity	Rf	Color	Identity	Rf	Color	Identity
0.49–0.67+	Pink	Okenone	0.77	Pink	Okenone	0	Orange	n.d.
						0.75	Pink	Spirilloxanthin
						0.84	Yellow	n.d.

+ The spot was a smear, probably because an excess of pigment was applied.

n.d. Not determined

? The spot was not examined spectroscopically, but a likely identity is suggested.

Table II-2. Separation of bacterial carotenoids on alumina with Rf values, colors of observed spots and the identities of the spots listed under each bacterial species.

References

Cloern, J.E., Cole, B.E., and Oremland, R.S., 1983. Seasonal changes in the chemistry and biology of a meromictic lake (Big Soda Lake, Nevada, USA), Hydrobiologia, 105: 195-206.

Good, T.W., 1973. Microbial carotenoids. In *Handbook of Microbiology Vol. III, Microbial Products* (A. I. Laskin and M. A. Lechevalier, eds.), CRC Press, Boca Raton, Fla, pp. 75-83.

Montesinos, E., Guerrero, R., Abella, C., and Esteve, I., 1983. Ecology and physiology of the competition for light between *Chlorobium limicola* and *Chlorobium phaeobacteroides* in natural habitats, Appl. Environ. Microbiol., 46:1007-1016.

Pfennig, N., 1978. General physiology and ecology of photosynthetic bacteria. In *The Photosynthetic Bacteria* (R.K. Clayton and W.R. Sistrom, eds.), Plenum Press, N.Y., pp. 3-18.

Pfennig, N. and Trueper, H.G., 1974. The phototrophic bacteria. In *Bergey's Manual of Determinative Bacteriology* (R.E. Buchanan and N.E. Gibbons, eds.), Williams and Wilkins Co., Baltimore, Md., pp. 24-64.

Thornber, J.P., Trosper, T., and Strouse, C.E., 1978. Bacteriochlorophyll *in vivo*: relationship of spectral forms to specific membrane components. In *The Photosynthetic Bacteria* (R.K. Clayton and W.R. Sistrom, eds.), Plenum Press, New York, pp. 133-160.

Trueper, H.G. and Pfennig, N., 1978. Taxonomy of the Rhodospirillales. In *The Photosynthetic Bacteria* (R.K. Clayton and W.R. Sistrom, eds.), Plenum Press, New York, pp. 19-27.

Trueper, H.G. and Yentsch, C.S., 1967. Use of glass fiber filters for the rapid preparation of *in vivo* absorption spectra of photosynthtic bacteria, J. Bacteriol., 94: 1255-1256.

van Gemerden, H. and Beeftink, H. H., 1983. Ecology of phototrophic bacteria. In *The Phototrophic Bacteria: Anaerobic Life in the Light* (J.S. Ormerod, ed.), Blackwell Scientific Publications, Oxford, England, pp. 146-185.

ANAEROBIC REDUCTION OF ELEMENTAL SULFUR BY *CHROMATIUM VINOSUM* AND *BEGGIATOA ALBA*

T.M. Schmidt

Introduction

Chromatium vinosum, a flagellated photosynthetic rod bacterium, and *Beggiatoa alba*, a gliding filamentous bacterium, both oxidize sulfide to sulfur, which is stored inside their cells in the form of sulfur globules. Although these bacteria are morphologically and physiologically distinct, they both belong to the purple bacterial group as determined by their 5S rRNA sequences (Krieg, 1984).

Filaments of *Beggiatoa* glide through sediments so that they are situated at the oxic/anoxic interface where sulfide and oxygen coexist. At this interface, sulfur is accumulated by the cells. Since this interface rises at night and falls during the day, *Beggiatoa* filaments must be able to generate energy under both oxic and anoxic conditions as they glide towards the interface. The aerobic oxidation of acetate by *Beggiatoa* has been well documented and shown to be responsible for energy generation (Strohl, 1981). However, there is no known mechanism by which *Beggiatoa* can generate energy in the absence of oxygen.

Chromatium is found in the anoxic layers of lakes. Electrons released from the oxidation of sulfide are used in anoxygenic photosynthesis. The sulfur that accumulates from this reaction increases the buoyant density of the cells. As sulfur globules accumulate, the cells sink out of the photic zone if the bacterial layer is concentrated enough to limit the light available for photosynthetic energy production. Once below the photic zone *Chromatium* gains maintenance energy from the oxidation of polyglucose to poly- -hydroxybutyric acid (PHB) and the reduction of sulfur to sulfide (van Gemerden, 1968). Decrease in the amount of intracellular sulfur globules reduces the buoyant density of the cell and may permit cells to return to the photic zone.

This project examined:

1) The effect of sulfur globules on the buoyant density of *Chromatium vinosum* and *Beggiatoa alba*,

2) The potential use of sulfur as a terminal electron acceptor in the anaerobic metabolism of *Beggiatoa alba*, and

3) The effect of the reduction of intracellular sulfur during dark metabolism on the buoyant density of *C. vinosum*.

Culturing Freshwater Strains of *Beggiatoa*
(Type strain: *B. alba* B18LD)

STOCK SOLUTIONS	BASIC GROWTH MEDIUM
Modified Pringsheim's Microelement Solution	5 ml/l
NH_4Cl (5 percent)	5 ml/l
$CaCl_2$ (15 percent)	5 ml/l
$MgSO_4 7H_2O$ (1 percent)	1 ml/l
KH_2PO_4 (1 percent)	1 ml/l
Sodium acetate	0.5 g/l
Sodium sulfide	0.24 g/l

Adjust the pH of the medium to 7.4 with 1N NaOH and autoclave. Add neutralized and sterilized sulfide to a final concentration of 1 mM. Use a 10 to 15 percent inoculum and gently agitate the culture for best growth. Cultures can be grown in the presence or absence of sulfide.

MODIFIED PRINGSHEIM'S MICROELEMENTS

H_3BO_3 - 0.001 percent
Na_2MoO_4 $7H_2O$ - 0.0001 percent
$FeSO_4$ $7H_2O$ - 0.07 percent
$MnSO_4$ $7H_2O$ - 0.0002 percent
$CoCl_2$ $6H_2O$ - 0.0001 percent
$ZnSO_4$ $7H_2O$ - 0.001 percent
$CuSO_4$ - 0.0000005 percent
EDTA - 0.2 percent

Prepare in ddH_2O and add 1 ml/l HCl to prevent precipitation of iron.

Maintaining Cultures on Agar Plates

Cultures can be maintained for two to three weeks on agar plates. Prepare the growth medium as described above except lower the acetate concentration to 0.1 g/l and add 0.1 g/l yeast extract. Sulfide should be added to 1 mM after autoclaving.

Transfer plate cultures every two to three weeks by cutting out a slab of agar and gently sliding it over the surface of a new plate.

Starting Suspension Cultures from Agar Plates

Prepare 100 ml of 2 percent agar in a 250 ml flask. Autoclave, then add neutralized and sterilized sulfide to a final concentration of 1 mM. After this solidifies, add 100 ml of basic growth medium (+ sulfide) and inoculate the flask with a section of the agar culture. Agitate gently. Growth should occur in two days. The agar plug will provide a continuous release of sulfide into the medium. *Beggiatoa* survives best under microaerophilic conditions.

Materials and Methods

Pure cultures of *Chromatium vinosum* and *Beggiatoa alba* were grown under conditions where elemental sulfur was accumulated by the cells. The cultures were then transferred to the apparatus diagrammed in Figure II-17. In the experiments with *Beggiatoa*, the culture was centrifuged and washed twice in basal salts (Strohl and Schmidt, 1984) before being transferred to the apparatus. Nitrogen was flushed through the system and the outflowing gas was bubbled through two test tubes that each contained 10 ml of 2 percent zinc acetate to precipitate sulfide. The zinc acetate tubes were changed every hour during the course of the experiments. This apparatus permitted the continuous removal of sulfide so that sulfide toxicity did not limit metabolic rtion of sulfur globules in the cell (Table II-3). *C. vinosum* and *B. alba* reduced the intracellular sulfur to sulfide at similar rates (Fig. II-18). *Beggiatoa* filaments that lacked sulfur inclusions produced no sulfide, suggesting that sulfur-containing amino acids were not the source of the sulfide measured.

The buoyant density of *Chromatium* cells was increased to 1.130 g/cm by providing illuminated cells with 1 mM sulfide 4 hours before the density measurement. This ensured that the 1fur to sulfide during six hours did not make a significant change in the buoyant density of the cells. Although sulfur reduction to sulfide with corelated decrease in buoyant density is not a mechanism by which *Chromatium* returns to the photic zone after 6 hours, it may be important to cell maintenance as the sulfur continues to decrease for several days.

Since *Beggiatoa* can also reduce sulfur to sulfide, we hypothesized that sulfur to sulfide is part of an anaerobic energy-generating system. This pathway was previously suggested to exist in *Beggiatoa* (Nelson and Castenholz, 1981). Our work provides evidence to confirm such a suggestion. Carbon stored as PHB may be oxidized with the concomitant reduction of sulfur to sulfide. Additional research is required to determine whether the oxidation of PHB using sulfur as a terminal electron source provides energy in *Beggiatoa* and whether this is sufficient to maintain cells and provide energy for movement back into the oxic zone.

References

Bradford, M.M., 1976. A rapid and sensitive method for the quantification of microgram quantities of protein utilizing the principles of proteus dye binding, Anal. Biochem., 72:248-254.

Figure II-17. Apparatus for continuous removal and measurement of sulfide.

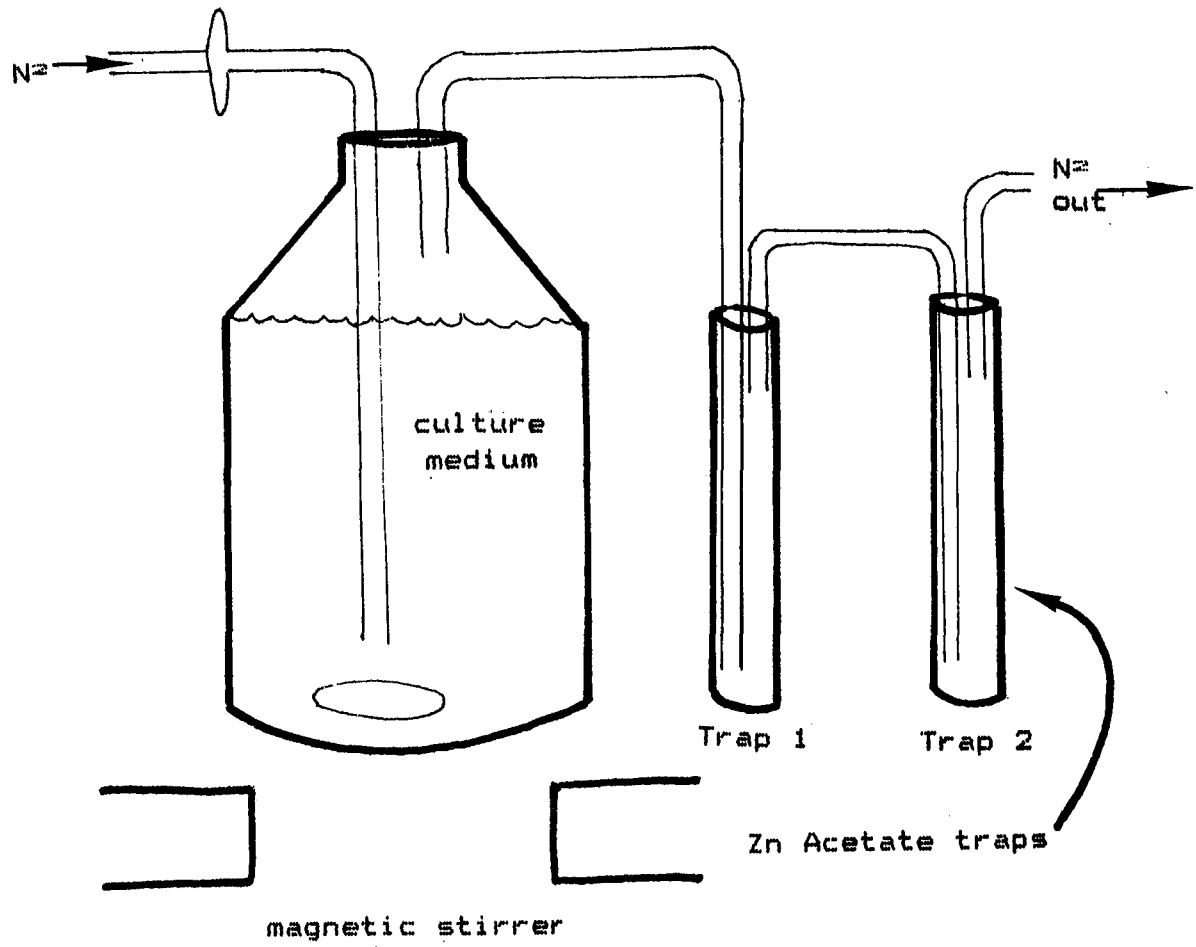

Organism	Sulfur inclusions	Buoyant density gm/cm^3
B. alba	+	1.115
B. alba	−	1.095
C. vinosum	+	1.087
C. vinosum	++	1.130
" " after 3 hours dark incubation	++	1.130
" " after 6 hours dark incubation	++	1.130

Table II-3. Buoyant densities of *B. alba* and *C. vinosum* with varying amounts of intracellular sulfur.

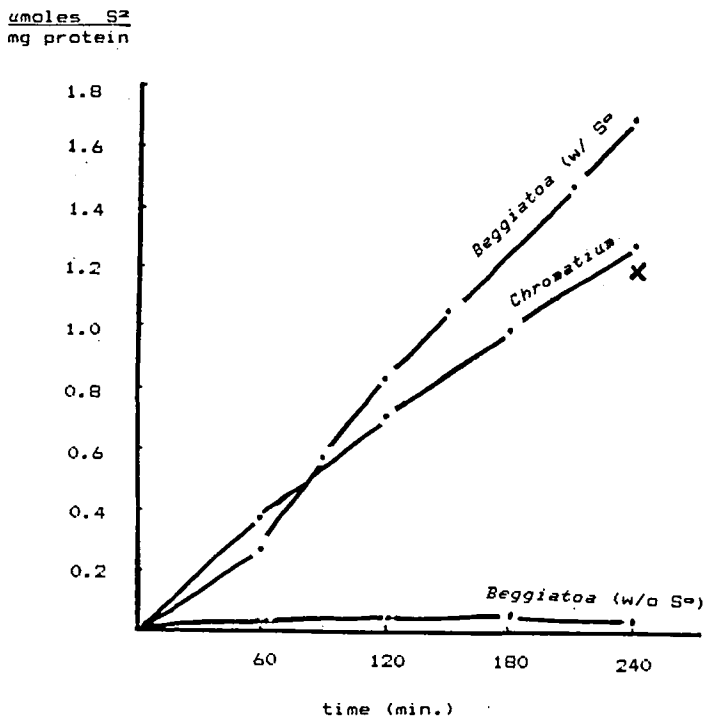

Figure II-18. Reduction of intracellular sulfur to sulfide.

Cline, J., 1969. Spectrophotometric determination of hydrogen sulfide in natural environments, Limnol. Oceanog., 14:454-459.

Guerrero, R., Mas, J., and Pedros-Alio, C., 1984. Buoyant density changes due to intracellular content of sulfur in *Chromatium warmingii* and *Chromatium vinosum*, Arch. Microbiol., 137:350-356.

Krieg, N.R. and Holt, J.G., 1984. In *Bergey's Manual of Systematic Determinative Bacteriology*, Vol. 1, Williams and Wilkins, Baltimore, Md.

Nelson, D.C. and Castenholz, R.W., 1981. Use of reduced sulfur compound by *Beggiatoa* sp., J. Bacteriol., 147:140-154.

Strohl, W. R., Cannon, G. C., Shivley, J. M., Gude, H., Hook, L. A., Lane, C. M., and Larkin, J. M., 1981. Heterotrophic carbon metabolism by *Beggiatoa alba*, J. Bacteriol., 148:572-83.

Strohl, W. R. and Larkin, J. M. 1978. Enumeration, isolation and characterization of *Beggiatoa* from freshwater sediments, Appl. Environ. Microbiol., 36:755-70.

Strohl, W. R. and Schmidt, T. M., 1984. Mixotrophy of the colorless, sulfide-oxidizing gliding bacteria *Beggiatoa* and *Thiothrix*. In *Microbial Chemoautotrophy* (W. R. Strohl and O. H. Tuovinen, eds.), Ohio State University Press, Columbus.

van Gemerden, H., 1968. On the ATP generation by *Chromatium* in darkness, Arch. Microbiol., 64:118-124.

BUOYANT DENSITIES OF PHOTOTROPHIC SULFUR BACTERIA AND CYANOBACTERIA

R Guerrero

The buoyant densities of bacterial cells can be greatly influenced by the accumulation of intracellular reserve material. The buoyant density of phototrophic bacteria that are planktonic is of particular interest, since these organisms must remain in the photic zone of the water column for optimal growth. Separation of cells by their buoyant density may also be of use in separating and identifying organisms from a natural population.

The bacteria used in this study were obtained from pure cultures, enrichments, or samples taken directly from the environment. Table II-4 lists the bacteria, their buoyant density, and the source of the sample.

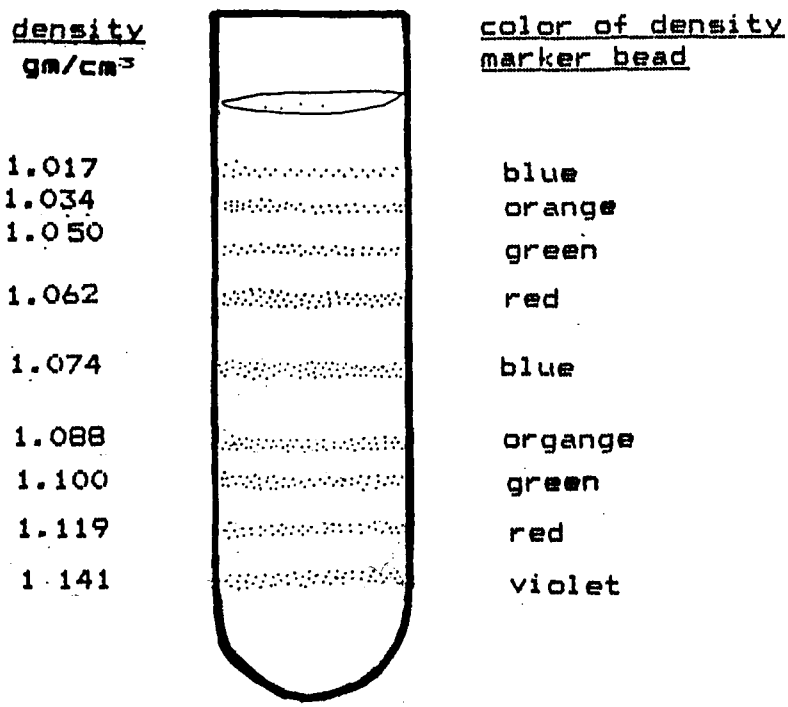

Figure II-19. Percoll gradient with density marker beads.

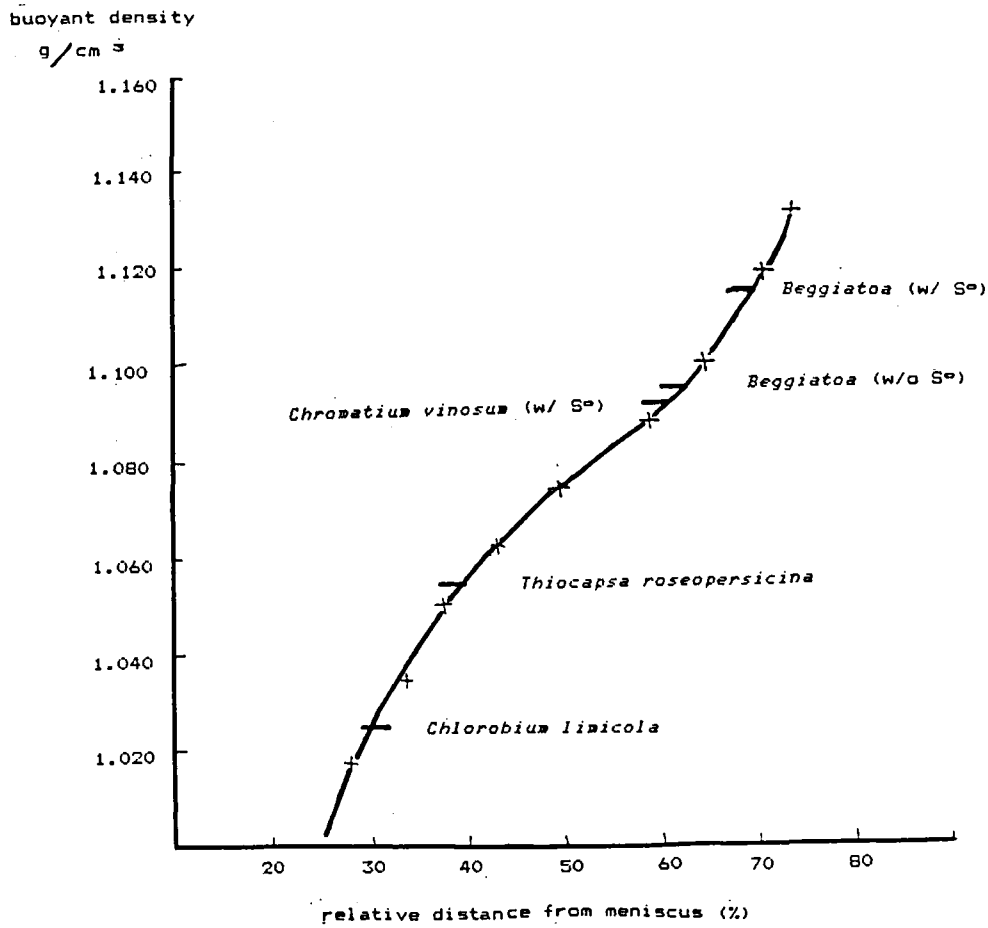

Figure II-20. Bouyant density of phototrophic sulfur bacteria and cyanobacteria.

ORGANISM	DENSITY g/cm³	SOURCE OF SAMPLE
Thiocystis gelatinosa	1.040	Pure culture
Thiocystis gelatinosa	1.030	Big Soda Lake
Thiocapsa roseopersicina	1.054	Pure culture
Chromatium vinosum	1.087-1.130	Pure culture
Chromatium minutissimum	1.078	Pure culture
Chlorobium phaeobacteroides	1.072	Pure culture
Chlorobium limicola	1.025	Pure culture
	1.014	Enrichment
Chlorobium vibrioforme	1.100	Pure culture
Prosthecochloris sp.	1.045	Enrichment Salt marsh
Rhodopsuedomonas sphaeroides	1.088	Pure culture
Rhodopsuedomonas capsulata	1.074	Pure culture
Rhodopsuedomona palustris	1.095	Pure culture
Ectothio rhodospira sp.	1.080	Big Soda Lake
Anacystis nidulans	1.119	Pure culture
Synechocystis sp.	1.020	Enrichment Alum Rock, Site III
Oscillatoria sp.	1.119	Enrichment Alum Rock, site III
Oocystis sp. (eukaryote; chlorophyte)	1.017	Big Soda Lake

Table II-4. Buoyant densities of purple and green phototrophic bacteria and cyanobacteria at 20°

INTERACTIONS AMONG SULFIDE-OXIDIZING BACTERIA

R. Poplawski

Introduction

Alternations between aerobic and anaerobic conditions prevail in aquatic environments. Such conditions promote various interactions among bacterium, including synergism, a phenomenon whereby bacterial growth is amplified as a result of proximity to another strain. Another is competition, whereby rivals interfere with each other's growth in a negative fashion (Atlas and Bartha, 1981). The aim of these experiments was to study the responses of different phototrophic bacteria in a competitive experimental system, one in which primary factors such as H_2S or light limited photometabolism. Two different types of bacteria shared one limited source of sulfide under specific conditions of light. The selection of a purple and a green sulfur bacteria and the cyanobacterium was based on their physiological similarity and also on the fact that they occur together in microbial mats. They all share anoxygenic photosynthesis, and are thus probably part of an evolutionary continuum of phototrophic organisms that runs from, strictly anaerobic physiology to the ability of some cyanobacteria to shift between anoxygenic bacterial-style photosynthesis and the oxygenic kind typical of eukaryotes. Hartman (1983) and Trueper (1982) suggest parallelism among such bacterial photosystems.

Chlorobium phaeobacteroides is a strictly anaerobic green sulfur bacterium that uses sulfide as an electron donor for carbon dioxide photoassimilation. In the course of carbon dioxide reduction sulfide is oxidized to sulfur which is stored outside the cells. Some strains further oxidize sulfur to sulfate. Production of sulfur corresponds with the equation:

$$2H_2S+CO_2 \rightarrow 2S+H_2O+(CH_2O)$$ (Kondratieva, 1979)

Oscillatoria limnetica is a facultatively oxygenic cyanobacterium which can use hydrogen sulfide anaerobically in a reaction that oxidizes hydrogen sulfide to S^o. The strain performs anoxygenic photosynthesis, driving electrons from hydrogen sulfide to PS I. *O. limnetica* is capable of anoxygenic photosynthesis at low H_2S concentrations (0.1-0.3 mM). A lag period of 2 hours is required for the shift. Once adaptation is complete, *O. limnetica* can grow photoautotrophically under anaerobic conditions with the same efficiency as it does by oxygenic photosynthesis (Cohen et al., 1975 a,b). Sulfide itself is a weak dibasic acid, with a pH of 6.76 and 11.96 at the ionic strength of the reactions. The concentration of the ionized and undissociated H_2S will drastically change in the pH between 7 and 8. Sulfide may cause deleterious effects on the cells and probably is the reason for the lag period. It is possible that the low redox potential

elicits a process in which reduction of an electron carrier causes it to become sulfide-resistant and thereby functional in the use of sulfide electrons. Addition of sodium thiosulfate to cell suspensions allows elimination of the preincubation period. It also decreases pH, turning most sulfide into H_2S (Belkins, unpublished). Sulfide is oxidized to sulfur according to the equation:

$$2H_2S+CO_2 \rightarrow (CH_2O)+2S+H_2O$$

S^o is expelled from the cells as refractile globules either free in the medium or adhering to the filaments.

Chromatium vinosum, a purple sulfur bacterium, forms S^o inside the cells during anoxygenic photosynthesis. These sulfur globules provide a reservoir of photosynthetic electron donors for CO_2 fixation. CO_2 is fixed as part of an anaerobic, obligately phototrophic metabolism. The final result of H_2S utilization corresponds to the equation:

$$H_2S+2CO_2+2H_2O \rightarrow H_2SO_4+2CH_2O$$

C. vinosum is inhibited by oxygen. Important redox enzymes are probably poorly protected.

MATERIALS AND METHODS

Semi-open system

A semi-open system was used with two of four 210 ml flasks taken from an Ecologen model E-40 (no. 57435, New Brunswick Scientific Co.). Each flask has two rubber-stoppered slits to facilitate sample extraction. The two flasks were connected by plastic covers attached with epoxy glue. Apertures (3.7 cm) for the filter membrane were drilled through the plastic covers. The membrane was glued with epoxy to a plastic and cardboard circular base from both sides to prevent leakage (Fig. II-21).

Light Measurements

Since light intensity can play an important role in determining the species composition among phototrophic bacteria in natural environments, the light emitted by one or two 60 watt incandescent lamps was measured by a Li Cor quanta meter which defined our light intensities. Under conditions of high light intensity (saturation conditions) the brown *C. phaeobacteroides* and the purple *C. vinosum* have similar generation times, although the latter need more light.

Millipore Membrane

A 3 *um* Millipore membrane was used between the two cell suspensions. The bacterial linear dimensions were smaller than the membrane pores (1.504 *um* in length as determined by Coulter Counter, 0.853 by transmission electron microscopy, 0.431 by scanning electron microscopy for *Chromatium vinosum*, and around 0.328, 0.225, and 0.053 um^3 for *Chlorobium* species (Montesinos et al., 1983)). Nonetheless, bacterial passage from one to the other system could not be confirmed by microscopy. Sulfur content per cell seems to determine cell volume in *Chromatium vinosum* (Guerrero et al., 1984). *O. limnetica* forms filaments larger than pore size.

Bacterial Strains

Chromatium vinosum UA 6001 was isolated by H. van Gemerden from Lake Ciso (Banyoles, Spain). *Chlorobium phaeobacteroides* UA 5001 was isolated from Vilar, Ciso, and other Spanish lakes. *Oscillatoria limnetica* was isolated from Solar Lake in the Gulf of Akaba in the Red Sea.

Growth Conditions

Cultures of *Chromatium* and *Chlorobium* were grown in Pfennig's medium under nitrogen atmosphere. Initial inocula were taken from stationary cultures (10 ml tubes) and inoculated into 150 ml bottles in Pfennig and Lippert medium (van Gemerden and Beeftink, 1983) for two to three days before experiments. Cultures were incubated at room temperature under light (20-30 $uE\ m^{-2}\ s^{-1}$ before inoculation in the semi-open system. *O. limnetica* was grown in agar tubes and inoculated to CHU11 medium improved by Y. Cohen (Waterbury and Stanier, 1981).

Chemical and Biological Parameters

Hydrogen sulfide was measured by colorimetric assay (Cline, 1969). Elemental sulfur was measured according to Bartlett and Skoog (1961). The difficulty in obtaining a standard sulfur solution was that only relative absorbance measurements are given but even these provide useful qualitative information. Sulfate was determined according to Tabatabai (1974). Protein determinations were carried out according to the method of Bradford (1976).

Experiments were done as follows: 210 ml cell suspension of each bacteria containing 25 mM buffer HEPES/NaOH, pH 7.1, and 100 mM Na_2CO_3 were illuminated by one or two 60 Watt incandescent lamps which provided 26-30 $uE\ m^{-2}\ s^{-1}$ between the bottom and surface of the flasks at 26°C. Inocula were maintained under N_2. The whole system was kept in the dark for fifteen minutes, after which samples for sulfide determination were taken. The system was

stored in the light, and sulfide was added in the initial defined concentrations. Samples were taken every four hours in the dark for H_2, S^o, and SO_4^{2-}. Every 8 hours protein was determined; samples, taken with disposable syringes, were immediately fixed, filtered, or frozen as required.

Chlorobium-Chromatium: Initial sulfide concentrations were 5.18 mM and 2.39 mM, respectively. Light intensity was set at 20-29 $uE\ m^{-2}\ s^{-1}$ for both systems.

Oscillatoria-Chlorobium: Initial sulfide concentration was 0.8 and 0.7 mM H_2S respectively and light intensities were set at 26-31 and 1.15-1.19 $uE\ m^{-2}\ s^{-1}$, respectively.
Low redox potential in the *Oscillatoria limnetica* system was obtained by the addition of 1.2 mM dithionite, which elicits a one to two hour lag period. pH was adjusted to 7.0 by 25 mM buffer HEPES/NaOH and 25 mM NaOH.

O. limnetica-C. vinosum: Initial sulfide concentration was established at 1.5 mM for both bacteria and light intensity was 26-31 $uE\ m^{-2}\ s^{-1}$ for both systems. As in the *Oscillatoria limnetica-Chlorobium* interaction, low redox potential was obtained by 1.2 mM dithionite and pH 7.0 was fixed by 25 mM buffer HEPES/NaOH.

Results and Discussion

Dissimilatory sulfide oxidation performed by two sulfur bacteria present together in aquatic habitats was examined experimentally to demonstrate H_2S oxidation to S^o and SO_4. In the *Chlorobium-Chromatium* experiment hydrogen sulfide was oxidized rapidly to S^o during the first 12 hours. *Chlorobium* more efficiently oxidized sulfide than *Chromatium* (0.33 mM $Na_2S\ h^{-1}$ and 0.23 mM $H_2S\ h^{-1}$ respectively.) Nevertheless, the rate of sulfide oxidation was higher in *Chromatium*. Apparently elemental sulfur was produced first by *Chlorobium* but only *Chromatium* oxidized S^o to sulfate. (Hydrogen sulfide at pH 7 represents 25 percent of the total sulfide). After 12 hours *C. vinosum* had left only about 0.115 mM H_2S free in the medium while increasing amounts of elemental sulfur produced by its counterpart were probably passively diffusing and used as an energy source. The use of either H_2S or elemental sulfur by *C. vinosum* to form H_2SO_4, the high light intensity, and the temperature were the main factors which inhibited sulfate formation by *C. phaeobacteroides*. *Chlorobium* may not have had high affinity for the elemental sulfur, which was used by its competitor.

Sulfate concentration only increased after 16 hours. Its rate of production was almost linear through the next 16 hours in the *Chromatium* system while *Chlorobium* did not oxidize sulfur.

Protein was synthesized at a high rate during the first 16 hours in *Chromatium vinosum* with a doubling time of 8 hours. The initial rate was 0.15 $\mu g\ ml^{-1}\ h^{-1}$, followed by a slower rate during the next 20 hours (0.004 $\mu g\ ml^{-1}\ h^{-1}$). *Chlorobium* failed to grow; it showed a negative rate of protein synthesis. This can be explained by the partial dilution of the cell suspension when sample volumes are replaced by fresh medium.

The changes in chemical and biological parameters are shown in Figures II-22 and II-23. As a preliminary conclusion, *Chlorobium* may have a higher affinity for sulfide than for S^o, but other factors such as light, high temperature, and the presence of possible toxic end metabolites produced by its counterpart did not permit more than a maintenance metabolism.

Oscillatoria-Chlorobium: Competitive interaction for H_2S was carried out in similar conditions as in the experiment above with *Chromatium* and *Chlorobium*. To prevent light saturation damage, intensities were lowered.

Both bacteria are capable of using H_2 as an electron donor. Sodium sulfide concentration decreased rapidly during the first 4 hours (Fig. II-24). *Chlorobium* used H_2S more efficiently than the cyanobacterium. Sulfide oxidation rates were 175 mM $Na_2S\ h^{-1}$ and 87 mM $Na_2S\ h^{-1}$, respectively. Both bacteria produced and expelled elemental sulfur which remained free in the medium. Only *Chromatium* further oxidized S^o to sulfate, providing itself another energy source besides H_2S. When *Chlorobium* grows under sulfide limitation the ability to use S^o can be observed.

Chlorobium probably uses the passively diffused S^o yielded by *Oscillatoria*. During 24 hours S^o increases in both systems, thus there is no evidence about the source of S^o used as electron donor by *Chlorobium*. However, sulfate increased after 4 hours with a rate of 45.8 μg sulfate $l^{-1}\ h^{-1}$ in the *Chlorobium* system (Fig. II-24). Sulfate is present in large amounts in CHU11 medium, thus some sulfate probably diffused to the *Chlorobium* system. Nevertheless, the rate of sulfate production decreased when sulfide was added (not shown).

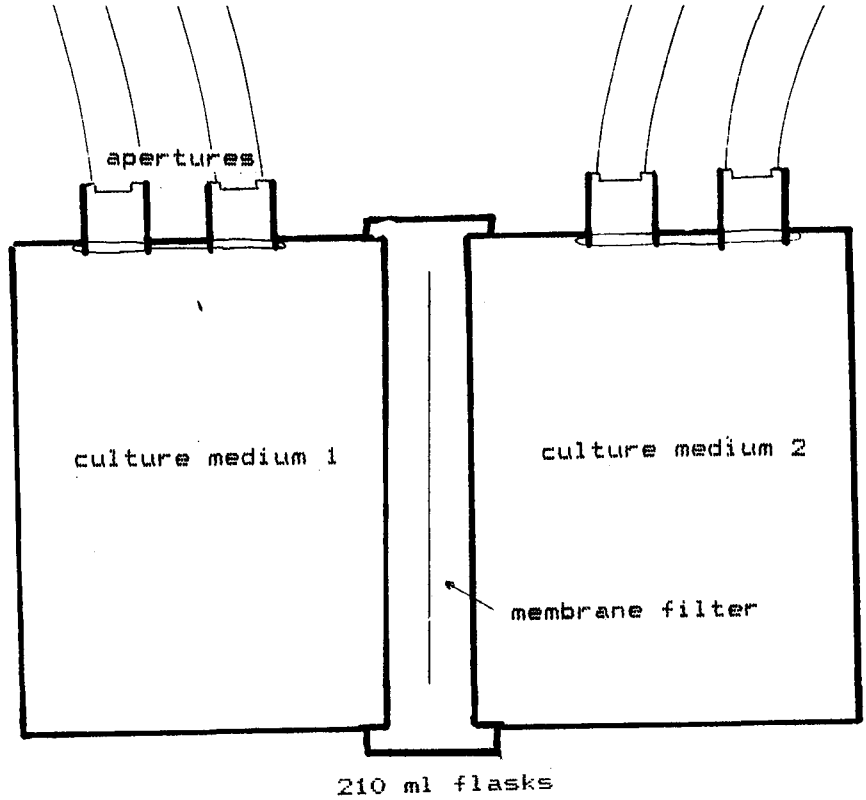

Figure II-21. Diagram of two culture media.

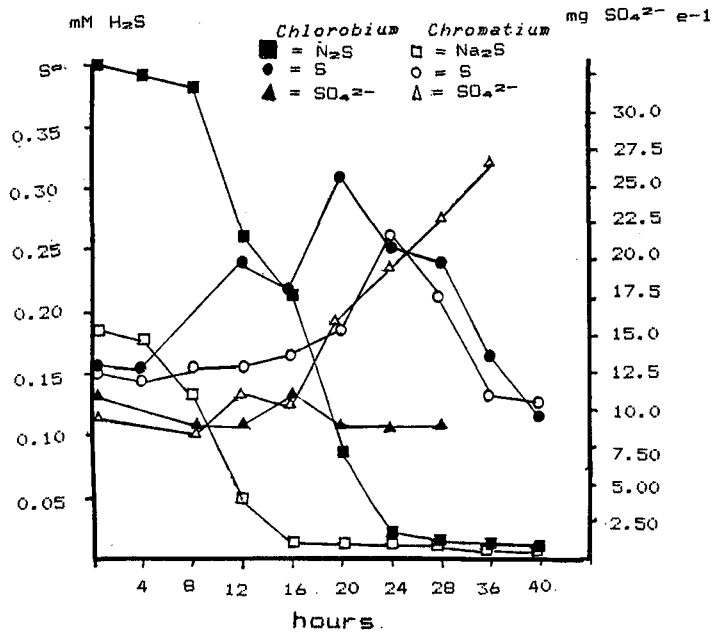

Figure II-22. Production and removal of sulfides and sulfates in *Chlorobium-Chromatium* cells grown in a semi-open system, illuminated by 60 Watt incandescent lamps, at 28o C. Sº served as electron donor only to *Chlorobium vinosum*, which performed full oxidation to SO_4^{2-}.

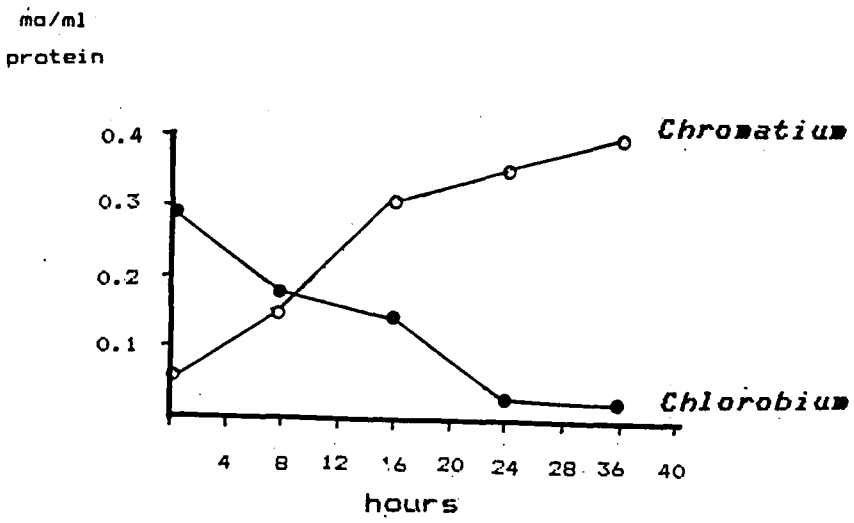

Figure II-23. Protein synthesis. Effective growth is performed only by *C. vinosum*. Descending *Chlorobium* line represents effect of semicontinuous dilution and/or death of the culture.

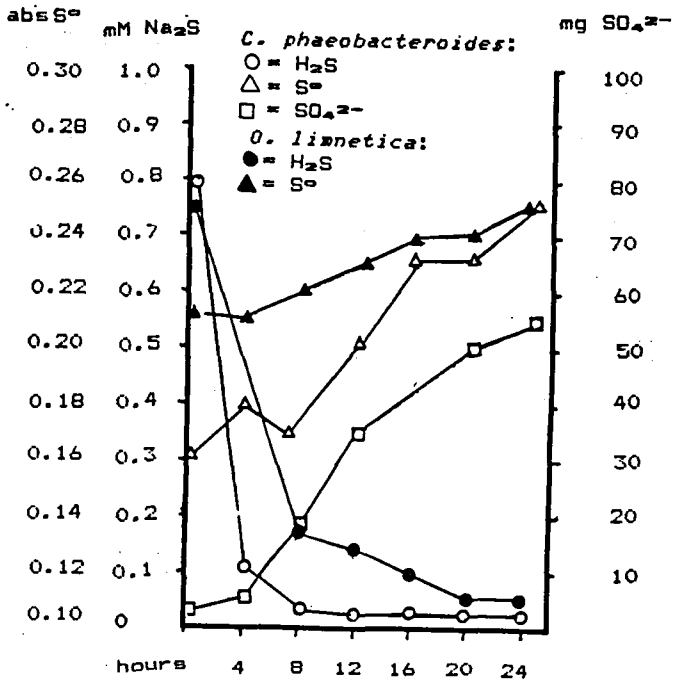

Figure II-24. Changes in chemical parameters during sulfide oxidation to sulfur and sulfate

The absence of sulfide available as electron donor for *O. limnetica* after 8-16 hours probably caused the shift to oxygenic photosynthesis, yielding oxygen toxic to the green sulfur bacterium. Protein synthesis increased during the first 8 hours, and some other growth occurred between 8 and 16 hours and then decreased rapidly after 16 hours (Fig. II-26).

Chlorobium phaeobacteroides' requirements for large amounts of sulfide, low light intensity, and low temperatures place this green sulfur bacterium in an ecological niche with no competitors. In aquatic habitats the uppermost limit of the green bacteria growth layer must be confined to a level of permanent sulfide production. *O. limnetica*, however, is substantially independent of H_2S, and it can shift between photosynthetic systems as environmental conditions require.

Oscillatoria-Chromatium were cultured together in the semi-open system to test competition for sulfide as it probably occurs in nature. Most *Chromatium* dependent upon sulfide are inhibited by oxygen. They lack an assimilatory sulfate reduction metabolism. *C. vinosum* can grow under low sulfide concentrations and high light intensities. Competition for sulfide in a semi-open system with the cyanobacterium grants an advantage to *C. vinosum* with respect to the use of S^o free in the medium, the sulfur being a product of hydrogen sulfide oxidation. Sulfuric acid is produced by photometabolism of *C. vinosum*.

Hydrogen sulfide was utilized by both bacteria as an electron donor. No net growth occurred during oxidation of S^o to sulfate as indicated by protein determination, perhaps due to damage caused by oxygen production by *Oscillatoria*. Some growth or maintenance metabolism possibly occurred since sulfate increased during the first 8 hours. This could not be determined accurately with our techniques (Fig. II-27).

Chlorobium cells are non-motile, strictly anaerobic, and sulfide-dependent. These cells will be found in the microbial community with no other phototrophic bacteria, i.e, over a sulfide-rich layer where they can absorb light energy from above. Yet purple sulfur bacteria, due to their motility and their ability to store S^o inside their cells, can adjust their sulfide environment and ambient light. Competition at low sulfide concentrations and at high light intensities favors *Chromatium vinosum*, which can efficiently utilize either hydrogen sulfide or sulfur. *O. limnetica*, occupying the surface layer in microbial communities, has another strategy since it can use either H_2S or water as an electron donor. Other strains, such as *Oscillatoria c-will*, isolated from Wilborg Spring in California, always perform oxygenic photosynthesis and have a high resistance to sulfide presence (Cohen, et al., unpublished data). When sulfide concentration is not limiting, phototrophic bacteria that seem to have a higher affinity and efficiency for sulfide are naturally selected over

Figure II-25

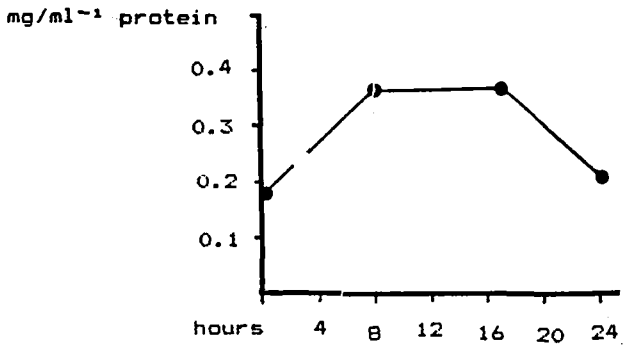

Figure II-27

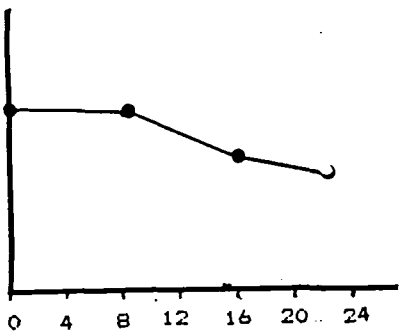

Figure II-25. Protein in *Chlorobium phaeobacteroides* during the first sixteen hours of experiment.

Figure II-27. Lack of growth of *C. vinosum* may have been caused by increasing toxic levels of O_2 due to shift back to oxygenic photosynthesis in *O. limnetica*.

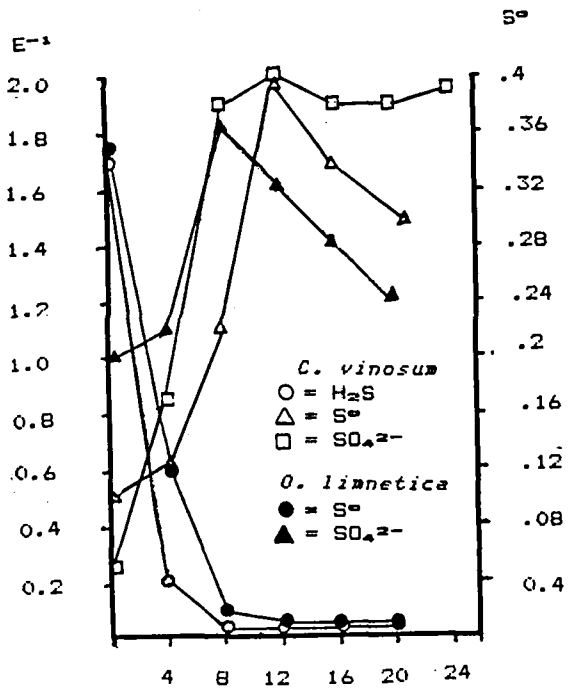

Figure II-26. Sulfur transformations in *Chlorobium-Oscillatoria* cultures.

cyanobacteria. Ecological niches for anaerobic phototrophs are provided in aqueous habitats, where metabolic end products are the primary compounds for their phototrophic metabolism. Maximum efficiency is accomplished by physiological stratification in the microbial populations. Stratification results from competition when primary elements such as H_2S and light become limiting factors.

References

Atlas, R.M. and Bartha, R., 1981. In *Microbial Ecology*, Chapter 8, Addison Wesley Publishing Co., pp. 249-281.

Bartlett, J. and Skoog, F., 1961. Method for sulfur estimation, Analyt. Chem., 26:1008-1011.

Bradford, M.M., 1976. A rapid and sensitive method for the quantification of microgram quantities of protein utilizing the principles of proteus dye binding, Anal. Biochem., 72:248-254.

Cline, J., 1969. Spectrophotometric determination of hydrogen sulfide in natural environments, Limnol. Oceanog., 14:454-459.

Cohen, Y., Padan, E., and Shilo, M., 1975a. Facultative anoxygenic photosynthesis in the cyanoboacterium *Oscillatoria limnetica*, J. Bacteriol., 12:855-861.

Cohen, Y., Jorgensen, B.B., Padan, E., and Shilo, M., 1975b. Sulphide dependent anoxygenic photosynthesis in the cyanobacterium *Oscillatoria limnetica*, Nature, 257:486-492.

Greenberg, A.E., Connem, J.J., and Jenkins, D., 1980. Sulfide/titrimetric method. In *Standard Methods for the Examination of Water and Wastewater*, 15th Ed, American Public Health Assoc. Inc., New York.

Guerrero, R., Mas, J., and Pedros Alio, L., 1984. Buoyant density changes due to intracellular content of sulfur in *Chromatium warmingii* and *Chromatium vinosum*, Arch. Microbiol., 137:350-356.

Hartman, H., 1984. The evolution of photosynthesis and microbial mats; a speculation of Banded Iron Formations. In *Microbial Mats: Stromatolites* (Y. Cohen, R.W. Castenholz, and M.O. Halvorson eds.) Alan R. Liss, Inc., New York.

Kondratieva, E.N., 1979. Intense review of biochemistry. In *Microbial Biochemistry* (J.R. Quayle, ed.), University Park Press, Baltimore.

Montesinos, E., Guerrero, R., Abella, C., and Esteve, I., 1983. Ecology and physiology of the competition for light between *Chlorobium limicola* and *Chlorobium phaeobacteroides* in natural habitats, Appl. Environ. Microbiol., 46:1007-1016.

Montesinos, E., Esteve, I., and Guerrero, R., 1983. Comparison between direct methods for determination of microbial cell volume; electron microscopy and electronic particle sizing, Appl. Environ. Microbiol., 45:1651-1658.

Tabatabai, M.A., 1974. Determination of sulfate in water samples, Sulfur Institute Journal, 10:11-13.

Trueper, H.G., 1982. Taxonomy of the Rhodospirillales. In *Mineral Deposits and the Evolution of the Biosphere* (H.D. Holland and M. Schidlowski, eds.), Dahlem Konferenzen, Springer Verlag, New York, p. 17.

van Gemerden, H. and Beeftink, H. H., 1983. Ecology of phototrophic bacteria. In *The Phototrophic Bacteria: Anaerobic Life in the Light.* (J.S. Ormerod, ed.), Blackwell Scientific Publications, Oxford, pp. 146-185.

Waterbury, J.B. and Stanier, R. Y., 1981. Isolation and growth of cyanobacteria from marine and hypersaline environments. Chapter 9. *The Prokaryotes* (M. P. Starr, H. Stolp, H. G. Trueper, A. Balows, and H. G. Schlegel, eds.), Springer Verlag, New York, pp. 221-223.

CHAPTER III

SULFUR REDUCTION IN SEDIMENTS OF MARINE AND EVAPORITE ENVIRONMENTS

Prof. M. Klug
P. Boston
R. Francois
R. Gyure
B. Javor
G. Tribble
A. Vairavamurthy

Introduction

Estimates of the earth's current crustal reservoirs of sulfur minerals indicate that 200-250 x 10^{18} moles of sulfur in the form of sulfate occur in evaporite deposits as gypsum ($CaSO_4$), 200-250 x 10^{18} moles of reduced sulfur (as FeS_2) are found in sediment, and only 40-42 x 10^{18} moles of sulfur are found dissolved in the oceans and in the atmosphere (R. Garrels, personal communication). During the Permian Period and at other times during the Earth's history, the development of large basins of restricted circulation, (i.e., evaporite environments,) resulted in widespread evaporite sedimentation ($CaCO_3$, $CaSO_4$, NaCl and potash minerals - see Fig. I-17). A result of this sedimentation was a sequestering of sulfur as $CaSO_4$. Although it is estimated that nearly 50 percent of the total sulfur pool is in the form of sulfate, little is known about the role of sulfur-reducing microorganisms as regards either the deposition or the diagenesis of this sulfate.

The microbial ecology of evaporite environments such as the Persian Gulf, the Great Salt Lake, and the Dead Sea are most often characterized by extensive microbial mat communities covering the sediments and/or high biological activity in the plankton of the brines. Although the distribution of microorganisms within these communities has been studied, the interrelationship of microbes and transformations in the sedimentary sulfur cycle environments remains poorly understood.

Geomicrobiological studies of evaporite environments have been retarded by logistical problems including the absence of adequate on-site laboratory facilities. It has been difficult to examine temporal developmental aspects of these environments such as the effects of increasing salinities over time on the geomicrobiology of evaporites.

Solar salt ponds serve as model systems for studying the geomicrobiology of sediments in normal marine and evaporite environments. A solar salt facility maintains seawater-concentrating ponds in a series of brines of increasing density, analogous to a river with a series of dams. Seawater enters the system and flows through the ponds so that $CaCO_3$ and $CaSO_4$ precipitate before the brines reach the stage

of NaCl saturation. The range of salinities in any one pond throughout the year depends on the management procedures of the salt company. These ponds provide opportunities to examine the effects of increases in salinity on the biological processes in the water column and sediments.

The accessibility of the PBME program to the Alviso salt ponds in San Francisco Bay Wildlife Refuge (Map 2) allowed us to examine transformations of sulfur in sediments of ponds ranging in salinities from that of normal seawater to those of brines saturated with sodium chloride.

Our investigations focused on the chemistry of the sediment and pore waters with emphasis on the fate of sulfate and sulfide and on the specific rate measurements of sulfate reduction. The effects of increasing salinity on both forms of sulfur and microbial activity were determined.

Site Description

The Alviso salt ponds, near the east side of the Dumbarton Bridge, are about 80 years old. On the average, brines have a residence time of about 5 years from the time they enter the system from San Francisco Bay until the time the brines are pumped from the NaCl crystallizer ponds to harvest salt. Table III-1 (provided by Leslie Salt Co.) summarizes the brine salinities measured between 25 March, 1983, and 20 July, 1984, in the ponds from which our sediment samples were taken. The data show that pond A2 varied the least (from 30 per mil to 80 per mil salinity). Pond 4 varied from roughly 43 per mil to 180 per mil, pond 5 varied from about 35 per mil to 133 per mil, and pond 1 varied from approximately 105 per mil to 250 per mil.

The ponds support very dense planktonic communities, especially when their salinity is greater than about 42 per mil salinity. Visibility through these brines was about 10 cm.

In ponds with brines ranging up to approximately 3 times seawater salinity, small fish (sticklebacks and topsmelt) are found. In ponds of higher density only a few invertebrates are found (*Ephydra* fly larvae and the brine shrimp *Artemia salina*). *A. salina*, a filter feeder, probably fails to limit phytoplankton both because it is harvested commercially and because of extremely high rates of primary productivity. Brine shrimp growth must also be limited by other factors; the shrimp do not thrive in brines of greater than about 200 per mil salinity. These brines typically have dense blooms of primary producers (the cyanobacterium *Aphanothece halophytica* and the green algae *Dunaliella salina* and *D. viridis*), *Halobacter*, and other halophilic bacteria. Microbial mat development on the surface of sediment occurs in ponds up to about 200 per mil salinity. The extent of mat development is limited by shading by dense plankton communities and rapid chemical precipitation of gypsum (at salinities of greater than 120 per mil) and halite (at salinities of greater than about 250

SALT PONDS
(see Map 2)

NAMES OF PONDS [b] (this study)	Date	Pond A2	Pond 1	Pond 4	Pond 5	S‰
		42	33 [c]	150	90 [d]	
	3/25/83	35	105	42.5	35	13
	4/8/83	35	113	42.5	35	14
	4/15/83	30	113	47.5	37.5	14
	4/29/83	40	115	47.5	42.5	14
	5/6/83	37.5	113	47.5	42.5	15
	5/13/83	40	115	50	45	15
	10/7/83	60	215	125	115	21
	11/4/83	60	200	148	133	19
	11/18/83	55	153	90	90	11
	12/2/83	52.5	158	90	90	11
	12/16/83	47.5	130	62.5	75	14
	1/6/84	45	128	60	67.5	13
	1/13/84	45	128	60	67.5	10
	2/3/84	47.5	130	65	70	12
	2/10/84	47.5	128	65	70	13
	2/24/84	47.5	125	65	67.5	14
	3/2/84	47.5	128	65	67.5	15
	3/16/84	50	128	67.5	67.5	16
	3/23/84	47.5	130	70	70	16
	4/6/84	50	140	80	80	15
	4/27/84	60	168	100	100	14
	5/25/84	80	220 [a]	133	113	16
	6/8/84	65	215	178	123	15
	6/29/84	42.5	225	155	125	19
	7/20/84	37.5	250	150	100	24

a Pond was essentially dry
b Named for quantity,
per mil, of salt measured in July 1984
c Salt marsh mean pond (map 2)
d Same as pond A4 (map 2)

Table III-1. Salinities and temperatures of Leslie Salt Co. concentrating ponds in 1983 and 1984. Salinities as per mil were calculated from salinometer readings.

per mil). Data obtained from sediments at an intertidal environment, the marsh site adjacent to the ponds, were used in comparison with those obtained from the pond sites.

Materials and Methods

Chemical Analyses

Salinities in the overlying water were measured with a hand-held refractometer (American Optical). Values of reported salinities are accurate to within 1 per mil.

Cores were obtained with hand-held extruded polycarbonate core barrels (7.5 cm inner diameters). Cores over 50 cm in length were obtained with the aid of an internal piston to avoid compaction of the core profile. Cores, stoppered and returned to the laboratory at S.J.S.U, were processed within 6 hours of collection.

Pore water from sediments was obtained by extruding the cores in an oxygen-free environment. The latter was obtained by placing a collar over the core and passing oxygen-free N_2 or carbon dioxide over the extruded section. Subsamples of the extruded material were placed in vials (10 cc) pre-flushed with oxygen-free N_2, stoppered with butyl rubber stoppers, and centrifuged for 30 minutes at 12,000 x g in an RG-2 Sorvall centrifuge. Pore water was removed and immediately analyzed for sulfate, sulfide, and chloride. Pore water for analyses such as volatile fatty acids not sensitive to oxygen was obtained by centrifuging larger samples in 50 cc polypropylene tubes.

Sulfate was analyzed turbidimetrically according to the method of Tabathabai (1974); sulfide was analyzed colorimetrically using the methylene blue technique (Cline, 1969). Chloride was determined titrimetrically with silver nitrate (American Public Health Assoc., 1976).

Volatile fatty acids were analyzed after the method of Lovley and Klug (1982). Briefly, 10 ml of pore water are made basic (pH 8.2) and slowly dried in a sand bath with a maximum temperature of 50°C to avoid basic hydrolyses of longer chain esters. Dried samples are made acidic with 10 percent phosphoric acid and vacuum steam distilled. The distillates were analyzed on a Hewlett Packard (Avondale, Pa.) HP 3830A gas chromatograph equipped with a flame ionization detector. Acids were separated on a 2 m glass column packed with 10 percent SP-1220 and 1 percent phosphoric acid coated on AWS Chromosorb 100/120 mesh (Suppelco, Avondale, Pa.). Operating conditions were: Column oven 135°C; detector 175°C; Injector 175°C; flow rate (N_2) 18 ml/minute. Output of the column was integrated with a HP 3830A integrator coupled to the above chromatograph.

At each sampling depth subsamples of sediment were also transferred to a preweighed vial and dried for 18 hours at

70°C in order to obtain a wet/dry conversion value. After drying, a subsample of the sediment was transferred to porcelain crucibles and combusted at 540°C for 20-24 hours in a muffle furnace. Organic content of the sediment was calculated as the percent weight loss following ignition.

For the analyses of acid volatile sulfide (AVS) soluble sulfur subsamples of sediments taken from cores including those used for other analyses were treated withe aqua regia (HNO_3-HCl 2:1) and frozen at -70°C in plastic bags. They were processed within one week. Samples were weighed and suspended in 30-50 ml distilled deionized water (ddw) warmed, and sparged with oxygen-free N_2 in a gas train. The train consisted of the flask with the sediment, followed by a flask with a 5 percent H_2SO_4 solution to trap any free chloride during acidification of the sample, and a tube containing 10 percent $AgNO_3$ to trap sulfide as an Ag_2S precipitate. After sparging, 25-30 ml of concentrated HCl was added to the sediment and the reaction was continued until no further Ag_2S precipitation was observed. The flask was again briefly warmed to remove the last traces of AVS. The Ag_2S precipitate was filtered on Whatman 50 paper, washed, dried, and weighed. The HCl-treated sediment was filtered on Whatman 50 paper and washed. The filtrate was analyzed for sulfate. The sediment was subjected to aqua regia oxidation by wetting the sediment with approximately 5 ml ddw and adding 20 ml aqua regia. The sediment was left at room temperature for 16 hours, heated to just below boiling for 2 hours, then filtered on glass fiber GF/A filters (Gelman Instrument Co.), washed with 80 ml ddw. The filtrate was analyzed for sulfate. Sulfate was estimated according to the method of Tabathabai (1974).

Sulfate Reduction Rates

Sulfate reduction rates were obtained using a modification of the technique of Ivanov (1964). Subsamples of sediments were obtained with 5 ml plastic syringes with the needle end cut off. The subcores were extruded into preflushed (oxygen-free N_2) 30 ml serum vials and stoppered. Each bottle received 3 microcuries (uc) $Na_2{}^{35}SO_4$ in 1 ml of anoxic sulfate-free seawater. Samples were mixed and incubated at *in situ* temperature (23°C) for 6-8 hours. The reaction was stopped by injecting 1 ml of 5 percent zinc acetate; then the samples were frozen (-70°C) until processing. All experiments were done in duplicate for each core section. Samples were assayed and rates determined using the procedure described by Smith and Klug (1981). These methods only accounted for the recovery of reduced sulfate in the free S^{2-} and AVS pool. Rates therefore should be considered underestimates of total sulfate reduction.

Results and Discussion

Chemical Profiles

Values measured for the sulfate, sulfide, and acid volatile sulfide (AVS) pools in sediments collected from an intertidal marsh site near pond 1 (33 per mil), pond A2 (42 per mil), pond A4 (90 per mil), pond 4 (150 per mil), and pond 1 (300 per mil) are shown in Tables III-2 through III-6 and Figures III-1 through III-5. Hereafter, sampling sites will be referred to by their salinities.

The percent sediment dry weight generally increased as a function of pond salinity due to the precipitation of gypsum and halite which are relatively dense constituents of hypersaline sediments. The organic content of the sediments (measured as a loss of weight upon ignition) was very high, ranging from about 10 percent to 20 percent of the dry weight. The lowest value recorded was 7.8 percent (300 percent salinity) and the highest value recorded was 23.1 percent (90 per mil site). Organic carbon content appeared to increase with salinity in sediments to a maximum in 90 per mil sediments, and then to decrease somewhat with continued concentration of brine. In all cases the organic content was higher than that found in the intertidal marsh sediment (33 per mil).

The salinity of the superficial brines in the salt ponds was estimated with a refractometer. Because calcium precipitates primarily as $CaSO_4$ in brines concentrated greater than four-fold (about 140 per mil) and NaCl precipitates when brines are concentrated to greater than about 250 per mil, the actual ion content of concentrated brines in the study sites could not be calculated by simply multiplying the concentration of each ion by the factor of concentration measured with the refractometer. With the exception of the 300 per mil site, estimates of seawater concentration were possible by measurements of Cl^- concentration, since this ion is conservative until the brine reaches the stage of NaCl saturation. For this reason, the calculation of sulfate/chloride ratios in sediment pore waters shown in Tables III-2 through III-6 and Figures III-1 through III-5 give a reasonable estimate of the amount of steady state sulfate reduced as a function of salinity and depth below the oxygen interface.

In every site except the 300 per mil site, the sulfate/chloride ratio decreased with depth in a manner typically found in marine sediments. The sediment profile in the 300 per mil site (Table III-6) may be complicated by the fact that although the chlorinity decreased with depth somewhat continuously, gypsum precipitation in various layers increased both the solid and soluble sulfate pools in localized horizons. Sulfate reduction rates (discussed on the following pages) were significant in this core; therefore the absence of biological activity can not explain the unpredictability in the pore water

Depth (cm)	S^{2-} mM	SO_4^{2-} mM	Cl^- M	$\frac{SO_4^{2-}}{Cl^-}$	% dry wt	% org matter	µmol[a] AVS	µmol[b] ARS
overlying water		27.5	0.345	0.080				
0-1	1.39	19.1	0.455	0.042	24.0	11.7	148	181
1-2	0.88	18.8	0.444	0.042	29.6	9.9	177	221
2-3	1.27	16.4	0.424	0.039	31.2	9.8	180	196
3-5	1.11	19.1	0.403	0.047	32.1	9.7	242	181
5-7	2.35	16.4	0.378	0.043	31.2	9.9	186	193
9-11	2.47	11.7	0.355	0.033	30.4	11.4	155	357
11-13	1.48	11.7	nd	nd	32.3	9.6	107	375
13-15	1.24	7.8	nd	nd	34.1	9.5	195	254
17-19	2.29	7.8	0.335	0.023	33.4	9.0	108	347
21-23	2.22	6.3	nd	nd	34.5	8.3	57	574
23-25	2.84	10.5	0.339	0.031	35.9	8.1	44	478
26-28	2.84	8.6	nd	nd	37.9	8.2	41	446
28-30	2.72	8.0	nd	nd	38.5	8.1	31	549
30-32	2.16	12.5	nd	nd	39.5	8.6	26	488

[a] acid volatile sulfur per g dry weight
[b] aqua regia soluble sulfur, per g dry weight

Table III-2. Chemical profiles of 33 per mil sediments.

Depth (cm)	S^{2-} mM	SO_4^{2-} mM	% dry wt	µmol[a] AVS	µmol[b] ARS
overlying water		21.9			
0-1	1.7	24.1	20.0	97	179
1-2	3.4	33.6	24.	156	187
2-3	3.4	28.9	26.5	161	155
5-7	5.0	24.5	23.3	124	206
9-11	5.0	18.2	26.6	108	315
13-15	nd	16.4	23.2	156	209

[a] acid volatile sulfur per g dry weight
[b] aqua regia soluble sulfur, per g dry weight

Table III-3a. Chemical profiles of 42 per mil sediments, 7/23/84.

Depth (cm)	SO_4^{2-} mM	Cl^- M	$\frac{SO_4^{2-}}{Cl^-}$	% dry wt	% org matter
0-3	28.1	0.818	0.035	25.1	14.9
3-6	20.9	0.856	0.027	24.7	17.7
6-9	17.8	0.930	0.023	37.6	10.8
9-12	13.5	0.975	0.019	30.9	14.1
12-15	11.1	0.980	0.017	27.3	16.3
15-18	9.2	0.988	0.009	27.3	16.3
18-21	8.6	0.975	0.009	28.5	19.4
21-24	4.3	0.978	0.004	26.2	19.8
27-30	4.8	0.973	0.005	27.7	17.2
3-36	3.9	0.973	0.004	32.1	13.4
39-42	3.9	nd	nd	28.2	15.8
45-48	4.3	0.983	0.004	32.2	15.4
51-54	4.5	nd	nd	30.6	15.9
57-60	3.9	nd	nd	31.1	15.6
63-66	2.5	0.980	0.003	29.6	15.9
69-72	3.9	0.963	0.004	29.2	15.0
72-72	5.2	0.955	0.006	30.6	14.6
78-81	3.7	0.968	0.004	36.2	13.5
83-86	4.1	0.968	0.004	34.9	12.9
86-89	5.3	0.949	0.006	38.3	11.9

Table III-3b. Chemical profiles of 42 per mil sediments, 7/28/84.

Depth (cm)	S^{2-} mM	SO_4^{2-} mM	Cl^- M	$\frac{SO_4^{2-}}{Cl^-}$	% dry wt	% org matter
0-1	0.9	61.7	1.17	0.053	17.9	20.9
1-2	2.3	46.9	1.19	0.039	23.2	15.1
2-3	8.7	46.9	1.24	0.038	23.1	17.2
3-5	10.2	32.8	1.28	0.026	22.5	17.9
5-7	9.9	25.8	nd	nd	19.2	23.1
7-9	12.0	16.4	1.29	0.013	19.	22.5
9-11	12.9	13.7	1.26	0.011	22.8	17.3
11-13	18.0	10.9	nd	nd	23.5	18.1

Table III-4. Chemical profiles of 90 per mil sediments.

Depth (cm)	S^{2-} mM	SO_4^{2-} mM	Cl^- M	$\frac{SO_4^{2-}}{Cl^-}$	% dry wt	% org matter
overlying water		105	2.25	0.047		
0-1	3.60	84.0	2.06	0.041	nd	nd
1-2	4.65	87.8	2.25	0.039	27.4	16.2
2-3	4.87	74.0	2.00	0.037	26.4	17.6
3-5	5.06	64.6	2.38	0.030	28.3	18.2
5-7	5.81	68.7	1.64	0.042	36.6	15.0
7-9	6.75	60.2	1.50	0.040	38.9	12.4
9-11	6.43	55.8	1.50	0.037	42.2	12.1
11-13	5.25	50.8	1.38	0.037	33.2	14.7
15-17	6.37	49.5	1.31	0.038	40.2	9.7
17-19	4.87	42.9	1.13	0.038	44.7	8.3
19-21	5.67	45.1	1.13	0.040	43.9	9.4

* gypsum layer in this sediment interval

Table III-5. Chemical profiles of 150 per mil sediments.

Depth (cm)	S^{2-} mM	SO_4^{2-} mM	Cl^- M	$\frac{SO_4^{2-}}{Cl^-}$	% dry wt	% org matter	µmol[a] AVS	µmol[b] ARS	mM $CaSO_4$
overlying water		196	6.38	0.0307					
0-1	2.01	162	6.0	0.0270	48.6	12.1	9.3	41.8	0.90
1-2	3.24	172	6.0	0.0287	43.7	14.0	38	46.4	1.10
2-3	3.55	162	5.81	0.0279	45.0	13.2	71	62	0.71
3-4	4.09	149	5.5	0.0271	46.0	13.5	62	88	1.61
4-6	6.10	122	4.56	0.0268	44.3	15.1	59	71	0.93
6-8	6.49	148	4.88	0.0303	44.6	15.2	62	10	.21
8-10	6.25	119	3.63	0.0328	44.6	16.0	67	163	0.99
10-12	8.73	108	2.63	0.0411	45.2	15.0	67	368	2.05
12-14	10.27	204	10.63	0.0192	40.1	14.5	70	203	0.38
14-16	10.81	117	4.44	0.0264	40.3	11.0	64	249	0.51
18-20	8.03	87	2.63	0.0331	39.4	10.9	78	185	0.28

[a] acid volatile sulfur per g dry weight
[b] aqua regia soluble sulfur, per g dry weight
[c] gypsum layer in this sediment interval

Table III-6. Chemical profiles of 300 per mil sediments, 7/28/84.

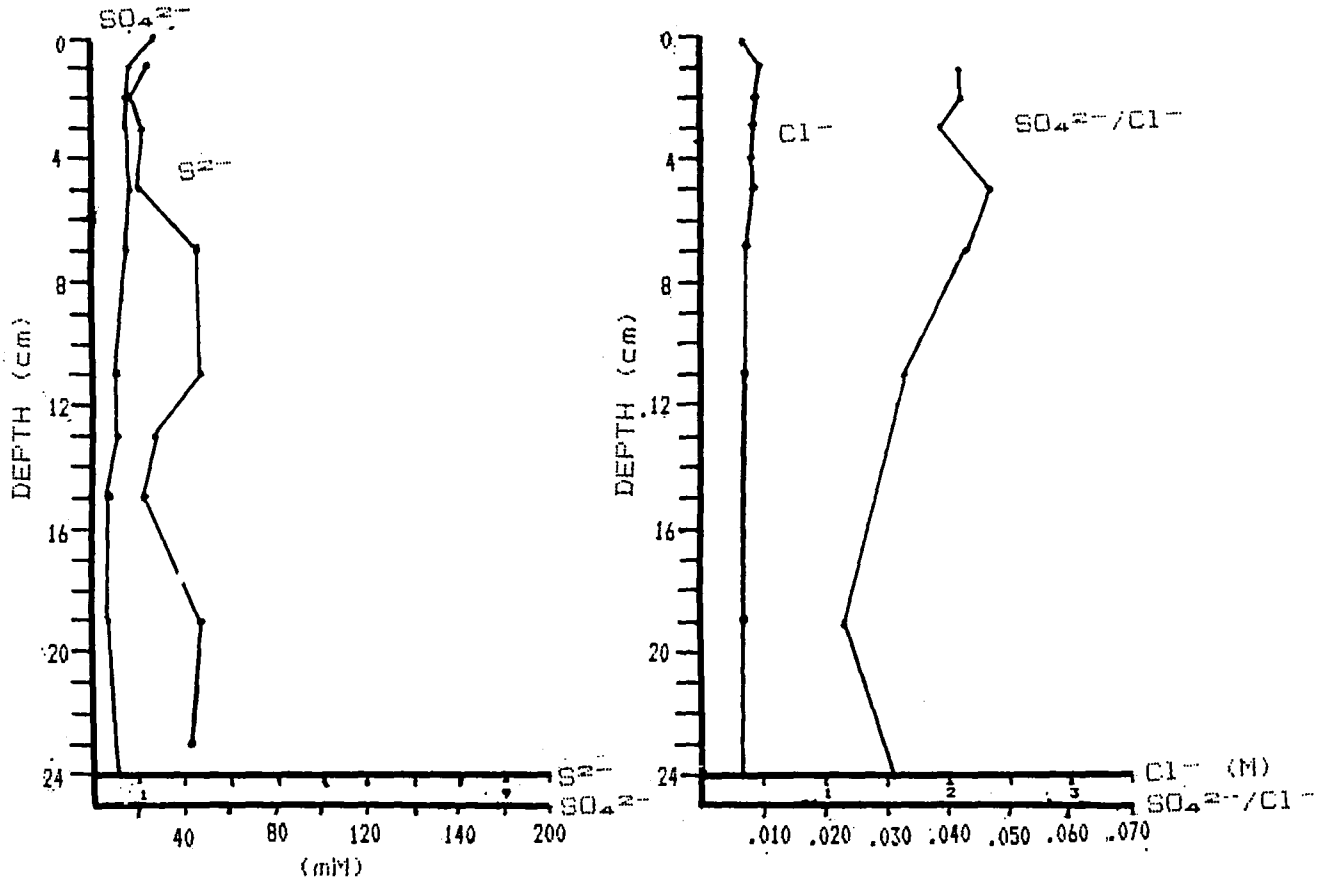

Figure III-1. (a) Sulfate and sulfide pool sizes in sediments from the 33 per mil site; (b) sulfate/chloride ratio and chloride pool size in sediments from the 33 per mil site.

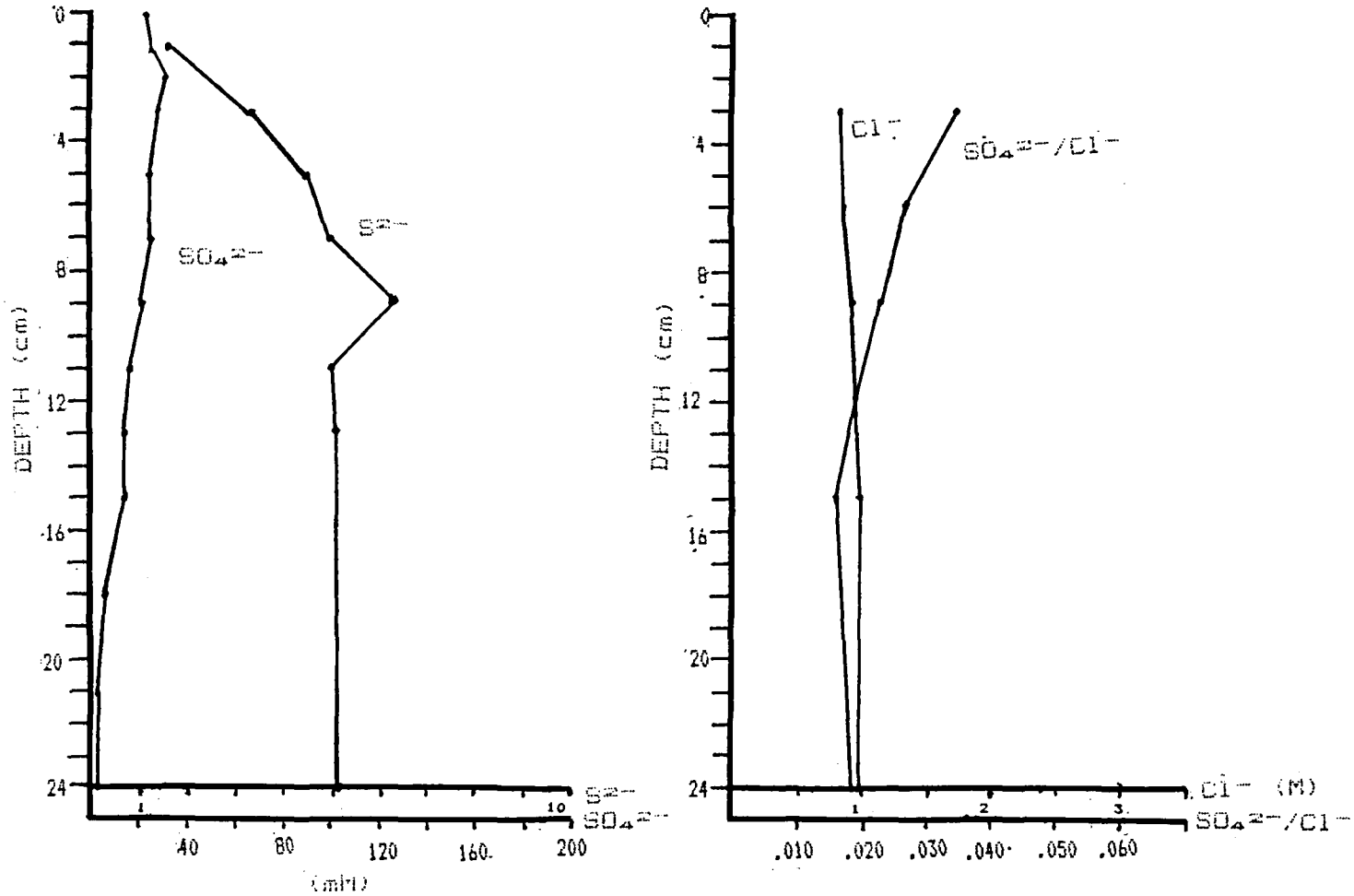

Figure III-2. (a) Sulfate and sulfide pool sizes in sediments from the 42 per mil site; (b) sulfate/chloride ratio and chloride pool size in sediments from the 42 per mil site.

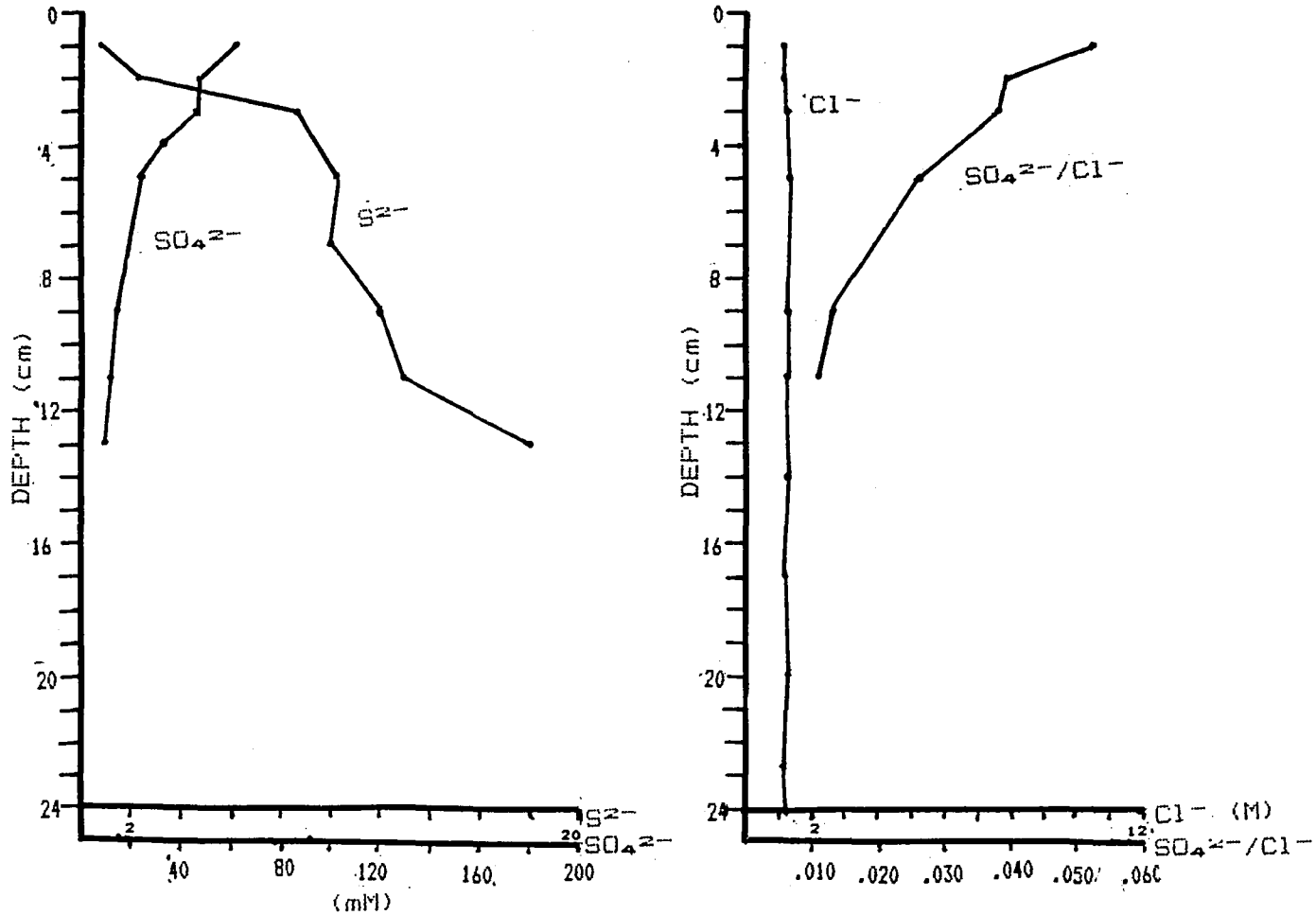

Figure III-3. (a) Sulfate and sulfide pool sizes in sediments from the 90 per mil site; (b) sulfate/chloride ratio and chloride pool size in sediments from the 90 per mil site.

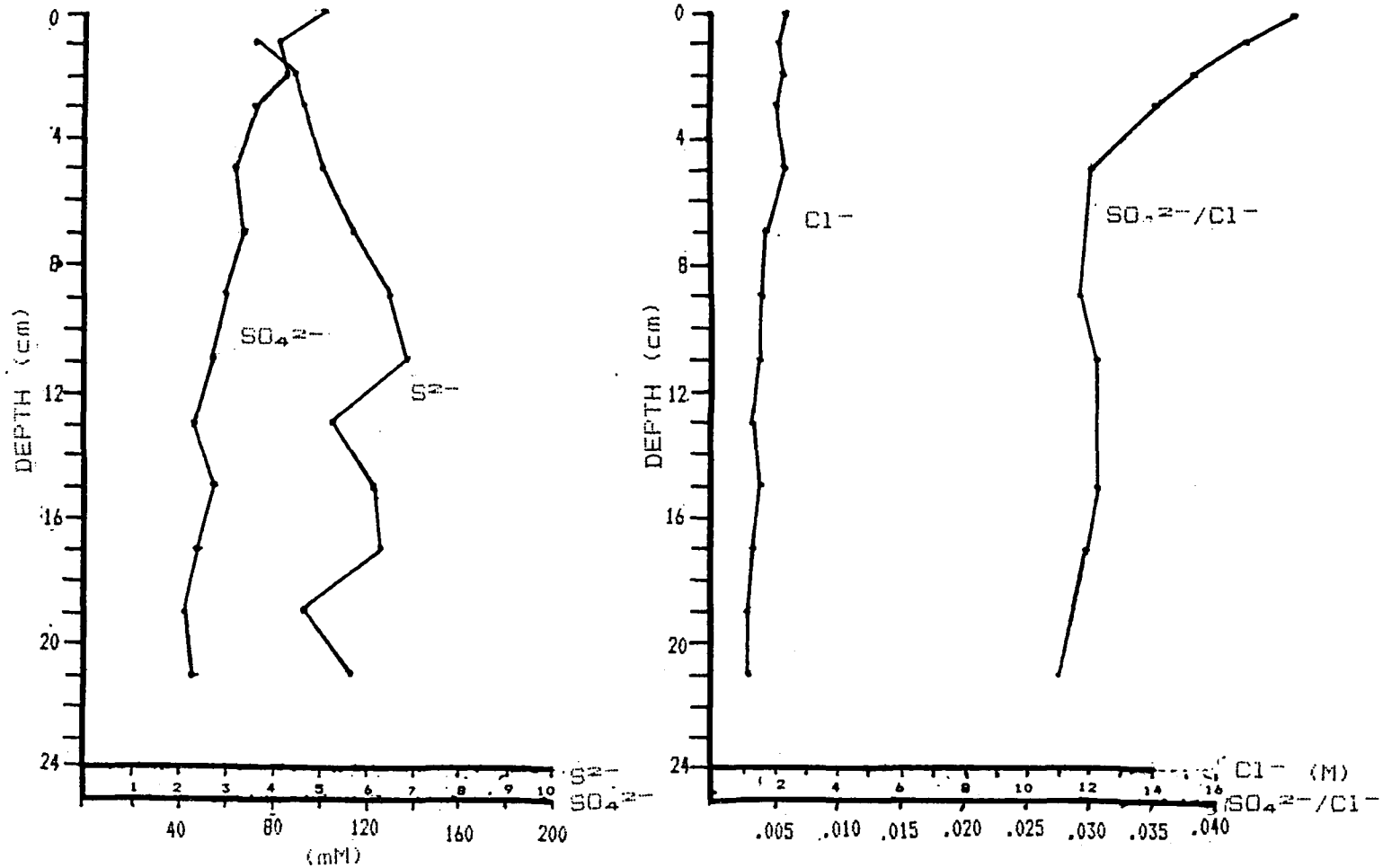

Figure III-4. (a) Sulfate and sulfide pool sizes in sediments from the 150 per mil site; (b) sulfate/chloride ratio and chloride pool size in sediments from the 150 per mil site.

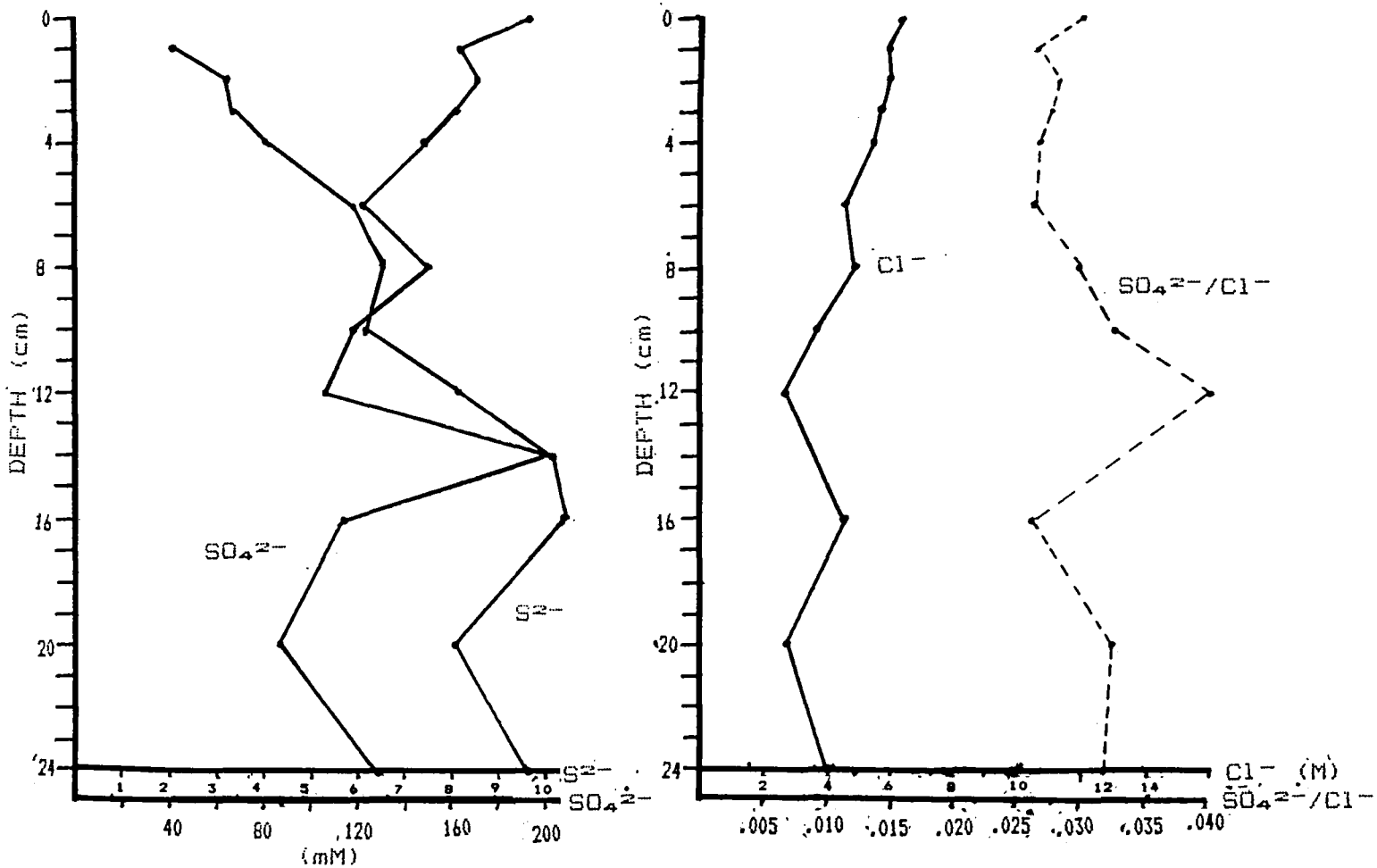

Figure III-5. (a) Sulfate and sulfide pool sizes in sediments from the 300 per mil site; (b) sulfate/chloride ratio and chloride pool size in sediments from the 300 per mil site.

(at 14 cm) but the variation may be due to a combination of a localized halite lamina and analytical error.

Sulfate is reduced to sulfide by sulfate-reducing bacteria, but sulfide may then react either biologically or non-biologically. Thus the sulfide pool is not an absolute indicator of the degree of sulfate reduction. It is therefore useful to measure the various sulfide pools as well as the sulfate/chloride ratios in order to evaluate the effects of bacterial sulfate reduction on the cycling of sedimentary sulfur.

In all sediment pore waters, sulfide was present in millimolar concentrations, typically between 1 and 10 mM. Sulfide typically increased with depth in all the salt pond sites. In the 42 per mil and 150 per mil sites, sulfide levelled off below about 10 cm depth, and in the 300 per mil site, it leveled off below around 14 cm. In the 90 per mil sediment sulfide increased with depth to at least 13 cm; no further profiles were measured below this point. Sulfide remained low with no general increase in the 33 per mil marsh sediment down to 32 cm. This type of profile may be typical of an intertidal marsh from which pore water is constantly pumped in and out with tidal changes in the nearby tidal creek. The steady-state values recorded for the salt pond sediments reflect sulfide concentrations that result from *in situ* sulfide production and passive diffusion in the absence of tidal pumping.

In anaerobic sediment in which Fe^{2+} is present, free sulfide reacts with Fe^{2+} to produce FeS and FeS_2. FeS is primarily responsible for the black color of reduced sediments. FeS is somewhat refractory to redissolution by microorganisms but it is readily oxidized by O_2. FeS reacts in an unknown way to form FeS_2 (pyrite), an extremely recalcitrant mineral that is not significantly oxidized non-biologically by O_2. Analyses of FeS and pyrite in sediment profiles through a wide range of salinities would indicate whether well-described trends in pyrite formation for marine sediments hold true for organic-rich evaporite sediments as well. For this study AVS and aqua regia-soluble sulfur profiles were determined in the 33 per mil, 43 per mil, and 300 per mil sediments. Pyrite was the major iron sulfide phase found in all three sediments (Figs. III-6 and 7). In the 42 per mil salinity site, the pyrite pool was nearly twice as large as the AVS pool within the top cm of the sediment. Pyrite content in all three sediment cores increased with sediment depth. In the 33 per mil core, as is typical for marine sediments, AVS decreased with sediment depth down to at least 32 cm. Because the 42 per mil sediment profile was only measured down to 14 cm no definite trend could be ascertained. The AVS pool increased with depth to at least 24 cm in the 300 per mil salinity sediment. These findings may be of importance in evaluating the mechanisms of FeS-FeS_2 transformations especially since the soluble and solid sulfate pools in this core were extremely large.

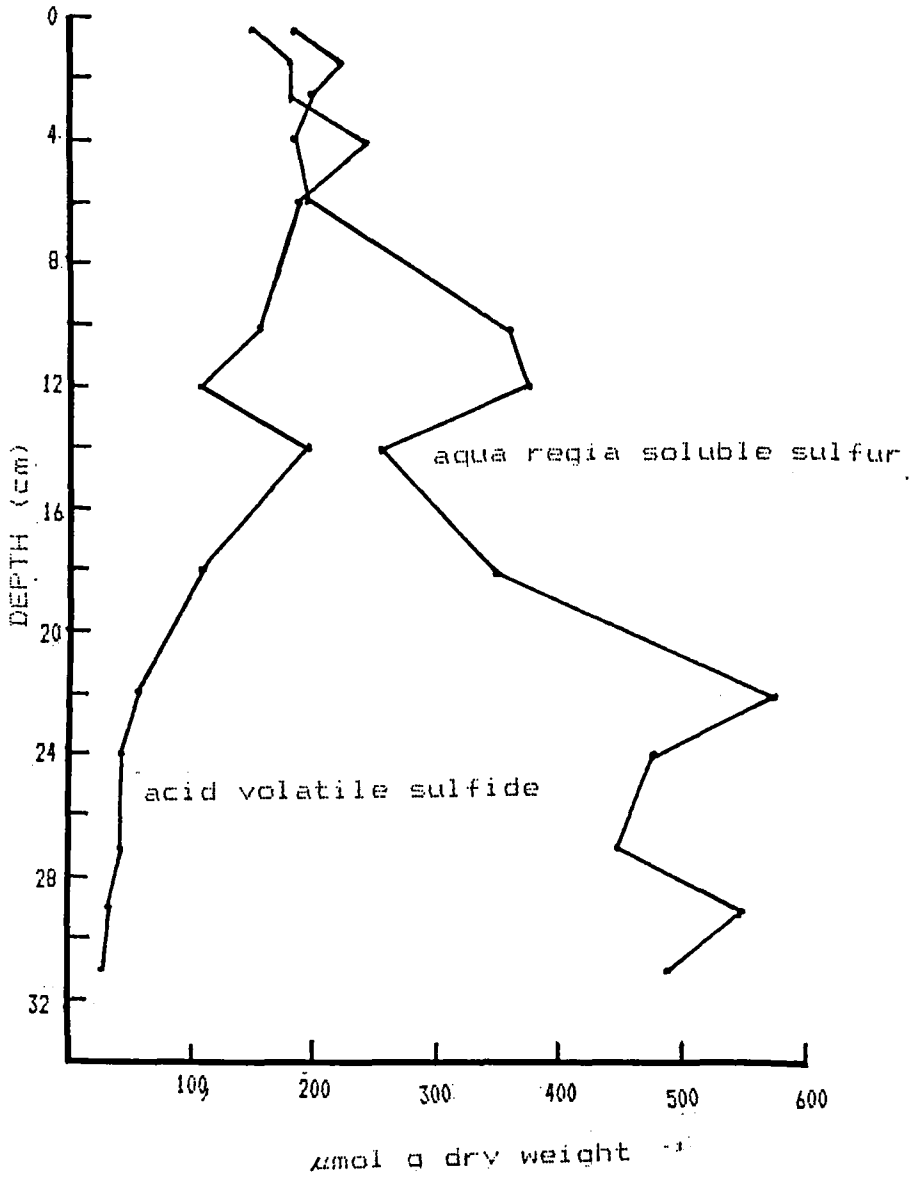

Figure III-6. Pool sizes of acid volatile sulfide and aqua regia soluble sulfur in sediments from the 33 per mil site.

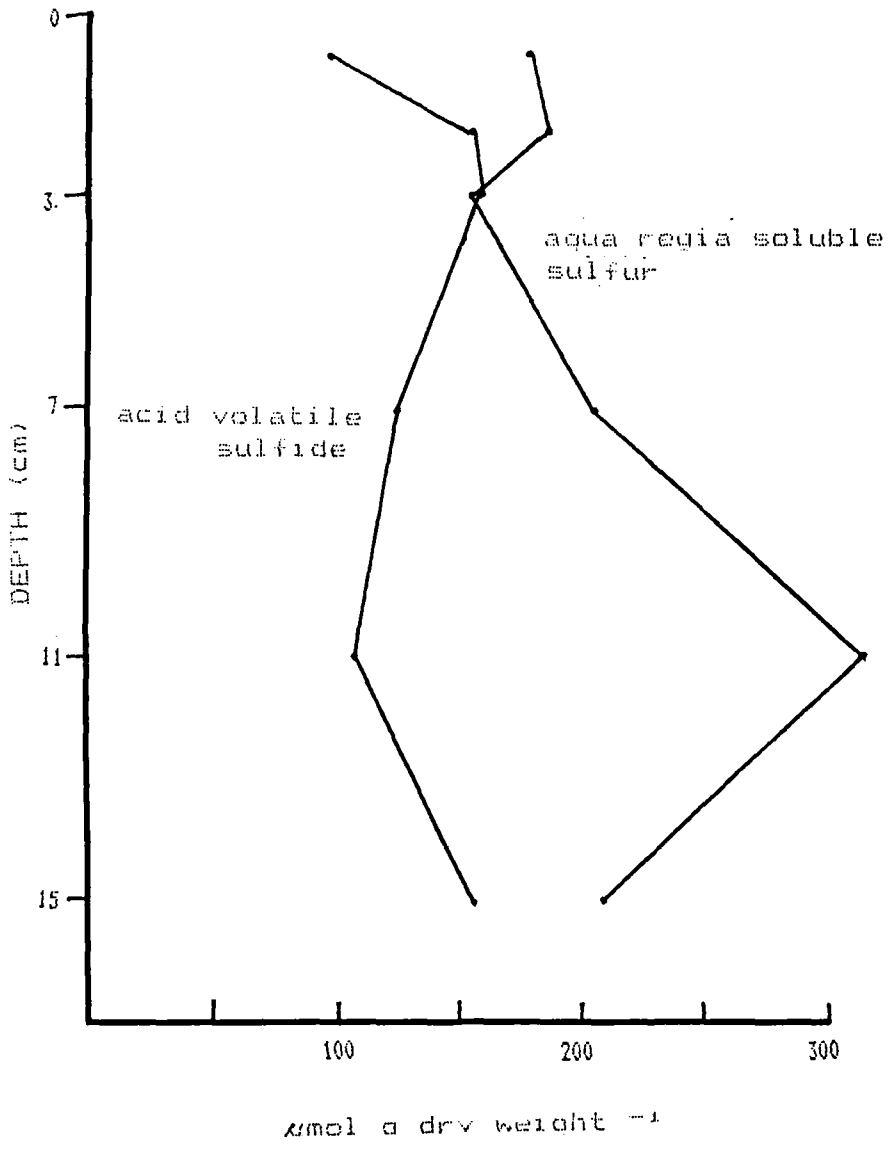

Figure III-7. Pool sizes of acid volatile sulfide and aqua regia-soluble sulfur in sediments from the 42 per mil site.

Total iron sulfides, estimated from the sum of AVS plus aqua regia soluble sulfide in the 33 per mil, 42 per mil, and 300 per mil salinity sediments, were compared. Total iron sulfides decreased with increasing salinity. The one anomalous point at 10-12 cm in the 300 per mil sediment corresponds to the sediment underlying a several mm-thick gypsum crust at this horizon. The relatively high concentration of iron sulfides at this sediment interval may have resulted from incomplete solution of gypsum in the HCl treatment which caused additional sulfate to appear after aqua regia treatment. Total iron was not measured in any of the sediments in this part of the investigation. The lack of iron in hypersaline sediments in combination with lower sulfate reduction rates may account for the lower abundance of iron sulfides in the evaporite sediments.

Sulfate Reduction

The rates of sulfate reduction were determined in duplicate samples at six different horizons in sediments of each pond (Figures III-8 and III-9). In all sediments except those from the 300 per mil salinity site, the greatest rates of sulfate reduction were recorded in the top first centimeter. Sulfate reduction measured in the first centimeter sediment of the 300 per mil pond may have been low because the surface, intermixed with halite crystals, was capped by a several mm-thick halite crust.

In sediments below 1 cm sulfate reduction rates were somewhat similar in most of the samples. In the 33 per mil salinity sediment, where the highest sulfate reduction rates were measured in the surficial 1 cm, negligible sulfate reduction was recorded below a depth of 7 cm. There was less than 1 mmol of dissolved sulfate in the pore water per gram wet weight, indicating that the sulfate reduction was most likely sulfate-limited.

Sulfate reduction rates in the top 1 cm of the 42 per mil salinity sediment were nearly ten-fold less than those recorded for the 33 per mil salinity sediment; both ponds harbored extensive microbial mat communities. However without data on the mat community productivity and on differences in bioturbation, an explanation for these differences is most likely not due to an increase in salinity since the values for reduction in the lower horizons are more comparable.

The higher rate of sulfate reduction recorded in the 13-15 cm interval of the 42 per mil sediment corresponds to the relatively high concentration of AVS and the low abundance of pyrite in this horizon. This is just below a point where sulfide reaches a maximum concentration.

Sulfate reduction rates in the 90 per mil salinity sediment were very high in the surficial 1 cm, and much lower below the

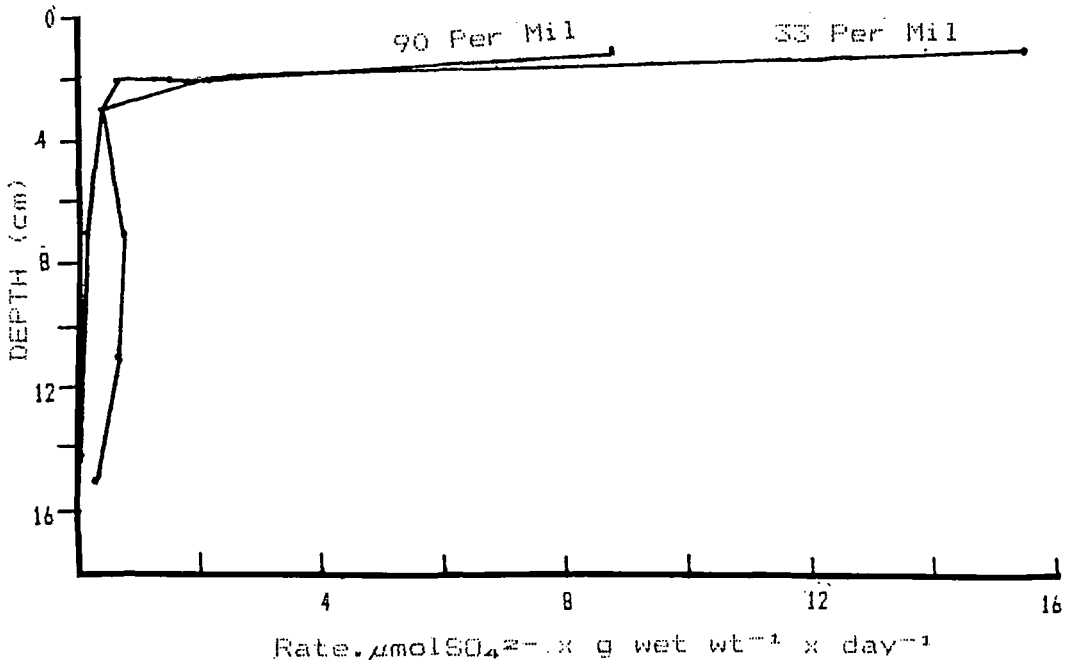

Figure III-8. Sulfate reduction rate in sediments from the 33 per mil site and 90 per mil sites.

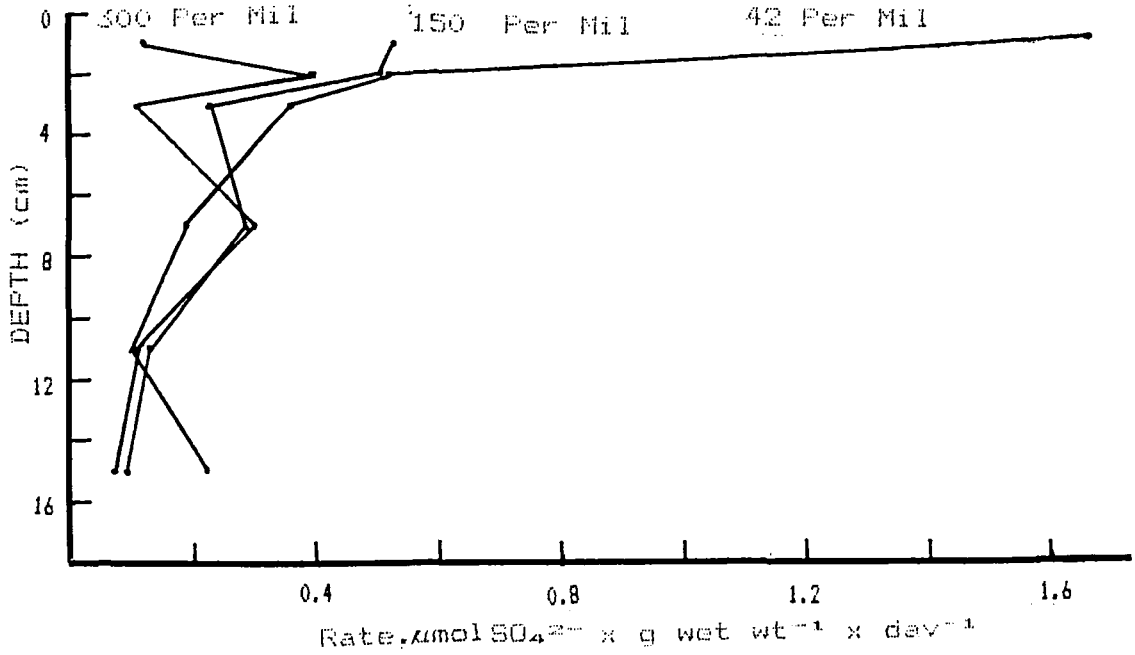

Figure III-9. Sulfate reduction rate in sediments from the 42 per mil, 150 per mil and 300 per mil sites.

surface, although they were never completely attenuated. The dissolved sulfate pool remained high in subsurface sediment, and was never less than 19 mM per gram wet weight in contrast to those measurements recorded for the 33 per mil sediment.

Gypsum deposition may have altered the typical sulfate reduction profiles in both the 150 per mil and 300 per mil salinity sediments. Gypsum precipitation probably precluded the local accumulation of organic-rich sediment found in lower salinity sediments, and increased the potential pool of soluble sulfate in adjacent horizons by acting as a sulfate reservoir.

In all but the 33 per mil site sulfate concentration did not seem to limit sulfate reduction. Organic matter content and concentrations of volatile fatty acids (Tables III-7 through III-11) increased in relation to increased salinity. When the sulfate reduction rates are compared on the basis of salinity, at depths below the top 1 cm a general trend of decreased activity is observed from ponds with a salinity greater than 70 per mil. To determine relationships of salinity to rates of sulfate reduction more studies are required.

Volatile Fatty Acids

Acetic acid was found in the greatest concentration of any volatile fatty acid (VFA) from the pore waters of sediments of any site (Tables III-7 through III-11). Isobutyric acid was the second most predominant VFA identified. It was followed by an unknown "acid volatile" compound which eluted between isovaleric and n-valeric acid at a retention time of 7.35 minutes. Another unknown acid eluted between butyric and isovaleric acids at a retention of 5.25 minutes. Figure III-10 (a-c) compares the chromatograms obtained for a standard series of VFA's (Fig. III-10a); chromatograms obtained from the depth interval of 19-20 cm in the 70 per mil site (Fig. III-10 b); and the composite chromatogram illustrating the elution pattern of the 7.35 minute peak (Fig. III-10c).

The number of identifiable VFA's increased markedly with an increase in salinity. No clear trend was noted in the concentrations of acetate to increased salinity except for the large increase noted in the 300 per mil site.

Acetate concentration generally followed that of sulfate in pore water (the 33 per mil and 42 per mil sites, Figures III-11 and III-12). This relationship did not strictly hold (Tables III-9, III-10, III-11). The concentration of acetate reached a minimum at the sulfate concentration minimum and subsequently increased with depth. These data strongly imply that acetate is a major precursor of sulfate reduction and that the reduction of sulfate and acetate consumption are linked. They further suggest that sulfate reducers are the major sink for acetate in these sediments. Another acetate-consuming process, methanogenesis, was examined in the 42 per mil site. The methane vs sulfate

Depth (cm)	a	b	c
0-1	19.7	-	0.12
1-2	20.59	0.14	0.12
2-3	19.62	0.83	0.51
4-5	9.62	-	-
7-8	10.44	-	-
10-11	10.44	-	-
14-15	8.69	0.68	0.45
18-19	8.20	0.581	0.37
23-24	5.47	0.028	0.99

a = acetic acid µmol/liter pore water
b = isobutyric acid µmol/liter pore water
c = volatile fatty acid 7.35 arbitrary unit/liter pore water

Table III-7. Volatile fatty acids in pore waters from the 33 per mil site. 7.35 refers to the retention time in relationship to acetic and isobutyric acids.

Depth (cm)	a	b	c	d
0-3	43.64	0.69	2.27	2.73
3-6	59.30	-	2.62	2.49
6-9	19.17	-	3.22	3.23
9-12	13.06	-	2.24	2.14
12-15	15.86	-	1.57	1.60
15-18	14.51-	1.02	0.99	
18-21	9.34	-	0.82	0.96
21-24	30.64	-	0.71	0.68
27-30	40.73	2.13	1.90	1.69
33-36	39.78	0.71	1.21	0.90
39-42	26.09	0.95	0.67	0.52
51-54	34.38	-	0.07	0.28
57-60	20.72	-	0.55	0.57
63-66	29-47	-	1.57	1.50
69-72	13-82	-	0.31	0.31
72-75	13.97	-	0.40	0.60
78-81	11.75	-	0.30	0.42
83-86	13.63	-	0.54	0.57
86-89	8.19	-	0.12	0.23

a = acetic acid µmol/liter pore water
b = isobutyric acid µmol/liter interstitial water
c = propionic acid µmol/liter interstitial water
d = volatile fatty acid 7.35 arbitrary unit/liter interstitial water

Table III-8. Volatile fatty acids in pore waters from the 42 per mil site. 7.35 refers to the retention time in relationship to acetic and isobutyric acids.

Depth (cm)	a	b	c	d	e
0-1	5.67	0.-	-	0.13	-
1-2	16.98	0.03	-	0.21	-
2-3	21.56	2.0	-	2.50	-
4-5	37.38	6.64	-	8.25	0.17
7-8	20.76	2.51	-	2.91	-
10-11	31.76	4.59	-	5.14	0.15
13-14	37.64	3.43	-	5.01	0.04
16-17	42.62	9.7	-	9.73	0.24
19-20	45.62	10.67	-	9.09	
22-23	16.79	5.67	-	4.73	0.18
25-26	32.34	8.68	-	8.33	-

a = acetic acid µmol/liter pore water
b = isobutyric acid µmol/liter interstitial water
c = n butyric acid µmol/liter interstitial water
d = volatile fatty acid 7.35 arbitrary unit/liter interstitial water
e = volatile fatty acid 5.25 arbitrary unit/liter interstitial water

Table III-9. Volatile fatty acids in pore waters from the 90 per mil site.

Depth (cm)	a	b	c	d	e
0-1	16.00	1.61	-	1.77	0.09
1-2	22.24	3.82	0.30	3.81	0.27
2-3	36.00	3.16	0.28	3.29	0.27
2-3	36.00	3.16	0.28	3.29	0.27
4-5	20.63	4.73	-	7.16	0.21
7-8	35.87	7.35	-	11.09	0.77
10-11	40.70	8.90	0.61	7.37	0.06
13-14	19.80	1.22	-	1.27	-
16-17	18.65	1.27	-	1.15	-
19-20	45.76	3.81	-	4.27	-
22-23	30.63	1.90	-	1.95	-
25-26	35.30	1.68	-	1.91	-

a = acetic acid µmol/liter pore water
b = isobutyric acid µmol/liter interstitial water
c = n. butyric acid µmol/liter interstitial water
d = volatile fatty acid 7.35 arbitrary unit/liter interstitial water
e = volatile fatty acid 5.25 arbitrary unit/liter interstitial water

Table III-10. Volatile fatty acids in pore waters from the 150 per mil site.

Depth (cm)	a	b	c	d	e	f	g
0-1	802.33	9.95	128.76	5.88	5.92	85.92	4.70
1-2	736.97	4.66	150.40	2.46	3.85	114.06	2.88
2-3	309.66	-	34.53	1.07	-	26.43	1.77
4-5	288.94	0.73	65.05	2.65	2.30	32.96	2.00
5-6	248.94	0.73	65.05	2.65	2.30	32.96	2.00
12-13	45.31	-	14.68	-	-	6.78	0.28
20-21	27.47	-	7.05	-	-	3.15	-
24-25	39.25	6.84	-	-	3.03	-	
28-29	57.36	-	7.3	-	-	3.71	-

a = acetic acid μmol/liter pore water
b = propionic acid μmol/liter interstitial water
c = isobutyric acid μmol/liter interstitial water
d = n butyric acid μmol/liter interstitial water
e = isovaleric acid μmol/liter interstitial water
f = volatile fatty acid 7.35 arbitrary unit/liter interstitial water
g = volatile fatty acid 5.25 arbitrary unit/liter interstitial water

Table III-11. Volatile fatty acids in pore waters from the 300 per mil site.

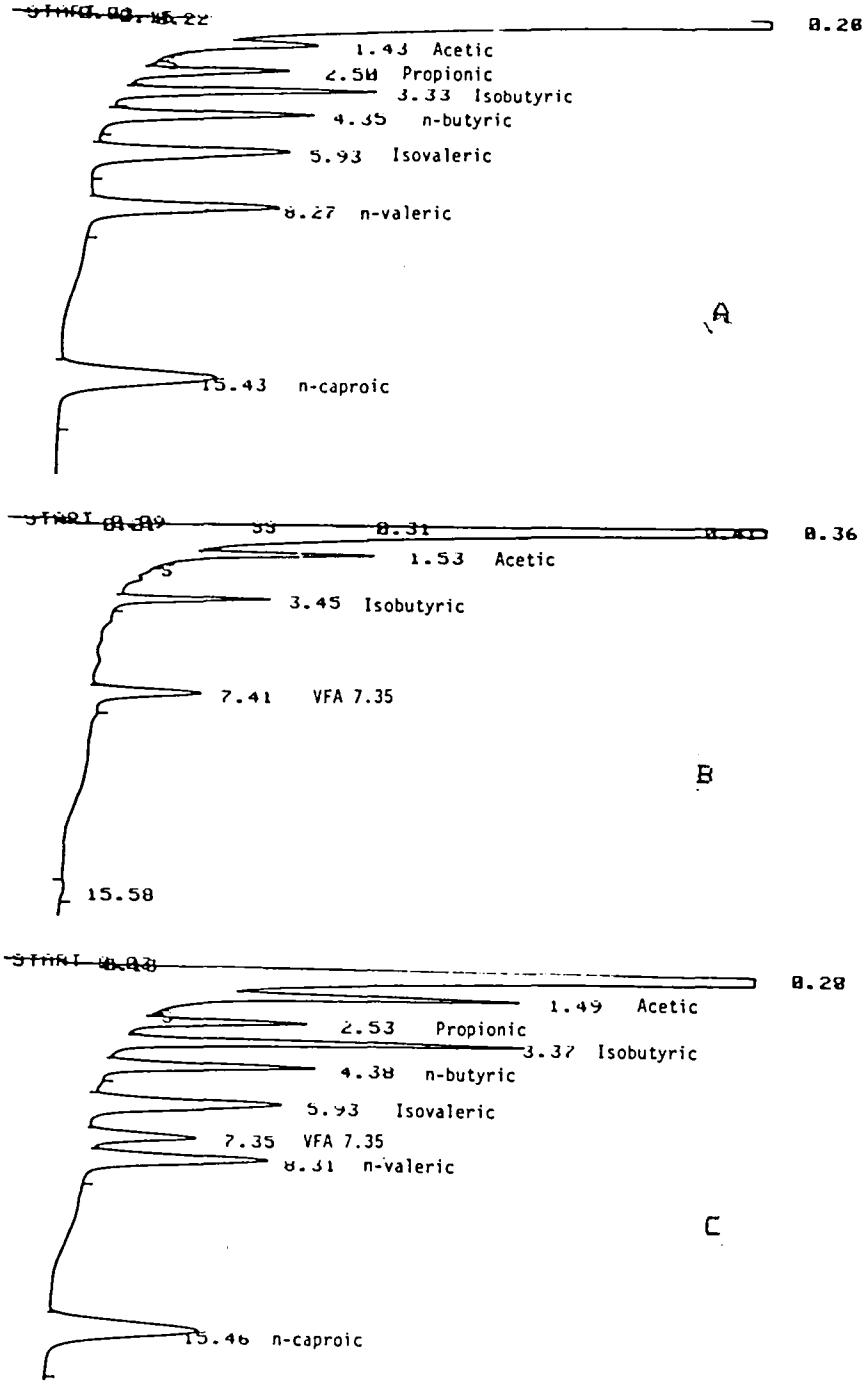

Figure III-10. (a) Chromatogram of standard volatile fatty acid mixture; (b) chromatogram of volatile fatty acids in the 19-20 cm profile of sediments from the 70 per mil site; (c) composite chromatogram of (a) and (b).

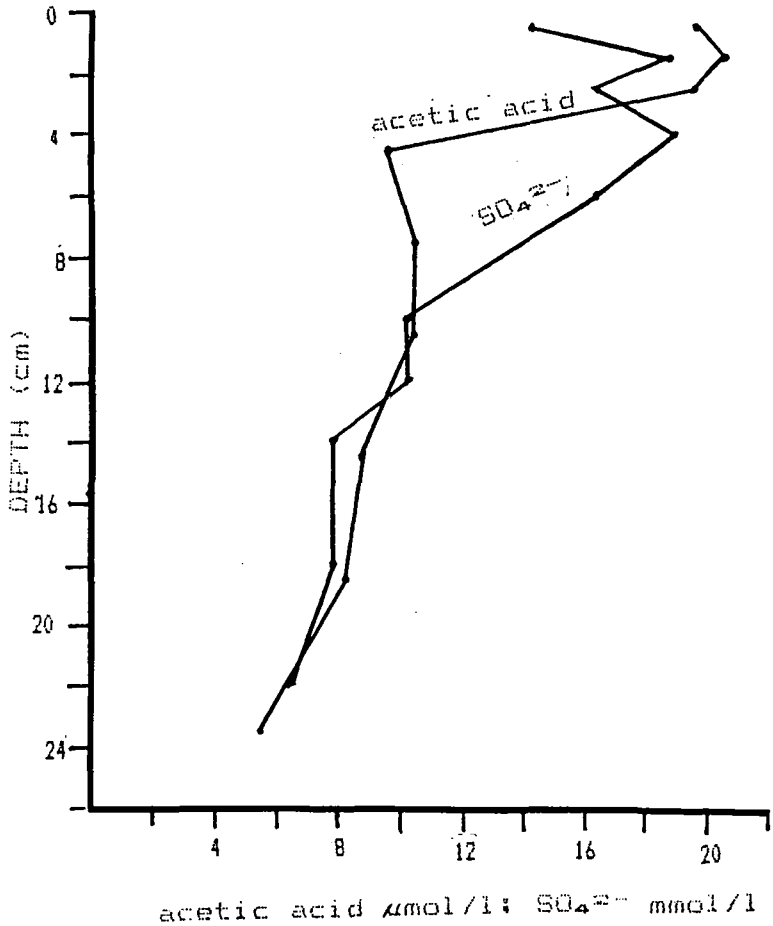

Figure III-11. Pool size of acetic acid and sulfate in sediments from the 33 per mil site.

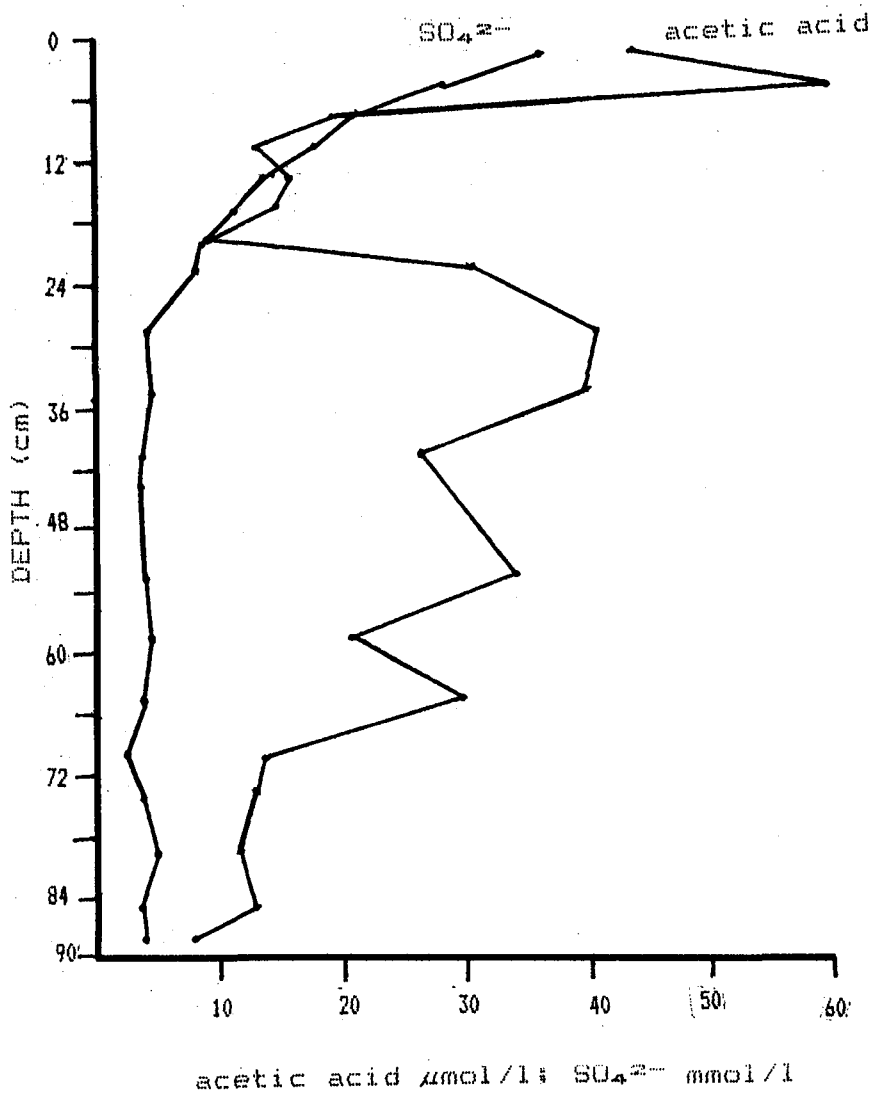

Figure III-12. Pool size of acetic acid and sulfate in sediments from the 42 per mil site.

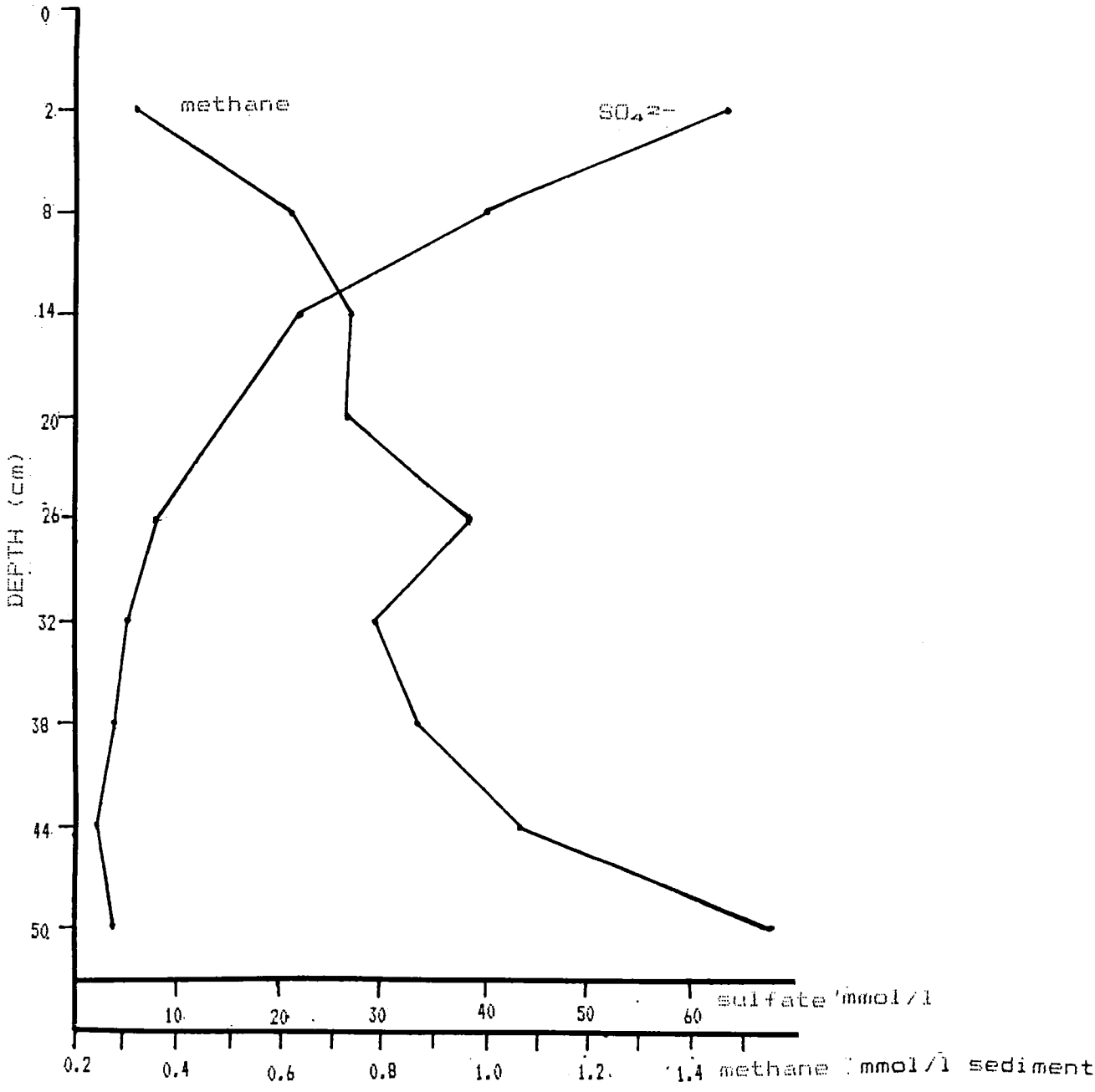

Figure III-13. Pool size of methane and sulfate in sediments from the 42 per mil site.

profiles are illustrated in Figure III-13. Although a steep gradient of methane was observed, no production of methane could be measured within a 60 cm profile from this site. Without further data, based on the observed profiles of sulfate, acetate, and sulfate reduction rates, we can only speculate that the major acetate consuming process is sulfate reduction.

The concentration and increase in diversity of total VFA's in relation to salinity suggests that the production of these compounds through fermentation exceeds their consumption. The general increase in chain length of the acids would be predicted if the products of fermentation, such as acetate are not consumed (Wolin, 1976). The presence of sulfate and acetate at concentrations well above the Km for sulfate reducers for sulfate and acetate down to 20 or more centimeters in sediments of the 90 per mil, 150 per mil, and 300 per mil sites, suggests that something other than low sulfate and acetate concentration inhibited sulfate reducers.

Conclusions

A unique set of chemical profiles and sulfate-reducing activity was found for the sediments of each of the sites examined. The quantity of organic matter in the salt pond sediments was significantly greater than that occurring in the adjacent intertidal site. The total quantitative and qualitative distribtion of volatile fatty acids was also greater in the salt ponds. Volatile fatty acids increased with salinity; the maximum quantitative and qualitative spectra of acids were found in the 300 per mil site. The general decrease in sulfate reduction rate in sediments of ponds of increasing salinity lead us to believe that organic matter was accumulating in these ponds because of the limited consumption of the fermentative intermediates.

Our sulfate reduction rates in sediments from the hypersaline ponds were comparable to those recorded in other evaporite environments (Skyring, 1984; Lyons et al., 1984). Sulfate reduction rates in surficial sediments of 33 per mil salinity were at least 2 and up to 50 times greater than those measured in other temperate salt marshes associated with microbial mats and in *Spartina* marshes. Howarth and Teal (1979) measured sulfate reduction rates of 0.25-6.0 μM per cm^{-3} per day in marsh sediments. In another study by Skyring et al. (1979), in a *Spartina* salt marsh, sulfate reduction rates were about 1 μM per gram per day in surficial sediments. Thus our rates of sulfate reduction were at least an order of magnitude higher than those in other salt marshes. Without knowledge of the extent of the surface mat development, organic production, and bioturbation in the sediments our results are difficult to extrapolate. The major point is that sulfate reduction in the pond sediments was apparently inhibited by salinity (or factors which accompanied the increases in salinity) since adequate sulfate and precursors (i.e., acetic acid) were available as metabolites for sulfate reducers. Iron sulfide

decreased in sediments of ponds of increasing salinity. Since sulfide values were generally higher than those recorded in the marsh site, iron limitations may limit iron sulfide accumulations. Iron limitations would also limit the activity of sulfate reducers, and thus sulfate reduction.

Although preliminary, these results indicate patterns which may serve as a basis for the examination of the chemical and microbiological changes occurring during the developmental stages of evaporite deposits.

References

American Public Health Assoc., 1976. *Standard Methods for the Examination of Water and Wastewater*, 14th ed., American Public Health Association, Inc., New York, pp. 303-304.

Cline, J.D., 1969. Spectrophotometric determination of hydrogen sulfide in natural waters, Limnol. Oceanog., 14:454-459.

Howarth, R.W., and Merkel, S., 1984. Pyrite formation and the measurement of sulfate reduction in salt marsh sediments, Limnol. Oceanog., 29:598-608.

Howarth, R.W., and Teal, J.M., 1979. Sulfate reduction in a New England salt marsh., Limnol. Oceanog. 24:999-1013.

Ivanov, M.W., 1964. Microbiological processes in the formation of sulfur deposits, Israel Program for Scientific Translation, Ltd., Jerusalem.

Lovley, D. R., and Klug, M. J., 1982. Intermediary metabolism of organic matter in sediments of a eutrophic lake., Appl. Environ. Microbiol., 43:552-560.

Lyons, W.B., Hines, M.E. and Gaudette, H.E., 1984. Major and minor element pore water geochemistry of modern marine sabkhas: the influence of cyanobacterial mats. In *Microbial Mats: Stromatolites*, (Y. Cohen, R.W. Castenholz and H.O. Halvorson eds.), Alan R. Liss, Inc., New York, pp. 411-423.

Smith, R.L. and Klug, M.J., 1981. Reduction of sulfur compounds in the sediments of a eutrophic lake basin. Appl. Environ. Microbiol., 41:1230-1237.

Skyring, G.W., Oshrain, R.L., and Wiebe, W.J., 1979. Sulfate reduction rates in Georgia marshland soil. Geomicrobiol. J., 1:389-400.

Skyring, G.W., 1984. Sulfate reduction in marine sediments associated with cyanobacterial mats in Australia. In *Microbial Mats: Stromatolites*, (Y. Cohen, R.W. Castenholz, and H.O. Halvorson eds.), Alan R. Liss, Inc., New York, pp. 265-275.

Tabathabai, M.A., 1974. Determination of sulfate in water samples, Sulphur. Int. J., 10:11-13.

Wolin, M.J., 1976. Interactions between H_2-producing and methane-producing species. In *Microbial Formation and Utilization of Gases (H_2, CH_4, Co).* (H.G. Schlegel, G. Gottschalk, and N. Pfenning, eds.), Goltze, Gottingen., pp. 141-150.

CHAPTER IV
CYANOBACTERIAL MATS: MICROANALYSIS OF COMMUNITY METABOLISM

Prof. Y. Cohen
D. Bermudes
U. Fischer
R. Haddad
L. Prufert
T. Scheulderman
T. Shaw

Introduction

Stromatolites, trace fossils of microbial communities, provide the oldest evidence of life on earth; they represent the beginning of our 3.5 billion year old record. Stromatolites are by far the most abundant fossils found in the Archean and Proterozoic Eons (3.5-0.6 billion years ago) (BYA). The other major sedimentary record of the Prephanerozoic are Banded Iron Formations (BIFs) deposited 2.2-1.8 BYA. Cyanobacteria are postulated to play a major role in the deposition of both stromatolites and BIFs. Cyanobacteria-like fossils have been described from cherts in many Prephanerozoic and Phanerozoic sediments. Some BIFs are associated with stromatolites. Cyanobacterial iron-dependent photosynthesis related to the deposition of Banded Iron Formations has been postulated (Hartman, 1984).

Even though stromatolites are scarce in the Phanerozoic Eon, they are still found today in specific environments where grazing metazoans are excluded. Cyanobacterial mats are presently found in hypersaline lagoons, hot springs, and alkaline lakes. The study of mat-forming cyanobacteria aids in the understanding of the environment of deposition of Prephanerozoic stromatolites and Banded Iron Formations as well as our study of evolution of photosynthesis among the most ancient groups of oxygenic phototrophs.

Cyanobacteria have long been known as oxygenic photosynthesizers. Other kinds of photosynthetic modes have been demonstrated for several mat-forming cyanobacteria, possibly indicating the antiquity of this group.

Facultative anoxygenic photosynthesis operating photosystem I independently of photosystem II and the use of hydrogen sulfide or hydrogen as electron donors have been shown in some strains of benthic cyanobacteria (Padan and Cohen, 1982). Recently others demonstrated oxygenic photosynthesis under high sulfide concentration (Jorgensen, et al., 1985). Fe^{++}-dependent carbon dioxide photoassimilation has been shown for conditions of intermediate redox potential.

Delta ^{13}C measurements of the cyanobacterial communities in recent mats have yielded the heaviest value ever recorded for per mil organic matter: -4 to -8 per mil. Yet similar measurements in ancient mats show values of 12 per mil to 16 per mil. The observed

discrepancy may be the result of the appearance of the bicarbonate pump in recent cyanobacteria that evolved in response to the decrease in atmospheric CO_2 concentration since the Phanerozoic Eon.

Two field sites were chosen for the study of cyanobacterial mats: the salt ponds in San Francisco Bay near the Dumbarton bridge where microbial mats develop under varying salinities, and the Alum Rock sulfur springs.

The microbial communities in these sites were studied using several approaches: a) light microscopy; b) the measurement of microprofiles of oxygen and sulfide at the surface of the microbial mat; c) the study of diurnal variation of oxygen and sulfide; d) *in situ* measurement of photosynthesis and sulfate reduction and study of the coupling of these two processes; e) measurement of glutathione in the upper layers of the microbial mat as a possible oxygen quencher; f) measurement of reduced iron as a possible intermediate electron donor along the established redoxcline in the mats; g) measurement of dissolved phosphate as an indicator of processes of break down of organic matter in these systems; and h) measurement of carbon dioxide in the interstitial water and its delta ^{13}C in an attempt to understand the flow of CO_2 through the systems.

Using these approaches we have analyzed microbial processes of primary production and initial degradation at the most active zone of the microbial mat. Our results can be compared to those obtained by those working on SO_4 reduction (Chapter III) in the deeper part of the sediment column.

Site Descriptions

Dumbarton Bridge Salt Ponds and Marsh

Salt Ponds

The study sites were the Dumbarton Salt Ponds (salinas) north of the Dumbarton Bridge (Map 2). These San Francisco Bay Wildlife Preserve salinas represent several environmentally distinct microbial mat communities. There are several salt evaporite ponds increasing from 42 per mil salinity (pond A2) to 90 per mil in pond 5 to 150 (145) per mil in pond 4. Sedimentary surficial microbial mats, collected from water at depths of 10-20 cm in these ponds have been microscopically examined (see Table IV-1).

The overall trends observed include a general decrease in the diversity of cyanobacteria. Population densities of *Oscillatoria* and *Anabaena* also declined with increasing salinity. *Anabaena* appeared in the 90 per mil pond probably because a niche was created for it due to the abundance of *Aphanothece halophytica* which causes a depletion of nitrogen.

MARSH	ORGANISMS
20 per mil	Cyanobacteria *Oscillatoria* 1,4,5,6,7,30 μ: Dominant *Anabaena* 4 μ: Fewer *Spirulina* 2 μ: Fewer Unicellular species: Fewer Other bacteria *Beggiatoa* (3 μ x 300 μ length): Abundant Spirochetes, *Chromatium*: Abundant *Thiospirillum*: Fewer Eukaryotes Diatoms: Dominant Ciliate and non-ciliate protists: Fewer
42 per mil	Cyanobacteria *Fischerella* - heterocysts: Fewer *Spirulina* (tightly coiled and loose type): Fewer Other bacteria *Beggiatoa*: Fewer Eukaryotes Small and large diatoms: Dominant Green algae, heterotrophic protists: Fewer
90 per mil	Cyanobacteria *Oscillatoria* 1,5 μ: Fewer *Fischerella*: Fewer *Spirulina* (tightly coiled and loose type): Fewer *Anabaena* 4 μ: Fewer *Aphanothece halophytica* (planktonic): Abundant Other bacteria Spirochetes: Fewer *Beggiatoa*: Fewer - Abundant Eukaryotes Diatoms: Dominant
145 per mil	Cyanobacteria *Aphanothece halophytica* (planktonic): Dominant *Oscillatoria* 1,2,4 μ: Fewer Purple filamentous bacteria 0.3,1 μ: Abundant Other bacteria Spirochetes, *Beggiatoa*: Fewer Eukaryotes *Dunaliella* (planktonic), Diatoms: Fewer Rod-shaped ciliated protists: Fewer
200 per mil	Cyanobacteria *Aphanothece halophytica*: Fewer Other bacteria Halophilic bacteria: Abundant Eukaryotes *Dunaliella*: Dominant

Table IV-1. Abundance and variety of organisms present in marsh sites of various salinities.

Yet *Aphanothece halophytica* increased as salinity increased. Diatom population densities also appear to decrease as a function of increasing salinity. The occurrence of *Beggiatoa* and spirochetes in all salinity ponds suggests that there is a relatively shallow oxygen/sulfide interface in these mats.

Marsh (33 Per Mil) Site

In addition to these saline environments a salt marsh with salinity around 33 per mil was studied. Mats from this site were collected as described above and examined microscopically (Table IV-1) (for site description see Chapter III).

Alum Rock Park Sulfur Spring Site

The site chosen at Alum Rock Park (Map 3) was a sulfide stream flowing down a rocky bank leading into a larger fresh water stream about 1.5 meters wide. The main sulfide stream split into two small streams about 35 cm down from the source and continued flowing down the bank. White filamentous bacteria grew along the two branches of the stream while cyanobacterial mats bordered the streams. The source water smelled strongly of sulfide. Elemental sulfur was evident along the edge of the stream leading from the source. Samples of microbial communities were taken along one of the main streams and across the dryer section between the streams (Figure IV-1). Communities appeared to vary significantly from high to low sulfide regions.

Materials and Methods

Microelectrode Calibrations and Data Calculations

Oxygen Microelectrode Calibration

The oxygen microelectrode (see Cohen, Sulfur Transformations, Chapter 1) was calibrated using three solutions of known oxygen concentration. The first consisted of distilled water that had equilibrated having N_2 gas bubbled through it. Similarly the second solution was distilled water that had had air bubbled through it, and the third was distilled water that had been equilibrated with O_2 gas. To determine the oxygen content of the solutions in micromoles a Keithley 480 picoammeter current meter hooked up to an electrode was employed. Winkler titrations using the iodometric method (*Standard Methods for the Examination of Water and Waste Water, 15th ed.*) were done for each of the three solutions. The values thus determined allowed the construction of a calibration curve for each electrode. Oxygen microelectrodes were recalibrated individually and frequently since in most media some agents pass through and poison the semipermeable membrane tip, causing a nonlinear response to oxygen concentration (Revsbech and Ward, 1984).

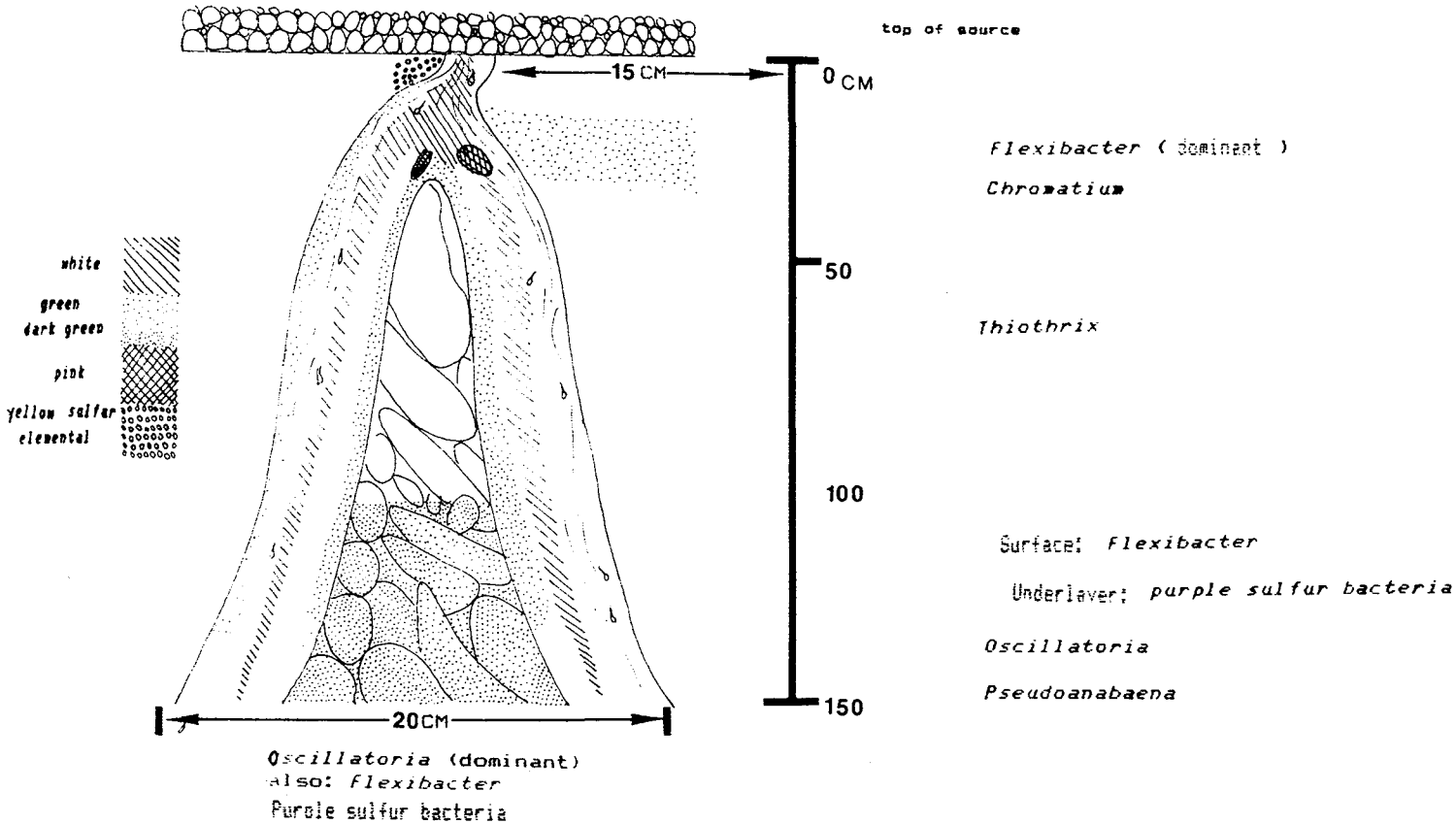

Figure IV-1. Schematic diagram of Alum Rock sulfur stream site 3.

Calculation of Sample Oxygen Concentrations

For a given profile and a given electrode the particular conditions at the time of profile measurement must be taken into account; otherwise O_2 concentrations from the ammeter readings may be invalid. An ammeter reading in the overlying water was taken and a corresponding Winkler titration done to determine the oxygen concentration of the water. Eventually, with depth in the profile, a constant baseline reading was achieved. This reading is taken as corresponding to a zero O_2 concentration value in this medium. This zero value reading is usually not the same as that in the calibration (N_2 solution) since the calibration was done in distilled water whereas the readings are done in complex ionic natural waters. The electrode still has a linear response to oxygen concentration but its absolute value shifts in response to the chemical environment. By taking the overlying water meter reading and subtracting the baseline reading, a value is obtained that corresponds to the O_2 concentration of the overlying water. Dividing these values into one another yields a slope factor. Therefore to obtain an oxygen concentration for a given reading one must first subtract the baseline reading and then multiply by the given calibration factor. Knowing that the electrode has a linear response, the effect of the given medium can be taken into account.

Sulfide Microelectrode Calibration

To calibrate sulfide electrodes readings were taken (in millivolts on a Keithley 160 B Digital Multimeter) for newly made standard solutions. As a check on the known standards methylene blue sulfide determinations (Pachmayr, 1960, modified by Trueper and Schlegel, 1964) were made on the standards. A calibration curve was drawn on 3 cycle log paper. The microelectrode measures S^{2-}, so to determine the H_2S profile one needs to take into account both pH and salinity. A pH profile should be taken with each sulfide profile. However, since the pH profiles we took showed that pH varies little with depth it was sufficient to determine the pH of the overlying water and assume constancy with depth. The simplest way to take pH and salinity into account is to follow the graphical determination presented in the Journal of Marine Research, 23, number 55 (1965), which shows the relationship between pH, salinity, and decimal fraction of undissociated hydrogen sulfide at 25°C. Readings were then taken on the meter (mV), converted to S^{2-} concentration via the calibration curve and then to H_2S concentration taking salinity and pH into account. Unfortunately, the sulfide electrodes were not very sensitive below about 100 μm and so many of our profiles which showed distinct trends in sulfide with depth could only be described as showing trace amounts.

pH Calibration

pH readings were taken in millivolts on a Beckman Model 3500 Digital pH Meter for solutions buffered at pH 5, 7, and 9. Good linear calibration curves were seen for all the microelectrodes although the values varied widely due to differences in the making of the electrodes.

Photosynthetic Rate Determinations

Light and Dark Profiles of Oxygen and Sulfide

To determine diurnal changes in these mat communities both dark and light oxygen and sulfide profiles were determined using microelectrodes that had been prepared by Cohen as described by Revsbech et al. (1983). Details may be found in the Microelectrode Calibrations and Data Calculations section above. The application of these electrodes to sediments and microbial mats has been described by Jorgensen et al. (1983), Revsbech and Ward (1984), and by Jorgensen et al., 1979. Profiles from the sulfur spring were taken *in situ*, whereas those from the microbial mats at the salinas were taken on cores brought back to the laboratory. The cores were taken by hand using 1 1/2 inch diameter acrylic tubing. These cores were kept in water baths in their own pond water and at ambient temperatures of 29°C, and were continuously aerated. Light profiles were taken at a light intensity of 1150 microEinsteins per meter^2 per sec ($\mu E\ m^{-2}\ s^{-1}$). In order to achieve very fine resolution when sampling these cores the microelectrodes were inserted into the mat with the use of micromanipulators (Stoelting Co.).

Anoxygenic Photosynthesis

To investigate the question of whether the microbial communities in the 42 per mil pond (A2) and at the marsh site were capable of anoxygenic photosynthesis using H_2S as an electron donor, the core was overlain with a known amount of pond water and then covered with paraffin oil after the light oxygen and sulfide profiles had already been taken. A known amount of sulfide was then inserted under the paraffin oil into the overlying water. The core was kept in the dark and continually monitored by sulfide and oxygen electrodes inserted at the depth of maximum photosynthetic activity before the paraffin was added. Once a steady sulfide reading was reached the light was switched on and the decrease in sulfide along with the increase in oxygen that occurred following illumination were monitored. After a steady-state oxygen concentration was reached the photosynthetic activity of the community was compared to that seen before the sulfide was added. Sulfide concentrations were increased until they became toxic to these microbial mats.

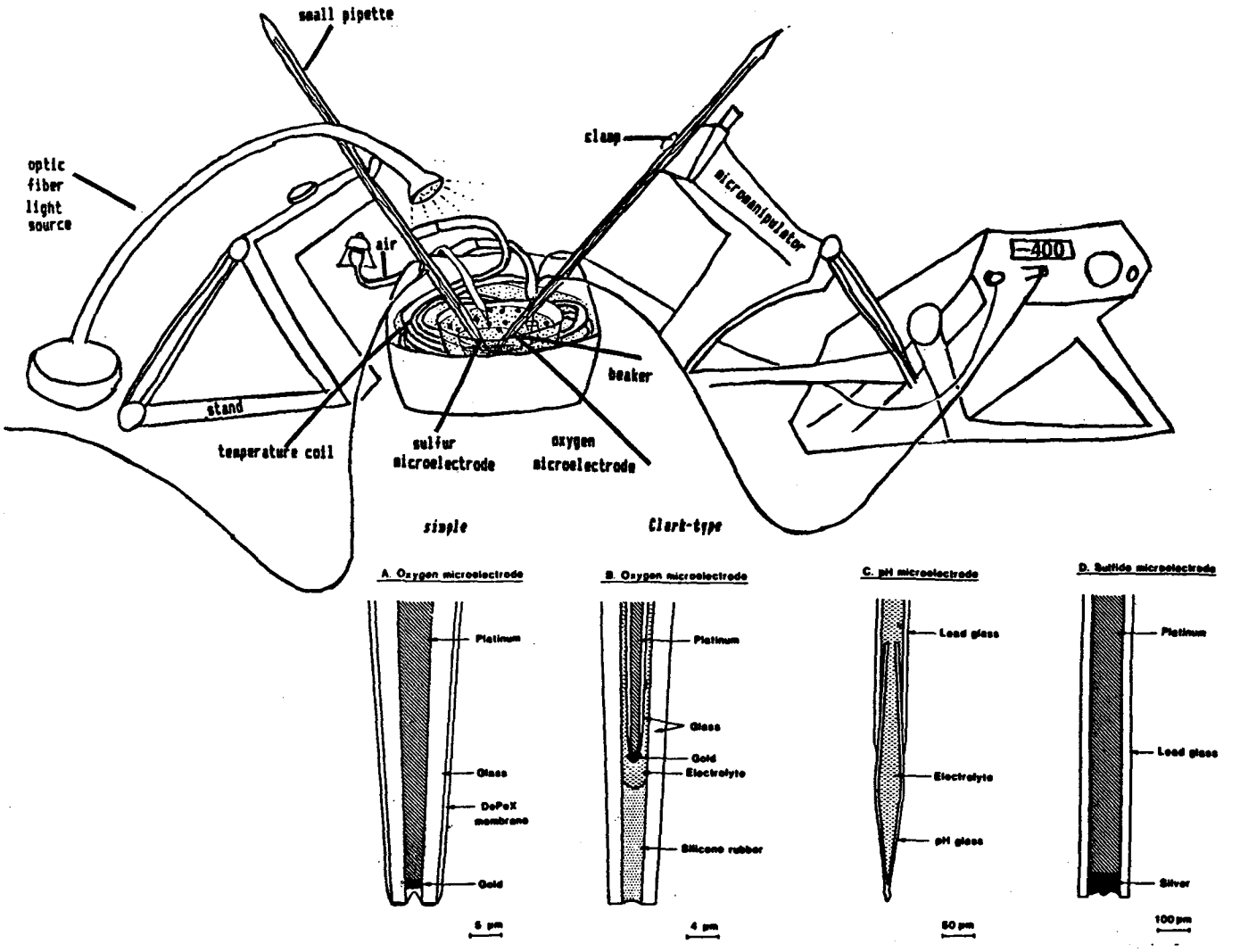

Figure IV-2. Oxygen, sulfide, and pH microelectrodes used by Cohen research group. For further details of the construction and use of these electrodes, see Revsbech and Ward (1984), and Revsbech, et al., (1983).

Oxygen Level Recovery

A core sample from the 150 per mil pond was studied. A light oxygen profile was taken (Fig. IV-3), the core then kept in the dark for approximately 2 hours, after which a dark O_2 profile was taken. After these baseline determinations were made the core was illuminated (1152 $uE\ m^{-2}\ S^{-1}$ from an optic fiber lamp) and profiles were taken after 17, 34, and 63 minutes of illumination.

Results

Light/Dark Profiles of Oxygen and Sulfide and Photosynthetic Rates

Introduction to Results

Dark and light oxygen profiles taken and photosynthetic rates determined in the microbial mats from the different salinity ponds using an O_2 microelectrode (Figures IV-4, IV-5 and IV-6) show two distinct layers of oxygenic photosynthetic activity in the mats at the marsh site and in the 42 per mil pond. This activity can probably be ascribed to the presence of diatoms in the top layer and cyanobacteria in the lower layer. The 90 per mil and the 150 per mil pond light O_2 profiles (Figures IV-5 and IV-6) show a single peak of photosynthetic activity, due to the presence of diatoms and some cyanobacteria. The *Aphanothece* sp. found in the 90 per mil pond were planktonic and therefore could not be responsible for this peak. The sediment of pond 4 (150 per mil) showed relatively poor mat development and the sediment was covered with a gypsum crust which accounts for data obtained from the O_2 profile. It was concluded that oxygenic photosynthetic activity decreases with increasing salinity.

Sulfide profiles were also taken from these mats both in the light and in the dark using a sulfide microelectrode. In almost all cases only trace amounts of sulfide were detectable. In the light, sulfide only appeared in deeper layers of the mat (in the marsh mat at about 0.5 mm in the 42 per mil site and at 1.75 mm). Only in the mat of the 150 per mil pond did sulfide occur in the light close to the surface (0.5 mm depth) in detectable levels (Figure IV-3, indicating that sulfate reduction rate at this site was high). In the dark nearly all mats looked reduced up to the surface. Hardly any oxygen was detectable after the cores had been incubated in the dark for 2 hours. However since there was no profound difference in sulfide profiles in light and dark, sulfate reduction is probably not limited by photosynthates.

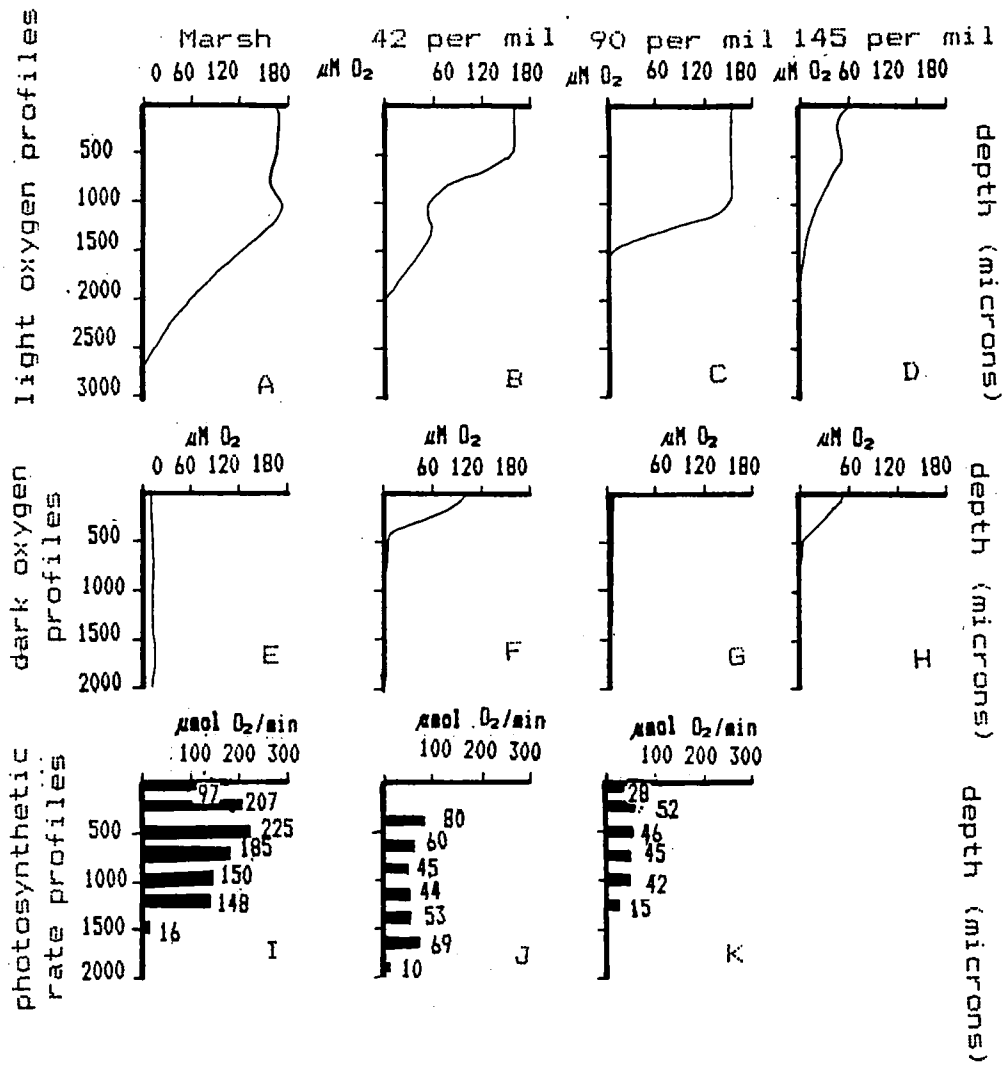

Table IV-2. Summary of site oxygen profiles and photosynthetic rate profiles.

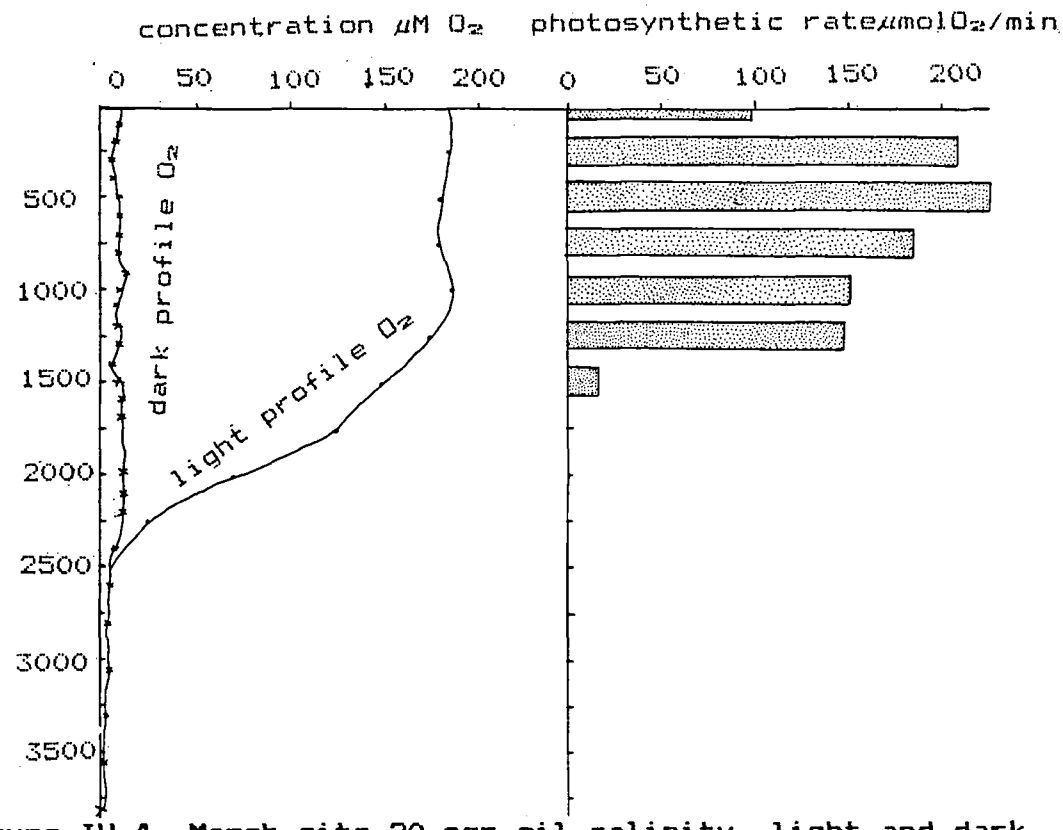

Figure IV-4. Marsh site 20 per mil salinity, light and dark oxygen profiles and rates of photosynthesis.

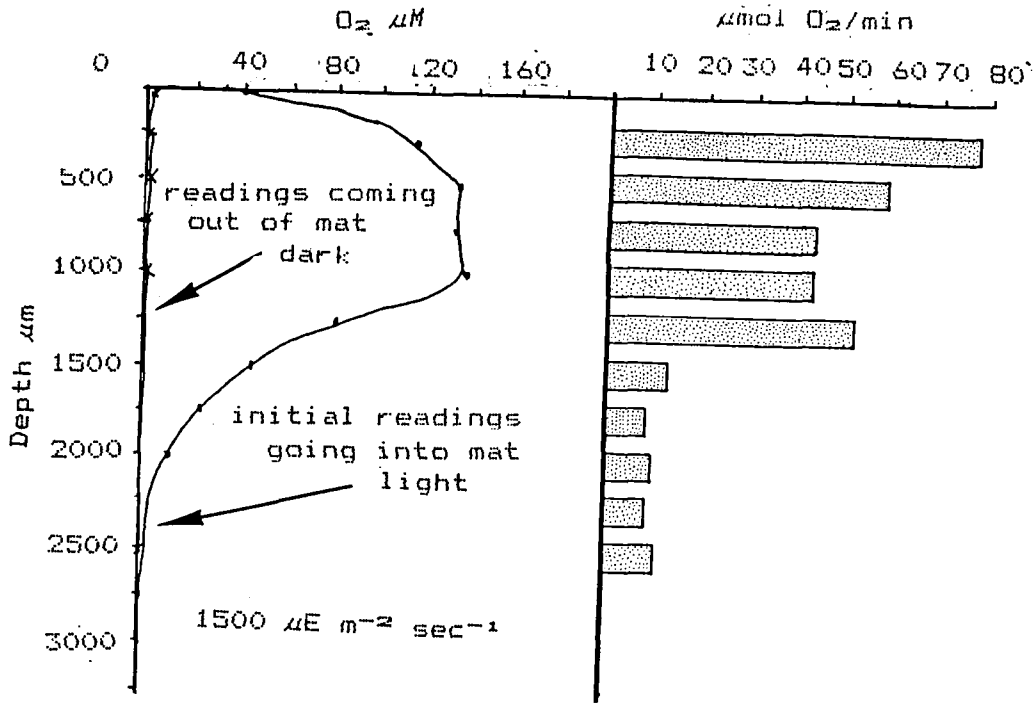

Figure IV-5. Oxygen profile and photosynthesis of 42 per mil pond.

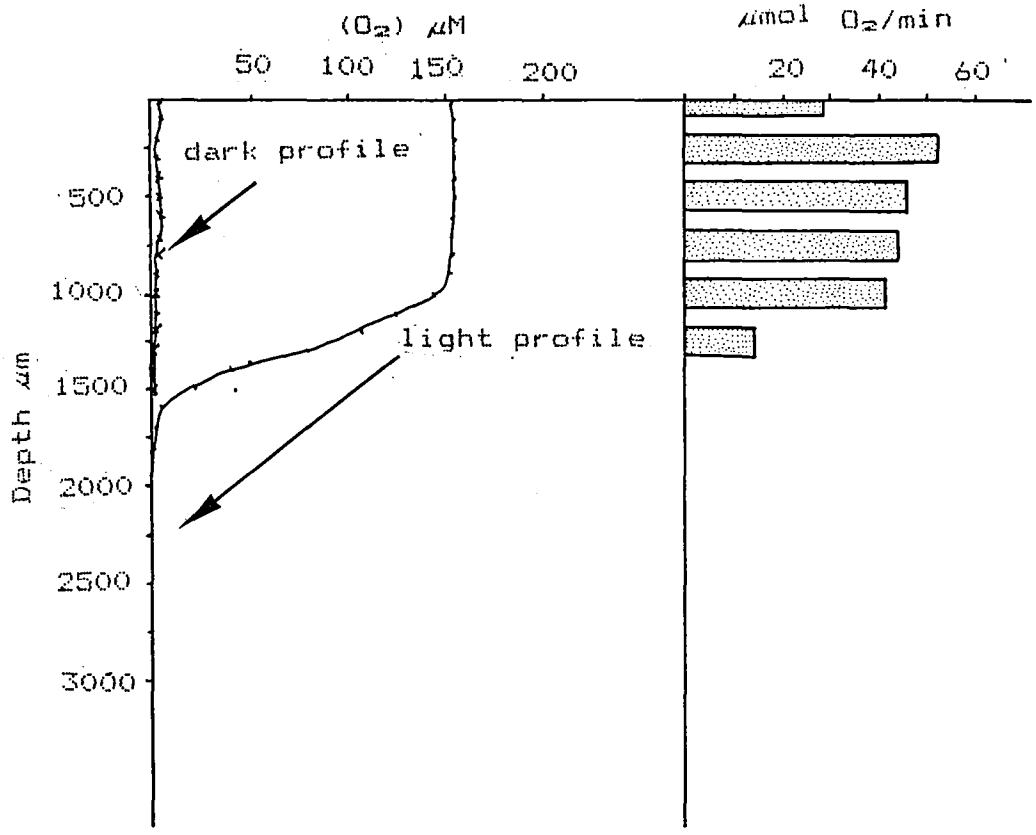

Figure IV-6. Profiles of 90 per mil salinity pond. Light and dark oxygen profiles and photosynthesis rates.

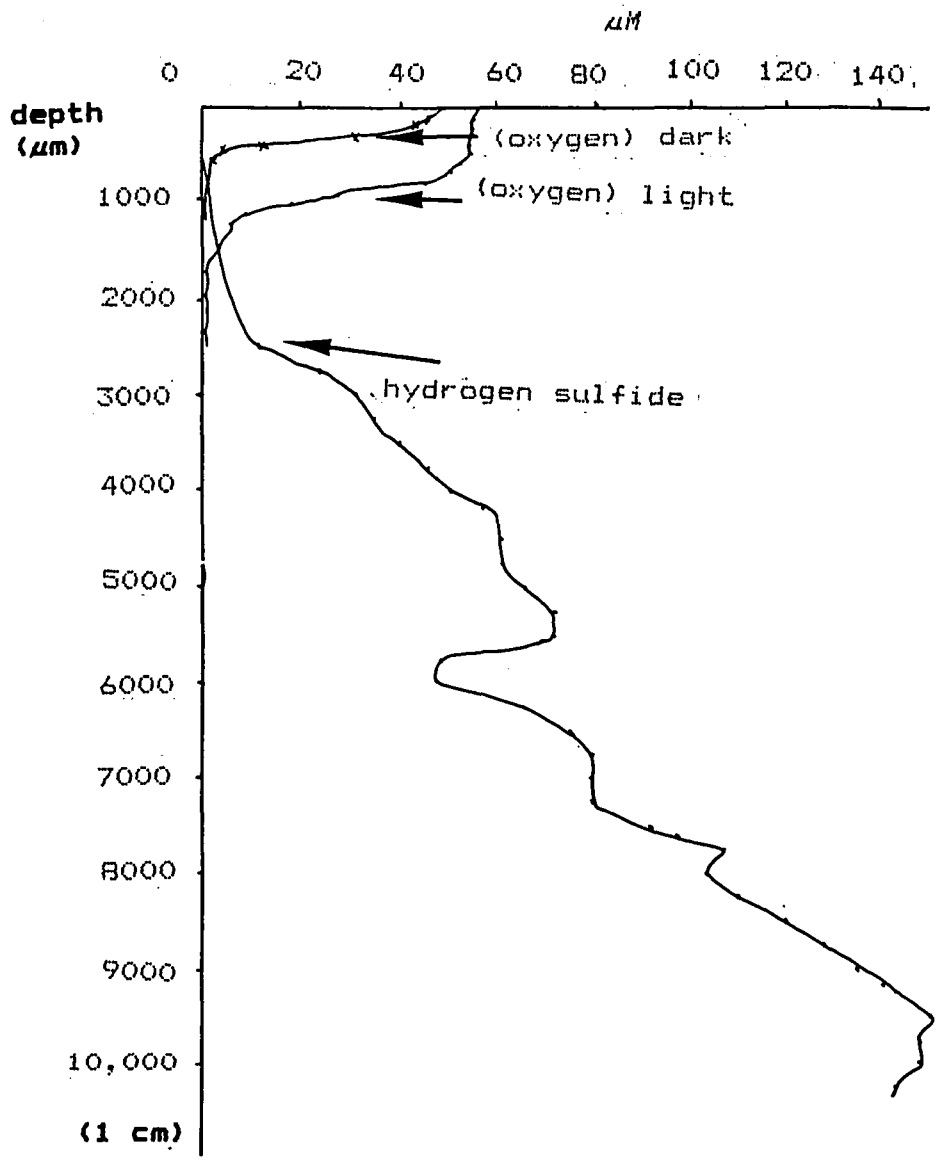

Figure IV-3. Profile of 145 per mil salinity pond. Light and dark oxygen profiles and light hydrogen sulfide profile. Collected at 23°, pH 8.4, and run at 28.5°C.

42 Per Mil Pond

Several light oxygen profiles were taken at the 42 per mil site (Fig. IV-5). These profiles show that the O_2 maximum is reached between 0.4 and 0.5 mm, and has a value of about 160 μM O_2.

90 Per Mil Site

The light O_2 profile showed relatively constant concentrations of about 154 μmol O_2/min from the surface down to a depth of about 900 μm. Below this depth the oxygen concentration decreased quickly reaching a zero reading at 1.5 mm.

150 Per Mil Site

The light oxygen profile for the 150 per mil site shows a drop in oxygen concentration from the high surface value of 57 μmol O_2/min, and an apparent second peak concentration of 55 μmol O_2/min at 5000 μm depth (Fig. IV-3).

Quantum Yield (μM O_2/μE)

The initial slope of a photosynthesis vs intensity plot is a function of the light photosynthetic reaction, and, according to Parsons, et al. (1972), is not usually influenced by other factors. Due to the nature of the sampling procedure, we did not actually derive the quantum yield (μM O_2/μE) but rather a value directly related to it (μM $O_2/m^2/\mu E$). Our calculations show that the greatest quantum yield (or efficiency) was found at 500 μm depth (Table IV-3). This is the same depth at which the maximum photosynthetic rates were found. The next highest yield was at 750 μm. Going to 1000 μm there was a fairly sharp drop in yield (from .024 to .017 μM $O_2/m^2/\mu E$, and by 1250 μm there was essentially zero yield at low light intensities. The values at the surface and 250 μm depth were about the same as that at 1000 μm (Table IV-4).

To determine these yields we measured incident light intensity and the amount of light that could be detected through a 1.5 mm slice of the mat. Using these two points, and assuming a linear relationship for simplicity, the intensities at the intermediate depths were estimated.

Anoxygenic Photosynthesis Results

We attempted to establish the occurrence of anoxygenic photosynthesis in the microbial mat of the 42 per mil pond. When the light was switched on after small amounts of sulfide (100 μM) were added to the mat the sulfide concentration decreased and the oxygen concentration increased accordingly. Large amounts of sulfide (1 mM) seemed to inhibit PS 2 since under

these conditions it took much longer for oxygen concentration to build up again. At low sulfide concentrations oxygenic and anoxygenic photosynthesis seemed to occur simultaneously, while at high concentrations only anoxygenic photosynthesis took place. No accurate measurements were possible, but a rough estimate of the anoxygenic photosynthetic activity is 5-10 micromoles sulfide per minute. Since no control measurement was possible, we are not sure whether the decrease in sulfide concentration was due to anoxygenic photosynthesis by cyanobacteria or to sulfide oxidation by *Thiobacillus*-like organisms.

Photosynthetic activity in the mat of the 42 per mil pond was not inhibited by light intensities up to 1150 μE m^{-2} s^{-1} (Figure IV-7). Inhibition occurred only at a depth of 2 mm (a conclusion based on only one point). Therefore the fact that the top layer of the mat was less photosynthetically active than the deeper layers cannot be ascribed to inhibition by high light intensity unless the light intensity encountered in the normal habitat is much higher. The mat reaches a maximum photosynthetic activity at the highest light intensity. With increasing depth the light intensity decreased (the light intensity values given in the graph are those measured at the surface of the mat and no light penetration could be detected through a 2 mm slice of the mat). Conclusions cannot be drawn from this experiment.

O_2 Level Recovery Experiment Results

Our results indicate that 2 hours was not enough time to achieve a baseline dark profile since the first recovery profile taken (after roughly 2 1/2 hours dark and 17 minutes light) showed lower O_2 levels than the "dark" profile. Nevertheless, recovery profile trends were seen. Surface O_2 concentrations dropped from 57 to about 50 μM O_2 but never below this level. In contrast, at 0.1 mm depth concentrations fell from 56 to 34 μM O_2. At 0.2 mm depth the O_2 level was probably even lower as the dark profiles show sharp decreases with depth in this range.

Thus this core shows a double peak profile with sharp O_2 concentration gradients in the upper half millimeter. After 34 minutes in the light this double peak profile is replaced by a smooth profile gently decreasing from the surface to about 0.2 mm depth and more rapidly decreasing after that to a baseline value of 3 μM at 0.6 mm depth. The shape of the profile remained basically the same on further illumination with concentrations increasing all through the profile but still reaching a baseline of 3 μM O_2 by 0.6 mm. An hour of illumination was not enough time to allow the core oxygen profile to fully recover to the original light profile values.

	Ponds		
	Salinity		
	20 per mil	42 per mil	90 per mil
maximum photosynthetic rate(μmol O_2/min)	225	80	52
depth of maximum photosynthetic rate (microns)	500	400	250
sum total photosynthetic rate in top 1 mm (μmol O_2/min	864	more than 229	213

Table IV-3. Summary of photosynthesis rate and depth data versus salinity (all determined at incident light intensity of 1150 μE m^{-2} sec^{-1}).

Depth	"quantum yield" μmol O_2 $m^2/\mu E$	Ik μE m^{-2} sec^{-1}
5	.014	349
250	.016	307
500	.035	189
750	.024	237
1000	.017	241
1250	0	109

where Ik is an indirect measure of the intensity at light saturation

Table IV-4. Quantum yield estimates and Ik where Ik is an indirect measure of the intensity at light saturation.

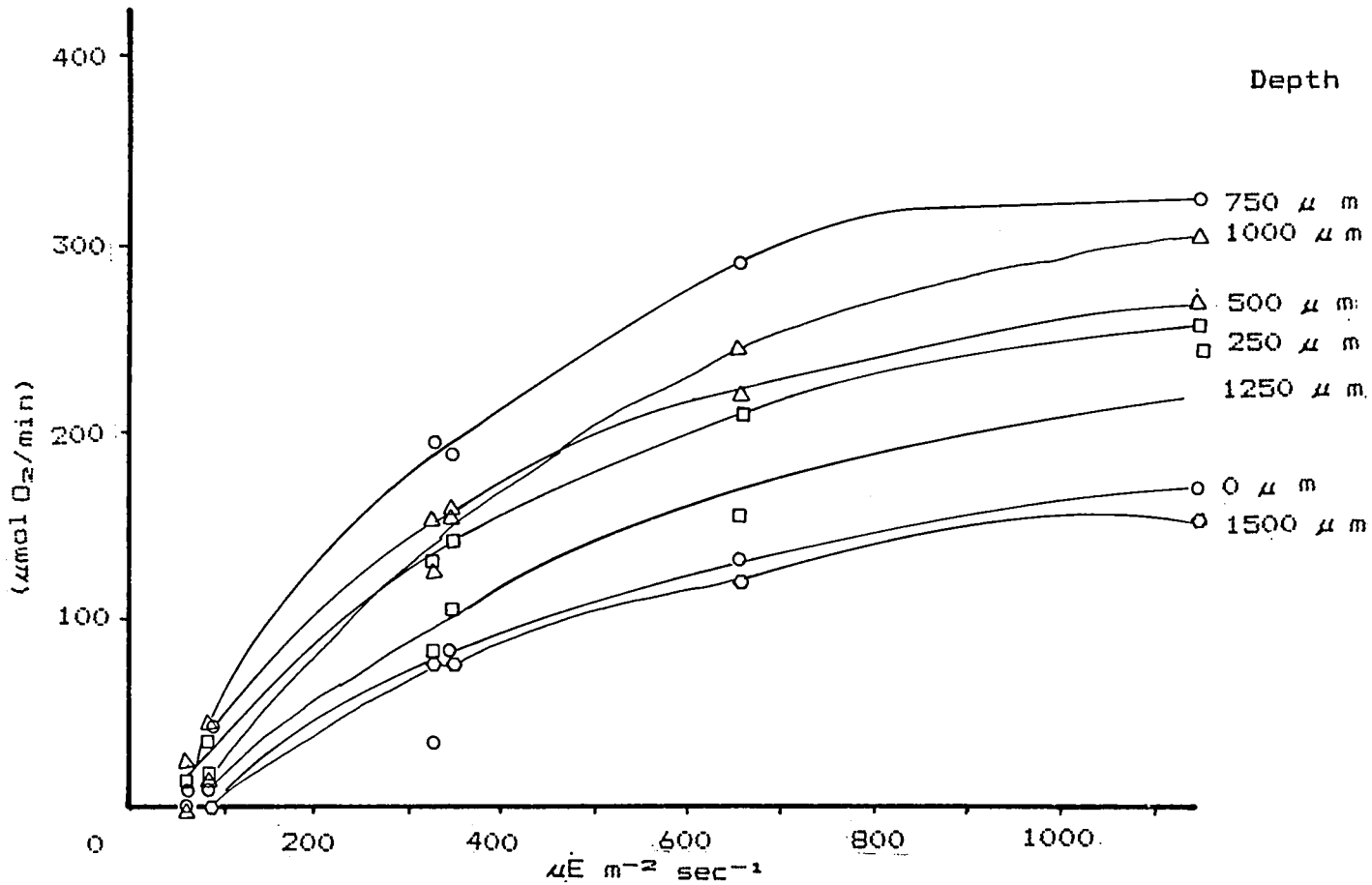

Figure IV-7. Light saturation curves for core from 42 per mil pond.

Discussion

Discussion of Oxygen Profiles and Photosynthetic Rates

The light oxygen profiles show similar characteristics at all sites examined: a zone in the upper portion of their profiles where O_2 content is fairly constant. The width of this zone varies slightly for the three lower salinity sites, being 1.0 mm at the mat, approximately 1.2 mm at the 42 per mil pond, and 0.9 mm at the 90 per mil pond. This zone is only 0.5 mm wide at the 150 per mil site. Though the profiles are fairly homogenous in their upper sections (Figures IV-3-6 or Table IV-2) the marsh (20 per mil) and the 42 per mil profiles do show some evidence for two zones of peak oxygenic photosynthetic activity. Microscopic examination of the 42 per mil mats showed both abundant diatoms and cyanobacteria, and it is likely that the apparent double peak of activity, which may be an artifact, is due to the presence of diatoms at the surface and cyanobacteria in a subsurface layer. The marsh site had cyanobacteria and diatoms; *Beggiatoa* was also very abundant. *Oscillatoria* sp. were by far the dominant photosynthetic species. The presence of abundant *Beggiatoa* is indicative of a shallow oxygen/sulfide interface which could easily shift position. Activity at the 90 per mil site peaked at 0.25 mm, probably due to pinnate diatoms since they are most abundant at this position. No photosynthetic rate determinations were made at the 150 per mil pond which was dominated by *Aphanothece*; oxygen concentrations, however, were low.

Since there were distinct areas of peak activity in profiles which showed much uniformity in the upper zones it is probable that bioturbation is a significant modifier of profiles in these mats. The shapes of these profiles support an interpretation of the presence of bioturbation rather than diffusion alone as the mechanism modifying the profiles. Bioturbation was quite evident at the 42 per mil site where tube-building polychetes (annelid worms) were abundant. Because of their high salinity tolerances, it is likely that polychetes and/or nematodes were the bioturbating agents at the marsh, whereas nematodes alone were probably the main agent at the 90 and 150 per mil sites. Protoctists, ciliates, and motile chlorophytes, found at all sites, could also be contributing to the bioturbation. The photic zone in all cases is less than 2 mm thick in these mats. In general the width of this zone decreases with increasing salinity (see photosynthetic rate profiles).

The depth of the maximum rate of photosynthetic activity tends to shift closer to the surface with increasing salinity. Both peak photosynthetic rates and O_2 production in the top 1 mm of these cores decreased with increasing salinity. Rates of production fell sharply from the marsh site (20 per mil) to the 42 per mil site. Between 42 per mil and 90 per mil the productivity showed a much more gradual decrease. Though there are no photosynthetic rate data for the highest salinity pond,

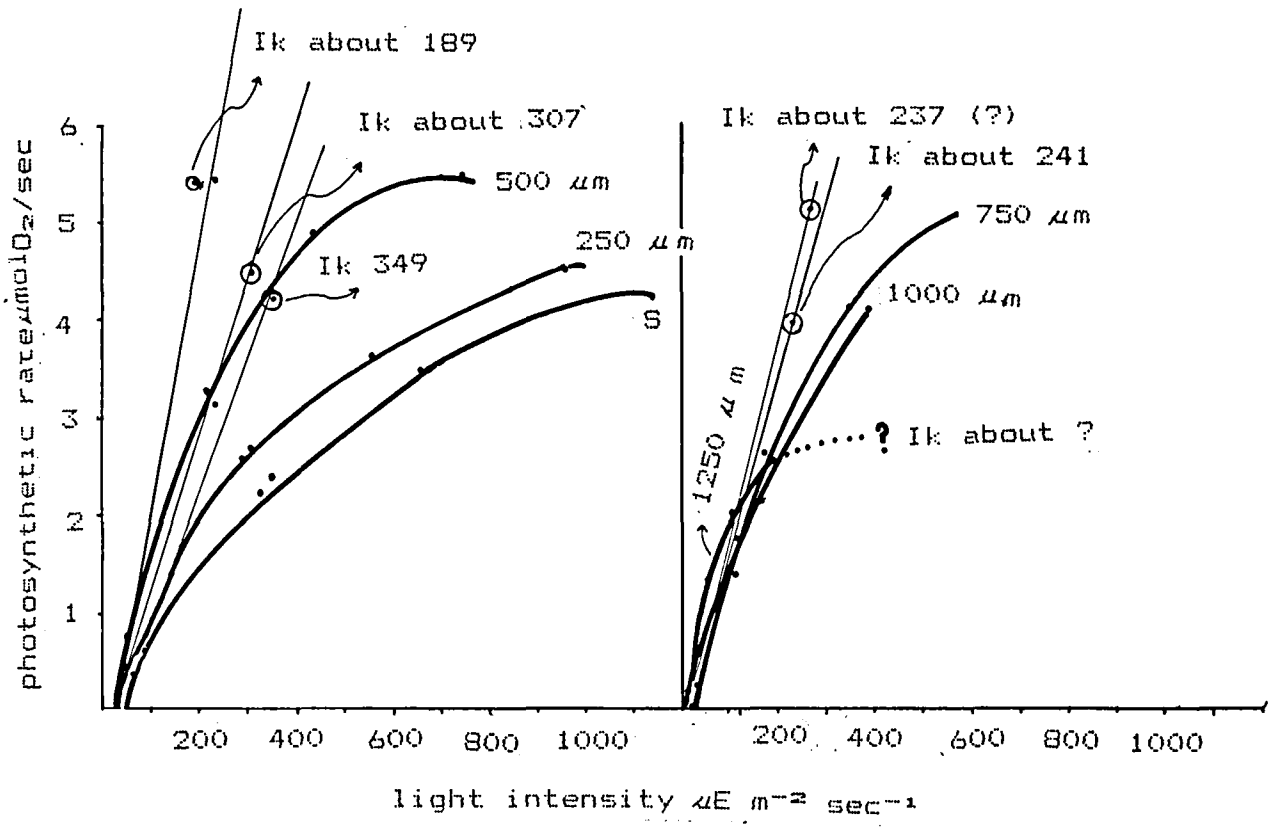

Figure IV-8. Photosynthesis at various depths of the sediment core and calculation of Ik values at the 42 per mil site.

the fact that its peak concentration profile was only 57 μM O_2 as compared to 150-170 μM at the other sites, suggests that another sharp drop in productivity occurs in going to this high salinity.

Sulfide Profiles

The sulfide profiles showed sulfide concentration below expected values, indeed below the resolution capabilities of our microelectrodes. The only exception was the profile of the 150 per mil site, where relatively high concentrations were found.

The light marsh profile shows essentially no free sulfide until a depth of 1.75 mm, where the concentration sharply increases, leveling off at 3.5 mm. The final concentration at this depth was approximately 30 μM. A dark profile taken 2 hours after incubation showed surface concentrations of about 30 μM (or about what the steady base level was in the light core) with concentration increasing slightly with depth and leveling off by a depth of 2.75 mm (Fig. IV-12). The 42 per mil sediment core (Fig. IV-12) light sulfide profile showed only a gradual increase in concentration between 3 and 10 mm. By 10 mm the concentration was probably still under 10 μM. A profile taken after 4 hours in the dark showed sulfide increasing much more quickly, beginning marked change about 0.25 mm to reach an approximate stable concentration (probably about 10 μM) at 2.5 mm. After 4 hours in the dark the 42 per mil core had some *Beggiatoa* scattered on its surface, verifying the profile's finding of a sulfide sink at the surface and indicating that this was the location of the oxygen/sulfide interface. In contrast, the marsh cores were completely covered by *Beggiatoa* after only about 20 minutes in the dark and by 2 hours had gone totally anoxic. No profiles were done for the 90 per mil site. The 150 per mil light sulfide profile shows a gradual though erratic increase in sulfide concentration with depth. The maximum concentration seen in this core was 150 μM H_2S at 9.5 mm (Fig. IV-3).

Comparative Analyses

The 150 per mil pond showed the highest sulfide concentrations (though in the upper 3 mm it appears quite similar to the marsh site), followed by the marsh, and then the 42 per mil pond. There is no direct corelation between the observed sulfide profiles and the salinity gradient. Either there is no corelation or the correlation is overshadowed by other factors. All three sites have available sulfate and since sulfate reduction rates depend on sulfate concentration (Martens and Berner, 1974), differences in concentrations of sulfate at the sites do not explain the differences in the profiles. One line of explanation for the profiles is that the activity of the sulfate-reducing bacteria differs at each site because of substrate availability, sedimentation rate, or some other factor or factors. However, the 150 per mil and the marsh site probably

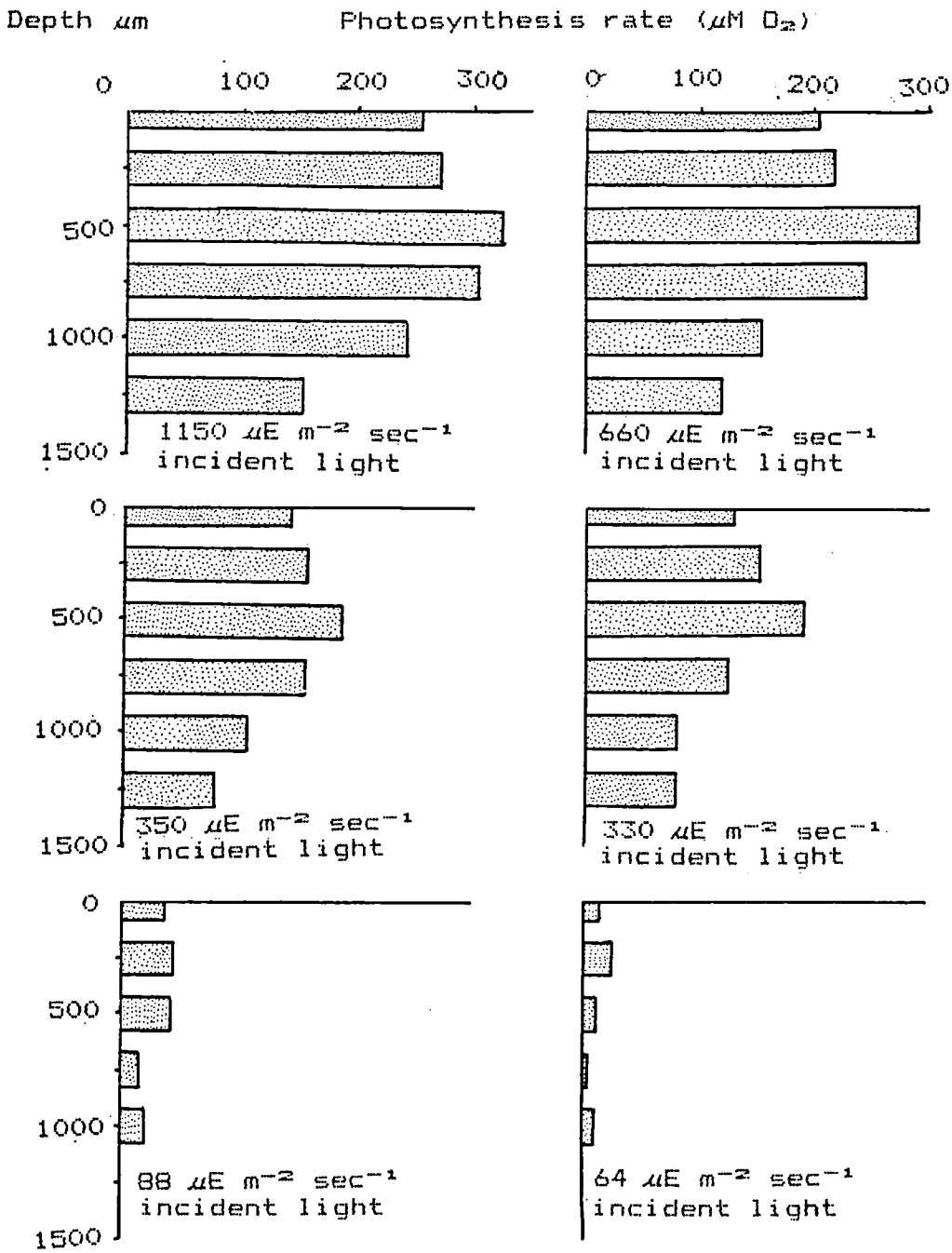

Figure IV-9. Photosynthesis rates at the various depths of sediment core at avarious light intensities (the 42 per mil pond).

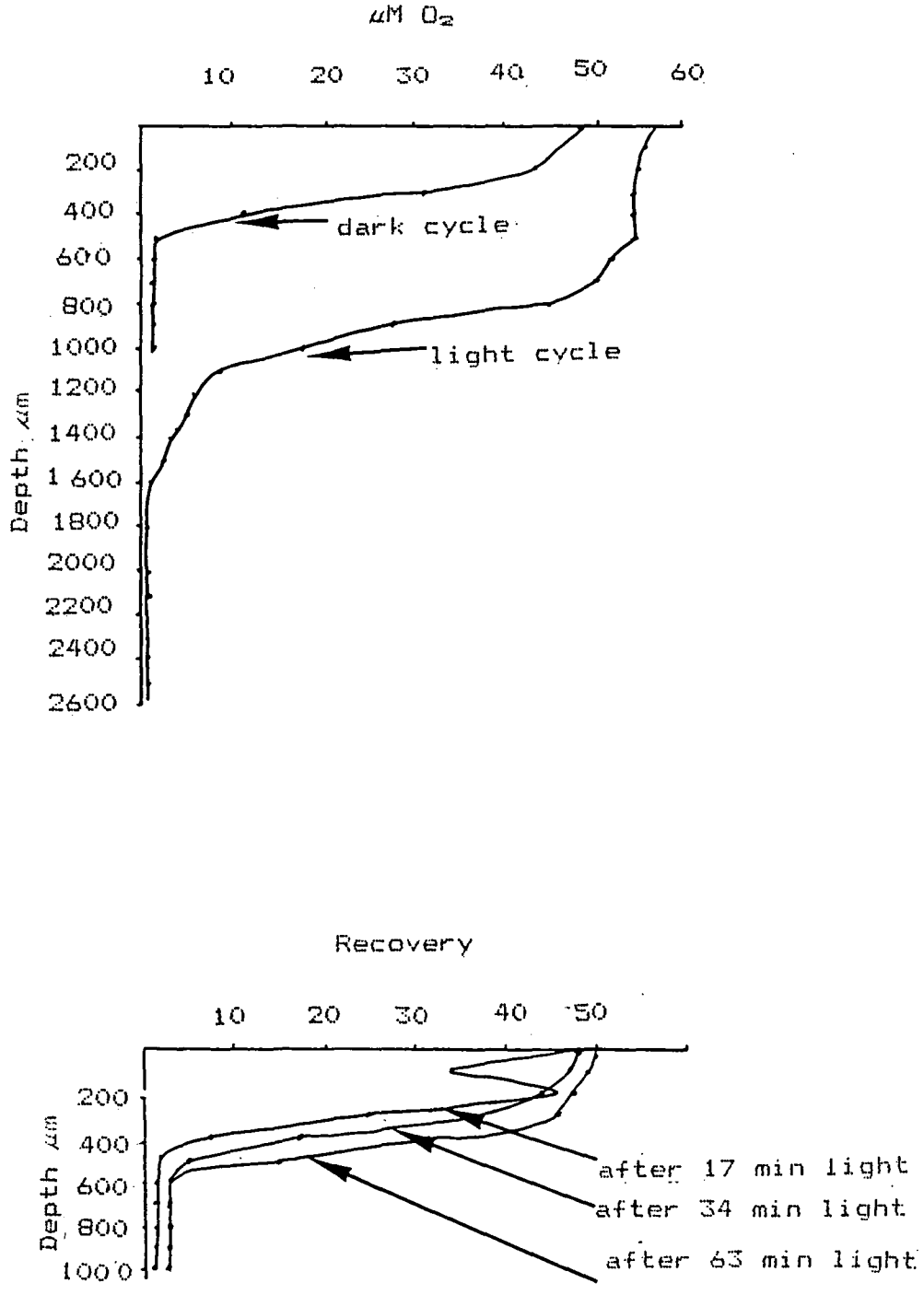

Figure IV-10. Changing oxygen profiles upon transfer from dark to light (145 per mil pond).

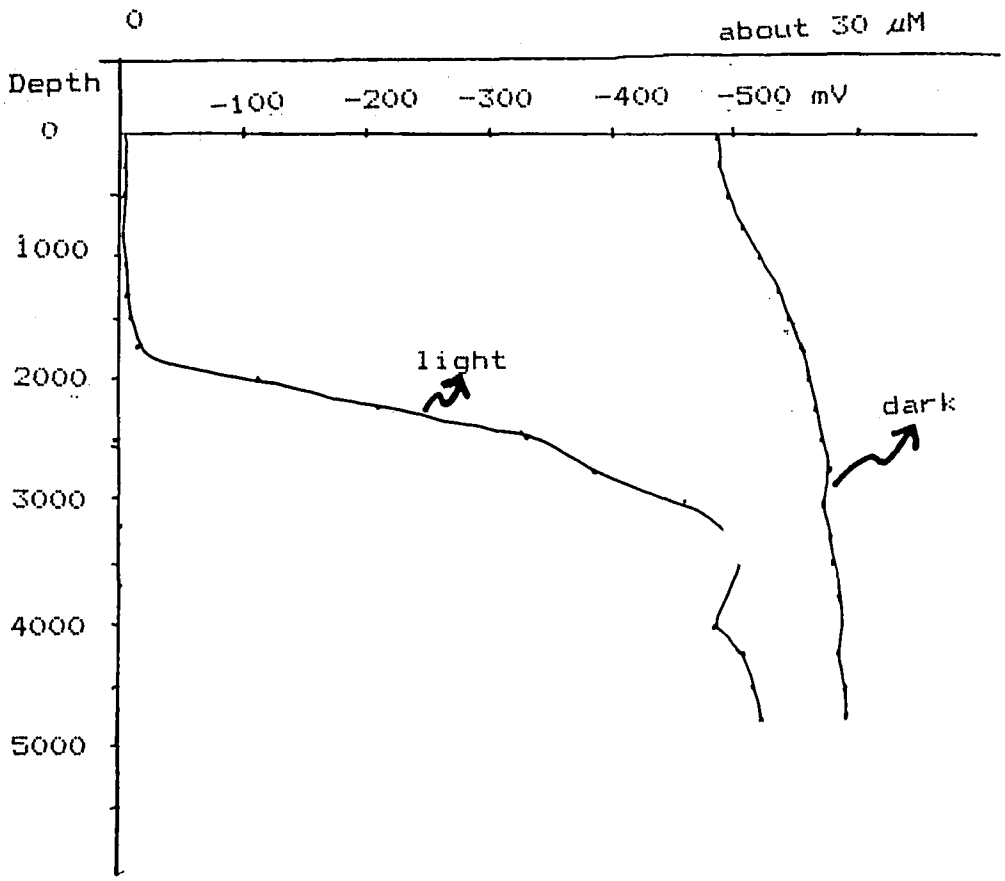

Figure IV-11. Marsh site sulfide profiles in the light (1500 μE m^{-2} sec^{-1}) and dark. Values are given in mV since, being smaller than 50 μM, they were all below the linear range of the sulfide electrode. pH = 8.83.
(1 cm)

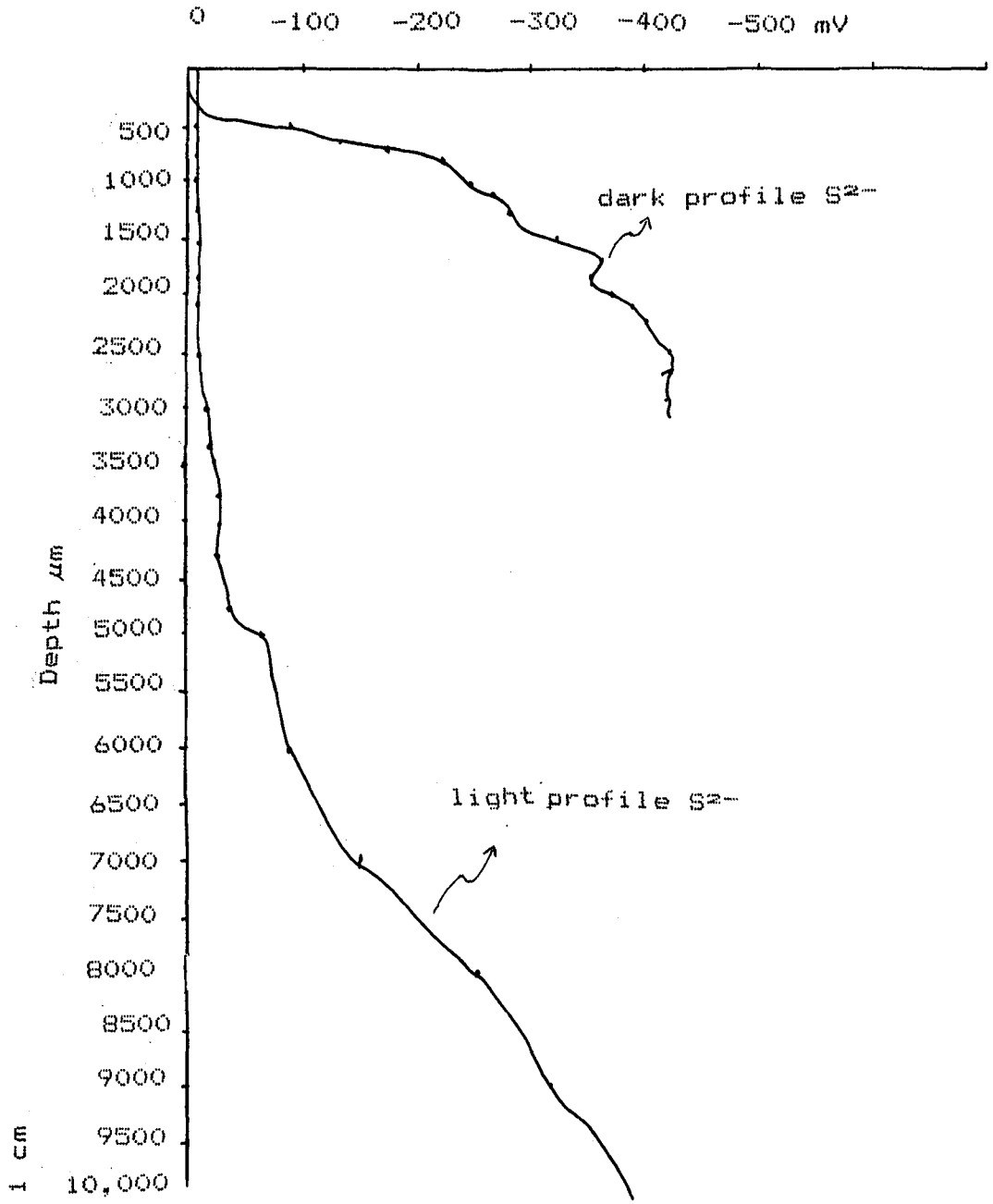

Figure IV-12. Sulfide profiles in the light (1500 µE m^{-2} sec^{S-1}) and the dark (42 per mil pond).

represent two extremes: the marsh site, open to mixing with bay waters, is surrounded by dense vegetation while the 150 per mil site is isolated at the end of a series of connected saline ponds with no surrounding vegetation growing on the evaporite, mineral-laden soil (abundant *Aphanothece* are present in the water column).

Another line of explanation for the anomolously low sulfide concentrations at the 42 per mil site is the existence of a sulfide "sink," such as ferrous iron, that does not operate at the other sites. Ferrous iron reacting with sulfide may form iron monosulfides and eventually pyrite. Roger François found significant pyrite formation in the sediments of the 42 per mil pond, the highest rates of formation being in the top centimeter. Other experiments by the Klug group indicate high rates of sulfate reduction; sulfide must be taken up in some way since very little free sulfide was measured. The 42 per mil pond is located immediately adjacent to the spillway pond whereas the 150 per mil pond is removed from direct sea water contact (Fig. IV-1). Thus the 42 per mil pond may receive iron via its closer contact with the bay water.

Microanalysis of Dissolved Iron and Phosphate in Pore Waters of Hypersaline Sediment

R. Haddad and T. Shaw

Introduction

Reduced iron, soluble in acidic pH, has an intermediate redox potential; it may serve as an intermediate electron acceptor-donor between O_2 and $S^{=}$. Furthermore, reduced iron is abundant in many fresh water and marine sediments. Iron may serve as an alternative electron donor in cyanobacterial photosynthesis (Cohen, personal communication).

Diurnal fluctuations of reduced iron concentrations, expected to occur in reduced sediments in the photic zone, were studied. Iron concentration was compared to O_2-H_2S, a microanalysis of sulfate reduction was performed, as well as an examination of diurnal concentration of dissolved phosphate and changes in interstitial CO_2.

Materials and Methods

Pore Water Iron Determination

Dissolved iron concentrations in sediment pore waters were determined colorimetrically by the ferrozine method (Stookey, 1970, modified by Murray and Gill, 1978). Further modifications of the original method were necessary to work with the limited sample size (0.5 ml) used with the millimeter pore water method described in the following section. A small amount (0.3 ml) of sample was added to 0.1 ml of ferrozine reagent, 0.1 ml hydroxylamine hydrochloride, and 1 ml of MilliQ purified water. The solution reacted for 10 minutes in an 80°C water bath. The samples were allowed to cool to room temperature and 0.1 ml of ammonium acetate buffer was added. The absorption of the resulting iron complex was measured at 562 nanometers in a 0.5 ml microcell. A standard curve and blank were measured with each set of pore water profiles.

Phosphate Assays

Dissolved phosphate concentrations in pore waters were determined colorimetrically by the stannous chloride method. Several modifications to the method were adopted to allow determination using 0.1 ml of sample. An acidic solution consisting of 0.1 ml of concentrated KCl in 100 ml of distilled water was used to dilute the pore water sample. The stannous chloride solution was diluted 1:5 with ethanol to allow more accurate addition of solution. To 1 ml of acidic solution were added 0.1 ml of sample, 0.02 ml of molybdate reagent, and 0.03 ml of stannous chloride solution. After ten minutes the absorption of the solution was measured at 690 nm.

Carbon Isotope Ratio Determination Methods

Sampling Procedure

3 to 5 cm-long sediment cores were collected using 1 1.2 cm diameter acrylic core tubes. These core tubes were specially designed; one end was tapered for easier sediment penetration and the other end was faced off for precise sectioning. The cores were returned to the San Jose State University laboratories within three hours of collection and incubation processes begun immediately.

Extruding Procedure

For sum CO_2 and ferrous iron analyses, the cores were transferred into a nitrogen atmosphere glove bag for processing. Procedural blanks indicated that the carbon dioxide concentration within the glove bag was less than 0.6 nM. Inside the glove bag, cores were extruded and sectioned into 1 mm or 2 mm sections using a .036 cm glass reinforced epoxy sheet. The error was estimated to be 1 mm plus or minus 0.5 mm sections. Pore water was obtained via ultracentrifugation for 10 minutes of the sliced sections, transferred and centrifuged a second time to insure particulate removal.

Total Carbon Dioxide Pore Water Procedure

A known volume of the particulate free pore water was transferred by syringe from the centrifuge tubes into 15.75 ml Pierce crimp-top vials. These were immediately crimped using septa and tear-away aluminum crimp tops. The stoppered vials were removed from the glove bag and stored at -76 degrees centigrade until isotopic analyses could be done (0.5-1 day).

Vacuum Line Procedures

Prior to isotopic analysis, the frozen pore water samples were allowed to equilibrate to ambient room temperature (approximately 25 °C). Two ml of 1 M sulfuric acid were added to liberate the total carbon dioxide as carbon dioxide gas. A 2 M sulfuric acid plus 2 M cuprous sulfate solution was experimented with in anticipation of high concentrations of sulfide; however, the lack of any CuS precipitate demonstrated that the concentration of hydrogen sulfide in the upper 1 cm of sediment would not interfere with the $^{13}C/^{12}C$ isotopic measurements. The CO_2 produced upon acidification was purified, isolated, measured for volume, and collected using vacuum line techniques in Dr. David DesMarais' carbon isotope laboratory at the NASA Ames Research Center (see PBME, 1982, NASA Technical Memorandum 86043 for details).

Stable Isotope Mass Spectrometer Procedure

$^{13}C/^{12}C$ isotpic measurements were made on a 6" nuclide stable isotope mass spectrometer and are presented in the usual del notation referenced to the Peedee belemnite (PDB) standard (See Table I-2 p).

Paratetramitus and Manganese-Oxidizing Bacteria

For methods see Read, et al, 1983. Manganese acetate plates were inoculated in the center with 1 mm^3 of sediment sample and flooded with 1 ml distilled water for each 1 mm depth for the 42 per mil site.

Results

Pore water from the upper centimeter of the 42 per mil pond was analyzed to determine the concentrations of dissolved iron and phosphate. The iron profiles suggest a strong corelation between iron remobilization and processes occurring in the light (see Fig. IV-13). Phosphate profiles (Fig. IV-14) suggest the removal of phosphate is strongly correlated with precipitation of oxidized iron in the upper 2-5 mm of the sediments. Phosphate concentrations were higher in the dark cycle cores where the iron diffusion gradient to the oxidized zone of the sediment is at a minimum. Although phosphate removal is associated with iron removal, there is little evidence for phosphate remobilization associated with iron remobilization. Phosphate appears to diffuse upward from below. This observation suggests that the mechanism of iron remobilization during the light cycle does not involve reduction of oxidized iron. Further, the corelation of iron remobilization with light cycle processes suggest that the mechanism of iron mobilization may be the result of an oxidative process.

Pore water ΣCO_2 concentrations and carbon isotope ratios are presented (Figure IV-15 and IV-17). These data are from the analyses of mini-sediment cores collected from the 42 per mil salt pond and incubated in the laboratory under light and dark conditions. The delta ^{13}C values in the light-incubated core decrease from -5.24 0.19 per mil at 0-1 mm to -7.89 per mil at 2-3 ml and increase back to about - 6 per mil at 6-10 mm. When sampling resolution is decreased to 2 mm intervals (Figures IV-15, 16, and 17) the major down core trends of heavy CO_2 at the surface are still evident but the fine-scale structure of the profile changes.

The large difference between the delta ^{13}C values in the 0-1 and 1-2 mm sections measured in the light-incubated cores is not present in the dark-incubated cores. In these cores, the isotope values are fairly constant over the upper 5 mm; they increase from 5-7 mm and level off in the 7-10 mm region.

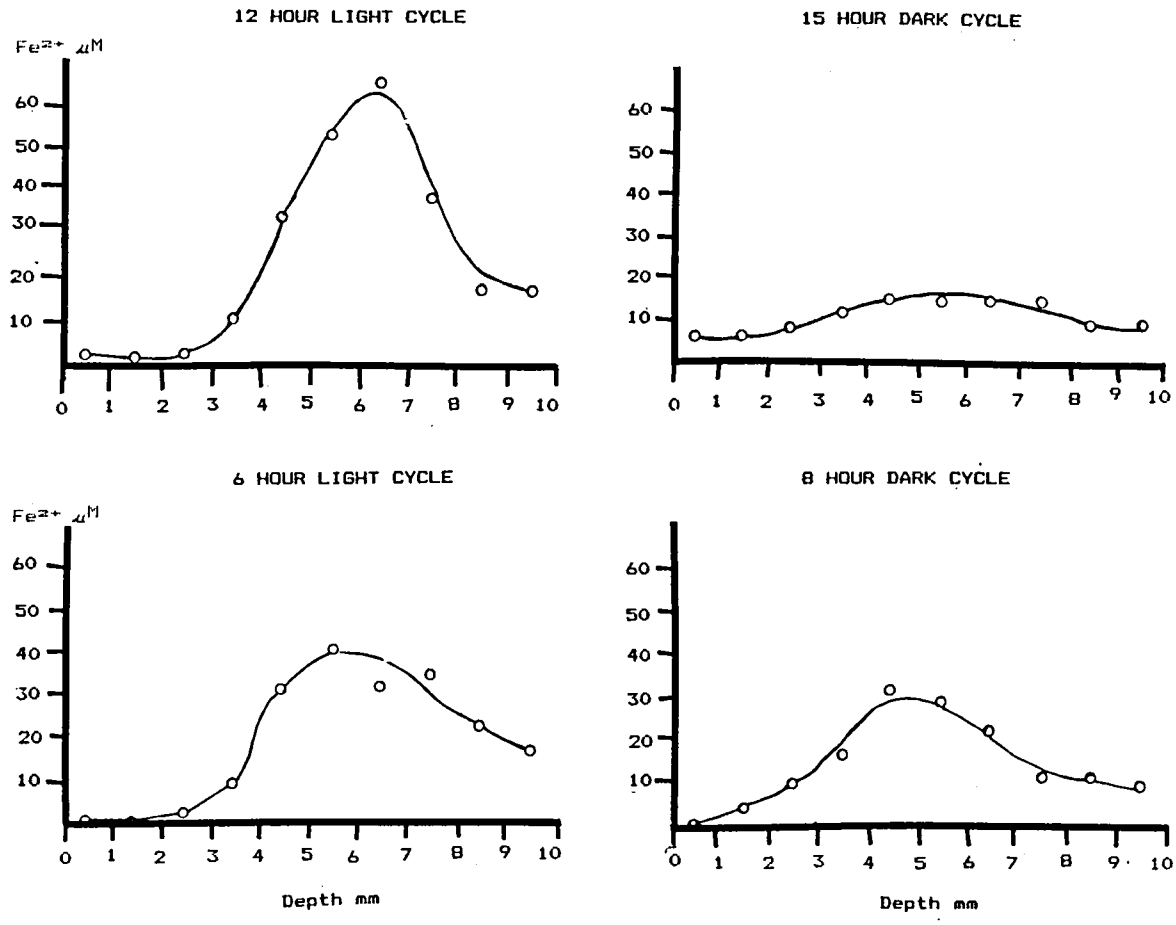

Figure IV-13. Iron profiles (42 per mil pond).

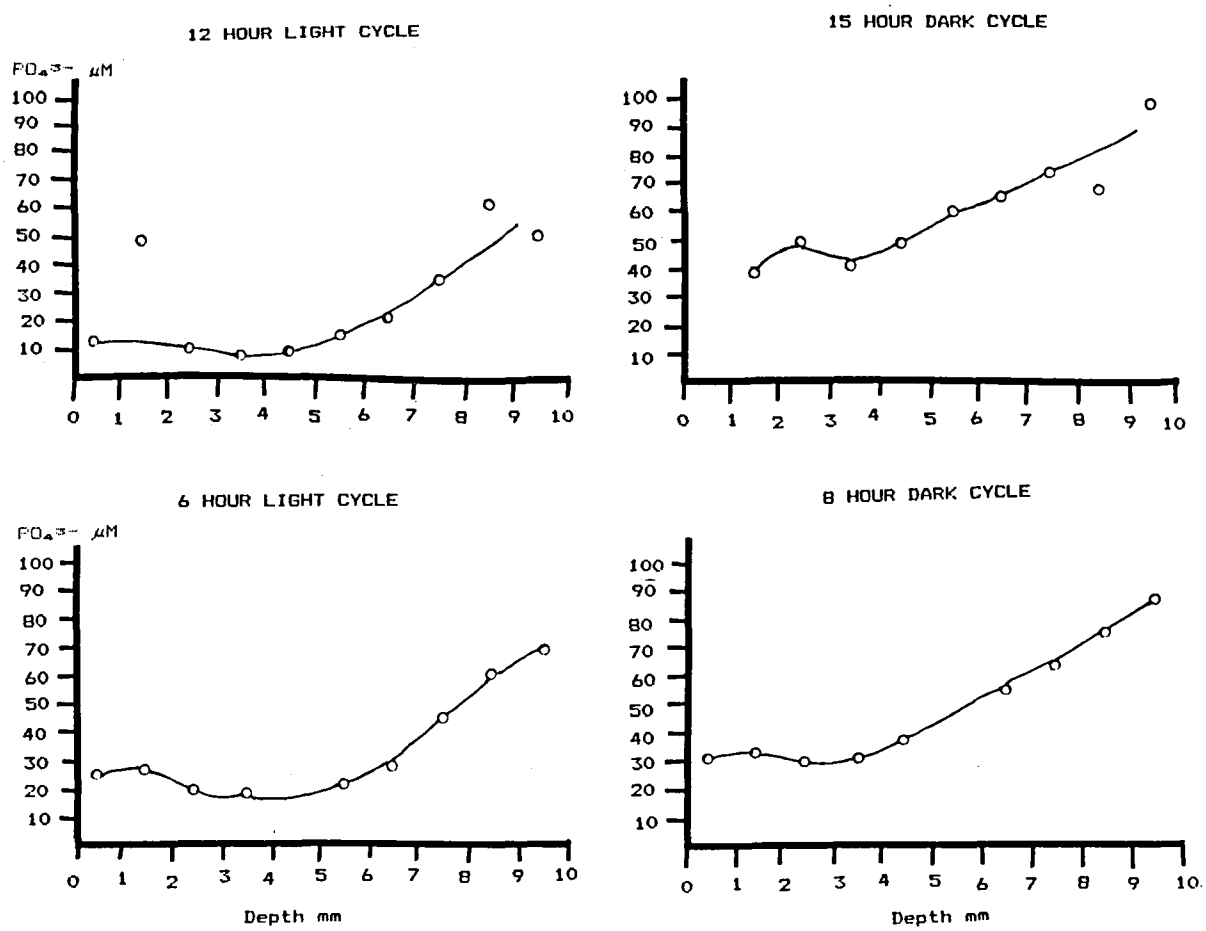

Figure IV-14. Phosphate profiles (42 per mil pond).

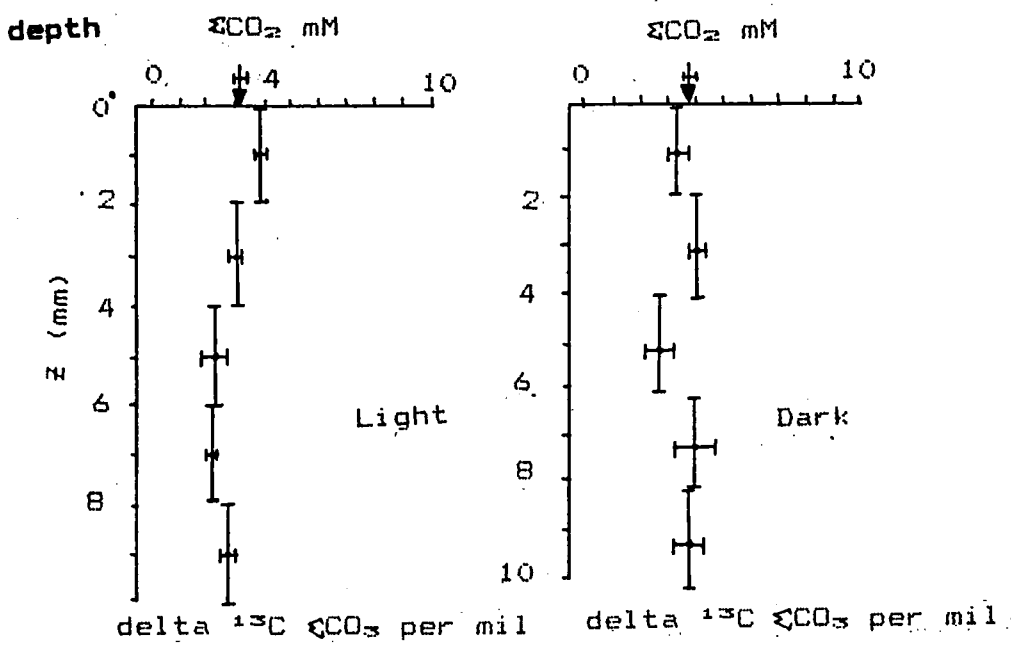
depth
ΣCO₂ mM
0
4
10
0
2
4
6
8
z (mm)
Light
delta ¹³C ΣCO₂ per mil
ΣCO₂ mM
0
10
2
4
6
8
10
Dark
delta ¹³C ΣCO₂ per mil

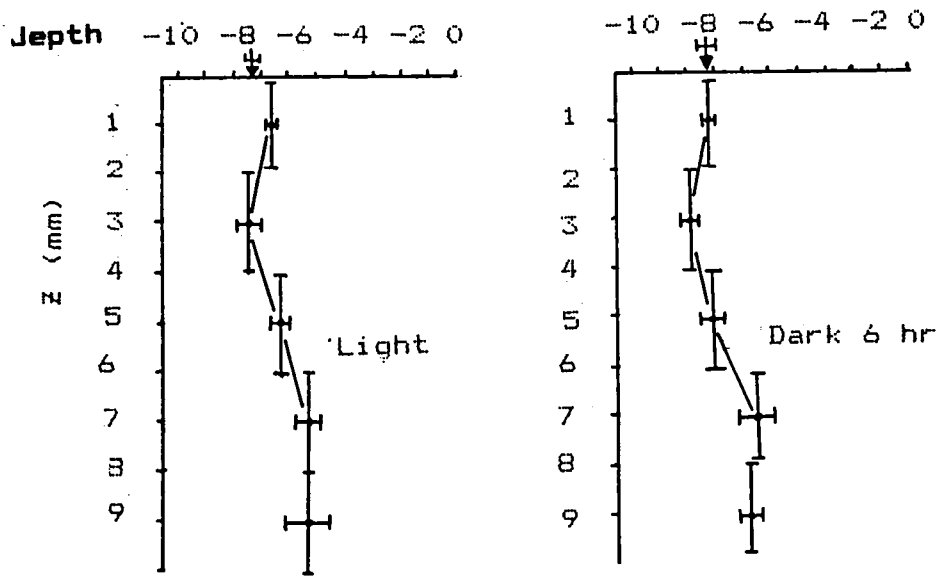
depth
-10 -8 -6 -4 -2 0
1
2
3
4
5
6
7
8
9
z (mm)
Light
-10 -8 -6 -4 -2 0
Dark 6 hr

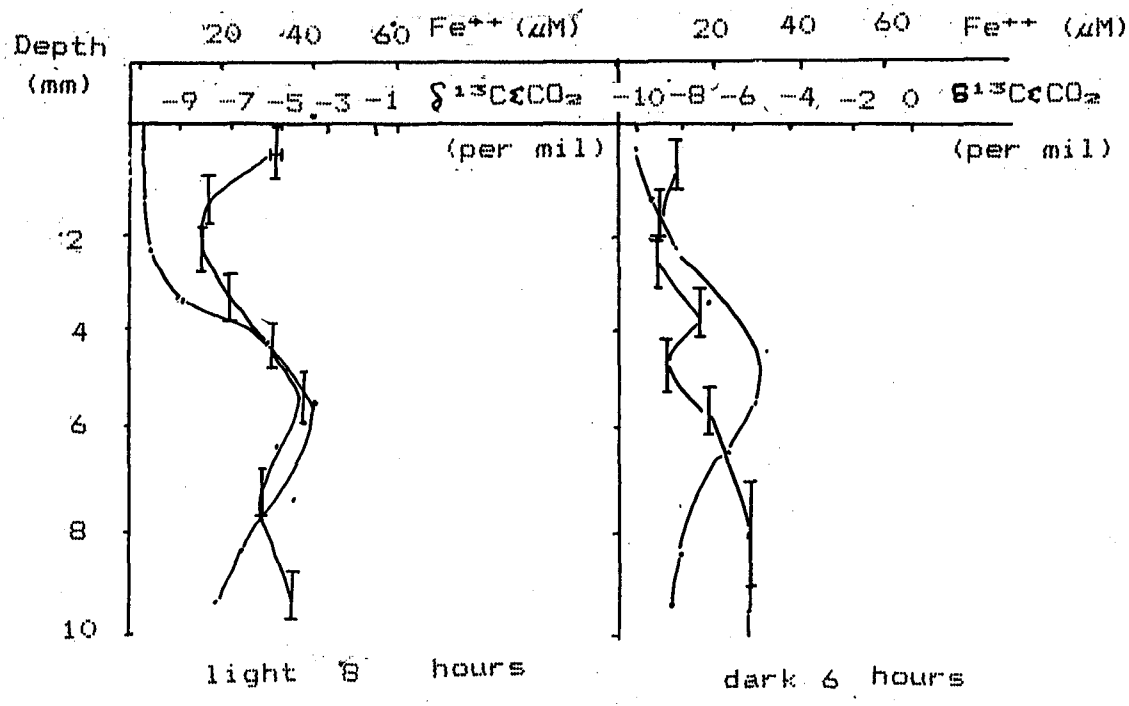

Figure IV-15. Comparison of concentration of dissolved Fe^{++} and delta $^{13}CO_2$ in the interstitial water.

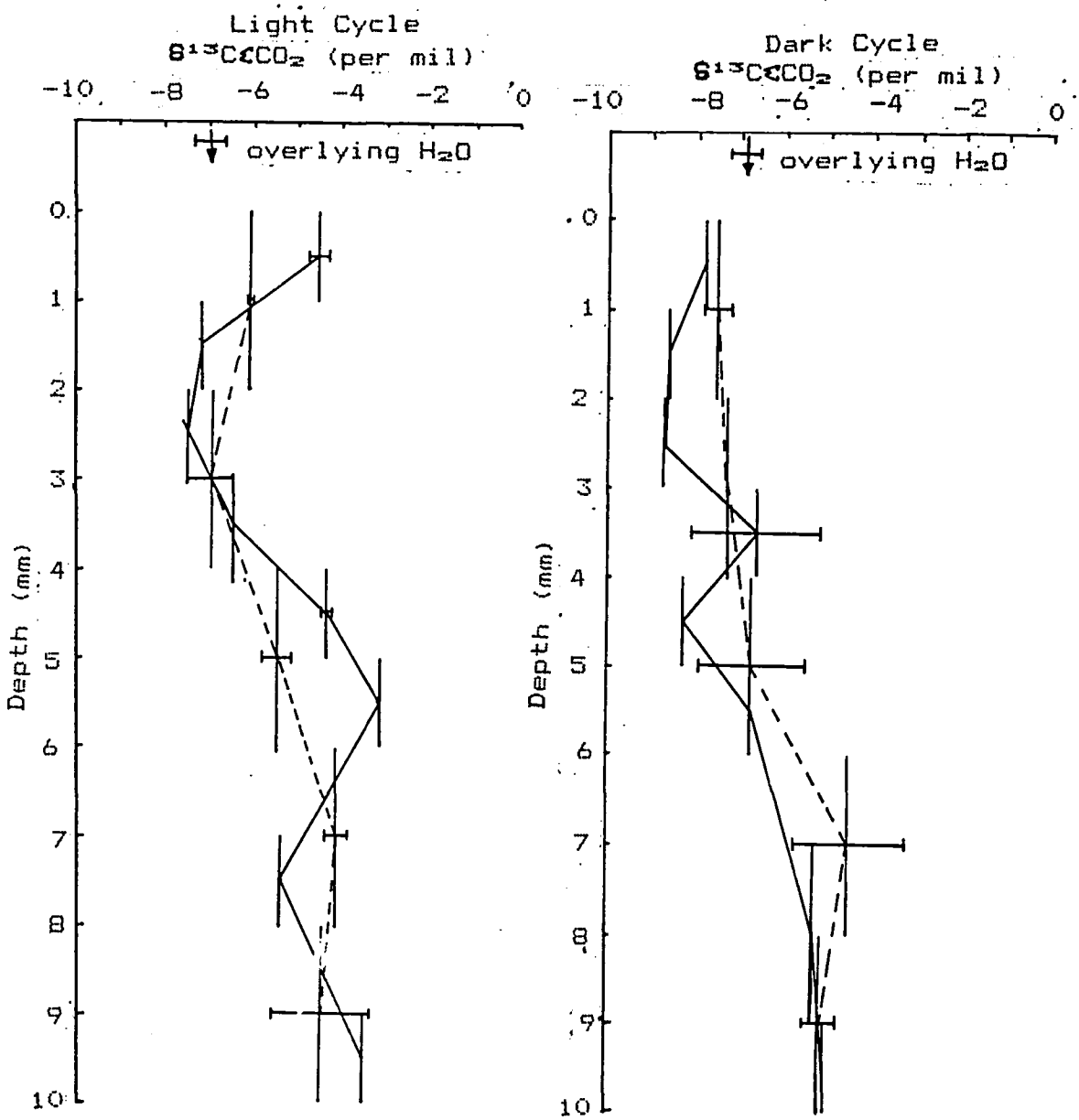

Figure IV-16. Light cycle delta $^{13}C \lessdot CO_2$ profile.

Figure IV-17. Dark cycle delta $^{13}C \lessdot CO_2$ profile.

The ΣCO_2 pore water concentrations are presented for the 2 mm sectioned cores only in Figure IV-15. In the light-incubated core, there is a gradual decrease in ΣCO_2 concentrations from 3.89 ± 0.14 mM at 0-2 mm to 2.11 ± 0.43 mM at 7-8 mm. No such trend is evident in the ΣCO_2 concentration profile in the dark-incubated core. In this core, CO_2 ranges from 2.74 ± 0.86 mM to 4.08 ± 0.37 mM.

Colonies of manganese-oxidizing bacteria appeared in all samples studied. Millimeter samples showed the most activity for both *Paratetramitus* and manganese oxidizers at 6 millimeters below the surface (Table IV-4).

Discussion

Partial oxidation of sulfide in the form of iron monosulfide may explain these iron profiles. The presence of elemental sulfur in the upper centimeter of these sediments (Chapter III) confirms the assumption that the sulfide is being oxidized in this zone but the presence of dissolved iron to depths of 8-9 millimeters suggests that very little free sulfide is available for oxidation in this zone.

An important aspect of the proposed mechanism is that iron monosulfide in the presence of elemental sulfur reacts to form pyrite, the ultimate sulfur sink in the sediments; these two reactants, however, are not usually found in the same sedimentary regime. The mechanism suggests that in this environment elemental sulfur and iron monosulfide can exist concurrently. Furthermore, rates of pyrite formation in these sediments are greatest in the top centimeter (see Chapter III).

Recent studies on microbial mat communities using microelectrodes have demonstrated that large gradients in oxygen (0-200 μM), sulfide (0-200 μM) and pH (1-9) exist within the upper 1-3 mm of the mat (Jorgensen 4et al., 1983). These profiles have been shown to be supported by microbially mediated processes (e.g., photosynthetic CO_2 fixation, CO_2 respiration, sulfate reduction, etc.) and they exhibit diurnal variations. One interesting observation from these studies is that both oxygen and sulfide coexist in low concentrations (200 μM and 50-100 μM respectively) in a narrow zone within the upper few mm of the mats. This chemical boundary is usually exploited by sulfur-oxidizing bacteria such as *Beggiatoa* and flexibacteria yet results from recent experiments using a new ^{35}S-sulfate reduction determination technique qualitatively demonstrate that sulfate reduction is occurring in this microaerophilic environment at significant rates (Y. Cohen, personal communication). In this microenvironment, photosynthetic products (amino acids, short-chained fatty acids, etc.) excreted by the phototrophic bacteria may be utilized as carbon sources by sulfate-reducing bacteria. Microbially-mediated degradation processes such as sulfate reduction and fermentation are assumed to be primarily by organic

matter produced *in situ* in the mat communities.

The results of the O_2 and sulfide profiles and pore water $\sum CO_2$ concentrations and carbon isotopic values do not support this hypothesis. Instead they argue that organic matter from the overlying water column limits degradative processes. During the light cycle, oxygen is present only in the upper 1-2 mm where active photosynthesis occurs. Concurrently, sulfide does not appear to be present in the pore water until 6-8 mm depth and even then only in trace quantities (less than 0.1 mM). During the dark period, oxygen is present in much lower concentrations, and sulfide apparently is present in trace amounts up to the sediment/water interface.

A comparison of the light and dark $\sum CO_2$ carbon isotope profiles (Fig IV-15) demonstrates a significant diurnal variation in the upper 1-2 mm due to the photosynthetic activity. During the light cycle, relatively light carbon dioxide (carbon dioxide enriched in ^{12}C with respect to ^{13}C) is fixed, thereby enriching the remaining sum carbon dioxide pool in ^{13}carbon dioxide with respect to ^{12}carbon dioxide. This results in an increase in the delta ^{13}C value. During the dark cycle, carbon dioxide is not fixed and respiration by heterotrophs produces light carbon dioxide thereby decreasing the delta ^{13}C sum carbon dioxide value in the pore water.

Directly below the photosynthetic zone, the proposed coupling of sulfate reduction with photosynthetic activity should result in lighter delta ^{13}C $\sum CO_2$ values in the pore water during the light cycle (when the light - roughly 30 per mil - photosynthate is being produced). The light/dark profiles demonstrate that the pore water delta ^{13}C CO_2 is actually lighter during the dark cycle presumably due to heterotrophic (fermentative) activity, and the absence of photosynthetic activity.

These isotopic data suggest that the degradation processes mediated by microbes are driven not by *in situ* photosynthetically derived organic matter, but by allochthonous organic matter (presumably from the overlying water column). This view is supported by the $\sum CO_2$ and delta ^{13}C values in the overlying water column. Comparing the measured values with predicted values based on concentrating seawater to 42 per mil, the measured $\sum CO_2$ concentration values range from 10-25 percent greater than the predicted values. Also, the delta ^{13}C values in the water column are 5-7 per mil lighter than the predicted value of about 0 per mil. In addition, there appears to be a net export of $\sum CO_2$ from the sediment to the overlying water column, completing a type of mini-carbon cycle which, for the most part, bypasses the processes of sedimentary CO_2 fixation.

A final curiosity is the increase in the $\sum CO_2$ delta ^{13}C profile in the 6-8 mm interval in which no diurnal variation is seen. These isotope values may be indicative of some type of chemoautotrophic CO_2 fixation. Although this would explain the heavy shift in isotope, no significant concentration change is seen. There appears to be a slight decrease in $\sum CO_2$ concentration in the dark profile; the precision of the light profile is such that no trend is clear. If these isotope profiles are superimposed upon those of the dissolved ferrous iron it can be seen that the maximum pore water ferrous iron concentration occurs in a zone where chemoautotrophic uptake of CO_2 is proposed. This maximal zone (6-7 mm in the light) seems to support the highest concentration of manganese-oxidizing bacteria and their predators, *P. jugosus* (an amoebomastigote, Table IV-5).

In summary, the $\sum CO_2$, isotope, and concentration profiles measured in a mm interval demonstrate that the upper 1 cm of this environment is extremely dynamic. There appears to be no direct relation between photosynthesis occurring in the mat community and microbially mediated degradation processes. Rather, the sedimentary microbial processes appear to be driven by allochthonous organic matter. The $\sum CO_2$ concentration and isotopic composition reflect microbially mediated degradation processes occurring within the sediment. In conclusion, we propose that the upper 10 mm of this environment can be viewed as having three geochemically distinct zones: 1) the upper 0-2 mm dominated by the diurnal variations in photosynthesis, 2) a middle 2-4 mm zone dominated by heterotrophic activity, and 3) a deeper 4-10 mm zone in which some chemoautotrophic activity is occurring together with ferrous iron and phosphate geochemical reactions.

Glutathione In Cyanobacteria

David Bermudes

Introduction

Glutathione, the tripeptide gamma glutamyl cysteinyl glycine (γ-glu-cys-gly), a nearly universal constituent of eukaryotic cells (Fahey, et al., 1984), has been found in many eubacteria (Fahey et al., 1978) including cyanobacteria (Fahey, personal communication). A related compound, γ-glu-cys, has recently been found in halobacteria (Newton and Javor, 1985). Numerous speculations on the function of glutathione have been put forth but they are based on scanty evidence. Glutathione may protect cells from peroxides (Mills, 1957). However, trends in glutathione production are not predictable; other functions for glutathione may exist for which the cell regulates its production.

The microelectrode and geochemical studies show that dramatic environmental gradients in microbial mat communities occur in the first 2 mm of the surface. Within this region steep gradients of oxygen, light, and hydrogen sulfide occur. The adaptations of several organisms to sulfide conditions by means of dissimilatory sulfur pathways have recently been described (Cohen, et al., 1975; Garlick, et al., 1977) which suggest an influence on local environments and the sulfur cycle.

Organisms adapt physiologically to their environment according to need, such as chromatic adaptation of phycobiliproteins in cyanobacteria. Similarly, changes in microbial mat environments of light, oxygen, and hydrogen sulfide may alter the need for glutathione. Light is responsible for both the photolytic damage to cells and oxygenic photosynthesis in cyanobacteria. The presence of O_2 and photolytically produced free radicals may increase the need for glutathione because of increased peroxide production. Conversely, the presence of H_2S, which combines with O_2 to form thiosulfate, may reduce the need for glutathione where the two gases coexist. We sought to determine the effects of light and O_2 on glutathione production. A preliminary study on the effects of the glutathione synthetase inhibitor, buthionine sulfoximine (S-n-butyl homocysteine sulfoximine or BSO for short), was also initiated.

Materials and Methods

Total glutathione, both oxidized and reduced forms of glutathione, and homoglutathione (Fahey and Newton, 1983) were assayed by the enzymatic method of Tietze (1969) modified by Fahey, et al., (1975) and expressed as nanograms of oxidized glutathione per mg residual dry weight.

Inhibition of glutathione synthesis by the -glutamylcysteine synthetase inhibitor BSO (S-n-butyl homocysteine sulfoximine) of molecular weight 232 (Griffith and Meister, 1979) was tested on *Anacystis nidulans* by its addition to the culture media in varying concentrations ranging from 10 uM to 5 mM. Cells were harvested by centrifugation and assayed for glutathione.

An axenic culture of *Anacystis nidulans* was obtained from Yehuda Cohen and grown on media BG-11 (Rippka, et al., 1979).

Aphanothece halophytica-dominated waters collected from the 150 per mil pond (Pond 4) were maintained at 25°C in closed vessels. A light period of 12 hours was followed by a dark period of 12 hours (40 to 0 $uE\ m^{-2}\ s^{-1}$ from incandescent 40 watt bulbs), very low light.

Growth curves of *Anacystis nidulans* and total glutathione were determined in a series of 9 2-liter Erlenmyer flasks fitted with cotton plugs and containing 750 ml BG-11 culture media and 75 ml. inoculum of stationary phase cells. Cell density was measured by absorbance at 550 nm. Cultures were sequentially harvested by centrifugation and total glutathione measured.

Light and dark effects on glutathione levels in *Anacystis nidulans* under normal oxygen tension were determined after placing 200 ml of log phase cells with a sterile supplement of 5 mM $NaHCO_3$ into 500 ml Erlenmyer flasks in light (20 and 0 $uE\ m^{-2}\ sec^{-1}$ Sylvania F40-GRO fluorescent lighting for 24 hours) and dark condtions. Aeration was provided at a rate of 0.35 liters per minute.

Light and dark effects on glutathione levels in *Anacystis nidulans* under reduced oxygen tension were determined after placing 200 ml of log phase cells with a sterile supplement of 5 mM $NaHCO_3$ in 500 ml Erlenmyer flasks in light (20 and 0 $uE\ m^{-2}\ sec^{-1}$ from Sylvania F40-GRO fluorescent light) and dark conditions for 24 hours. Oxygen tension was lowered by passing cotton filtered N_2 through the media at a rate of 0.35 liters per minute.

Results and Discussion

Results of light and dark studies under normal and reduced oxygen tensions were compared to determine the effect of reduction in oxygen tension on glutathione levels.

The growth rate of *Anacystis nidulans* and concurrent production of glutathione is presented in Figure IV-18. The generation time of *Anacystis nidulans* was approximately 12 hours. Throughout growth, glutathione levels remained between

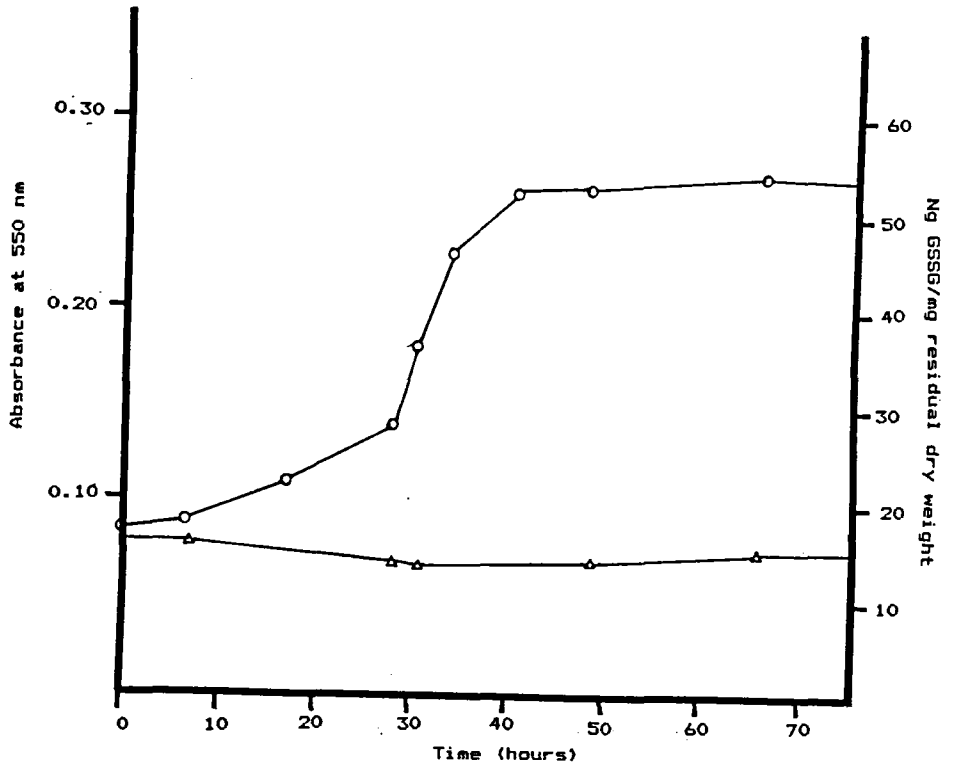

Figure IV-18. *Anacystis nidulans* growth curve comparing levels of oxidized glutathione (GSSG) per mg of residual dry weight. —△— = glutathione levels; —○— = growth

16.0 and 13.0 ng glutathione per mg residual dry weight of cells when grown under incandescent lighting of 40 $\mu E\ m^{-2}\ sec^{-1}$, thus showing a slight trend toward reduced levels during log phase. This allowed the subsequent comparison between light and dark incubated cells which would presumably no longer exist in the same growth phase.

Results of light and dark incubation of *Aphanothece halophytica*-dominated planktonic microbial community from Pond 4 and *Anacystis nidulans* under high and low oxygen tension is presented in Table IV-5. Unexpectedly, both *Aphanothece halophytica* samples and *Anacystis nidulans* cultures show increased levels of glutathione after 24 hours of continuous dark. While *Aphanothece* samples exhibited only approximately a 10 percent increase, *Anacystis* (O_2) and *Anacystis* (N_2) cultures showed approximately a 100 percent and 50 percent increase, respectively, thus revealing a diurnal variation.

Different light sources were used for growing *Anacystis* and for the light and dark study under normal and reduced oxygen tension. The former used 40 $\mu E\ m^{-2}\ sec^{-1}$ from 40 watt incandescent lamps and the latter 20 $\mu E\ m^{-2}\ sec^{-1}$ from F40-GRO fluorescent lighting. Apparently, there is an increased glutathione level; the lower intensity presumably also differs qualitatively.

It appears that light-grown *Anacystis nidulans* cells have equal amounts of glutathione while dark-grown cells produce more glutathione in the presence of increased O_2. Since *Aphanothece halophytica*-dominated planktonic communities grow under reduced oxygen tensions in this high salinity pond, this may account for the relatively lower percentage increase at night.

The results of the glutathione synthesis inhibition by BSO are presented in Table IV-6. Although some concentrations of BSO apparently result in approximately one third of the control level of glutathione, the highest concentration of BSO used (5 mM) showed no inhibition. Thus BSO is not an effective inhibitor of glutathione synthesis in *Anacystis nidulans*. It is not known whether the lack of inhibition is due to lack of sensitivity by the enzyme, lack of transport into the cell, or detoxification by intracellular or extracellular means.

These preliminary studies do show an environmentally determined pattern of cellular glutathione. The effects, if any, of H_2S, organic sulfur, or other metabolites remain to be tested.

Acknowledgement: I thank Barbara Javor and Robert Fahey for their assistance in this study.

Plate		Manganese oxidizers		
Depth (mm) (plates)	*P. jugosus* (presumptive)	quantity	diversity	spread away from sediment inoculum
1	—	+	+	+
2	++	+	—	—
3	+	+	—	—
4	++	+	—	—
5	++	++	+	+
6	+++	+++	+++	+++
7	+	+	+	—
8	+	+	+	—
9	++	+	+	—
10	+	+	+	—

Key to diversity

—	absent
+	present, more than or equal to 3 different colony morphotypes
++	present, more than or equal to 3-5 different colony morphotypes
+++	present, more than or equal to 6 different colony morphotypes

Table IV-5. Colonies of *Paratetramitus jugosus* and manganese-oxidizing bacteria as a function of depth.

	Light	Dark
Aphanothece (7/10/84)	4.9	5.6
Aphanothece (7/24/84)	4.4	5.4
Anacystis (O_2)	41.4	82.5
Anacystis (N_2)	43.2	57.1

Table IV-6. Effect on glutathione levels by light and dark conditions of *Aphanothece halophitica*-dominated planktonic community and on axenic cultures of *Anacystis nidulans* under high (O_2) and low nitrogen (N_2)

BSO Concentration (μM)	0	10	100	500	1000	5000
ng glutathione ag^{-1} residual dry weight	60	33.9	22.4	20.4	20.8	56.2

Table IV-7. Effect of increasing concentrations of BSO on glutathione levels in *Anacystis nidulans*

		sulfide concentration (μM)							
aerobic	anaerobic								
no sulfide	0	0.01	0.02	0.05	0.1	0.2	0.5	1	2	4
++	+++	+++	+++	+++	++	++	++	+	+-	-

+++ = very good growth; ++ = good growth; + = little growth; +- = more or less growth - = no growth.

Table IV-8. Anaerobic growth of *Oscillatoria* from Alum Rock spring site 3 in the presence of sulfide after 5 days.

Microbial Communities and Microprofiles of Sulfide and Oxygen of Alum Rock Sulfur Springs

U. Fischer

Introduction

Microbial Community of Alum Rock Spring Field Site

The microbial community of Alum Rock sulfur spring site 3 was studied along one branch of the main stream and between the two branches, 150 cm distant from the source. The community at the source (sample J) was dominated by green sulfur photosynthetic bacteria of the genus *Chlorobium*. At 15-35 cm from the source (samples I and H) dominance in the community shifted to the genus *Flexibacter* at the surface of the mat and purple sulfur bacteria of the genus *Chromatium* underneath. At 50-80 cm (samples G and F) colorless sulfur-oxidizing bacteria of the genus *Thiothrix* began to appear. At 100 to 150 cm (samples D and E), the surface of the mat was still dominated by *Flexibacter* but underneath dominance shifted to purple sulfur bacteria as above, as well as cyanobacteria of the genus *Oscillatoria* and *Pseudonabaena*. The measurements of temperature along the stream showed no significant gradient. We believe that community variations are controlled more by sulfide than temperature. The temperature along the stream was 29°C at positions J and I, and 28°C at positions E and D. At position L, which was shaded, the temperature decreased to 19°C.

Ten ml of the overlying water were taken at position G and fixed immediately with 20 ml of 2 percent Zn-acetate to determine the sulfide concentration by the methylene blue method. A sulfide concentration of 106 uM was calculated for the overlying water.

Isolation of Cyanobacteria

Samples from positions E and L of the Alum Rock sulfur spring site 3 were taken to isolate cyanobacteria. The samples were placed on agar plates (containing the standard mineral medium BG 11 and 2 percent agar) and incubated at 27°C at a light intensity of 15-20 $uE\ m^{-2}\ sec^{-1}$. After 3 days single cyanobacterial colonies were transferred onto fresh plates and the microorganisms were studied under the microscope. This procedure was repeated several times, until only a single cyanobactrium species was detected by microscopic observations. From position E an *Oscillatoria* species, 5 um in width, was isolated (with some heterotrophic bacteria).

The *Oscillatoria* sp. was transferred from the plates to 10 ml of liquid BG 11 medium and grown for 5 days under the same conditions as described above for the plates. Then 5 ml of this preculture were transferred to 100 ml of liquid BG 11 medium and allowed to grow for 5 days. Some drops of this culture suspension were mounted on an agar slide as a preparation for photmicrographs using a Zeiss

Photomicroscope II. The filamentous cyanobacterium *Oscillatoria* is illustrated in Figure IV-19a. To determine whether the organism contains phycocyanin, an epifluorescence microscope with a 550 nm interference filter for the excitation light and a cut-off filter at 680 nm for the emitted light was used. The red color in the cyanobacterium is due primarily to excitation of phycocyanin. *Synechocystis* did not grow in a liquid medium. For photomicrographs, some colonies of *Synechocystis* were taken directly from the agar plate and mounted on an agar slide. The morphology is shown in Figure IV-19b. The presence of phycocyanin in *Synechocystis* as detected by its red color is also demonstrated by the use of an epifluorescence microscope (Figure IV-19d).

Materials and Methods

Culture Medium for Cyanobacteria

For the cultivation of cyanobacteria, the mineral medium, BG 11, described by Rippka et al., (1979) was used. Distilled water was replaced by Alum Rock spring water.

BG 11 medium (1 liter)

$NaNO_3$: 1.5 g
$K_2HPO_4.3H_2O$: 0.04 g
$MgSO_4.7H_2O$: 0.075 g
$CaCl_2.2H_2O$: 0.036 g
Citric acid: 0.006 g
Ferric ammonium citrate: 0.006 g
EDTA (disodium magnesium salt): 0.001 g
Na_2CO_3: 0.02 g
Trace element solution: 1 ml
Alum Rock Spring water: 1000 ml

After autoclaving and cooling, the medium had a pH of 7.4. For aerobic growth of cyanobacteria a 250 ml Erlenmeyer flask containing 100 ml of medium was used.

For the enrichment and isolation of cyanobacteria on solid media, 20 g of agar were added to the BG 11 medium.

Composition of Trace Element Solution
(Rippka et al., 1979)

Ingredient	Amount (g/l distilled water)
H_3BO_3	2.86
$MnCl_2.4H_2O$	1.81
$ZnSO_4.7H_2O$	0.222
$Na_2MoO_4.2H_2O$	0.390
$CuSO_4.5H_2O$	0.079
$Co(NO_3)_2.6H_2O$	0.0494

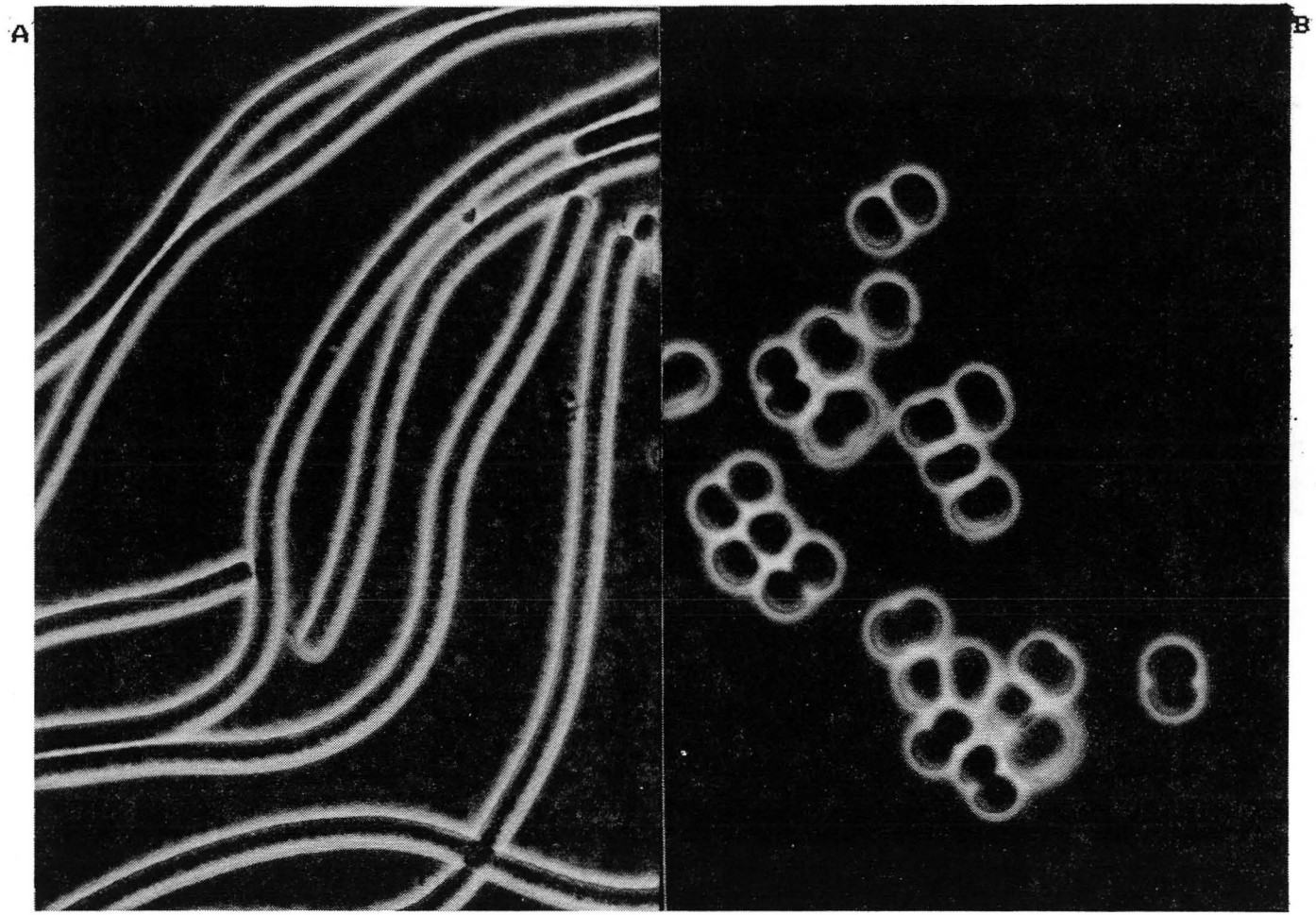

Figure IV-19. (A) *Oscillatoria sp.* isolated from Alum Rock spring, 7 mm = 10 μm; (B) *Synechocystis sp.* isolated from Alum Rock spring. 4 mm = 10μm.

Anaerobic Growth of Cyanobacteria in the Presence of Sulfide

Anaerobic growth in the presence of sulfide of isolated cyanobacterial strains from Alum Rock sulfur springs was achieved in 8 ml screw-cap test tubes. The tubes contained the standard BG 11 medium described above and, in addition, different concentrations of sulfide. Each of the tubes was inoculated with 1.5 ml (about 20 percent) of an anaerobically grown liquid culture.

Preparation of a Sulfide Stock Solution (6.25 mM) (Modified After Pfennig and Trueper, 1981)

$Na_2S.9H_2O$	0.75 g
Na_2CO_3	0.5 g
Distilled water	50 ml

The solution was autoclaved and after cooling was partially neutralized with 2 ml of a sterile 2M H_2SO_4 solution. (The carbonate was added to increase the growth yield of the cyanobacteria.)

Culture Medium for *Thiothrix*

For the enrichment and isolation of *Thiothrix* species of Alum Rock spring on agar plates, I used the following medium (Wiessner, 1981):

Per 1 liter:

NH_4Cl	50 mg
K_2HPO_4	100 mg
$CaSO_4.2H_2O$	2 mg
$MgSO_4.7H_2O$	10 mg
$ZnSO_4.7H_2O$	0.1 mg
$MnSO_4.4H_2O$	0.02 mg
H_3BO_3	0.1 mg
$Co(NO_3)_2$	0.01 mg
$NaMoO_4.2H_2O$	0.01 mg
$CuSO_4.5H_2O$	0.0005 mg
$FeSO_4.7H_2O$	7 mg
EDTA (Na_2-salt)	9.2 mg
Na-acetate	10 mg
$Na_2S.9H_2O$	300 mg
agar	12.5 g

Adjust the pH of the medium to about 7.0
Important: $FeSO_4$ and EDTA must be mixed separately and added to the medium after a short period of boiling.

Culture Medium for *Flexibacterium.*

For the enrichment and isolation of *Flexibacteria* species of Alum Rock sulfur springs only agar plates were prepared. The medium used was Number 27; Vy/2 agar medium (Reichenbach and Dworkin, 1981).

The medium contained per 100 ml:

Baker's yeast	0.5 g
$CaCl_2$	0.1 g
Agar	1.5 g
Cyanocobalamine	50 *ug*

pH is adjusted to 7.2

Absorption Spectra of Cyanobacterial Chlorophyll

Absorption spectra were determined in a Varian Techtron double beam spectrophotometer model 635, connected to a recorder.

In vivo spectra were obtained by suspending cell material in 50 percent sucrose to avoid settling of whole cells in the cuvette. *In vitro* spectra of chlorophylls were obtained by extracting wet cell material either in 100 per cent methanol or acetone. The cell material was harvested by centrifugation (12,000 rpm for 10 minutes) in a Sorvall RC2-B. To the pellet, 5 ml of methanol or acetone were added and then allowed to stand in the dark at 4°C for 10 minutes before the suspension was centrifuged the same way a second time. The supernatant was used to determine the absorption spectra of extracted pigments. All spectra were recorded in the range of 750 nm to 350 nm.

Field Experiments with Oxygen and Sulfide Microelectrodes

To study the microprofile of oxygen and sulfide in an Alum Rock sulfur spring (see profiles of salt ponds and marsh site), handmade microelectrodes (Fig. IV-2) were attached to a micromanipulator which was held in place on a stand. Profiles were obtained with microelectrodes from the overlying water and from the microbial mats, with measurements taken at 100 *um* or 250 *um* increments. In addition, in the overlying water, sulfide concentration was determined by the methylene blue method (below) and oxygen was determined using the method of Winkler (below).

Sulfide Determination by the Methylene Blue Method

Determination of sulfide used the method of Pachmayr (1960) as modified by Trueper and Schlegel (1964).

The assay was done in 100 ml volumetric flasks which contained:

10 ml Alum Rock spring water
20 ml 2 per cent Zn-acetate[a]
10 ml DMPD-solution[b]
0.5 ml FAS-solution[c]

[a,b,c]: for preparation, see below

This reaction mixture was shaken vigorously and allowed to stand for 10 minutes at room temperature. The flask was then filled up to 100 ml with distilled water. The absorption was measured at 670 nm against a blank without Alum Rock spring water.

Preparation of (a) Zn-acetate, (b) DMPD and (c) FAS solutions:

a) Zn-acetate: 20 g Zn-acetate were dissolved in 1000 ml distilled water and 1-2 drops of acetic acid were added.

b) DMPD: 2 g dimethyl-p-phenylene-diamine chloride were suspended in 200 ml distilled water. Then 200 ml of concentrated H_2SO_4 were carefully added. Distilled water was added to make a 1 liter solution which was stored in a 1000 ml volumetric flask wrapped with aluminum foil.

c) FAS: 50 g $NH_4Fe(SO_4)_2.12H_2O$ were dissolved in 100 ml distilled water by adding 10 ml concentrated H_2SO_4. The solution was then filled up to 500 ml with distilled water and kept in a 500 ml volumetric flask wrapped with aluminum foil.

Results

Isolation of *Thiothrix* and *Flexibacter*

No attempt to enrich or isolate *Thiothrix* or *Flexibacter* from Alum Rock sulfur spring on agar plates was successful.

Absorbance Spectra of Isolated Cyanobacteria

To determine the composition of the pigments from the isolated cyanobacteria strains, absorbance spectra were taken from whole cells or extracted pigment preparations. Three major groups of pigments are normally present in cyanobacteria: chlorophyll a, biliproteins, and carotenoids. The *in vivo* spectrum (Fig. IV-20) of the isolated *Oscillatoria* strain shows maxima at 680 nm and 435 nm, indicating chlorophyll a (for isolated *Synechocystis*: 685 nm and 445 nm, Fig. IV-21), at 632 nm indicating phycocyanin (for *Synechocystis* at 632 nm), and at 488 nm indicating carotenoids (for *Synechocystis* at 500 nm).

When the pigments of *Oscillatoria* and *Synechocystis* were extracted by methanol or acetone, the absorption maxima were more distinct and were shifted towards shorter wavelengths. This is

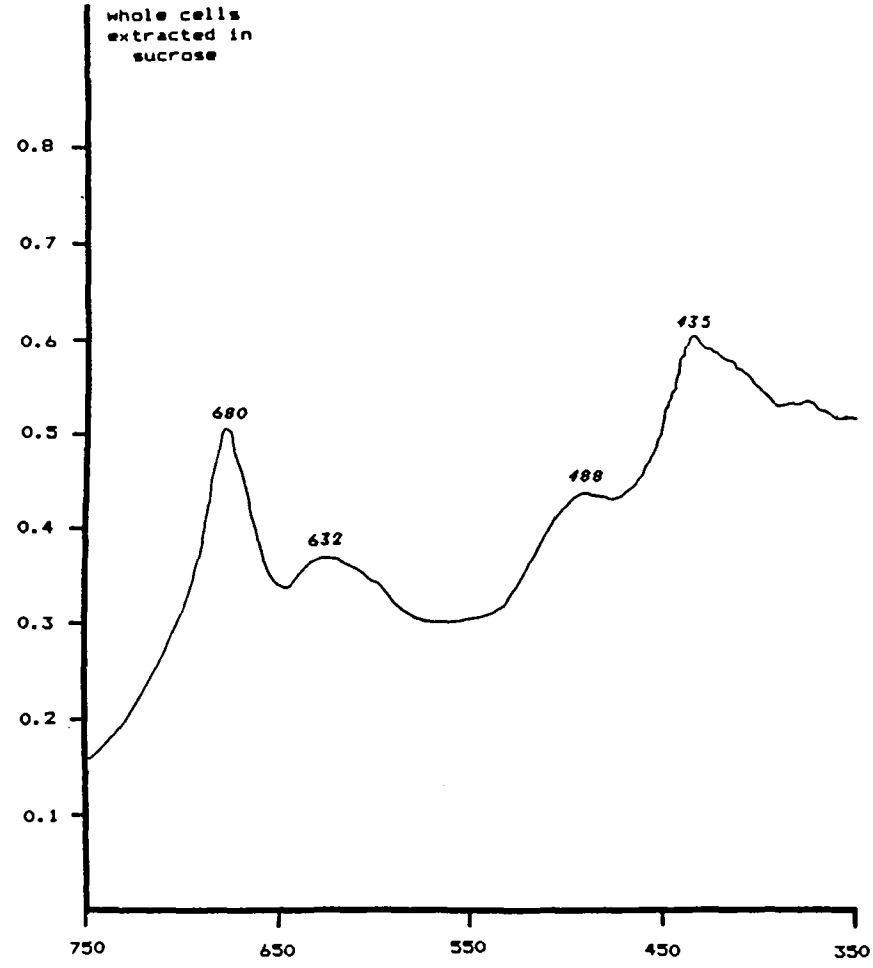

Figure IV-20. Absorbance spectrum of *Oscillatoria*.

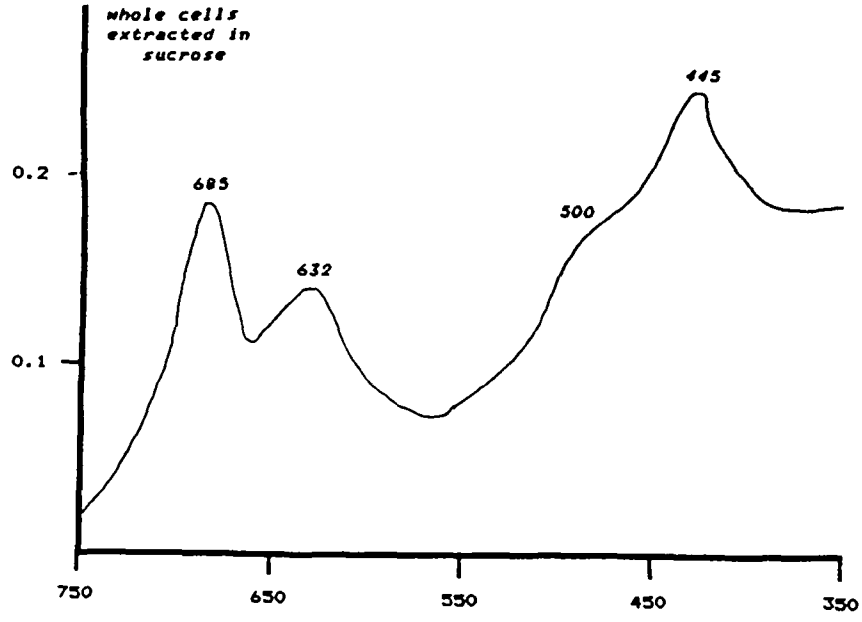

Figure IV-21. Absorbance spectrum of *Synechocystis*.

illustrated in Figures IV-22 and 24 for *Oscillatoria* and for *Synechocystis* in Figures IV-23 and 25.

Anaerobic Growth of *Oscillatoria* in the Presence of Sulfide

Some cyanobacteria perform oxygenic or anoxygenic photosynthesis in the presence of sulfide. Cyanobacteria of Alum Rock sulfur springs may be able to carry out photosynthesis when sulfide is present. Attempts were made to determine how isolated *Oscillatoria* grow under anaerobic conditions with different sulfide concentrations. The anaerobic growth experiment was carried out as described in the Methods section. The sulfide concentration ranged from 0 to 4 mM. The control contained no sulfide. For aerobic growth conditions, one screw-cap test tube contained only 1.5 ml of the cell suspension and 5 ml of the BG 11 medium. The inoculated 8 ml screw cap test tubes were incubated for 5 days at 27°C and 15-20 $\mu E\ m^{-2}\ sec^{-1}$. The result is shown in Table IV-7 (see end of preceding subchapter).

During the 5 days after the inoculation period the generation of a gas, probably oxygen, was observed in the culture tubes containing 0 to 0.05 mM sulfide. Under these growth conditions, *Oscillatoria* had a dark green color and showed very good growth at the bottom of the culture tubes. At higher sulfide concentrations (from 0.1 to 1 mM) the color of the culture was more or less light green and the organisms formed a thin layer from the bottom to the surface. The culture exposed to 4 mM sulfide did not grow, sank down to the bottom of the tube, and showed a yellow-brownish color two days after inoculation. Whether this *Oscillatoria* strain shows the same behaviour concerning photosynthesis found for *Oscillatoria limnetica* from Solar Lake remains to be studied.

Microprofile of an Alum Rock Sulfur Spring

The distribution of sulfide and oxygen in the overlying water and microbial mat at Alum Rock spring site 2 was measured with handmade microelectrodes. This sulfur spring was choosen for measurements because it was easy to place the tripod with the micromanipulator and microelectrodes directly in front of the spring. Since the mat of the spring was growing on a vertical rock substrate, it was necessary to insert the microelectrodes more or less horizontally into the mat. Three profiles of oxygen and sulfide were taken across the spring, 5-10 cm down from the top of the source. The main stream in the middle of the spring had a white color and the community was comparable to that of spring site 3 at positions H and J. The borders on both sides of the main stream had a dark green color and the community was nearly the same as that described for positions C and D of the spring site 3. In the overlying water the sulfide concentration was determined by the methylene blue method (see Methods section above) along the stream. From Figure IV-26 it can be seen that there is a decrease in sulfide concentration from the top, at the source, to the bottom. Light intensity decreases from 60 $\mu E\ m^{-2}\ sec^{-1}$ at the top to 50 $\mu E\ m^{-2}\ sec^{-1}$ at the bottom. From the top to the ground there is a

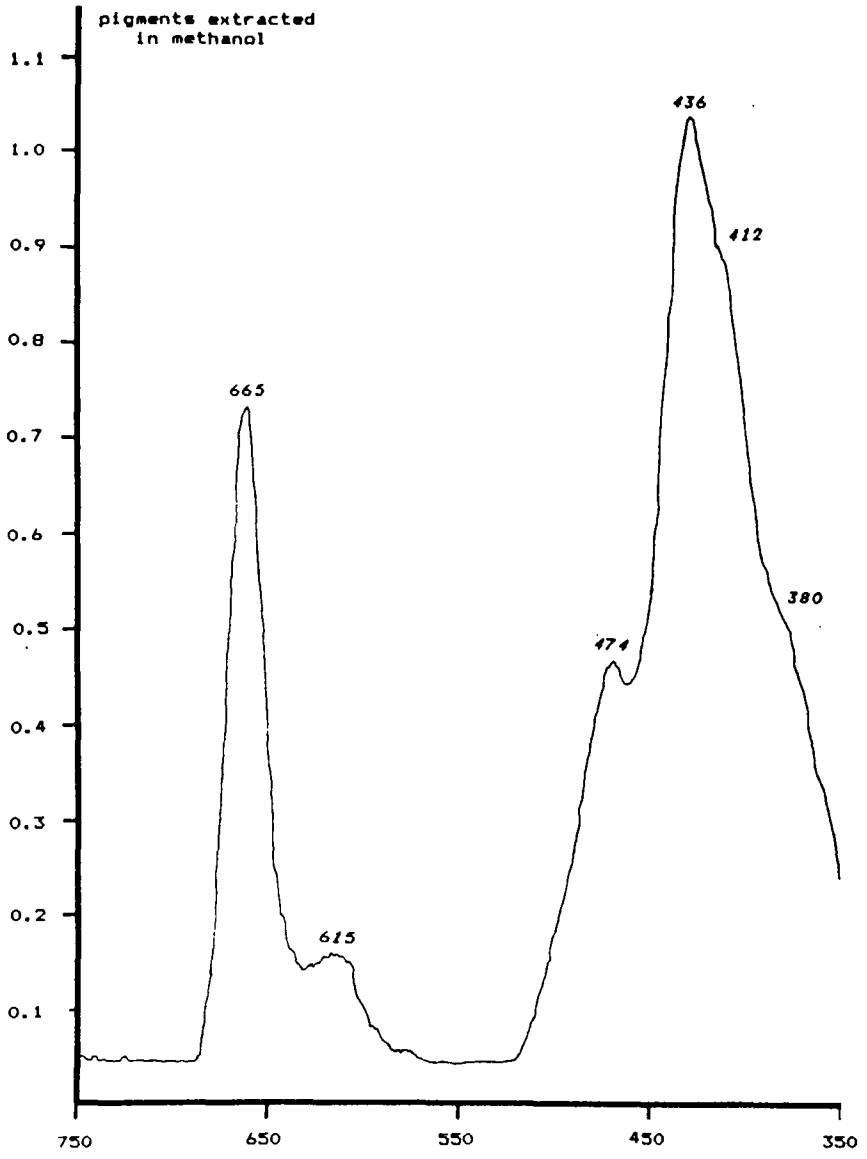

Figure IV-22. Absorbance spectrum of *Oscillatoria*.

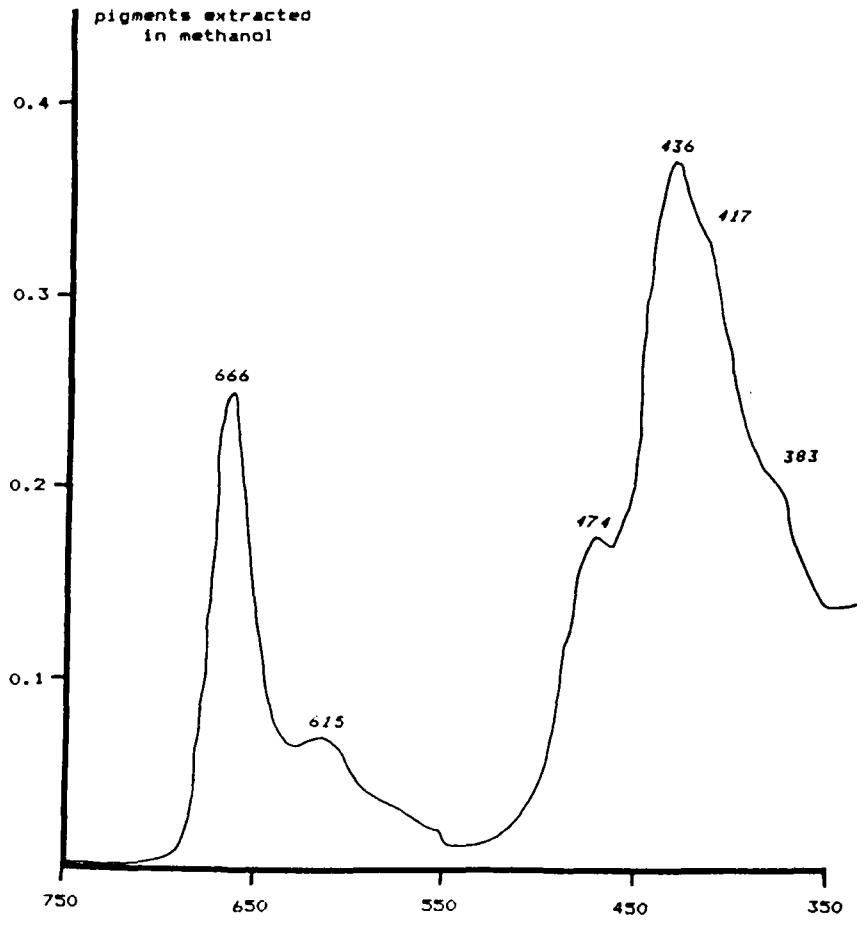

Figure IV-23. Absorbance spectrum of *Synechocystis*.

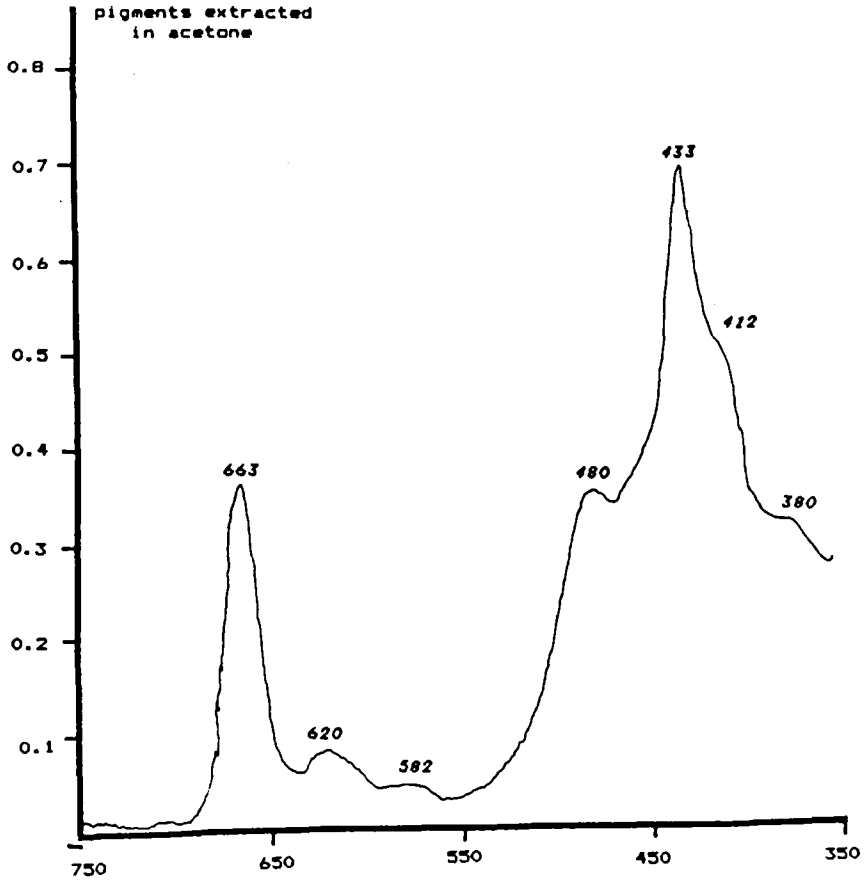

Figure IV-24. Absorbance spectrum of *Oscillatoria*.

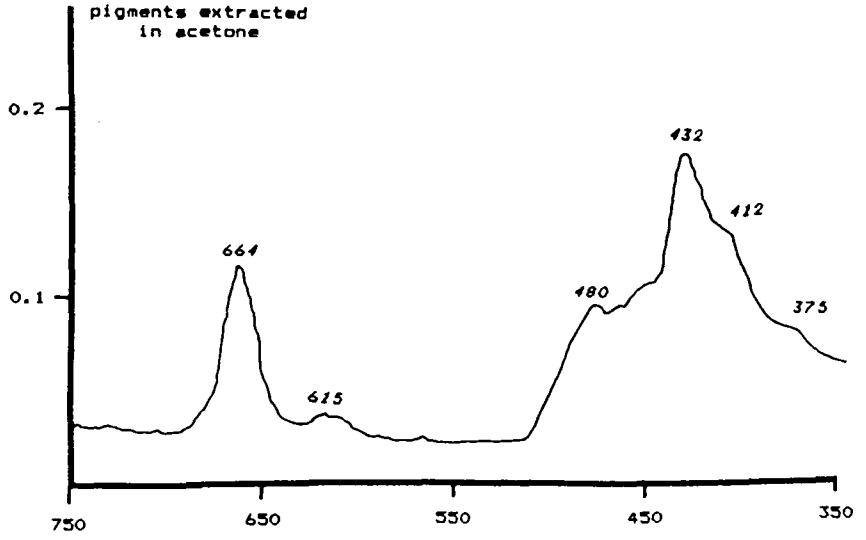

Figure IV-25. Absorbance spectrum of *Synechocystis*.

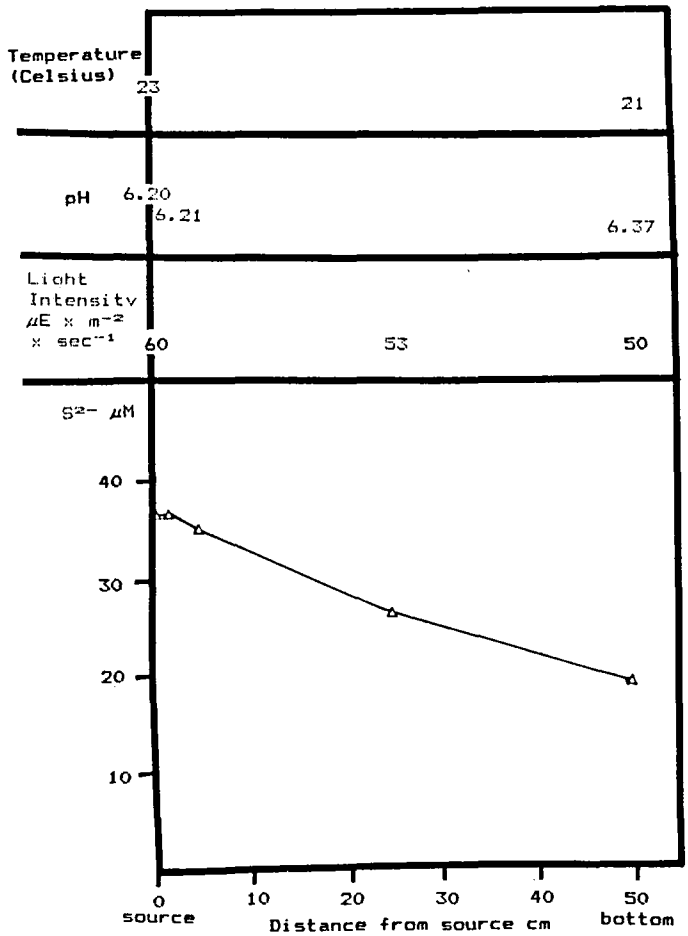

Figure IV-26. Sulfide, light intensity, pH, and temperature in the main stream of Alum Rock (at site 2). Air temperature 28° by the spring (in the shade).

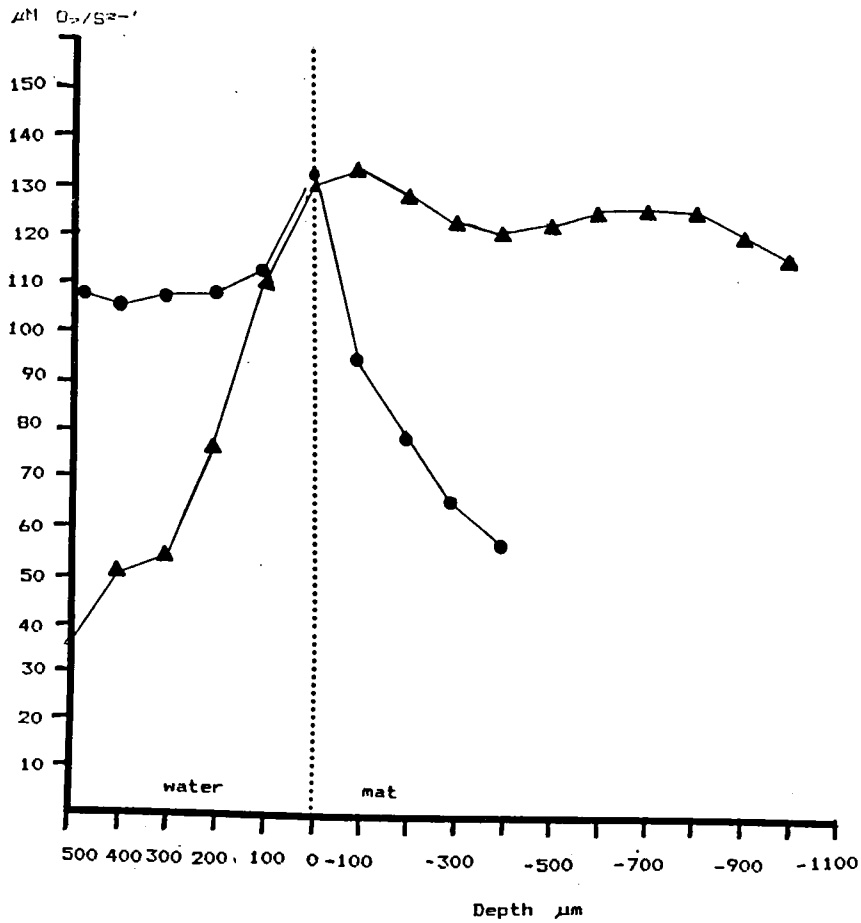

Figure IV-27. Oxygen and sulfide in the main stream and at microbial mat (white). (Alum Rock, site 2; 10 cm below top of spring).

▲ = S^{2-}; ● = O_2

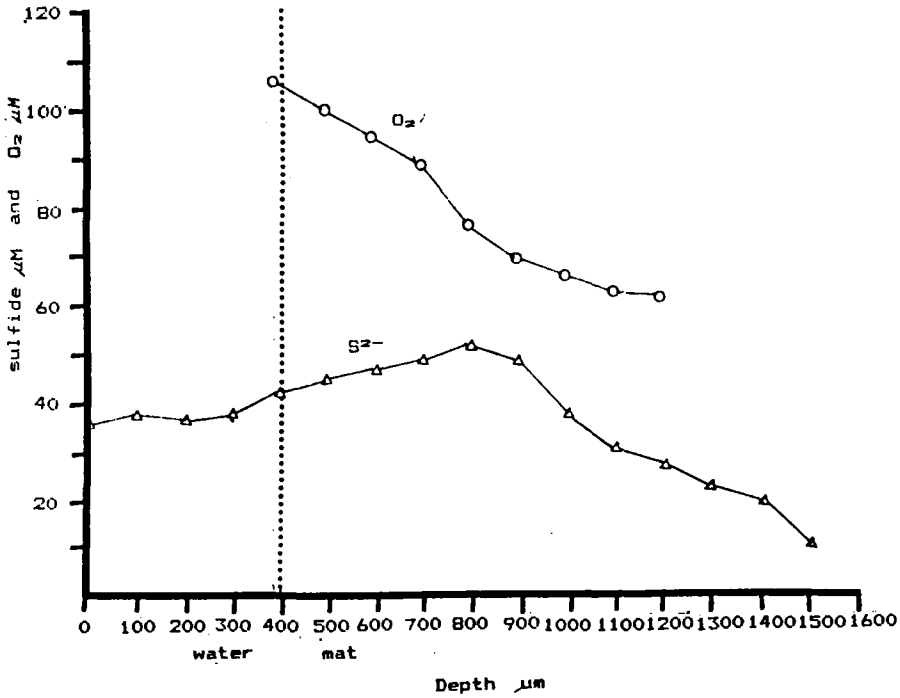

Figure IV-28. Oxygen and sulfide in the overlying water and microbial mat (border of the main stream, green). Alum Rock, site 2; 10 cm below top of spring.

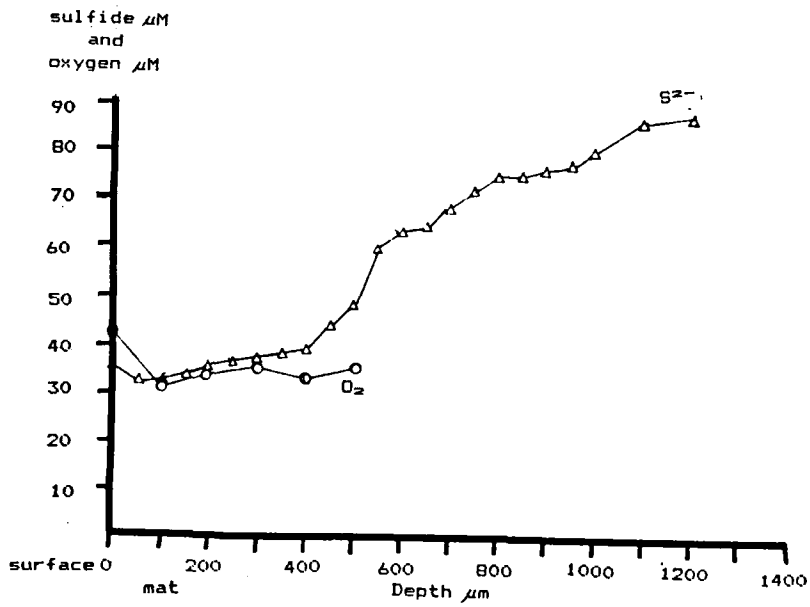

Figure IV-29. Oxygen and sulfide at a microbial mat (border of the main stream, green). Alum Rock, site 2; 5 cm below top of spring.

temperature difference of 2°C. The pH increases from 6.2 to 6.37. In the overlying water of the main stream (white color of the mat), an enormous increase in sulfide was measured with depth, while in the mat a low decrease was measurable (Figure IV-27). By contrast, the oxygen concentration decreased rapidly in the first 500 *um* of the mat. One explanation for this steep decrease in oxygen in this part of the mat is that a predominantly heterotrophic community is present, with only a small number of cyanobacteria producing oxygen during photosynthesis. The other profiles were taken at the border of the main stream, in very well developed (dark green) cyanobacterial mats (Fig. IV-28 and 29). The oxygen concentration decreases very slowly during the first 500 *um* of depth because of the oxygenic photosynthesis activity of cyanobacteria, the dominant organisms at this part of the spring. The sulfide concentration in the mat increases with depth when oxygen decreases.

References

Baumgartl H., and Lubbers, D.W., 1973. Platinum needle electrodes for polarographic measurement of oxygen and hydrogen. In *Oxygen Supply*, (M. Kessler, D.F. Bruley, L.C. Clark Jr., D.W. Lubbers, I.A. Silver, J. Strauss eds.), Urban and Schwarzenberg, Munich, pp. 130-136.

Cohen, Y., 1984. Oxygenic photosynthesis, anoxygenic photosynthesis and sulfate reduction in cyanobacterial mats. In *Perspective in Microbial Ecology*, (M. Klug, ed.), ASM publ.

Cohen, Y., Castenholz, R.W., and Halvorson, H.O. (eds.), 1984. *Microbial Mats: Stromatolites*, Alan R. Liss, N.Y.

Cohen, Y., Jørgensen, B.B., Padan, E., and Shilo, M., 1975. Sulphide-dependent anoxygenic photosynthesis in the cyanobacterium *Oscillatoria limnetica*. Nature 257:489-492.

Fahey, R.C., Brody, S., and Mikolajczyk, S.D., 1975. Changes in the glutathione thiol-disulfide status of *Neurospora crassa* conidia during germination and aging, J. Bacteriology, 12: 144-151.

Fahey, R.C., Brown, W.C., Adams, W.B., and Worsham, M.B., 1978. Occurrence of glutathione in bacteria, J. Bacteriology, 133:1126-1129.

Fahey, R.C. and Newton, G. L., 1983. Occurrence of low molecular weight thiols in biological systems. In *Functions of Glutathione: Biochemical, Physiological, Toxicological, and Clinical Aspects.* (A. Larsson, et al., eds.), Raven Press, New York.

Fahey, R.C., Newton, G.L., Arrick, G., Overdank-Bogart, T., and Alev, S. B., 1984. *Entamoeba histolytica*: a eukaryote without glutathione metabolism, Science, 24:70-72.

Garlick, S., Oren, A., and Padan, E., 1977. Occurrence of facultative anoxygenic photosynthesis among filamentous and unicellular cyanobacteria, J. Bacteriology, 129:623-629.

Griffith, O.W. and Meister, A., 1979. Potent and specific inhibition of glutathione synthesis by buthionine sulfoximine (S-n-butyl homocysteine sulfoximine), J. Biol. Chem., 254: 7558-7560.

Hartman, H. 1984. In *Microbial Mats: Stromatolites* (Y. Cohen, R.W. Castenholz, and H.O. Halvorson, eds.), Alan R. Liss, N.Y.

Ho, K.K., and Krogmann, D.W., 1982. Photosynthesis in cyanobacteria. In *The Biology of Cyanobacteria*, Vol. 19, (N.G. Carr and B.G. Whitton, eds.), Blackwell Scientific Publications.

Howarth, R.W., and Marino, R., 1984. Sulfate reduction in salt marshes with some comparisons to sulfate reduction in microbial mats. In *Microbial Mats: Stromatolites*, (Y. Cohen, R.W. Castenholz and H.O. Halvorson, eds.), Alan R. Liss, N.Y., pp. 245-264.

Jørgensen, B.B., and Cohen, Y., 1977. Solar Lake (Sinai), The sulfur cycle of the benthic cyanobacterial mats, Limnol. and Oceanog. 22:657-666.

Jørgensen, B.B., Revsbech, N.P., Blackburn, T.H. and Cohen, Y., 1979. Diurnal cycle of oxygen and sulfide microgradients and microbial photosynthesis in a cyanobacterial mat sediment, Appl. Environ. Microbiol. 38:46-58.

Jørgensen, B.B., Revsbech, N.P., and Cohen, Y., 1983. Photosynthesis and structure of benthic microbial mats: microelectrode and SEM studies of four cyanobacterial communities, Limnol. Oceanog. 28:1075-1093.

Jørgensen, B.B., Revsbech, N.P., and Cohen, Y., 1985. Transition from anoxygenic to oxygenic photosynthesis in a *Microcoleus chthanoplastes* cyanobacterial mat, Limnol. Oceanogr., (in press)

Martens, C.S., and Berner, R.A., 1974. Methane production in the interstitial waters of sulfate depleted marine sediments, Science, 185:1167-1169.

Mills, G.C., 1957. Hemoglobin catabolism. I. Glutathione peroxidase, an erythrocyte enzyme which protects hemoglobin from oxidative breakdown, J. Biol. Chem. 229:189-197.

Murray, J.W., and Gill, G., 1978. The geochemistry of iron in Puget Sound, Geochim. Cosmochim. Acta, 42:9-19

Newton, G.L. and Javor, B., 1985. Gamma-glutamylcysteine and thiosulfate are the major low molecular weight thiols in halobacteria, J. Bacteriology, (in preparation).

Pachmayr, F., 1960. Vorkommen und Bestimmung von Schwefelverbindungen in Mineralwasser. Doctoral thesis, Univ. Munich, West Germany.

Padan, E. and Cohen, Y., 1982. Anoxygenic photosynthesis. In *The Biology of Cyanobacteria*, (N. G. Carr and B. A. Whitton, eds.), Blackwell Scientific Publications, Oxford, 688 pp.

Parsons, T.R., Takahashi, M., and Hargrave, B., 1977. *Biological Oceanographic Processes*, Pergamon Press.

Pfennig, N. and Trueper, H.G., 1981. Isolation of members of the families Chromatiaceae and Chlorobiaceae. In *The Prokaryotes*. (M.P. Starr, H. Stolp, H.G. Trueper, A. Balows and H.G. Schlegel, eds.). Vol. 1, Springer Verlag, New York, pp. 279-289.

Read, L.K., Margulis, L., Stolz, J.F., Obar, R., and Sawyer, T., 1983. A new strain of *Paratetramitus jugosus* from Laguna Figueroa Baja California, Mexico, Biological Bulletin, 165:241-264.

Reichbach, H. and Dworkin, M., 1981. The order Cytophagales (with addenda on the genera *Herpetosiphon*, *Saprospira*, and *Flexithrix*). In *The Prokaryotes*. (M.P. Starr, H. Stolp, H.G. Trueper, A. Balows, and H.G. Schlegel, eds.). Vol. 1, Springer Verlag, New York, pp. 356-379.

Revsbech, N.P., Jørgensen, B., and Cohen, Y., 1983. Microelectrode studies of the photosynthesis and O_2, H_2S, and pH profiles of a microbial mat, Limnol. Oceanog., 28:1062-1074.

Revsbech, N.P., Jørgensen, B., and Brix, O., 1981. Primary production of microalgae in sediments measured by oxygen microprofile, H14 CO_3 fixation and oxygen exchange methods, Limnol. Oceanog. 6:717-730.

Revsbech, N.P. and Ward, D.M., 1984. Microprofiles of dissolved substances and photosynthesis in microbial mats measured with

microelectrodes. In *Microbial Mats: Stromatolites*, (Y. Cohen, R.W. Castenholz, and H.O. Halvorson, eds.), Alan R. Liss, N.Y.

Rippka, R., Deruelles, J., Waterbury, J.B., Herdman, M., and Stanier, R.Y., 1979. Generic assignments, strain histories and properties of pure cultures of cyanobacteria, J. Gen. Microbiol., 111:1-61.

Skyring, G.W., 1984. Sulfate reduction in marine sediments associated with cyanobacterial mats in Australia. In *Microbial Mats: Stromatolites*, (Y. Cohen, R.W. Castenholz, and H.O. Halvorson, eds.), Alan R. Liss, N.Y., pp. 265-276.

Stookey, L.L., 1970. Ferrozine: a new spectrophotometric reagent for iron, Anal. Chem., 42.

Tietze, F., 1969. Enzymic method for quantitative determination of nanogram amounts of total oxidized glutathione: applications to mammalian blood and other tissues, Anal. Biochem. 27:502-522.

Trueper, H.G. and Schlegel, H.G., 1964. Sulphur metabolism in Thiorhodaceae. I. Quantitative measurements on growing cells of *Chromatium okenii*, Antonie van Leeuwenhoek J. Microbiol. Serol., 30:225-238.

Wiessner, W., 1981. The family Beggiatoaceae. In *The Prokaryotes*. (M.P. Starr, H. Stolp, H.G. Trueper, A. Balows, and H.G. Schlegel, eds.). Vol. 1, Springer Verlag, New York, pp. 380-389.

CHAPTER V

MICROBIAL COLONIZATION AND GROWTH ON METAL SULFIDES AND OTHER MINERAL SURFACES

Prof. D.E. Caldwell
A.R. Sundquist
J. Lawrence
A.P. Doyle

Introduction

Sulfur-containing minerals present in soils, sediments, and other environments are often coated with a film of actively metabolizing microorganisms. Because these films are difficult to study, cell suspensions are frequently used. Laboratory studies have formed the basis of knowledge concerning microbial activity and the chemical development of Earth. Because there could be important differences between the activities of microbes in uniform cell suspensions and those in nature, this research aimed to document the presence and formation of mineral films. It was found that microbial films formed rapidly on all of the (SbS_2), barite ($BaSO_4$), selenite ($CaSO_4$), amorphous elemental sulfur, and hematite (Fe_2O_3). Gradients of soluble sulfur compounds (cysteine, glutathione, thioglycolate, sulfite, and thiosulfate) did not increase the rate of attachment or growth of bacterial populations colonizing these surfaces. Microbial activities, including metabolism, growth, behavior varied substantially depending upon whether the cells were in suspension or in surface films.

Materials and Methods

In Situ Incubation of Membrane Enrichments

A membrane filter (polycarbonate capillary membrane, 0.05 um pores, 25 mm diameter, Nucleopore, Pleasanton, CA) was cemented to the ground flat surface of one tube of a Bellco Parabiotic Chamber (catalog no. 1945) (Fig. V-1). This was done by coating the surface with an uninterrupted ring of silicone rubber and applying the filter with the shiny side out. The assembled "J-tube" was autoclaved to sterilize the apparatus and to solidify the silicone rubber. Care was taken to protect the outer surface of the filter from pore-clogging debris.

50 mM solutions of the following five sulfur compounds were prepared: L-cysteine, reduced glutathione, and the sodium salts of sulfite, thiosulfate, and thioglycolate. The compounds were dissolved in water and the pH adjusted to neutrality.

Acridine orange, a fluorescent stain, was used to stain the incubated filters. A 0.1 percent stock solution was first prepared by dissolving acridine orange in 10 mM potassium phosphate buffer at pH 7.2. A 1:10 dilution of the stock into

Surface	N (cells/field)	A (cells/field-hr)	$N=A/\mu(e^{\mu t}-1)$ μ solved(hr^{-1})	$\mu=\ln(N/ci+1)/t$ μ calculated(hr^{-1})
pyrite (natural)	70.0	3.1	0.051	0.23
	67.6	2.8	0.060	0.19
pyrite polished	99.6	3.9	.066	0.22
	43.4	1.8	0.062	0.20
pyrite polished	73.7	2.7	0.074	0.20
oblique	44.9	2.0	0.054	0.22
average	66.5±21	2.7±0.78	0.061±0.008	0.21±0.02
pyrrhotite natural	73.9	2.9	0.066	0.20
	98.7	4.3	0.052	0.23
pyrrhotite polished	120	4.0	0.085	0.19
top	124	3.8	0.094	0.19
" " side	79.3	3.4	0.057	0.18
average	99.2±22.8	3.7+=0.6	0.071±0.018	0.20±0.02
galena	71.2	2.5	0.076	0.28
	47.6	1.9	0.04	0.22
stibnite	80.2	2.9	0.076	0.19
	50.3	2.4	0.044	0.24
sulfur	57.4	2.4	0.061	0.21
	41.6	1.7	0.064	0.23
glass	55.7	2.4	0.056	0.22
	45.8	2.3	0.040	0.21
average	56.2±13.3	2.3±0.4	0.060±0.013	0.23±0.03
calcite	32.2	1.2	0.071	0.21
	69.4	2.2	0.083	0.21

Table V-1. Bacterial colonization of sulfide mineral surfaces.

	cells per field	colonies per field	attachment rate (cells field^{-1}h^{-1})	specific growth rate (h^{-1})
cystine	18.0	13.0	1.9	0.29
glutathione	8.9	5.5	0.78	0.21
thioglycollate	7.5	6.0	0.85	0.18
sulfite	11.0	7.2	1.0	0.23
thiosulfate	14.0	10.0	1.4	0.20
control	15.0	9.2	1.3	0.23

note: 4,900 μM^2 per field

Table V-2. Effect of sulfur compounds on bacterial attachment to mineral surfaces.

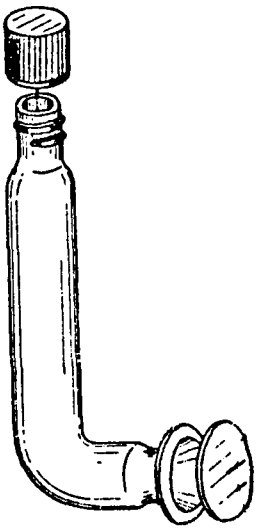

Figure V-1. "J-tube" with filter.

the above phosphate buffer yielded a 0.01 percent working solution. Both solutions were kept refrigerated between uses.

A 4 percent solution of formalin was used as fixative.

Six assembled J-tubes were autoclaved and cooled. Into five separate J-tubes were added approximately 25 ml of the five sulfur-compound solutions. The sixth J-tube, the control, was left empty. The J-tubes were capped and fastened to a test tube rack with the membranes facing down. This positioning ensured that solution was always in contact with the filter and that no debris settled on the filter surface. The rack and J-tubes were submerged in the sulfur spring-fed pool at Alum Rock Park (Fig. V-2, site 1). After a seven hour incubation period (7:30 AM to 2:30 PM) the J-tubes were removed from the creek and the remaining solutions were poured out. The attached filters were rinsed with distilled water and the J-tubes were placed into a beaker of 10 percent formalin. The J-tubes were kept refrigerated in the formalin until the filters were to be examined.

The filters were stained while attached to the J-tubes. After rinsing away the formalin with water the filters were flooded with 0.01 percent acridine orange for 30 seconds and rinsed with water. The J-tubes were then placed into a beaker of water for 5 minutes. The latter ensured that the staining of the background was minimized. The cells of interest were those irreversibly attached to the filters so that loss of cells from a filter surface during rinsing, staining, or storage was insignificant. The filters were then peeled away from the J-tubes and placed onto glass slides with the colonized side up. After trimming the filters, cover slips were placed on the filters and sealed with vaspar, an equal mixture of petroleum jelly and paraffin.

A Zeiss Photomicroscope III with epifluorescence was used to view the filters at 1000X magnification. Twenty fields were selected randomly from each filter. Fields containg debris were discarded. All bacteria and microcolonies that fell within or intruded upon a 65x65 μm grid were counted as being in that field. A microcolony was defined as an accumulation of morphologically similar cells that were no further than a cell-length away from a neighboring cell. The number of microcolonies containing 1, 2, 3-6, 7-12, 13-24, or more cells as well as the total cell count were noted for each filter. From the distribution of cells within these microcolonies the growth and attachment rates for *in situ* colonization of the filters were determined.

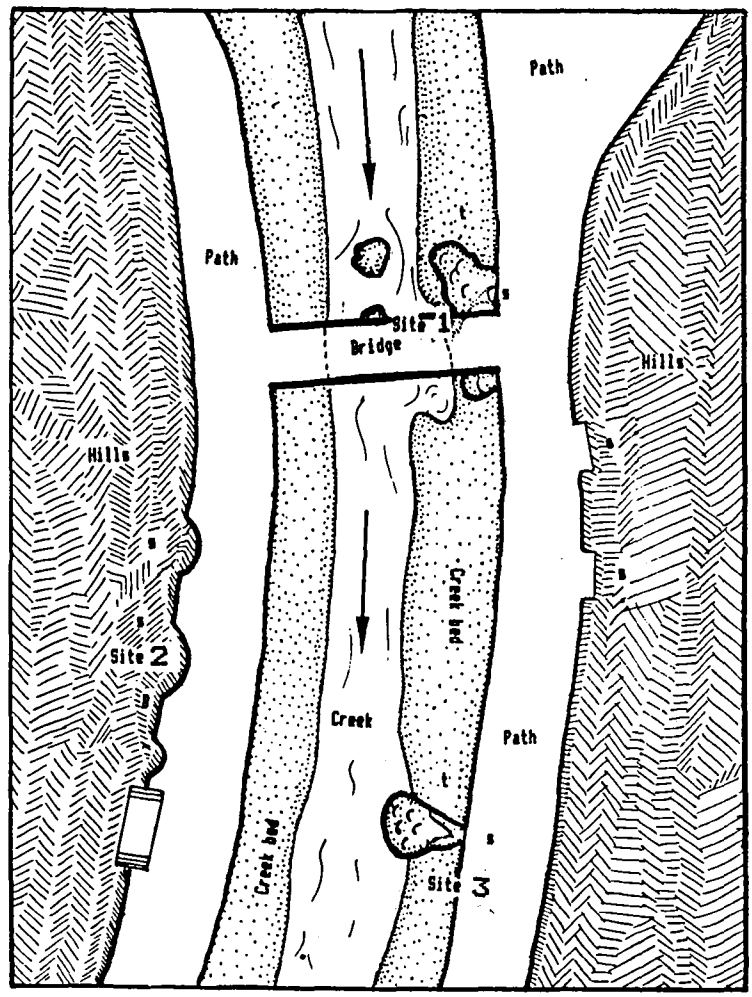

Figure V-2. Close-up of Penitencia Creek inset, Alum Rock Park Map 3.

Calculations of total cell count, N, and colony count, Ct, of attachment rate, A, and growth rate, μ, were done for each field. These field values were totaled and averaged to give the mean field value for each filter. All results were repeated as average counts and rates for a filter.

μ_1 and μ_2 were also corelated by first averaging the cell count for the filters and then using these averages in the growth rate equation of Caldwell.

Field values of A were correlated by counting the attachment events (i.e., all microcolonies) and dividing by the incubation period. From these values $\bar{A}$ (the average of the field values) was determined. (Three different values for A and $\bar{A}$ were calculated depending on the value of Ct used, which depended in turn on the value of C chosen - see A_1, A_2, and A_3).

Individual growth rates, μ, were calculated with the following equation:

$$\mu = 1 \ (N/Ct + 1)/t$$

Four values, $\mu 1$-$\mu 4$ were calculated. A second equation was used to caluculate μ; three values were determined, μ-$\mu 7$, for each field.

In Situ Incubation of Minerals

Either natural crystal faces or cleavage faces were used as colonization surfaces. In some cases the crystals were polished using 0.2 micron diamond abrasive. In the case of pyrite and pyrrhotite, oblique faces (with respect to cleavage and crystal planes) were obtained by grinding and the colonization of these faces compared to that of the natural faces (Fig V-3). Crystal faces were cleaned before use by wiping with petroleum ether. Crystals were submerged at Site 1, Penitencia Creek Alum Rock State Park.

Study of Pure Cultures and Natural Communities in Continuous Slide Culture

Perfilev capillaries (Perfilev and Gabe, 1969) were used to construct continuous slide cultures in which a laminar flow velocity of 10 cm per second was maintained during microbial colonization and growth. The capillaries were two mm in depth and 1 mm in width (internal dimensions). The small size of these capillaries made it difficult to properly focus the condenser on the cells for phase microscopy. In addition the capillaries contained stretch marks that resulted in optical distortions. As a result, capillaries were produced by bonding cover slips between glass slides using silicone seal. The dimensions of this culture system were 2 by 2 mm. Liquid was supplied via 22 gauge hypodermic needles inserted through the silicone. Sterile medium or sterile filtered stream water was supplied continuously and the inoculum was injected through a silicone septum. The inoculum was pulsed repeatedly or continuously until the

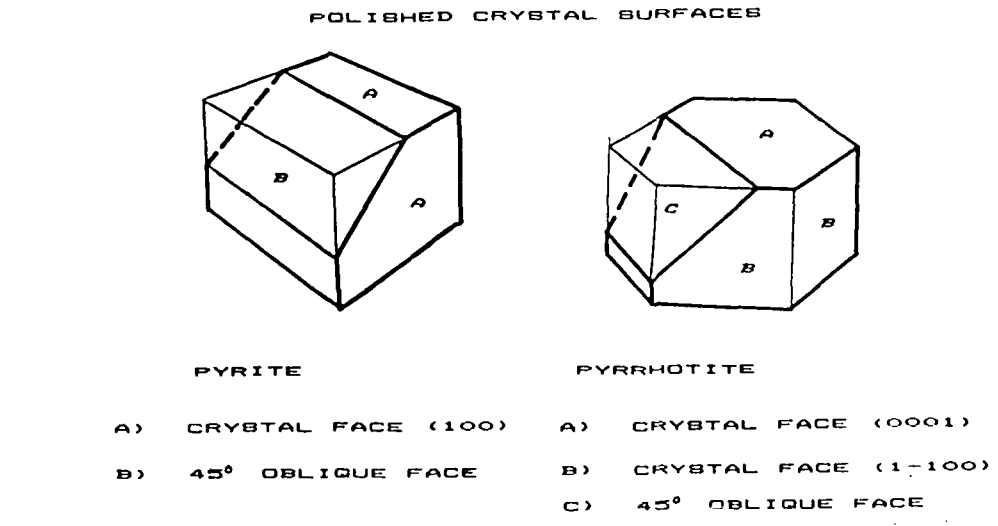

Figure V-3. Diagrams of polished crystal surfaces of pyrite and pyrrhotite. Numbers in parentheses refer to mineralogists' code for either crystal face or cleavage plane.

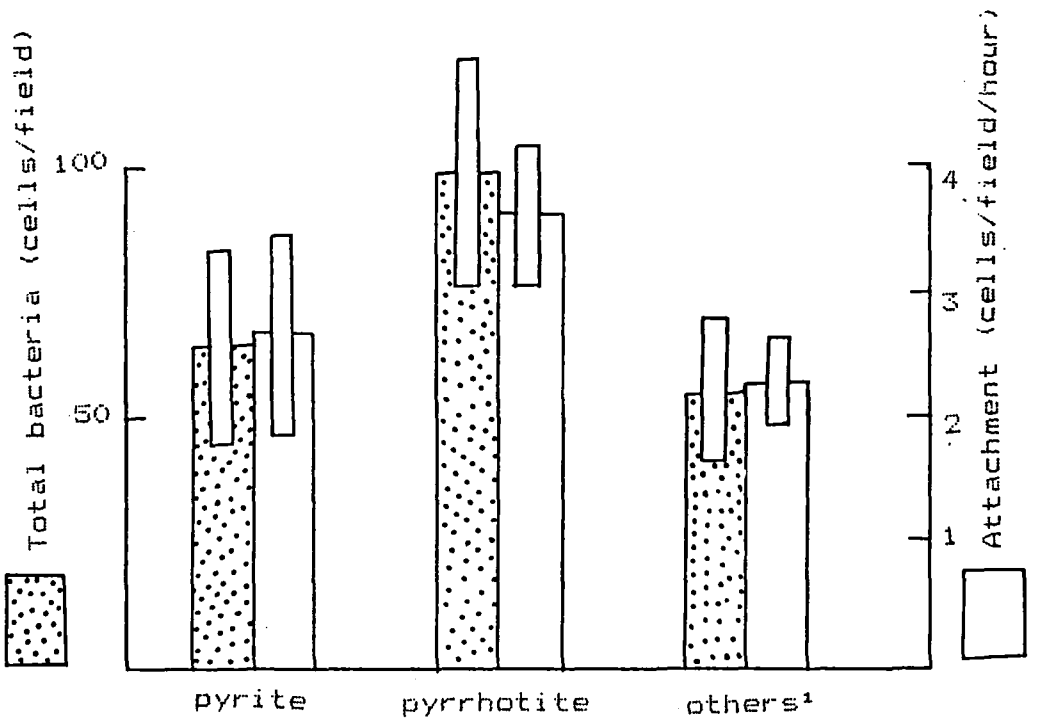

Figure V-4. Distribution of colony occurrence on mineral surfaces: bacterial attachment to pyrite, pyrrhotite, and other minerals.

density of cells was 5 to 50 per field (4,900 square microns per field).

Fluorescent Staining

Bacterial cells on mineral and filter surfaces were visualized using epifluorescent microscopy to observe cells stained with a 0.01 percent (w/v) solution of acridine orange in a 10 mM phosphate buffer (pH 7.2).

A novel stain, MBBR, was also evaluated as a potential staining technique. It gives a blue fluorescence upon reaction with thiols (Kosower et al., 1978; Newton et al., 1981).

A 50 mM stock of MBBR (Calbiochem-Behring - now called Behring Diagnostic) in acetonitrile was made. Acetonitrile (CH_3CN) is used because it will dissolve MBBR and it is only a poorly nucleophilic solvent. This solution can be kept refrigerated for months. 3 mM solutions are made by diluting the stock into Tris buffer (50 mM Tris, pH 8.0, 3 mM EDTA). This working solution should be made fresh daily since the MBBR will react slowly with water. Also, since uv radiation speeds up the nucleophilic attack on MBBR, hydrolysis can be greatly reduced by shielding the 3 mM solution from light. This will prolong the "lifetime" of the working solution.

Results and Discussion

Incubation of Minerals Under *In Situ* Conditions

To determine whether a bacterial film forms on sulfur minerals *in situ*, various sulfur-containing and other minerals were incubated at Site 1 in Penitencia Creek. The rate of cell growth and attachment within the surface microenvironment of mineral surfaces was also determined (Caldwell et al., 1981, 1983). Minerals studied included pyrite, pyrrhotite, galena, stibnite, barite, selenite (calcite), amorphous ingots of elemental sulfur, and hematite. A film rapidly formed on each of the minerals, however, no differences between the rate of colonization of various minerals were observed (Table V-1) with the exception of pyrite and pyrrhotite which were more rapidly colonized than other minerals. This confirms results previously obtained in continuous culture but which evaded repetition under *in situ* conditions (Kieft and Caldwell, 1984).

Data for bacterial colonization of each mineral are presented in Table V-1. The average number of cells in each field (N) and the hourly attachment rate (A) are given in the first two columns. No outstanding differences between minerals in final population could be seen there. Because the number of replicates for each surface type was small, pyrite, pyrrhotite and the remaining surfaces were compared as groups as shown in the histogram in Figure V-9. Pyrrhotite had fifty percent more bacteria than other surfaces, but this difference may be due to errors in the estimates. The error bars represent one standard deviation of the five to ten surfaces compiled in each group.

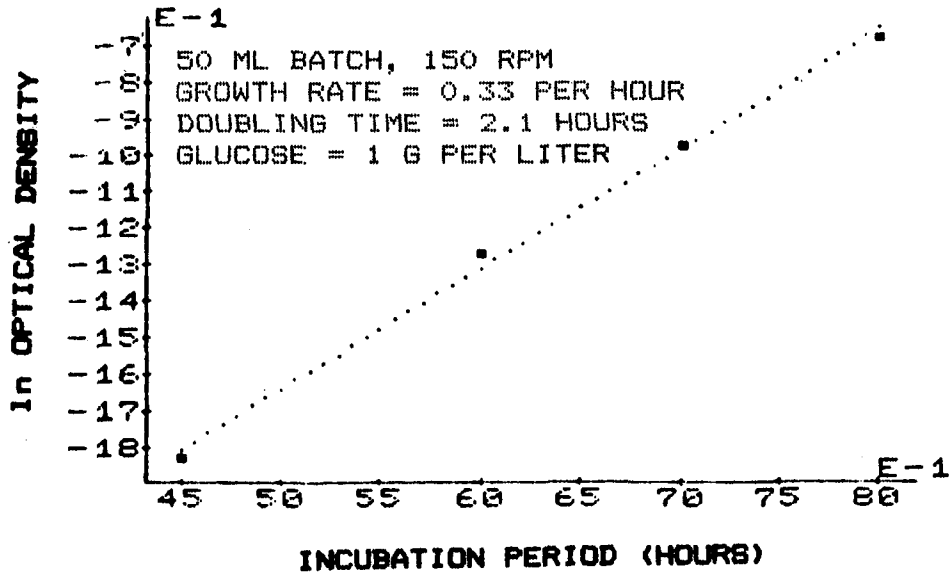

Figure V-5. Exponential growth of *Pseudomonas fluorescens* batch culture (50 ml volume, 150 rpm shaking) μ =0.331 hr^{-1}. Ta =2.09 h.

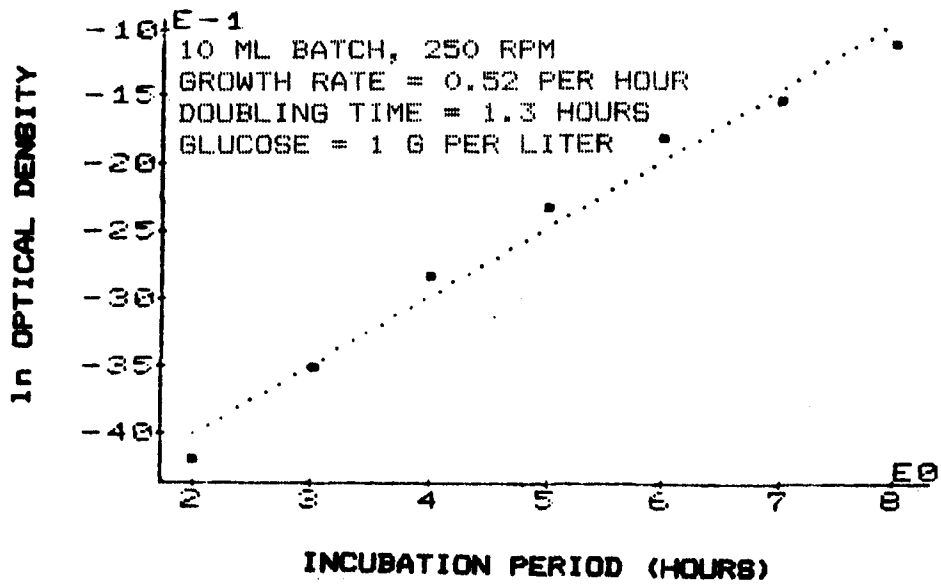

Figure V-6. Exponential growth of *Pseudomonas fluorescens* batch culture (10 ml volume, 250 rpm shaking) μ =0.515 hr^{-1}. Ta =1.346 h.

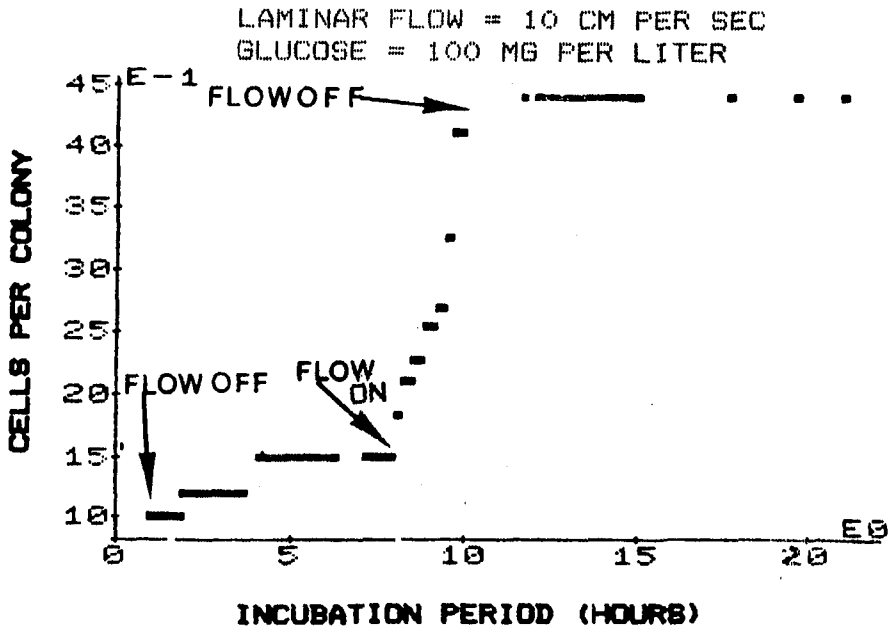

Figure V-7. Growth of *Pseudomonas fluorescens* colonies in a Perfil'ev capillary with and without laminar flow at a glucose concentration of 100 g/liter.

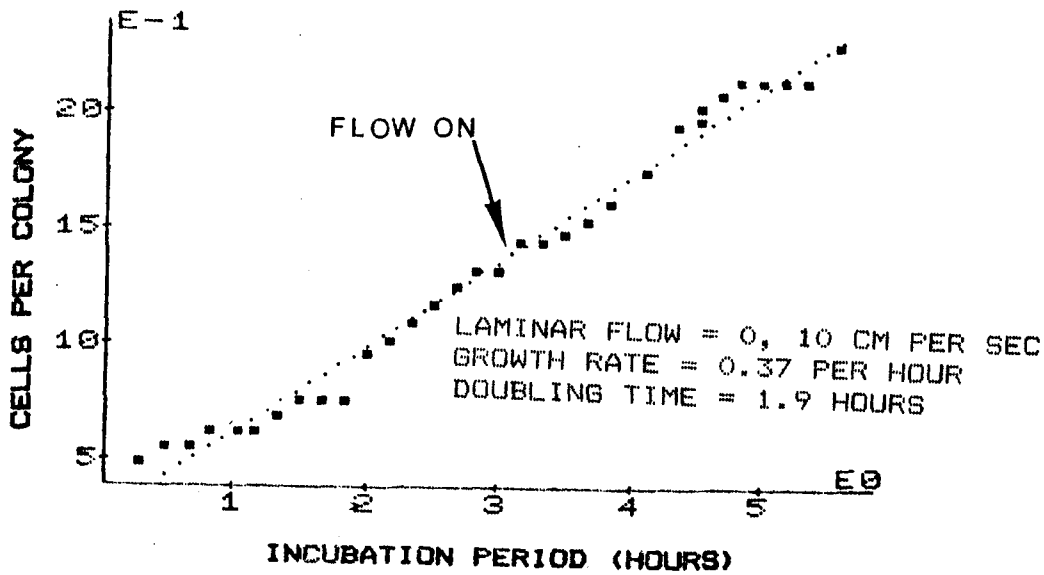

Figure V-8. Growth of attached colonies of *Pseudomonas fluorescens* without and with laminar flow at a glucose concentration of 1 g/liter

Two growth rates were calculated for bacteria on each surface. Although these values differed by about a factor of four depending on the method of calculation, they were constant from sample to sample within experimental error. The lack of a significant enhancement of growth by one mineral type indicates that either the substrates had a negligible effect on growth or that the bacterial community was too heterogenous to reveal enhanced growth. Sulfide oxidizers were probably not the predominant bacteria in the incubation site.

The growth equation developed by Caldwell et al. (1981) was used to obtain growth rates from the observed bacterial populations. With values for total cells (N) and attachment (A), a looping, trial-and-error computer program was used to solve the equation for growth (u).

$$N = A/u\ (\exp(ut) - 1) \qquad (1)$$

This gave the first growth rate listed in Table V-1. With the assumption that the colonies reached steady growth and attachment rates, a second equation was derived by Caldwell et al. (1983). In this equation growth could be directly calculated.

$$u = \ln(N/Ci + 1)/t \qquad (2)$$

Ci was the average number of occurrences that a colony size class (1-, 2-, 4-, 8-, 16-cells, etc.) was seen on a surface and t was the incubation time. This growth rate is the second value given in Table V-1. Direct observation of two actively growing colonies described earlier in this chapter gave an average growth rate of 0.58/h. The second growth rate was closer to this value, but this may have been an artifact.

The surfaces of the selenite crystals dissolved markedly, so the results from their colonization were not included here. One polished side and both polished oblique surfaces of the pyrrhotite were microscopically streaked or blemished, so their counts were not included either. A visual comparison of the polished pyrrhotite and pyrite indicated that there was more shallow pitting on the pyrrhotite, which may have been due to its faster weathering. Quantitative examination with such techniques as scanning electron microscopy or computer-aided image enhancement of these surfaces before and after colonization are needed to confirm this observation.

In Situ Incubation of Membrane Enrichments

To determine whether surfaces enriched with soluble sulfur substrates (cysteine, glutathione, thioglycolate, sulfite, and thiosulfate) increased the rate of growth or attachment of natural communities, membrane enrichments were incubated at Site 1. These rates were determined as described by Caldwell et al. (1981, 1983). The enrichments were incubated slightly downstream from sulfur springs which released sulfur-oxidizing bacteria. This ensured that the *in situ* concentration of sulfur substrates would be below that supplied by the membrane enrichments and that appropriate communities would be

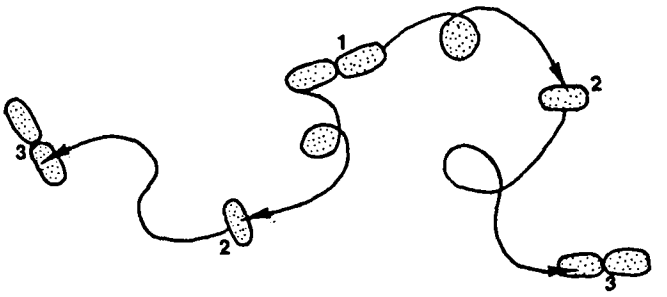

Figure V-9. Drifting mode of surface colonization.

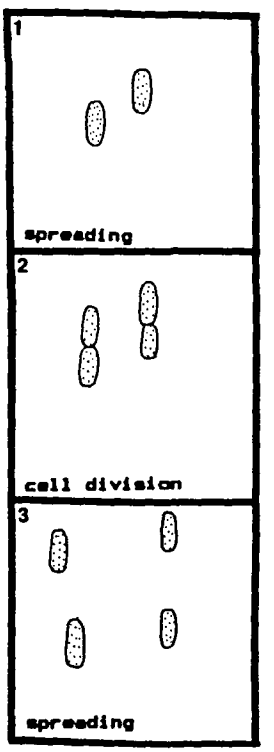

Figure V-10. Spreading mode of surface colonization.

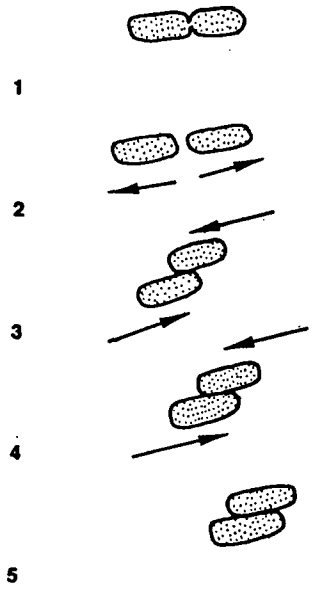

Figure V-11. Static mode of surface colonization.

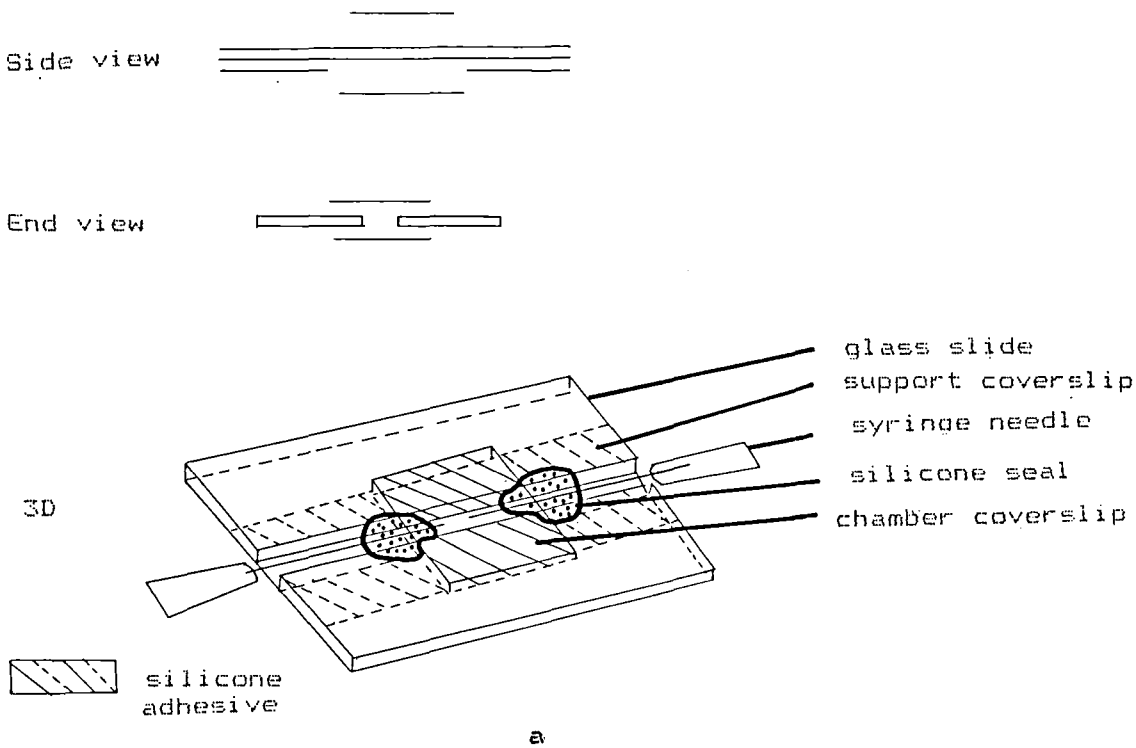

Figure V-12. (a) Schematic diagram of colonization and chamber culture apparatus; (b) diagrams of observation chamber.

present. The results of this study (Table V-2) showed no significant difference between the experimental treatments and the control membranes which lacked substrate.

Differences between Microbial Growth Kinetics in Cell Suspensions and in Films

The growth of *Pseudomonas fluorescens*, a heterotrophic sulfur oxidizer, was studied in batch cell suspensions and in continuous culture. In batch culture the cells were oxygen limited (growth rate 0.33 per hour under oxygen limitation and 0.52 per hour when vigorously aerated, Fig V-5 and 6). As shown in Fig V-7 and 8, growth within the film was glucose limited. Glucose limitation could be eliminated by increasing laminar flow and consequently decreasing the thickness of the hydrodynamic boundary layer. It can be seen that the attached cells are capable of growth rates equal to or faster than the rates achieved in liquid culture.

Differences between Microbial Behavior in Cell Suspension and in Biofilms

Several behavioral phenomena were observed for cells growing within the hydrodynamic boundary layer that have not previously reported. Despite a flow of 10 cm per second in the environment, the bacteria were able to move freely in both directions within the hydrodynamic boundary layer which apparently provides a calm zone within which turbulence is avoided and in which bacterial motility is remarkably effective. During the division of cells on surfaces unique mechanisms of remaining attached during cell division were observed as the colony formed. In the drifting mode the cells tumble and drift across the surface at a very slow rate as they divide. In the spreading mode of surface colonization the cells spread outward from the center of the colony as they divide. In the static mode of surface colonization the cells stay tightly grouped within the colony although they do undergo separation and reorientation. (Figures V-9-11.)

References

Baldensperger, J., Guarraia, L.J., and Humphreys, W.J., 1974. Scanning electron microscopy of thiobacilli grown on colloidal sulfur, Arch. Microbiol., 99:323-329.

Bennet, J.C., and Tributsch, H., 1978. Bacterial leaching patterns on pyrite crystal surfaces, J. Bacteriol., 134:310-317.

Caldwell, D.E., Brannan, D.K., Morris, M.E., and Betlach, M.R., 1981. Quantitiation of microbial growth on surfaces, Microbial Ecol., 7:1-11.

Caldwell, D.E., Malone, J.A., and Kieft, T.L., 1983. Derivation of a growth rate equation describing microbial surface colonization, Microbial Ecol., 9:1-6.

Kieft, T.L., and Caldwell, D.E., 1984. Weathering of calcite, pyrite, and sulfur by *Thermothrix thiopara* in a thermal spring., Geomicrobiol. J., 3:201-216.

Kieft, T.L., and Caldwell, D.E., 1984. Chemostat and *in situ* colonization kinetics of *Thermothrix thiopara* on calcite and pyrite surfaces, Geomicrobiol. J., 3:217-229.

Kosower, E. M., Pazhenchevsky, B., and Hershkowitz, E., 1978. 1,5-diazabicyclo(3.3.0)-octadienediones (9,10-dioxabimanes). Strongly fluorescent syn isomers, J. Am. Chem. Soc., 100:6516-6518.

Lord, C.J. and Church, T.M., 1984. The geochemistry of salt marshes: Sedimentary ion diffusion, sulfate reduction, and pyritization. Geochim. Cosmochim. Acta, 47:1381-1391.

Newton, G.L, Dorian, R., and Fahey, R.C., 1981. Analysis of biologcal thiols: Derivation with monobromobimane and separation by reverse-phase high-performance liquid chromatography, Anal. Biochem., 114:383-387.

Perfiliev, B.W. and Gabe, D.R., 1969. *Capillary Methods of Investigating Microorganisms*, (J. M. Shewan, Transl.), University of Toronto Press, 627 pp.

SULFUR CYCLE

BY R. HARRISS AND H. NIKI

CURRENT ISSUES

Human activities strongly influence the tropospheric sulfur cycle in certain regions of the world, particularly in and downwind of populated areas. The literature on the reaction and transformation of SO_2 and its distribution and transport in eastern North America and western Europe is voluminous. A reading of even selected portions of the literature on sulfur cycling illustrates that measurements and models of sulfur on the regional scale are providing a relatively consistent understanding of the sources, transport, and fate of anthropogenic emissions of SO_2. However, with the possible exception of reasonably well-understood processes related to local and mesoscale impacts of anthropogenic SO_2, global sulfur cycle studies are in the infancy stage.

Among the general categories of tropospheric sulfur sources, anthropogenic sources have been quantified the most accurately, particularly for the OECD countries. Research on fluxes of sulfur compounds from volcanic sources is now in progress. However, very few generally accepted measurements are available for either concentrations or fluxes of SO_2, H_2S, DMS, DMDS, CS_2, COS, and other sulfur species derived from natural biogenic sources. Measurement techniques have been inadequate until recently; serious questions still remain concerning flux determinations. Tables 7.4, 7.5, and 7.6 summarize most of the data available in the open literature.

What do the existing data indicate in terms of interesting hypotheses and the design of future global studies? First, natural sources of reduced sulfur compounds are highly variable in both space and time. Variables, such as soil temperature, hydrology (tidal and water table), and organic flux into the soil, all interact to determine microbial production and subsequent emissions of reduced sulfur compounds from anaerobic soils and sediments. For example, fluxes of H_2S, COS, CS_2, $(CH_3)_2S$, $(CH_3)_2S_2$, and CH_3SH can vary by several orders of magnitude on time scales of hours and space scales of meters in a coastal environment. A second interesting aspect of existing data on biogenic sources of reduced sulfur relates to the origin of relatively high SO_2 values measured in the mid-troposphere over the tropics and in the southern hemisphere during GAMETAG.

SOURCES AND DISTRIBUTIONS

Current estimates of global sources of atmospheric sulfur are based on very few data and will not be discussed in detail here. Several recent comprehensive reviews are cited at the end of this section for the reader unfamiliar with previous attempts to estimate sulfur sources. We briefly summarize available information on sources of COS, CS_2, DMS, and H_2S to the troposphere in the following paragraphs; these are the major biogenic sulfur species with a clearly identified role in tropospheric chemistry.

Carbonyl Sulfide (COS)

Carbonyl sulfide is the most abundant gaseous sulfur species in the troposphere. Concentrations of COS are approximately 500 + 50 pptv, with no detectable systematic variations vertically or latitudinally. This constant concentration with altitude and latitude suggests a relatively long atmospheric lifetime, estimated to be around 2 years.

Current estimates of global sources and sinks of COS are summarized in Table 7.6. It is important to note that these source and sink estimates are derived by extrapolation of a very limited data base and are subject to large uncertainties. Recent data suggest that oceanic regions of high biological productivity and organic content, particularly coastal waters and upwelling areas, are a major global source of COS. Experiments in coastal waters

TABLE 7.4 Approximate Tropospheric Concentration Range of Selected Sulfur Compounds in Unpolluted Air

	Atmospheric Concentrations[a] (ng/m^3)				
Location	H_2S	DMS	CS_2	COS	SO_2
Ocean boundary layer	<5-150	<2-200	1200-1550	50-70	<15-300
Temperate continental boundary layer	20-200	PD	1200-1550	PD	<15-300
Tropical coastal boundary layer	100-9000	PD	1200-1550	PD	PD
Free troposphere	PD	<2(PD)	1200-1550	<10	30-300

[a]PD indicates poorly determined at this review.

TABLE 7.5 Biogenic Emissions of Sulfur Compounds (emission rate in g S/m^2/yr)

Location	H_2S		DMS		CS_2		COS	
	Avg.	Max.	Avg.	Max.	Avg.	Max.	Avg.	Max.
Salt marsh	0.55	41.5		3.84				
			0.006					
	0.5	100	0.66	2.5		0.2		0.03
	72	381	0.093			1.13		6.36
Freshwater marsh	0.6	1.27						
Inland soils (U.S.)	0.001				0.001		0.002	
Swamps and tidal flats	0.044							
Sediments of shallow coastal area	~19	~2000						
Soils of humid equatorial forests	0.07	2.6						
Soils of temperate regions	0.044	0.24						
Open ocean			0.106					

indicate that COS is produced by photooxidation of dissolved organic matter independent of salinity, plant metabolism, or bacterial activity.

Some authors have suggested that the oceans may be a net sink for COS from the atmosphere. An intensive research program concerned with the production, distribution, and emissions of COS from coastal and oceanic environments will be required to quantify the role of the marine environment as a source of this compound.

Soils can also be a source of COS to the troposphere. Coastal salt marsh soils appear to be a "hot spot" for COS emissions, but the small area of these soils limits the role of marshes as a major global source. Measurements from a variety of soils in the United States were used to calculate the global soil source of COS shown in Table 7.6. The total absence of data on COS emissions from tropical soils introduces significant uncertainties into estimates of the global soil source. Efforts to quantify COS emissions from soils will probably be complicated by large variations in both space and time. Microbial processes that produce COS are influenced by soil moisture, nutrients, soil organic content, and other physiochemical variables.

Combustion processes are also thought to be a significant global source of COS. These processes include biomass burning, fossil fuel burning, and high-temperature industrial processes involving sulfur compounds. Again, it must be emphasized that these estimates are based on very limited data and may change significantly as new data become available.

During periods of low volcanic activity, COS may be a major source of sulfur to the stratosphere, resulting in the formation of the stratospheric aerosol layer that influences the earth's climate. The anthropogenic sources of COS identified in Table 7.6 represent approximately 25 percent of the total source strength, supporting speculations of possible effects on climate within the next century. Because of the importance of COS in the global sulfur cycle, its sources, atmospheric chemistry, and sinks are a critical scientific issue.

Carbon Disulfide (CS_2)

The abundance and distribution of CS_2 in the troposphere are not well known. Available measurements in the literature at this date show a typical range from approximately 15 to 30 pptv in surface nonurban air to 100 to 200 pptv in surface polluted air. The concentra-

TABLE 7.6 Global Sources and Sinks of Carbonyl Sulfide

	Estimate	Range
Sources (Tg/yr)		
Oceans	0.60	0.3-0.9
Soils	0.40	0.2-0.6
Volcanoes	0.02	0.01-0.05
Marshes	0.02	0.01-0.06
Biomass burning	0.20	0.1-0.5
Coal-fired power plants	0.08	0.04-0.15
Automobiles, chemical industry and sulfur recovery processes	0.06	0.01-0.3
Subtotal	1.4	≤3
CS_2-COS: CS_2-photochemistry and OH reactions	0.60	0-2
Total	2	≤5
Global burdens (Tg)	4.7 (500 pptv)	3.8-5.2
Lifetime (yr)	2-2.5	≥1
Sinks (Tg/yr)		
OH reaction	0.8	0.1-1.5
Stratospheric photolysis	0.1	≤0.2
O reaction	0.03	—
Other	1.1	≤3.3

NOTES: The estimated emissions are consistent with observed distributions of COS and CS_2 according to a global mass balance. All combinations of emissions within the ranges given above may not be consistent.

SOURCE: From Khalil and Rasmussen, 1984.

tion of CS_2 appears to decrease rapidly with altitude, indicating ground sources and a relatively short atmospheric lifetime. The primary removal mechanism for CS_2 in the troposphere is thought to be reaction with OH, producing COS and SO_2. The reaction rate constants for oxidation of CS_2 are poorly known, and the relative importance of CS_2 as a precursor for atmospheric COS and SO_2 is an unresolved issue.

The primary natural sources of COS and CS_2 are thought to be similar. The one available set of measurements of CS_2 in seawater indicates that concentrations are highest in coastal waters.

Dimethylsulfide $(CH_3)_2S$

Dimethylsulfide (DMS) is the most abundant volatile sulfur compound in seawater with an average concentration of $\sim 100 \times 10^{-9}$ g/l. This compound is produced by both algae and bacteria. The evidence for a biogenic origin for DMS has come from laboratory measurements of emissions produced in pure, axenic cultures of marine planktonic algae and field measurements of emissions from soils, benthic macroalgae, decaying algae, and corals. Extensive oceanographic studies have shown direct correlations between DMS concentrations in seawater and indicators of phytoplankton activity. The vertical distribution, local patchiness, and distribution of DMS in oceanic ecozones exhibit a pattern very similar to primary productivity. Selected groups of marine organisms such as coccolithophorids (i.e., a type of marine planktonic algae) and stressed corrals are particularly prolific producers of DMS. The calculated global sea-to-air flux of sulfur as DMS is ~ 0.1 g S/m^2/yr, which totals to approximately 39×10^{12} g S/yr. A more limited set of measurements has been made in coastal salt marshes with DMS emissions commonly in the range of 0.006 to 0.66 g S/m^2/yr.

Hydrogen Sulfide (H_2S)

Knowledge of natural sources of H_2S to the troposphere is still rudimentary. Preliminary studies have shown that anaerobic, sulfur-rich soils (e.g., coastal soils and sediments) emit H_2S to the atmosphere, albeit with strong temporal and spatial variatons. Hydrogen sulfide fluxes at a single location can vary by a factor of up to 10^4 depending on variables such as light, temperature, Eh, pH, O_2, and rate of microbial sulfate reduction in the sediment. The presence of active photosynthetic organisms or a layer of oxygenated water at the sediment surface can reduce or stop emissions due to rapid oxidation of H_2S.

Agricultural and forest soils can also be a source of H_2S to the atmosphere. Measurements by several investigators suggest that maximum emissions from nonmarine soils are associated with wet tropical forest soils. It is likely that many soils that appear to be aerated contain anaerobic microhabitats suitable for microbial sulfate reduction; the magnitude of H_2S emissions will depend on the net effects of many processes that influence production, transport in the soil, oxidation rates, and exchange at the soil-air interface.

Photochemical sources for atmospheric H_2S have been proposed to occur through a combination of the following reactions:

$$\begin{aligned}
OH + COS &\rightarrow SH + CO_2, \\
OH + CS_2 &\rightarrow COS + SH, \\
SH + HO_2 &\rightarrow H_2S + O_2, \\
SH + CH_2O &\rightarrow H_2S + HCO, \\
SH + H_2O_2 &\rightarrow H_2S + HO_2, \\
SH + CH_3OOH &\rightarrow H_2S + CH_3O_2,
\end{aligned}$$

and

$$SH + SH \rightarrow H_2S + S.$$

Removal of H_2S is thought to be accomplished by

$$OH + H_2S \rightarrow H_2O + SH,$$

resulting in a lifetime of approximately 1 day. In situ photochemical production from COS and CS_2 precursors is the most likely source of H_2S measured in remote ocean air. Atmospheric concentrations of H_2S in continental air are highly variable, resulting from a complex interaction of factors determining ground emissions, in situ photochemical production, and atmospheric lifetime.

TRANSFORMATIONS AND SINKS

The oxidation of SO_2 to H_2SO_4 can often have a significant impact on the acidity of precipitation, currently an issue of national and international concern. A schematic representation of some important transformations and sinks for selected sulfur species is illustrated in Figures 5.11, 5.13, and 7.5. The oxidation of reduced sulfur compounds, such as H_2S, CS_2, $(CH_3)_2S$, and others, leads to the production of acids or acid precursors such as SO_2, $SO_4^=$, and CH_3SO_3H. Subsequent oxidation steps involving a combination of homogeneous and heterogeneous reactions lead to the production of H_2SO_4, which is removed from the atmosphere by wet and dry deposition processes (see Chapter 5). Carbonyl sulfide appears to be relatively inert in the troposphere and is primarily destroyed in the stratosphere.

In terms of experiments to elucidate the fast photochemistry of this system, measurement schemes will be

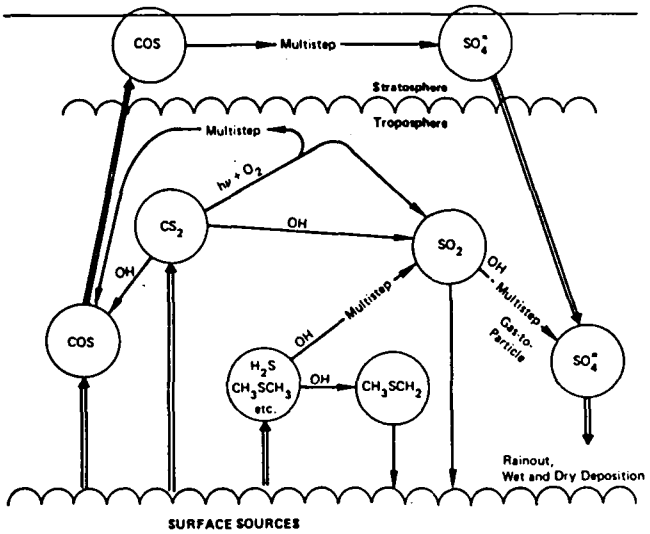

FIGURE 7.5 A tentative scheme for the oxidation and removal of atmospheric sulfur species.

needed to verify the chemical pathways by which reduced sulfur species are oxidized to SO_2 and $SO_4^=$. It is probable that it will be useful to carry out these experiments in a variety of different environments, including areas of intense sulfur emissions (e.g., swamps, tidal flats, and marshes) as well as remote marine areas. Unfortunately, present understanding of the distributions of atmospheric sulfur species and the elementary chemical reactions involved in the previously described oxidation chains is quite poor. In addition, the instrumentation necessary to measure many of the key atmospheric constituents has yet to be developed. Once this task is completed, it will be possible to design specific fast-photochemistry experiments to selectively study various facets of the atmospheric sulfur system.

In the case of H_2S oxidation, for instance, it is believed that oxidation is initiated by reaction with OH, i.e.,

$$H_2S + OH \rightarrow H_2O + SH,$$

and is followed by an as yet unconfirmed reaction sequence that produces SO_2 as an end product. The lifetime of H_2S in the atmosphere seems highly variable based on limited field measurements. In situ studies of H_2S oxidation kinetics in a variety of environments (e.g., swamps, salt marshes, and mangroves) would be extremely useful to improved understanding of the sulfur cycle.

Recent studies of DMS photooxidation provide important data on reaction mechanisms and products. The major gas-phase sulfur product produced in outdoor smog chamber experiments was SO_2. Substantial formation of light-scattering aerosol particles was observed, with inorganic sulfate and methane sulfonic acid as major components of the aerosol. Fourier transform infrared methods have been used to quantify products of the reaction of HO + CH_3SCH_3 in the presence of C_2H_5ONO and NO. Methyl thionitrite (CH_3SNO) was observed as an intermediate product, with SO_2 and CH_3SO_3H as major products. These studies serve as models of important photooxidation sinks for reduced sulfur species.

ROLE OF CLOUDS AND AQUEOUS-PHASE CHEMISTRY

As indicated in Chapter 5 of this report, aqueous-phase chemistry (i.e., in cloud and raindrops) plays a major role in the oxidation of SO_2 to H_2SO_4. Current thinking also suggests that clouds may be the dominant transport conduit for movement of SO_2 and other relatively short-lived reduced sulfur species to mid-tropospheric altitudes. Sulfur dioxide produced below cloud base may be injected directly into the free troposphere by updrafts associated with clouds or may dissolve or react with cloud droplets, depending on a variety of poorly quantified physical and chemical variables. Evaporation of cloud droplets may produce small sulfate-rich aerosol particles that subsequently act as cloud condensation nuclei. If the transport and reaction mechanisms mentioned in this paragraph are active over large areas of the nonurban troposphere, they contribute to explanations for acid rain in remote oceanic regions and higher SO_2 in the free troposphere than in underlying ocean boundary layer air. Once in the middle to upper troposphere, SO_2 may have a much longer lifetime with potential for long distance transport beyond the synoptic scale.

Future field experiments will need to measure a variety of species including SO_2, $(CH_3)_2S$, H_2O_2, and methane sulfonic acid in gas, liquid, and solid phases where appropriate. Combined ground and aircraft measurements focused on the role of cloud and aqueous-phase processes are a high priority.

BIBLIOGRAPHY

Andreae, M. O. (1980). Dimethylsulfoxide in marine and freshwaters. *Limnol. Oceanogr. 25*:1054-1063.

Andreae, M. O., and H. Raemdonck (1983). Dimethyl sulfide in the surface ocean and the marine atmosphere: a global view. *Science 221*:744-747.

Aneja, V. P., A. P. Aneja, and D. F. Adams (1982). Biogenic sulfur compounds and the global sulfur cycle. *J. Air Pollut. Control Assoc. 32*:803-807.

Barnard, W. R., M. W. Andreae, W. E. Watkins, H. Bingemer, and H. W. Georgi (1982). The flux of dimethyl sulfide from the oceans to the atmosphere. *J. Geophys. Res. 87*:8787-8793.

Brown, K. A. (1982). Sulfur in the environment: a review. *Environ. Pollut. 3*:47-80.

Chatfield, R. B., and P. J. Crutzen (1984). Sulfur dioxide in remote oceanic air: cloud transport of reactive precursors. *J. Geophys. Res.* (in press).

Delmas, R., J. Baudet, J. Servant, and Y. Baziard (1980). Emissions and concentrations of hydrogen sulfide in the air of the tropical forest of the Ivory Coast and of temperate regions in France. *J. Geophys. Res. 85*:4468-4474.

Ferek, R. J., and M. O. Andreae (1984). Photochemical production of carbonyl sulfide in marine surface waters. *Nature 307*:148-150.

Graedel, T. E. (1977). The homogeneous chemistry of atmospheric sulfur. *Rev. Geophys. Space Phys. 15*:421-428.

Graedel, T. E. (1979). Reduced sulfur emission from the open oceans. *Geophys. Res. Lett. 6*:329-331.

Herrmann, J., and W. Jaeschke (1984). Measurements of H_2S and SO_2 over the Atlantic Ocean. *J. Atm. Chem. 1*:111-123.

Husar, R. B., J. P. Lodge, and D. J. Moore (1978). *Sulfur in the Atmosphere*. Pergamon, New York.

Ingvorsen, K., and B. B. Jorgensen (1982). Seasonal variation in H_2S emission to the atmosphere from intertidal sediments in Denmark. *Atm. Environ. 16*:855-864.

Jones, B. M. R., R. A. Cox, and S. A. Penkett (1984). Atmospheric chemistry of carbon disulphide. *J. Atm. Chem. 1*:65-86.

Jorgensen, B. B. (1982). Ecology of the bacteria of the sulfur cycle with special reference to anoxic-oxide interface environments. *Phil. Trans. Roy. Soc. London B298*:543-561.

Khalil, M. A. K., and R. A. Rasmussen (1984). Global sources, lifetimes, and mass balances of carbonyl sulfide (COS) and carbon disulfide (CS_2) in the earth's atmosphere. *Atm. Environ.* (in press).

Kritz, M. A. (1982). Exchange of sulfur between the free troposphere, marine boundary layer, and the sea surface. *J. Geophys. Res. 87*:8795-8803.

Lawson, D. R., and J. W. Winchester (1979). Atmospheric sulfur aerosol concentrations and characteristics from the South American continent. *Science 205*:1267-1269.

Logan, J. A., M. B. McElroy, S. C. Wofsy, and M. J. Prather (1979). Oxidation of CS_2 and OCS: source for atmospheric SO_2. *Nature 281*:185-188.

Maroulis, P. J., A. L. Torres, A. B. Goldberg, and A. R. Bandy (1980). Atmospheric SO_2 measurements on Project GAMETAG. *J. Geophys. Res. 85*:7345-7349.

McElroy, M. B., S. C. Wofsy, and N. Dak Sze (1980). Photochemical sources for atmospheric H_2S. *Atm. Environ. 14*:159-163.

Moller, D. (1984). On the global natural sulphur emission. *Atm. Environ. 18*:29-39.

National Research Council (1978). *Sulfur Oxides*. Committee on Sulfur Oxides, Assembly of Life Sciences, National Academy of Sciences, Washington, D.C.

National Research Council (1981). *Atmosphere-Biosphere Interactions: Toward a Better Understanding of the Ecological Consequences of Fossil Fuel Combustion*. Commission on Natural Resources, National Academy of Sciences, Washington, D.C.

Nguyen, B. C., B. Bonsang, and A. Gaudry (1983). The role of the ocean in the global atmospheric sulfur cycle. *J. Geophys. Res. 88*:10903-10914.

Niki, H., P. D. Maker, C. M. Savage, and L. Breitenbach (1980). Fourier transform study of the OH radical initiated oxidation of SO_2. *J. Phys. Chem. 84*:14-16.

Rasmussen, R. A., M. A. K. Khalil, and S. D. Hoyt (1982). The oceanic source of carbonyl sulfide. *Atm. Environ. 16*:1591-1594.

Servant, J., and M. Delapart (1982). Daily variations of the H_2S content in atmospheric air at ground level in France. *Atm. Environ. 16*:1047-1052.

Shriner, D. S., C. R. Richmond, and S. E. Lindberg (1980). *Atmospheric Sulfur Deposition*. Ann Arbor Science, Ann Arbor, Mich.

Slatt, B. J., D. Natusch, J. M. Prospero, and D. L. Savoie (1978). Hydrogen sulfide in the atmosphere of the northern equatorial Atlantic Ocean and its relation to the global sulfur cycle. *Atm. Environ. 12*:981-991.

GARREL'S EUGAIAS

1.) LIFE (bacteria) CONTROLS SEA FLOOR SPREADING

A. Bacteria produce soil CO_2 from organics and thus control the rate of weathering.

B. The rate of weathering controls the rate of isostatic uplift of continents.

C. The rate of uplift controls the rate of thinning of the continental crust.

D. The thickness of the continental crust alters the heat flow, the convection flow from the mantle is impaired.

E. When the heat flow is altered, the spreading rate is changed. High spreading rates raise the sea level and flood continents. Low spreading rates lower sea level and expose continents to more weathering.

F. Bacteria, by controling weathering, control the spreading rate; high spreading rates raise the sea level and flood continents. Therefore bacteria control sea floor spreading.

2.) LIFE CONTROLS VOLCANOES

A. Limestone is biogenic.

B. When subducted, limestone reacts with silica at low temperatures to release CO_2, primarily through volcanoes. (Note volcanoes in South America north of the Nazca plate.)

Editor's Note: Two independent lines of argument, the first from L. Margulis and the second from J. Lovelock, support Garrel's first Eugaia:

First line of argument (Margulis'):

1) In the absence of life the Earth's carbon dioxide would be in the atmosphere just as it is on Mars and Venus. Greenhouse effects would follow.

2) The heat gradient from the mantle to the atmosphere would resemble much more that of Venus than now, and water would be vaporized.

C) Biogenic limestone is the repository of atmospherc carbon dioxide, therefore water is liquid. The oceans maintain an enormous heat discontinuity, segregating a hot mantle from a cold atmosphere and lithosphere. Heat from the mantle escapes at the edges only of lithospheric plates. Therefore life, the remover of atmospheric CO_2, controls the movement of lithospheric plates.

Second line of argument (Lovelock's:)

A) The amount of salt in the present ocean threatens life. Salt-protein attractions are higher than protein-protein attractions at high salt concentrations.

B) Salt is removed from the ocean by the evaporation of huge quantities of NaCl in tropical regions. This requires low flat extensive tropical exposures.

C) Life, by some unknown method, moves low edges of plates to tropical regions, effectively protecting its proteins from falling apart.

Prediction: lithospheric plate movement, like life, will not be found elsewhere in the solar system.

OTHER NOTEWORTHY COMMENTS

1) "We all build more and more complicated geochemical models until no one understands anyone else's model. The only thing we do know is that our own is wrong." Robert Garrels

2) "We only have two sexes, we can't conceive of a third. All we can imagine are interesting combinations of the two." Robert Garrels

3) "Deep sea sediments are trivial. I don't know why they've wasted all that time drilling all those little holes." Robert Garrels

4) "What's this Intercourse Memo all about?" Penny Boston

5) Lynn Margulis - "Do you know about the framboids that are so popular in the geological literature?

Doug Caldwell (hands outstretched) - "Yeah, I've got two big ones with lesions on them."

6) "The language of science is just another metaphor to describe our perception of reality." Sherwood Chang

7) "The chief purpose of models is not to be right or wrong but to give us a place to store our data." Robert Garrels (as reported by Christopher Martens)

8) "Without explanatory mechanisms, scientists will deny the existence of phenomena (e.g., atmospheric regulation by the biota; Wegener's discovery of continental drift)" Lynn Margulis

9) "Nature doesn't like definitions." Dorion Sagan (on the differences among autopoiesy, replication, and life).

10) "The abundance and perversity of Proterozoic stromatolites is remarkable." Stanley Awramik

11) "There are three kinds of lies: white lies, bold face lies, and statistics." Mark Twain via Stanley Awramik

12) "Nature abhors a pure culture of microbes." Lynn Margulis

13) "Reality is a figment of someone's imagination." George Fox

14) "My students tell me that the experiment failed because the data didn't come out right. Then they try again until it works. Experiments fail when they don't fit our preconceived ideas." Ken Nealson

15) "Before the genetic take-over our ancestors were clay (aluminosilicates)." Graham Cairns-Smith (Editors' corollary: After the computer takeover our descendants, the computers, will also be (alumino-)silicates).

15) "There are no one-celled animals, no one-celled plants, and no protozoa. Furthermore, no live organisms are higher than any others." Lynn Margulis

A final note: This document, NASA technical publication , is available from the NASA Headquarters Life Sciences Office, Washington DC 20546. Because there is strong interest in publication and wider distribution of "Microbes and the Global Sulfur Cycle," participants and others are urged to send corrections, comments, and suggestions to Dorion Sagan or any of the editors at the addresses listed in the front of this pamphlet.

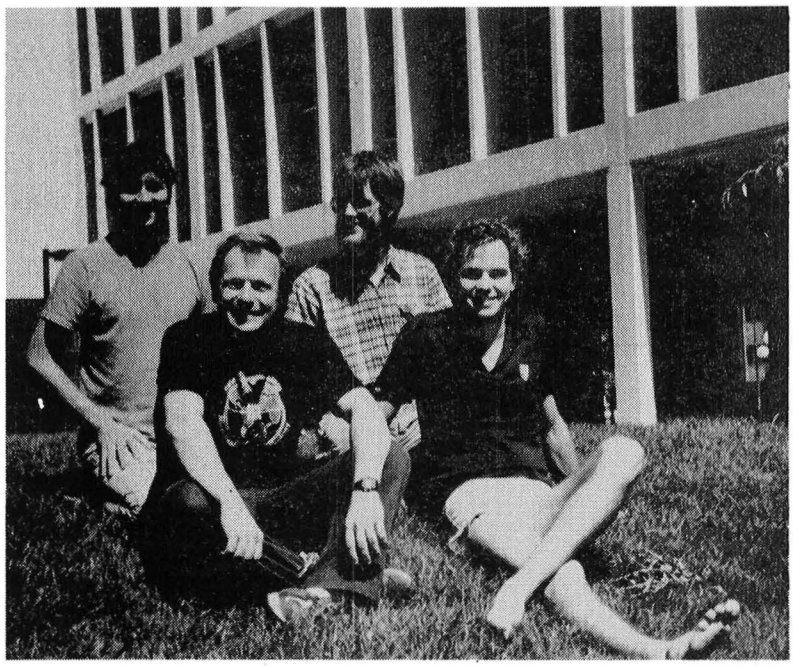

So committed were they to field and laboratory investigation that these eminent Planetary Biology and Microbial Ecology scholars nearly irretrievably missed the group photograph

Left to right:

Gordon Tribble, Kenneth Nealson, Allan Doyle and Alfred Sundquist

☆U.S. GOVERNMENT PRINTING OFFICE:1985 -537 -086/ 20001 REGION NO. 4

1. Report No.	2. Government Accession No.	3. Recipient's Catalog No.
NASA TM-87570		

4. Title and Subtitle	5. Report Date
The Global Sulfur Cycle	July 1985
	6. Performing Organization Code: EBR

7. Author(s)	8. Performing Organization Report No.
Dorion Sagan, Editor	
	10. Work Unit No.
9. Performing Organization Name and Address: Life Sciences Division, NASA Office of Space Science and Applications, Washington, DC 20546	11. Contract or Grant No.
	13. Type of Report and Period Covered: Technical Memorandum
12. Sponsoring Agency Name and Address: National Aeronautics and Space Administration, Washington, DC 20546	14. Sponsoring Agency Code

15. Supplementary Notes

16. Abstract

This report summarizes the results of the Planetary Biology Microbial Ecology's 1984 Summer Research Program, which examined various aspects of the global sulfur cycle. This interdisciplinary program integrated the contributions of university and NASA scientists and student interns of NASA's Exobiology Program. The Program investigated ways in which sulfur flows through the many living and chemical species that inhabit the surface of the earth. Major topics studied included sulfur cycling and metabolism of photo-tropic and filamentous sulfur bacteria; sulfur reduction in sediments of marine and evaporite environments; recent cyanobacterial mats; microanalysis of community metabolism in proximity to the photic zone in potential stromatolites; and formation and activity of microbial biofilms on metal sulfides and other mineral surfaces. Relationships between the global sulfur cycle and our understanding of the early evolution of the earth and biosphere and current processes that affect global habitability were stressed.

17. Key Words (Suggested by Author(s))	18. Distribution Statement
Exobiology Sulfur Cycle Microbial Ecology	Unclassified - Unlimited Subject Category 51

19. Security Classif. (of this report)	20. Security Classif. (of this page)	21. No. of Pages	22. Price
Unclassified	Unclassified	306	A14

N-305

For sale by the National Technical Information Service, Springfield, Virginia 22161

National Aeronautics and
Space Administration

Washington, D.C.
20546

Official Business
Penalty for Private Use, $300

SPECIAL FOURTH CLASS MAIL
BOOK

Postage and Fees Paid
National Aeronautics and
Space Administration
NASA-451

U.S.MAIL

NASA

POSTMASTER: If Undeliverable (Section 158
Postal Manual) Do Not Return